Liquid Rocket Analysis (LiRA)

Development of a Liquid Bi-Propellant Rocket Engine Design, Analysis and Optimization Tool

R.R.L. Ernst

supervisor: Ir. B.T.C Zandbergen

AE5810 Master of Science Thesis

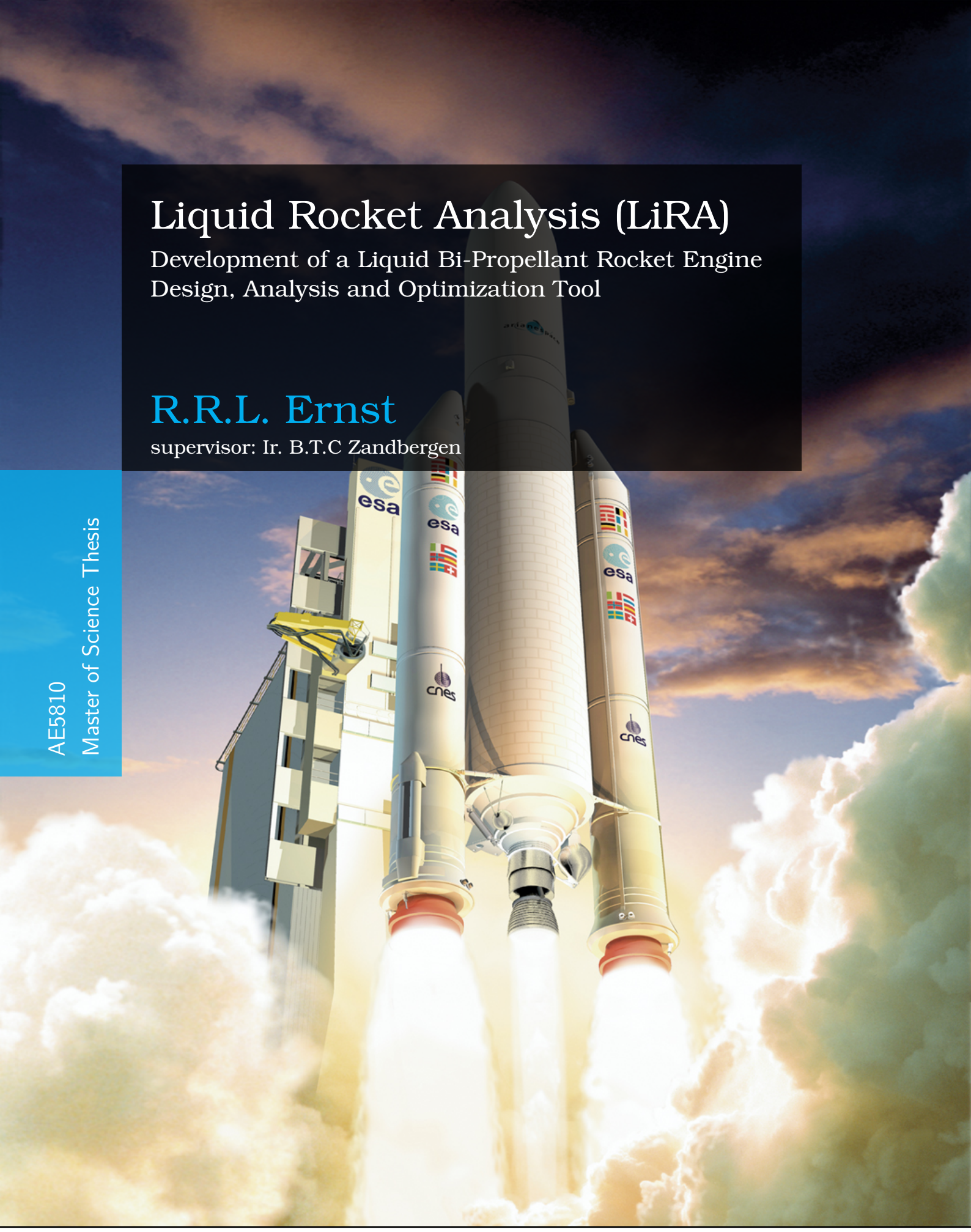

TU Delft Delft University of Technology

Space Systems Engineering

Liquid Rocket Analysis (LiRA)

Development of a Liquid Bi-Propellant Rocket Engine Design, Analysis and Optimization Tool

Master of Science Thesis

AE5810

For the degree of Master of Science in Spaceflight at Delft University of Technology

R.R.L. Ernst

Student nr. 1539833

supervisor: Ir. B.T.C Zandbergen

May 8, 2014

Faculty of Aerospace Engineering (AE) · Delft University of Technology

Cover photo: Artist's Impression of
an Ariane 5 ECA ©ESA-D. Ducros
http://spaceinimages.esa.int/

Delft University of Technology
Department of
Space Systems Engineering (sse)

The undersigned hereby certify that they have read and recommend to the Faculty of Aerospace Engineering (AE) for acceptance a thesis entitled

Liquid Rocket Analysis (LiRA): Development of a Liquid Bi-Propellant Rocket Engine Design, Analysis and Optimization Tool

by

R.R.L. Ernst

in partial fulfillment of the requirements for the degree of

Master of Science

Dated: May 8, 2014

Chairman of thesis committee: _____
Prof.dr. E.K.A. Gill

Supervisor of thesis: _____
Ir. B.T.C Zandbergen

Member of thesis committee: _____
Dr. A. Gangoli Rao

Abstract

The need to increase specific impulse of rocket launcher engines has lead design engineers to start development of ever more complex engine cycles starting from simple gas pressure fed engines to the very complex staged combustion cycle engines. Currently a wide range of different cycles does exist. These cycles not only differ in terms of performance, but also in terms of mass, cost, reliability etc., which in general makes it difficult to quickly determine which cycle is best suited for a certain mission or task. For this a tool that is capable of analysing different cycles and the impact of design choices has been developed. The tool, named LiRA, has as goal giving the user better system level understanding of the different possible engine cycles and the functions of the components; it can therefore provide valuable and time saving assistance during design or in analysis and optimisation studies. A modular approach is applied where engine components are sized using a performance, dimension and mass model who make use of corrected ideal rocket theory and empirical relations. This work focuses mainly on the methodology and the construction of the models, and further includes the optimisation of an upper stage and a verification, validation and uncertainty and sensitivity analysis of the tool and the optimisation to assess its accuracy, precision and applicability. The completed program has proved to confirm known trends and known cycle characteristics like the mass savings that can be achieved when using turbo-pump fed engines instead of pressure fed engines for mid- to high-thrust booster applications. Further the superior performance of closed cycles, especially staged combustion cycles has been confirmed, and some cycle specific design choices like the need of bypasses in expander cycles have been explained. The tool however is not complete and should be expanded; the addition of a cost and reliability assessment model is for example strongly recommended. There also remain issues with the accuracy and uncertainty of certain estimates which make that the current version should only be used for comparative studies.

Table of Contents

Acknowledgements

First I'd like to thank my parents Myriam Van Nuffel and Erich Ernst for their unconditional support and giving me the opportunity to study.

Next I want to thank my thesis supervisor ir. Barry Zandbergen for the extensive counsel and guidance he provided during the creation of this work.

Further a note of thank goes to my house mate Tom Stokkermans who has proof-read my thesis and with whom I had several insightful discussions on the content of this thesis.

And lastly I would like express my appreciation for the help received of my fellow students, especially Roy Bijster, Remco Schoemaker, Ivan Krusharev and Alexandru Mancas, during the creation of this work.

Delft, University of Technology
May 8, 2014

R.R.L. Ernst

Glossary

List of Acronyms

be	bleed expander engine cycle
ce	closed expander engine cycle
gg	gas generator engine cycle
pf	pressure fed engine cycle
sc	staged combustion engine cycle
Ariane 5 ME	Ariane 5 Midlife Extension
CEA	Chemical Equilibrium with Applications
COPV	composite over-wrapped pressure vessels
DARE	Delft Aerospace Rocket Engineering
DLR	Deutsches Zentrum für Luft- und Raumfahrt
EPS	Etage à Propergols Stockables
ESA	European Space Agency
ESC-A	Etage Supérieur Cryogénique type A
ESC-B	Etage Supérieur Cryogénique type B
GUI	Graphical User Interface
LH2	Liquid Hydrogen
LiRA	Liquid Rocket Analysis
LOX	Liquid Oxygen
LRE	Liquid Rocket Engine

LRP2	Liquid Rocket Propulsion 2
MMH	Monomethylhydrazine
NASA	National Aeronautics and Space Administration
N2O4	Dinitrogen Tetroxide
NIST	National Institute of Standards and Technology
RP1	Rocket Propellant 1
RPA	Rocket Propulsion Analysis
SCORES	SpaceCraft Object-oriented Rocket Engine Simulation
TCA	Thrust Chamber Assembly
TPA	Turbo-Pump Assembly
TU Delft	Delft University of Technology

List of Symbols

α	Nozzle half angle
Δ	Difference
δ	Thrust chamber inner wall thickness
ϵ	Nozzle area ratio
η	Efficiency
Γ	Van Kerckhove function
γ	Ratio of specific heats
μ	Viscosity
ϕ	Equivalence ratio
ρ	Density
ρ_0	Total density
σ_{ult}	Ultimate strength
ζ_s	Specific impulse corrections factor
$\dot{m}$	Mass flow
$\hat{M}$	Molar mass
(L/d)	Length-over-diameter ratio
A	Cross-sectional area
c^*	Characteristic velocity
C_F	Thrust coefficient
c_p	Specific heat capacity at constant pressure
c_v	Specific heat capacity at constant volume
d	Diameter

e	Height of the wall roughness
F	Thrust
f	Friction loss coefficient
F/W	Thrust-to-weight ratio
f_s	Safety factor
g_0	Standard gravitational constant
h	Enthalpy
h_c	Coolant side convective heat transfer coefficient
h_g	Gas side convective heat transfer coefficient
Isp	Specific impulse
K	Mass estimation correction factor
k	Conductivity
L	Length
L^*	Characteristic length
M	Mach number
m	Mass
MR	Mixture Ratio
n	Amount of moles
P	Power
p	Pressure
p_0	Total pressure
P_ρ	Power density
Pr	Prandtl number
R	Specific gas constant
r	Radius
R_A	Absolute gas constant
Re	Reynolds number
rf	Recovery factor
RSD	Relative Standard Deviation
RSE	Relative Standard Error
SD	Standard deviation
SE	Standard error
SEE	Standard error of estimation
T	Temperature
T_0	Total temperature
V	Volume
v	Velocity
x	Distance measured from the throat towards the nozzle exit
Z	Compressibility factor
AVG	Average
MEOP	Maximum Expected Operating Pressure
$_{adiabaticwall}$	T

a	Atmosphere
bo	Boil-off
b	Boiling
$crit$	Critical
c	Coolant side
$disch$	Discharge
$evap$	Evaporation
e	Exit
$fuel$	Fuel
f	Final
gg	Gas generator
g	Hot gas side
inj	Injector
in	In(let)
i	Initial
mcc	Main combustion chamber
MC	Monte Carlo
mix	Mixture
m	Mechanical
$nozzle$	Nozzle
OAT	One-At-the-Time
out	Out(let)
ox	Oxidiser
$press$	Pressurant
$prop$	Propellant
pu	Usable propellant
p	Pump
r	Reference
sl	Sea level
tc	Thrust chamber
tp	Turbo-pump
$trap$	Trapped
T	Turbine
t	Throat
ull	Ullage
u	Longitudinal
vac	Vacuum
wc	Wall coolant side

Chapter 1

Introduction

The design of an engine always comes down to maximising the performance and reliability while minimising mass, volume and cost. Since these parameters are correlated, different design philosophies are found in the past, current and future engine architectures. The engine requirements, and therefore the importance of the aforementioned parameters, are application dependent which makes an optimisation to meet these often conflicting requirements not evident.

From studying the past, current and future proposed engine cycles in literature, a clear evolution from simple pressure fed towards complex turbo-pump fed engine cycles can be observed. Turbo-pump fed systems are said to have better performance, lower mass and are often compacter but nevertheless pressure fed systems are still widely used today. So one may ask himself at what point turbo-pump fed systems become the preferred choice over pressure fed systems. Further an evolution from classic gas generator and staged combustion cycles towards new turbo-pump fed cycles such as expander cycles is seen. Completed and ongoing studies for new generation upper stage cryogenic engines in Europe which have the objective of increasing reliability, increasing performance, have engines with restart capability and low recurring cost identify expander cycles as a promising technology. [1]

The different turbo-pump cycles have as the name suggests one thing in common, namely two pumps driven by a single or double turbine; the approaches on how to drive the turbine is what defines the different turbo-pup engine cycles. A dedicated gas generating device could be used, or hot gaseous fuel could be tapped of from either the thrust chamber or the heat exchanger. And what to do with the gas after it has passed the turbine, dump it, or inject it back in the main combustion chamber?

Apart from the engine architecture a designer is also confronted with other considerations such as an oxidiser and fuel choice and the design of the thrust chamber. These tremendous amount of possibilities lead exactly to the needs of means to quickly assess engine cycles and design choices in order to quickly and efficiently select the most suitable candidates for a certain set of requirements. This is where a liquid rocket analysis tool like Liquid Rocket Analysis (LiRA) comes in place.

In the space systems engineering department at Delft University of Technology (TU Delft) and in the Delft Aerospace Rocket Engineering (DARE) association some projects have been done or

are still ongoing that require engine cycle design, analysis and optimization. For example in his master thesis graduation project 'Assisted-Launch Performance Analysis - Using Trajectory and Vehicle Optimization' [2], Jan Vandamme builds a launch-vehicle model consisting of a liquid engine performance and a mass model that is used to perform multi disciplinary optimization. While the tool developed by Vandamme is adequate for the goals aimed at in his thesis, it could be replaced or extended by introducing more detail, more possible engine cycles and more propellant combination choices. In an other master thesis, Menno van Kesteren has created a solid rocket engine analysis and design model; implementation or combination of his tool and the tool developed in this thesis would create a more powerful new tool capable of also considering different engine types (solid or liquid).

Further Astrium Space Transportation in Germany together with Herakles in France and the Von Karman Institute in Belgium have had the assignment by the European Space Agency (ESA) to jointly research the applicability of solid gas generator technology to, among others, drive the turbine of a gas generator cycle engine. An small study into the solid gas generator technology and applicability has already been performed by the author of this report during an internship at Astrium Space Transportation in Bremen, Germany; it was requested to build an tool in Microsoft Excel to assess the impact of using this technology on the mass and volume of the engine. A tool like LiRA offers a more detailed way to objectively compare the conventional and newly proposed systems and allow to help to conclude on this technology. When designing engines a trade-off between different possibilities is needed; the trade criteria are among others for example the dry mass, wet mass, reliability, cost, specific impulse, etc. Each criterion has its own weight in the trade, but in order to assign scores a single tool that calculates the parameter values related to these criteria offers an objective evaluation method. However as it is not possible to publicly find the properties of the solid considered to be used in the solid gas generator this study is not performed.

In order to perform system analysis of Liquid Rocket Engine (LRE) it is common to calculate feed system and performance data to compare different LREs and to evaluate the influence of key parameters on the behaviour of a certain engine. [3] Several companies, institutes or organisations like the Deutsches Zentrum für Luft- und Raumfahrt (DLR) and the National Aeronautics and Space Administration (NASA) built in-house tools to check or predict the behaviour of a certain engine cycle) and to help designers make the right design choices. TU Delft has expressed the desire for such tool to be used by students and academic professionals affiliated to the Space Systems Engineering chair and/or the University to study and analyse several liquid rocket engine cycles. While performance, mass and optimization models have already been (multiple times) created as part of projects at TU Delft, no project has been dedicated yet to build a general tool that can be extended, adapted to project needs and used by everyone to perform these and other tasks. The availability of such a tool should lead to time savings in project schedules, as one doesn't have to invent the wheel again.

The aim of the project is to create in a 30 week effort (the basis of) a tool to support the design, analysis, modelling, performance prediction and optimization of liquid bi-propellant rocket propulsion system and apply it in an example upper stage optimisation. The tool is to be suitable for the use in preliminary or conceptual design phase or can be used for data validation. In its current state LiRA is capable of performing performance analysis, total propulsion system mass estimation, total propulsion system dimension estimation and propulsion system optimization for five different engine cycles at systems level; supported engine cycles are the pressure fed cycle, gas generator cycle, staged combustion cycle, closed expander cycle and bleed expander cycle. The tool has several simplifications, such as neglecting pressure losses in lines connecting components, inside the cycle and could and should be extended; however due to the limited time

available this is left for future projects. Since the tool is hence to be extended, it is build in an easy to understand modular way. It will be the basis for a larger more extensive tool which is the ultimate aim of the faculty space chair and the associated interested parties. MATLAB has been chosen as software package to build the tool. Real engine data will be used to validate the tool and finally two study goals have been set to demonstrate the capabilities of the tool.

The first goal is to develop a tool capable of modelling a liquid rocket engine on systems level. Second goal is to simultaneously demonstrate the capability of the tool in the optimisation of an upper stage based on the Ariane 5 upper stage and to study the impact of engine cycle choice on the stage in order to be able to conclude on different engine cycle technology advantages and disadvantages.

First a literature and state of the art study is performed in Chapter 2. The chapter starts with the exploration of literature in order to gain a broad overview of the different existing engine cycles, their operation and advantages and disadvantages. Next publications about engine cycle analysis and modelling are shortly reviewed in order to gain insight in the work methods of others. This is followed by a review of different existing tools and identification of their strengths and shortcomings. Finally concluding remarks and a pan of approach is made.

The literature study is followed by the development of the models used in LiRA; starting with the performance model in Chapter 3, followed by the mass and sizing model in Chapter 4.

The description of the models developed is followed by a discussion of the program in Chapter 5.

Before verification and validation of the tool for engine analysis in Chapter 7, first a short recap in Chapter 6 of important statistical analysis principles is given and the statistical theory needed for verification, validation, sensitivity study and uncertainty analysis are discussed.

After the verification and validation of the engine analysis capability of LiRA, a stage propulsion system optimisation routine is developed in Chapter 8 and applied in an example optimisation of an upper stage based on the Ariane 5 ESC-A. The optimisation is validated and based on the results conclusions are drawn on the different engine cycles.

As a proper design or optimisation should also address the sensitivity of the results to the uncertainty in the model parameters a sensitivity and uncertainty analysis routine is developed in Chapter 9 and applied to the optimised upper stage example. From this study more conclusions on the obtained results for the optimised upper stage are drawn and points of improvement are identified.

Finally the thesis ends with Chapter 10 where the final conclusions of the thesis are given and recommendations for points of improvement and future work are given.

During the creation of this work many tables with data and figures were created; in order to improve readability the choice was made to put only the most essential figures and tables into the main text and move similar figures and tables to the end of each concerning chapter in a separate section called 'Large Figures and Tables'.

Further some generated data that is not used in discussion but can help in checking or reproducing calculations made has been put in a separate Appendix document. This Appendix further also gives examples that help understand calculations made and contains a user guide for the program.

Chapter 2

Literature Study and State of the Art Review

In this chapter a short introduction into the different engine cycles and their characteristics is given. It becomes apparent that due to the many design variations in engine cycle architectures and the accompanying large amounts of variable parameters, the need of a tool to find optimum design is already found early in rocket engine design literature. Interesting here are the modelling approaches taken and especially the parameters that were found most important during modelling and optimisation. Several tools to assist the designer in his or her task exist and are reviewed in order to find their strengths and shortcomings.

2-1 Liquid Rocket Engine Cycle Theory

A Liquid Rocket Engine (LRE) generally has two types of applications, either as boost propulsion or as auxiliary propulsion. Sutton gives in [4] an overview of typical characteristics of these categories; Table 2-1 summarises the most important differences and characteristics. This work will focus only on design, analysis and optimization of liquid rocket engines of the first category, the boost propulsion, as for these engines many different and rather complex engine cycles exist. Each cycle has its advantages and disadvantages in dry mass, wet mass, reliability, cost, specific impulse, etc. When looking to the history of rocket engines one can see a trend in time towards higher combustion pressures, M. Kaufmann identifies that the reasons for this are [5]:

- a more compact overall design
- higher specific impulse
- and the resulting higher payload percentages of launch vehicles with high pressure engines.

Table 2-1: Characteristics of the two main categories of liquid rocket engines [4]

Purpose	Boost Propulsion	Auxiliary Propulsion
Mission	Propel vehicle along flight path	Minor manoeuvres to adjust flight pad, adjust attitude or orbit maintenance
Applications	Launch vehicle boost and upper stages, large missiles	Spacecraft, satellites, top stages of small missiles, space rendezvous
Total impulse	High	Low
Thrust level	$4500\,\text{N} - 7.9 \times 10^5\,\text{N}$	$0.001\,\text{N} - 4500\,\text{N}$
Feed system	Mostly turbo-pump type; occasionally pressurised feed system for smaller thrusts	Pressurized feed system with high-pressure gas supply
Propellants	Cryogenic and storable liquids	Storable liquids, monopropellants and/or stored cold gas
Chamber pressure	$24\,\text{bar} - 210\,\text{bar}$	$14\,\text{bar} - 21\,\text{bar}$
Cumulative duration of firing	Up to a few minutes	Up to several hours
Shortest firing duration	Typically $5\,\text{s} - 40\,\text{s}$	$0.02\,\text{s}$ is typical for small thrusters

Turbo-pump-fed versus pressure-fed.

In order to achieve high pressures, one can see that progressively in time designers start to favour pump fed systems instead of pressure-fed engines for large rocket stages. For example the first Aestus engine is a pressure-fed one, while the next one, Aestus 2, is planned to be turbo-pump fed. Liquid rocket stages that are currently being developed are turbo-pump fed. An overview of the key advantages and disadvantages of both architectures is given in Table 2-2.

Differences among turbo-pump fed cycles.

Further, among turbo-pump fed systems different design philosophies can be noted between the countries where the engines are made; the United States of America has a great interest in staged combustion cycles (topping cycles) while Europe focuses more on gas generator and expander cycles and the Russians mainly use staged combustion and gas-generator cycles. Further a difference in propellant choice and mixture ratio can also be noted between different nations; the Russians tend to use often the oxygen rich (or fuel lean) semi-cryogenic combination of RP-1 (Kerosene) as fuel combined with LOX (Liquid Oxygen) for their turbo-pump fed engines, while European and US turbo-pump fed engines often use a oxygen lean (or fuel rich) combination of LOX and LH2 (liquid hydrogen), a fully cryogenic propellant combination. [6]

In the early days of rocketry hypergolic storable propellant combinations of N2O4 (Nitrogen-Tetroxide) with pure N2H4 (Hydrazine) or mixtures of Hydrazine such as UDMH (Unsymmetrical Dimethylhydrazine) or MMH (Monomethylhydrazine) were almost exclusively used. [6] Now they are, despite having a less favourable specific impulse and having toxic properties, still widely used for upper stage engines and satellite propulsion due to their storability and hypergolic properties that hence don't require the need of an igniter in the system. [6] Modern booster engines use more high performant propellant combinations such as LOX/LH2 and LOX-RP1. [6] According to Martensson et al. [7] the most important property of propellant choice is density as it determines in the first place the mass and volume of the propellant and the tanks containing it but also the pump head and thus turbo-pump size and mass. Other important properties to take into account when making a propellant choice are [7]:

Table 2-2: Characteristics of Pressure-Fed and Pump-Fed Engines [8]

Characteristic	Pressure-fed	Pump-fed
Complexity	Simple	Complex
Recurring cost	Inexpensive	Expensive
Specific impulse	Good	Slightly higher than pressure fed
Development cost	Low	High
Development risk	Low	Moderate
Development schedule	Short	Long
Reliability*	High	Low
Number of parts	Few	Many
Tolerances	Low	Very high
Start up / shut down	Easy and short	Difficult and long
Tank stiffness	High	Low
Handling robustness	High	Low
Cross-sectional area†	High	Moderate
Failure type	Benign	Catastrophic
Weight‡	Heavy	Light

* High speed rotating components at elevated temperatures in turbo-pump fed systems lead to lower reliability.
† In turbo-pump fed systems a higher chamber pressure is possible which leads to a smaller thrust chamber with a better (smaller) nozzle area ratio, hence a smaller engine.
‡ Due to the need for more components the engine mass of a turbo-pump fed systems is larger, however due to the decrease in needed propellant tank pressure these tanks are lighter than the propellant tanks in a pressure-fed system.

- its lubricating and cooling properties
- the soot/particles created during the combustion as these could lead to erosion, wear and clogging of components. This is especially the case for hydrocarbons such as methane and kerosene
- material compatibility such as embrittlement caused by hydrogen or oxidation caused by oxygen.

Further, as noted before, the mixture ratio also plays an important role. Rocket engines usually do not operate at the stoichiometric mixture ratio but at fuel rich mixture ratios; the reason is that operating with fuel rich mixtures increases the specific impulse [4]. If MR denotes the (oxidiser over fuel) mixture ratio and ϕ the equivalence ratio defined as [9]:

$$\phi = \frac{MR_{actual}}{MR_{stoichiometric}} \tag{2-1}$$

then a mixture is stoichiometric[1] when $\phi = 1$, fuel lean[2] when $\phi > 1$ and fuel rich[3] when $\phi < 1$. [9]

Most engines, with exception of for example the Russian RD-180 pre-burner, run fuel rich propellant combinations. For LOX/LH2 engines fuel rich combinations mean a minimal creation of (atomic) oxygen that could cause oxidation of materials; especially at high pressures this is an issue. However the production of water is higher and the formation of condensation droplets should be avoided for combustion stability. LOX/RP-1 has the problem of the formation of carbon

[1] the stoichiometric mixture ratio has just enough of oxidiser that all fuel is completely consumed.
[2] a fuel lean (or oxygen rich) mixture ratio has excess oxidiser.
[3] a fuel rich (or oxygen lean) mixture ratio has excess fuel.

in fuel rich mixtures and thus possible problems with erosion, wear and clogging of components of the turbine; this could explain why for the RD-180 a fuel lean mixture ratio was chosen.

While Table 2-2 only compares a pressure-fed engine with a turbo-pump fed system, also between the several open and closed turbo-pump engine cycle configurations advantages and disadvantages exist. A main difference between an open and a closed cycle is that because the warm gas produced in an open cycle is not needed in the combustion chamber any more after it has passed the turbine, it can be expanded to atmospheric conditions over the turbine, and thus more energy can be extracted by the turbine than is the case for a closed cycle where the turbine exit pressure must take the required main combustion chamber pressure into account. As the expansion over the turbine and after that over the main combustion chamber injector significantly lowers the pressure, the pressure before the turbine needs to be significantly higher, which also leads to higher pump discharge pressures, than is the case for a open cycle.

Overview and description of common engine cycles.

Now a discussion follows on several common open and closed engine cycles and their characteristics [10] [11]:

1. gas generator engine cycle (gg) (see Figure 2-1a)
   Open cycle. Pumps increase the propellant pressure before they are injected into the thrust chamber. The turbine that actuates the pumps is driven by a hot gas generator which combusts propellant tapped off from the main feed lines after the pumps. After it has passed the turbine, the gas is dumped into the atmosphere, sometimes through smaller nozzles to generate additional thrust, or alternatively injected back in the thrust chamber at the end of the nozzle. The portion of the fuel which does not go to the gas generator, passes first the nozzle where it is used for cooling before being injected in gaseous state into the thrust chamber. e.g. HM7B and Aestus 2 upper stage engines and the Vulcain main stage engine of Ariane 5

2. bleed expander engine cycle (be) (see Figure 2-1b)
   Open cycle. Pumps increase the propellant pressure before they are injected into the thrust chamber. The turbine that actuates the pumps is driven by hot gaseous fuel after it has passed as a liquid the nozzle where it is used for cooling. The gaseous fuel is dumped into the atmosphere after it has passed the turbine. The thrust chamber uses the gaseous fuel which is not send to the turbine. e.g. engine of the Japanese LE5

3. combustion tap-off cycle (see Figure 2-1c)
   Open cycle. Pumps increase the propellant pressure before they are injected into the thrust chamber. The turbine that actuates the pumps is driven by hot combustion gas which is tapped of from the thrust chamber e.g. US J2S engine

4. pressure fed engine cycle (pf) (see Figure 2-2a)
   Closed cycle. No pumps are present, the oxidiser and fuel are injected directly in the thrust chamber. Because of the absence of pumps to increase the pressure after the tanks, the propellants have to be stored at high pressure. e.g. Aestus upper stage engine of Ariane 5 and the AJ-10 engine of the Delta II Launcher

5. staged combustion engine cycle (sc) (see Figure 2-2b)
   Closed cycle. Pumps increase the propellant pressure before they are injected into the

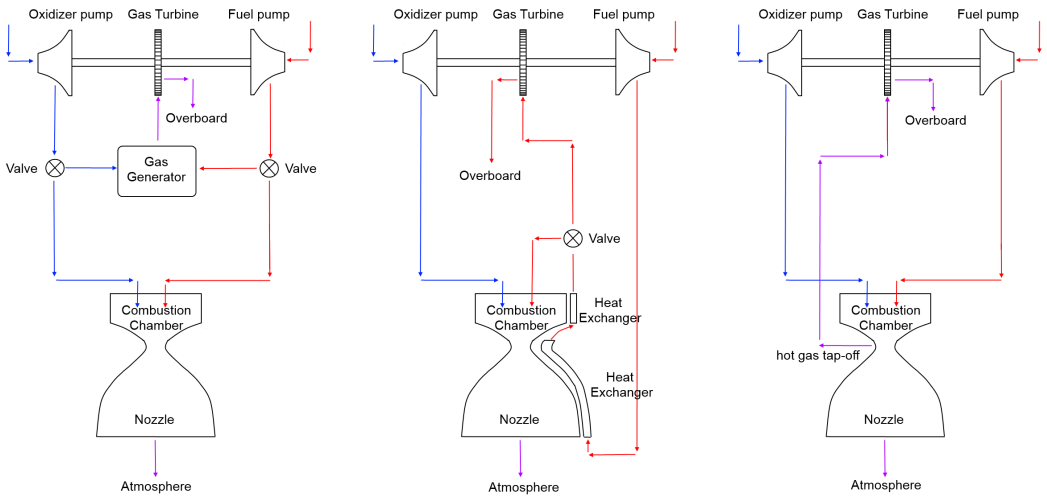

(a) Gas generator cycle **(b)** Open bleed expander cycle **(c)** Combustion tap-off cycle

Figure 2-1: Open engine cycles

thrust chamber. The turbine that actuates the pumps is driven by a warm gas generator which combusts oxidiser tapped off from the main oxidiser feed lines after the pump and gaseous fuel after the liquid fuel has passed the pump and the nozzle where it is used for cooling. in the warm gas generator the combustion is incomplete and the generated gas is injected in the thrust chamber where it combusts (in the ideal case) completely. e.g. the Russian RD-120, RD-170 and RD-253 rockets, the US SSME and High Thrust Engines for next generation launchers

6. closed expander engine cycle (ce) (see Figure 2-2c)
   Closed cycle. Pumps increase the propellant pressure before they are injected into the thrust chamber. The turbine that actuates the pumps is driven by hot gaseous fuel after it has passed as a liquid the nozzle where it is used for cooling. After the gaseous fuel has passed the turbine it is injected into the thrust chamber. e.g. American RL-10 and the VINCI engine which is foreseen for Ariane 5 ME

Though all cycles in Figure 2-1a to Figure 2-1c are depicted with a single turbine, and when applicable a single gas generator or pre-combustion chamber, also cycles with a separate turbine, sometimes also driven by a separate gas generator or pre-combustion chamber, for each pump exist. Further often the fuel is used as coolant for parts of the thrust chamber; hence cycle architecture variations with heat exchangers on nozzle, throat and/or combustion chamber parts are possible as well.

Cycle advantages and disadvantages

In [12] Sisco gives a overview of most liquid rocket engine cycles and their advantages and disadvantages, based on this overview Table 2-3 was made. Further Sutton also gives an overview in [13] of the qualitative characteristics of the turbo-pump cycles considered in this work; Table 2-4 summarises the most important entries.

Table 2-3: Engine cycle advantages and disadvantages (based on overview given in [12])

Cycle	Advantages	Disadvantages
Pressure fed	• Simple reliable design • No turbo-pump	• Limited to low burn times and low thrust • Limited throttling capabilities • High pressure tanks • Tank bladders can be required
Gas generator	• Fairly simple • Wide thrust operating range	• Turbine exhaust gas has low specific impulse and leads to effective loss in performance • Gas generator required
Staged combustion	• High performance • High chamber pressure and thrust capability	• Very complex with lower reliability • Advanced turbine and pumps required to cope with high pressures • Pre-burner (gas generator) required
Closed expander	• Good performance • Simple design with a low weight and wide thrust operating range • No gas generator required	• Limited to low chamber pressures • Limited to cryogenic fluids
Bleed expander	• No gas generator required	• Limited to cryogenic fluids • Pressure and thrust limited by fuel thermal properties

Table 2-4: Qualitative characteristics comparison of the turbo-pump cycles considered (based on overview given in [13])

	Gas generator cycle	Staged combustion cycle	Expander cycle
Engine specific impulse as % of gas generator cycle	100 %	102-108 %	102-106 %
Turbine mass flow, as % of total propellant flow	1.5-7 %	60-80 %	75-96 % of the fuel flow or 12-20 % of total propellant flow
Typical pressure drop, across turbine as % of chamber pressure	50-90 %	60-100 %	5-30 %
Pump discharge pressure in % of chamber pressure	135-180 %	170-250 %	150-200 %
Relative inert mass of engine	Low	High	Moderate
Thrust control, typical	Regulate flow and/or mixture ratio in gas generator	regulate pre-burner mixture ratio and propellant flows	Control bypass of some gasified fuel flow around turbine
Maximum pressure in feed system	Low	High	Moderate

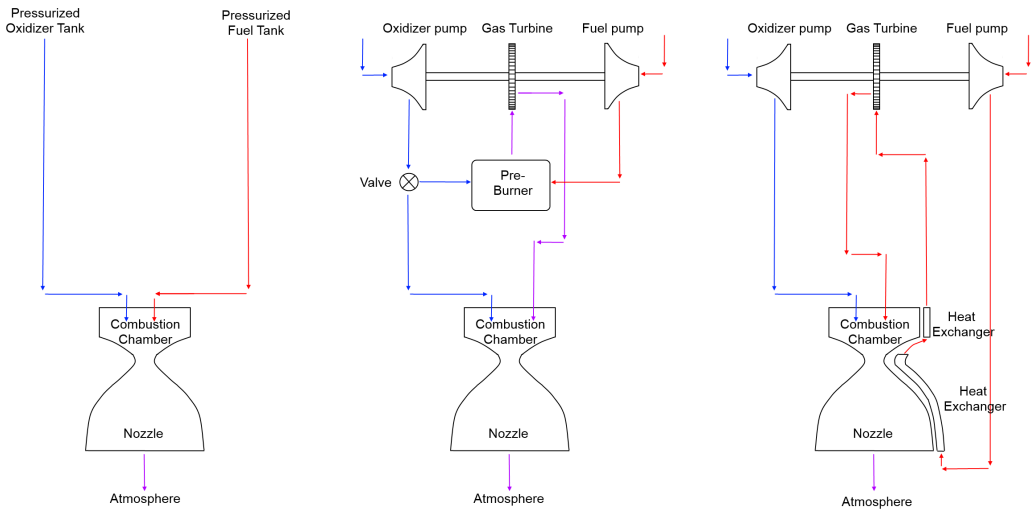

(a) Pressure-fed cycle **(b)** Staged-combustion cycle **(c)** Closed expander cycle

Figure 2-2: Closed engine cycles

In the nine-teen-sixties M. Kaufmann wrote a report, see [14], where he demonstrates the superior performance of a topping cycle[4] above other cycles by studying the analytical relation between pump and chamber pressure for topping cycle engines and considering or optimizing for several parameters like propellant combinations, mixture ratios, thrust level, efficiencies, pressure drops, etc. His goal was to present the maximum achievable chamber pressure, and thus maximum achievable specific impulse, for a topping cycle engine as he identifies high specific impulse and small engine size are important performance objectives for chemical propulsion rockets.

2-2 Software Development and Existing Models with Similar Purpose

In the nine-teen-eighties and nine-teen-nineties efforts by rocket researchers like C. Goertz, S. Gordon, D. Manski and J. Martin lead to several conference papers discussing methods to analyse and optimize (advanced) rocket launcher systems. The software developed was used to predict or verify propulsive parameters such as chamber pressure, specific impulse, thrust, mass flow, volume flow and to analyse the nozzle extension, engine cycle selection, study new technology effects, etc. [15] [16] NASA and DLR have combined their software codes in order to analyse and optimize rocket launcher systems; the combined software has a engine mass model including the feed system, a performance model and a cycle model. [15]

While a large amount of different liquid bi-propellant engine cycles exist and are proposed, most of them basically consist out of similar components such as pumps, turbines, gas generator, combustion chamber, nozzle. [3] Therefore Goertz proposed to use a modular approach for the analysis of engine cycles [3]; he found that a relatively small component library is sufficient for the analysis of most complex engine cycles. He makes use of a sequential method where the

[4] a topping cycle is another name for staged combustion cycle, sometimes also called a pre-burner cycle

components of an engine cycle are calculated iteratively in a predetermined order until the desired solution state is found. Goertz also notes that a major advantage of this modular approach is that a wide range of modelling is possible; from simple to sophisticated depending on the accuracy required and on the data available. Existing and new models and subroutines can be integrated easily, thus the program can be easily extended and allows for independent development of parts for the program which can be integrated when needed. Also he argues that using a sequential method is more intuitive and more easily understood. Finally complex engine systems can be constructed partially, allowing for intermediate checks and early flaw detection or code errors.

Notable existing liquid rocket analysis tools are, among others, CEA [17], SEQ [3], LRP [18], RPA [19], SCORES [20], RedtopPRO [21] and EcoSimPRO [22].

CEA

CEA is a tool developed by Gordon and McBride at NASA Glenn/Lewis Research Center. [23] The tool calculates chemical equilibrium product concentrations from any set of reactants and determines thermodynamic and transport properties for the product mixture. [17] Applications are for example assigned thermodynamic states, theoretical rocket performance, Chapman-Jouguet detonations, and shock-tube parameters for incident and reflected shocks. [17] NASA claims it is widely used by the aerodynamics and thermodynamics community. [17]

RPA

Rocket Propulsion Analysis (RPA) is a tool that works very similar to CEA; the minimal set of input parameters consist of: combustion chamber pressure, propellant combination, mixture ratio or oxidiser excess coefficient or mass fractions of each component, list of components at standard conditions or at assigned temperature, assigned enthalpy. RPA calculates combustion equilibrium and the properties of the reaction products. [19] Additionally if the the nozzle exit pressure, or alternatively the nozzle area ratio, is defined together with a chamber contraction area or mass flux, then the conditions at the nozzle throat, nozzle exit and the theoretical rocket engine performance are determined as well. [19] This tool hence only performs combustion calculations and estimates the thruster performance.

SCORES

SpaceCraft Object-oriented Rocket Engine Simulation (SCORES) is a web-based rocket engine analysis tool for conceptual design which provides thrust, specific impulse and thrust to weight estimates for a given mixture ratio, chamber pressure, throat area and expansion ratio. [20] The code, according to [24], works again very similar to CEA regarding its equilibrium analysis and capabilities, but adds some additional features such as an 'expert-system database of engine efficiencies to account for engine cycle effects' such as staged combustion, expander and gas generator. In other words the tool does not model the entire engine cycle, just the thrust chamber but uses a database of stage specific efficiencies to account for cycle differences.

SEQ and LRP2

In papers published by DLR or people affiliated to DLR (such as [25], [26], [18] and [27]) often make use of the tools called SEQ and Liquid Rocket Propulsion 2 (LRP2); LRP2 is based on SEQ

[18] which in its turn is based on the modular DLR code [27] described by Goertz in [3]. According to [28] and [18] the modular approach used in LRP2 allows quick arrangement of components, especially the turbo-pump assembly, through the use of an input file and then calculates the fluid properties sequentially following specific thermodynamic processes in the components along the flow path. In LRP2 conditions are linked to component settings which result in a system of non-linear equations that is solved by an external subroutine. [18] LRP2 appears to be only capable of performing engine performance analysis and needs to be used with other tools such as TDK for calculating the nozzle performance and heat exchange rate in the regenerative cooling part, NCC for combustion chamber and nozzle contour pre-dimensioning and preliminary mass estimation, and LRP_mass which sizes and estimates the mass of the turbo-pumps, extend its capabilities as can be read in [26] and [18]. From comparing publications using the tool it can be concluded that the operation mode is very similar to that of LiRA; a modular approach with components such as storage tanks, pumps, valves, flow separators, gas generator or pre-burner, turbines, injector, combustion chamber, nozzle and more.

RedtopPRO

RedtopPRO is a commercial software package dedicated to the modelling of liquid propulsion rocket engines. A comparison between RedtopPRO and LiRA is performed in Table 2-5 and Table 2-6.

EcoSimPRO

An other similar software package is EcoSimPRO which also uses a modular approach by using multidisciplinary component libraries and a schematic user interface [22]. It is capable of modelling zero dimensional and one dimensional continuous-discrete systems in both steady state a transient studies; it does this by constructing and solving systems of linear, non-linear differential-algebraic or ordinary-differential equations. While EcoSimPRO is a very capable tool and has much detail in it, it is stated on their website that the modelling skills of the user increase with complexity. [22] As it is also stated that the tool can be used for solving simple differential-algebraic equations to modelling complete spacecraft vehicles [22], the latter hence requires high user skills; it therefore seems that EcoSimPRO is intended for advanced design modelling phases, also due to the extensive component library and component detail which also have a large required amount of input parameters. LiRA requires no user modelling skills and therefore is ideal for system level studies, however it currently cannot model transient behaviour nor components in such detail as offered in EcoSimPRO.

2-3 Conclusions on User Requirements and Plan of Approach

The red line found throughout literature is that there exists the need for a versatile tool that can be used to quickly verify or predict engine performance, mass, dimensions, reliability and cost. Ideally this tool should also be able to optimise a design and be able to assess the sensitivity of the output to certain parameters.

So in summary from literature it can be seen that already many tools exist; however the freely available tools are often limited to a certain aspect like combustion or thruster design only and do not model the feed system and thus do not take engine cycle options into account. Commercial

Table 2-5: Software comparison with REDTOP PRO (1/2)

	LiRA	REDTOP PRO (sources: [21], [29])
Purpose:	Idem	For use in conceptual and preliminary design of space transportation systems utilising liquid propulsion rocket engines
Modelling approach	Full power and pressure balance with fluid analysis starting in combustion chamber, through nozzle, injector, cooling channels, pre-combustion device, turbine(s), pumps, propellant storage tanks and pressurant tank.	Full power balance with fluid analysis starting at pump inlet, through turbine(s), pre-combustion device(s), valve(s), injectors, main chamber(s), and nozzle(s)
# of input parameters	19-33 (depending on cycle modelled)	80-150 (depending on cycle modelled)
First order input	See Table 5-1	• Engine cycle • Engine configuration • Required thrust, mass flow rate or throat area • Chamber and pre-burner/gas generator mixture ratio(s) • Desired chamber pressure • Turbo-machinery (pump and turbine) efficiencies • Valve, injector and heat exchanger pressure drops • Regenerative, radiative and ablative nozzle area ratios • Chamber/throat and nozzle heat fluxes • Nozzle shape, half angle, equilibrium flow fraction and length fraction (% of conical nozzle)
Second order input	See Table 5-1	Varies by engine type and are often component specific. e.g. • Average material densities and yield strength • Burst pressures • Safety factors • Unit weights • Other

Table 2-6: Software comparison with REDTOP PRO (2/2)

	LiRA	REDTOP PRO (sources: [21], [29])
Components	Main combustion chamber, pump, turbine, gas generator, flow divider, injector, heat exchanger, nozzle	Chamber, pump, turbine, valve, flow divider, injector, heat exchanger, nozzle
Key Outputs	Engine thrust, Isp, weight, dimensions, power, internal pressures, temperatures and more	Engine thrust, products of combustion, Isp, weight, reliability, cost, turbo-machinery speeds & power, internal pressures, geometries & areas, and more
Engine Cycles	Pressure-fed, gas generator, staged combustion, closed expander and bleed expander	Staged-combustion, gas-generator, expander, split-expander, tap-off, and pressure-fed designs for "real life" engines
Configuration	Single pre-burner/gas generator or none	Dual pre-burner, single preburner/gas generator, catalyst pack or none
Turbine flow sequence	Parallel	Series, parallel, separate
Fluid Properties and Combustion Chemistry	Chemical equilibrium flow analysis using data tables storing combustion temperature, density, molar mass, specific heat capacity, ratio of specific heats, viscosity and conductivity as function of pressure and mixture ratio in ASCII text files created with NASA CEA (which uses minimization of Gibbs Free Energy). Fluid properties tables storing density, specific heat capacity, viscosity and conductivity in ASCII text files constructed using NASA CEA and NIST chemistry webbook, molar mass is fixed for fluid and specific heats of evaporation is fixed for reference pressure and temperature and obtained from TU Delft.	Fluid property database tied to dynamic equilibrium chemistry model; Frozen and equilibrium flow analysis via minimization of Gibbs Free Energy. Approximately 30 species available in database. Thermodynamic properties for any species considered in system are stored in an ASCII text file containing density, entropy, and enthalpy values versus temperature and pressure. Species properties in both liquid and gaseous forms are contained in the same table; property tables compiled from number of sources including JANAF.
Cycle Losses	Only pressure loss over injector, cooling channel and from gas generator to turbine inlet are taken accounted for	Detailed tracking of losses based on results of power balance and fluid flow rate requirements (e.g. gas generator drive gas, etc.), heat transfer losses, etc.
Nozzle Analysis	Corrected ideal rocket nozzle expansion theory	Rao nozzle analysis with flow divergence loss calculation
Engine Mass	Regression analysis fit equation or approximation relations with correction factors used for overall and engine component mass estimation	Component-level weight analysis using various physics-based, historical, or scaling relationships for engine parts and systems.
Engine Cost	None	Local implementation of the Liquid Rocket Engine Cost Model (LRECM) from NAFCOM. For Government customers only.
Engine Reliability	None	Top-level estimate of engine reliability and safety
Engine dimensions	Regression analysis fit equation used for overall and engine component dimension estimation	Overall length

tools are very expensive and thus often only purchased by very specialised companies; some tools even have features that can exclusively be used by the US government. These restrictions often in combination with high purchase prices have led the aerospace industry and aerospace research centres and organisations to develop their own in-house tools. However often these tools are most of the time initially only focusing on one aspect of the design, analysis or optimisation and such as thrust chamber design, or mass estimation, combustion, etc. Usually they are created by different persons over the years and have to be used parallel or in sequence when designing an engine. Attempts to merge these tools in a single tool is often desirable and attempted, however as it is time-consuming and difficult especially since knowledge tends to get lost as soon as the creator(s) of the tool leave(s) the company, this is not always successful.

Further one should note that with the exception of the in-house tools, which usually aren't available for particular use because of confidentiality, the publicly available tools, both free and commercial, don't allow for much modifications and expansion of the tool as the source code is often protected.

Concerning the tool structure, the modular approach is found back in all tools that model complete engine cycles; the recurring components found in these models are propellant tanks, pumps, turbines, gas generator, combustion chamber, nozzle, injector and heat exchanger. The component or engine cycles properties are determined using a mass, dimensioning, mass, reliability or cost model.

Therefore to meet the user requirements, the tool created in this work needs to be a single tool that is cheap, easy to understand, easy to use and easy to expand and capable of preliminary design or design (choice) verification, optimisation and sensitivity and uncertainty study.

Chapter 3

Performance Model

The performance model of LiRA has the objective to calculate the pressure, temperature, density of the propellant in the components and lines; from this the required power in the pumps and turbine will follow as well as the engine thrust and specific impulse. This calculation process is an iterative process as pressures and powers must be balanced such that the system is in equilibrium.

First the thruster (assembly of injector, main combustion chamber and nozzle, also called thrust chamber assembly (TCA)) is sized and the combustion and flow expansion properties are calculated. Next the feed system and heat exchanger calculations are performed iteratively until the the feed system is capable of sustaining itself and delivers the right amount of oxidiser and fuel at the correct amount of pressure to the thrust chamber injector. The model consists of a fluid property database, combustion thermodynamic database, engine components and balancing algorithms; the latter have as goal to find the right amount of pressure rise over the pumps needed to account for all losses and have the needed pressure in the main combustion chamber and at the same time size the turbine, and if applicable gas generator, such that the right amount of power is delivered to the pumps to realise this pressure rise. The feed system requirements follow from the thruster sizing as the thruster must be such that the right amount of thrust (which is often coupled to a change in velocity, often called 'delta v', requirement) is delivered from which a pressure and mass flow requirement follows; the feed system must then be sized such that the right amount of oxidiser and fuel is supplied at the right pressure.

As each engine cycle has many components in common, the performance modelling of each component is discussed separately prior to going into the balancing of the engine cycles. However first the use of substance property and combustion thermodynamic data tables is explained as these are called upon in the lion's share of the calculations.

3-1 Substance Property and Combustion Thermodynamic Data Tables

The model uses several pure and mixed substances in liquid or gaseous state. Substance properties like combustion temperature, molar mass, ratio of specific heats, specific heat capacity, density,

Table 3-1: Error introduced for mixture properties using linear interpolated CEA tabulated values with respect to using CEA directly

Mixture	Pressure [bar]	Mixture ratio [−]	CEA value	LiRA value	$E_{\%}$ [%]
			Combustion temperature [K]		
LOX-LH2	112	5.78	3498.30	3494.1	0.1
LOX-RP1	504	0.23	1219.61	1214.6	0.4
N2O4-MMH	13.7	31.4	865.63	867.6685	0.2
			Specific heat ratio [−]		
LOX-LH2	25	1.7	1.3010	1.3022	0.1
LOX-RP1	213	4.3	1.1332	1.1333	0.0
N2O4-MMH	374	8.6	1.2259	1.2258	0.0
			Molar mass [g/mol]		
LOX-LH2	318	9.26	17.794	17.8	0.0
LOX-RP1	0.007	3.2	22.690	22.6	0.4
N2O4-MMH	41	1.2	18.047	18.0	0.3

viscosity, conductivity vary with pressure, temperature and/or mixture ratio. Other flow properties such as Reynolds number and Prandtl number vary as well with pressure, temperature and/or mixture ratio but can be calculated from aforementioned properties. Combustion and mixture properties could be estimated when the properties of the pure substances that make the mixture are known, however this is very complex chemistry or could be obtained empirically. Pure substance properties are often determined empirically. As for the latter trustworthy data is readily available, there is no reason not to use this data. Concerning mixtures and combustion modelling a dedicated model could be created, however models using proven methods with good results are already available; these can either be integrated or in case this is difficult, output data generated for certain input ranges can be generated and stored in lookup tables.

Combustion thermodynamic data tables.

The ideal case would be to completely make a thermodynamic model that can model the combustion process the same as or similar to the NASA Chemical Equilibrium with Applications (CEA) [17] code developed by Gordon and McBride [23]. An alternative solution could be to completely integrate CEA in the model, however due to time constraints this cannot be done and the approach of using property data tables constructed using CEA has been chosen. As the data in the table is at certain pressure-mixture ratio combinations, one will need to perform a two-dimensional (linear) interpolation in order to obtain the value for a desired pressure-mixture ratio combination. The assumption and weakness here is hence that one on one hand has to trust that the NASA CEA code is accurate and precise enough for modelling reality to an extend that is acceptable by the user, and on the other that the use of tables does not lead to additional significant loss in accuracy. The latter is tested in Table 3-1 where for random pressure and mixture ratio combinations, the values of certain properties obtained using the tables and those obtained directly with CEA are compared. As can be seen from Table 3-1 the differences for these random samples are less than half a percent and thus negligible. A validation of CEA is hence desirable. The main goal of combustion modelling in LiRA is to obtain a value for the specific impulse (and from this value a thrust). When calculating the specific impulse of several real engines using the data tables constructed with NASA CEA, see Table 3-8, one can see an average overestimation of about 10%. To address this inaccuracy, the specific impulse obtained is corrected using a correction factor; therefore any inaccuracy in CEA is automatically accounted

Table 3-2: supported mixture thermodynamic properties pressure and mixture ratio ranges

Mixture	p_{min} [bar]	p_{max} [bar]	MR_{min} [−]	MR_{max} [−]
LOX-LH2	0.001	800	0.5	10
LOX-RP1	0.001	1000	0.1	60
N2O4-MMH	0.001	400	0.5	35

for the most important thrust chamber performance parameters.

Table 3-2 gives an overview of all supported mixtures and their supported mixture ratio and pressure ranges. It should be noted however that for some very low or very high pressure ranges not all data for every mixture ratio was generated and put in the tables, this is because very high pressures are usually only found in the gas generator or pre-burner which operates fuel or oxygen rich; therefore for the very high pressures only data is found at very fuel rich or very oxygen rich mixture ratios. The very low pressures are only encountered in the nozzle and as the main combustion chamber mixture is usually fuel rich, no data for oxygen rich mixtures at very low pressures was generated and put in the tables. Further for some properties like combustion temperature the available ranges are larger than others like viscosity; this is because properties like viscosity and conductivity are only needed in heat exchange in the nozzle where the pressures and mixture ratios are usually moderate and fuel rich respectively. LiRA is not capable of extrapolating data and therefore will return an error when the model attempts to request the value of a pressure and mixture ratio combination which is out of the supported range. However nor during the modelling of the many real engines in this work, nor during sensitivity analysis or optimisation LiRA has failed to lookup a value in the table which was not available, hence in practice the aforementioned 'gaps' and the range limits should not form any limitations as they are located at pressure and mixture ratio combinations that are very unlikely to occur.

Substance property data tables.

Pure substance properties are dependent on temperature and pressure and are difficult to be predicted but sources like the National Institute of Standards and Technology (NIST) chemical web-book [30] or CEA allow to obtain substance properties under certain specified conditions. Therefore the approach was chosen to create data tables for the oxidisers and fuels considered in LiRA for a wide range of pressure and temperature ranges, see Table 3-4, that can be encountered in LiRA. Attempting to look up a property value for a pressure and temperature combination that is out of range will yield an error, in practice the tables are extensive enough that one should not have this error with the exception in the heat exchanger where in some cases extreme high pressures and temperatures, that in reality would be unacceptable, in theory could occur. For LOX and LH2 the tables were created using NIST and for N2O4, MMH and RP1 the CEA tool has been used. In case the tables are not extensive enough, and thus a certain property cannot be found under the needed conditions, an error will be returned stating which property could not be found in the tables for which conditions. The tables can easily be extended by adding data generated using NIST, CEA or data originating from other sources. As the data in the table is at certain pressure-temperature combinations, one will need to perform a two-dimensional (linear) interpolation in order to obtain the value for a desired pressure-temperature combination. Unlike the combustion tables in these tables no gaps are present. The fuels have a larger range of temperatures because they can also be used as coolant while the oxidiser in LiRA can't. The loss in accuracy when using tables instead of CEA directly is assessed in Table 3-3. The error

Table 3-3: Error introduced for pure substance properties using linear interpolated CEA tabulated values with respect to using CEA directly

Substance	Pressure [bar]	Temperature [K]	CEA value	NIST value	LiRA value	$E_{\%}$ [%]
				Density [kg/m^3]		
LOX	2.4	200	-	4.6518	4.6532	0.0
LH2	43	304	-	3.3454	3.3465	0.0
MMH	124	405	72.281	-	72.3083	0.0
N2O4	168	284	218.21	-	218.3748	0.1
RP1	0.7	1047	0.11969	-	0.1202	0.4
				Specific heat capacity [kJ/kgK]		
LOX	2.4	200	-	0.92077	0.92060	0.0
LH2	43	304	-	14.432	14.431	0.0
MMH	124	405	2.2148	-	2.2183	0.2
N2O4	168	284	0.9537	-	0.9537	0.0
RP1	0.7	1047	5.6866	-	5.6569	0.5
				Viscosity [millipoise]		
LOX	2.4	200	-	0.14707	0.14752	0.3
LH2	43	304	-	0.091327	0.091322	0.0
MMH	124	405	0.16823	-	0.16823	0.2
N2O4	168	284	0.19243	-	0.19241	0.0
RP1	0.7	1047	0.22682	-	0.22662	0.1
				Conductivity [mW/cmK]		
LOX	2.4	200	-	0.18455	0.183	0.8
LH2	43	304	-	1.9099	1.910	0.0
MMH	124	405	0.6574	-	0.660	0.4
N2O4	168	284	0.2560	-	0.256	0.0
RP1	0.7	1047	4.3351	-	4.337	0.1

Table 3-4: Pure substance supported pressure and temperature ranges

Pure substance	p_{min} [bar]	p_{max} [bar]	T_{min} [K]	T_{max} [K]
LH2	0.5	220	20	1350
LOX	0.5	300	90	200
MMH	0.1	170	280	1000
N2O4	0.5	170	280	500
RP1	0.5	700	280	1200

introduced in the considered samples by using tables and interpolation is for none of the samples larger than one percent and hence can be considered negligible.

Again here LiRA relies on data from external sources (NIST and CEA), but as these are sources with a good reputation, validation is assumed to be not necessary.

3-2 Thrust Chamber

The thrust chamber is the heart of a propulsion system as it is the component which generates the thrust. In this section the performance calculations of the thrust chamber are discussed in three parts; the injector, the main combustion chamber and nozzle. A summary of the most important thrust chamber characteristics in LiRA are:

Table 3-5: Characteristic design mixture ratios given by Haidn [6] and Sutton [4] and chosen typical optimisation search ranges of model supported liquid propellant combinations

Oxidiser	Fuel	Characteristic design MR		MR optimisation search range	
		Haidn [-]	Sutton [-]	Min [-]	Max [-]
LOX	$RP1$	2.77	2.5	2.0	4.0
	LH_2	4.83	4.5-6.0	3.0	7.0
N_2O_4	MMH	2.37	-	1.5	3.0

- **component function(s)**: generate thrust
- **component modelling goal(s)**: model combustion and flow expansion
- **important assumption(s)**: fixed percentage pressure drop over injector, instantaneous chemical equilibrium, steady isentropic inviscid flow.
- **important limitation(s)**: nozzle shape options limited to conical, no engine throttling

3-2-1 Main Combustion Chamber and Nozzle

Main combustion chamber mixture ratio.

oxidiser, fuel, pressure and mixture ratio determine the start characteristics of the flow in the main combustion chamber, the thrust chamber geometry then affects how the flow further develops towards the nozzle exit. In [6] and [4] Haidn and Sutton respectively give for various typical propellant combinations, among others, the characteristic mixture ratio. The third column of Table 3-5 shows the characteristic oxidiser over fuel mixture ratios given by Haidn for the propellants supported in this model, while the fourth column of Table 3-5 gives the typical ranges for LOX/RP1 and LOX/LH2 as stated by Sutton. In case no mixture ratio in the thrust chamber is defined by the user, the characteristic mixture ratio by Haidn is assumed. However these mixture ratios are design values and should in a good design be optimised for; as one would like to have high specific impulse for efficient propellant consumption, the ranges of mixture ratio of certain propellant combination can be limited.

Considering the models of LiRA support main combustion chamber pressures as low as 10 bar (typical lower pressure for a pressure fed engine) up till pressures above 100 bar (often encountered in staged combustion cycles), it is desirable to know what the influence of the mixture ratio choice for a certain propellant combination at a given pressure on the performance is and what the ideal mixture ratio range is for pressures of this order of magnitude.

Figure 3-1, Figure 3-2 and Figure 3-3 show for various propellant combinations the relation between ideal specific impulse [1] and the mixture ratio. An area expansion ratio (A_e/A_t) of 45 has been chosen to simulate in LiRA the same conditions as Haidn. From these figures and available mixture ratio data of actual engines (see Appendix D, Table D-5), it can be concluded that typical mixture ratios are in the ranges given in the fifth and sixth column of Table 3-5.

[1] Figure 3-1 and Figure 3-2 were obtained using ideal rocket motor theory in combination with the flow thermodynamic property data tables that were constructed using CEA

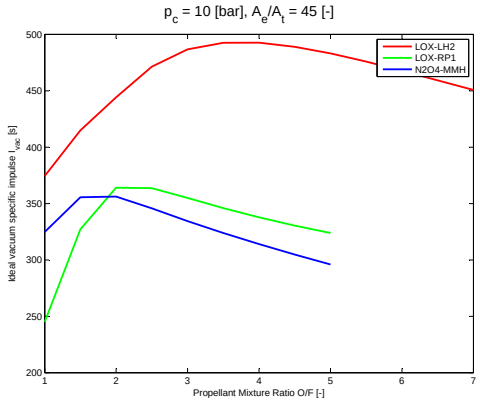

Figure 3-1: Ideal specific impulse of various propellant combinations (at $10\,\mathrm{bar}$ with $A_e/A_t = 45$) calculated with LiRA

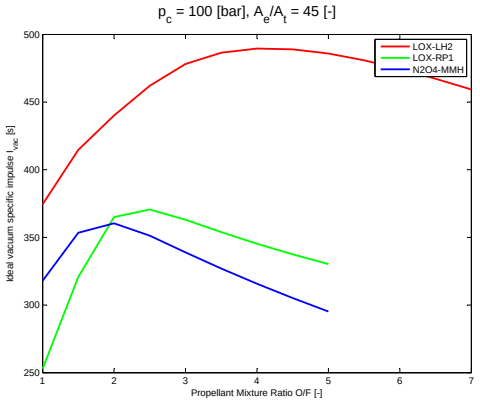

Figure 3-2: Ideal specific impulse of various propellant combinations (at $100\,\mathrm{bar}$ with $A_e/A_t = 45$) calculated with LiRA

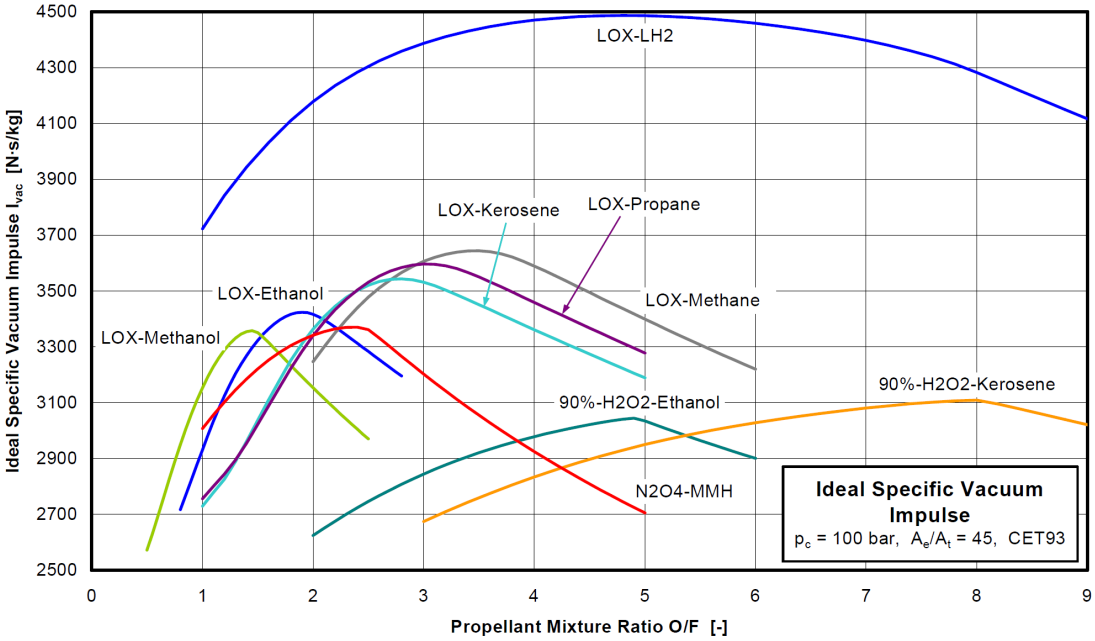

Figure 3-3: Ideal specific impulse of various propellant combinations (at $100\,\mathrm{bar}$ with $A_e/A_t = 45$) taken from Haidn [6]

The chemical equilibrium during expansion in the nozzle is modelled under the assumption that the flow in the nozzle is in chemical equilibrium. This means that there is instantaneous chemical equilibrium among all molecular species and that it is maintained under the continuously variable pressure and temperature conditions of the nozzle expansion process. A consequence is that the gas composition is different in the chamber and the nozzle exit. Sutton states that this method usually overstates the performance values, such as the characteristic velocity or specific impulse, typically by 1% to 4% [4].

Main combustion chamber combustion and flow properties.

The specific heat ratio (γ), the combustion temperature (T), the molar mass ($\hat{M}$), the density (ρ) and the specific heat capacity (c_p) for mixtures of fuel and oxidiser are obtained from data tables which have been constructed using CEA.

If the combustion process would lead to ideal gasses the specific heat capacity could be calculated using:

$$\left.\begin{aligned} \gamma &= \tfrac{c_p}{c_v} \\ R &= \tfrac{R_A}{\hat{M}} = c_p - c_v \end{aligned}\right\} c_p = \frac{\gamma}{\gamma - 1} \cdot \frac{R_A}{\hat{M}} \tag{3-1}$$

where c_p is the specific heat capacity at constant pressure, c_v is the specific heat at constant volume, (R) the specific gas constant calculated using Eq. (3-2):

$$R = \frac{R_A}{\hat{M}} \tag{3-2}$$

where the absolute gas constant (R_A) has a value of 8.314 462 1 J/molK.

The density could be calculated using the ideal gas law:

$$\rho = \frac{p}{\frac{R_A}{\hat{M}} \cdot T} \tag{3-3}$$

In order to check if the assumption of ideal gas is valid, in Table 3-7 the density and specific heat capacity are calculated, for random pressures with a typical mixture ratio, from the ideal gas relations (Eq. (3-3) and Eq. (3-1)) using the the molar mass, temperature and ratio of specific heats given by CEA; these are tabulated in Table 3-6. The obtained values are compared to the result for the density and specific heat capacity calculated by CEA. This shows that while the assumption of ideal gas leads to negligible ($< 5\%$) differences in density, significant ($> 5\%$) differences in specific heat are introduced and thus for the calculation of specific heat the gases in the combustion chamber and nozzle it was chosen to not treat the flows as ideal gases in order to not introduce additional errors in the heat exchange during regenerative cooling.

From the specific heat ratio, the value of the Van Kerckhove function Γ can be calculated:

$$\Gamma = \sqrt{\gamma} \cdot \left(\frac{2}{\gamma + 1}\right)^{\left(\frac{\gamma+1}{2\cdot(\gamma-1)}\right)} \tag{3-4}$$

The Mach number (M) at any point in the thrust chamber is found from solving the area-Mach number relation, given by Eq. (3-5), for M given the local area ratio:

$$\left(\frac{A}{A_t}\right)^2 = \frac{1}{M^2} \cdot \left[\frac{2}{\gamma + 1} \cdot \left(1 + \frac{\gamma - 1}{2} \cdot M^2\right)\right]^{\frac{\gamma+1}{\gamma-1}} \tag{3-5}$$

Table 3-6: Combustion chamber flow molar mass, temperature and ratio of specific heats calculated with CEA for given propellant combination at various pressures for a typical mixture ratio

	p [bar]	$\left(\hat{M}\right)_{\text{CEA}}$ [g/mol]	$(T)_{\text{CEA}}$ [K]	$(\gamma)_{\text{CEA}}$ [−]
LOX-LH2	1	11.3900	2900.4	1.1241
MR: 5.0	5	11.5575	3052.9	1.1355
	10	11.6335	3120.7	1.1412
	25	11.7268	3202.9	1.1490
	50	11.7905	3258.6	1.1550
MMH-N2O4	1	21.0102	2904.9	1.1254
MR: 1.9	5	21.2977	3057.5	1.1364
	10	21.4291	3126.8	1.1418
	25	21.5947	3213.1	1.1492
	50	21.7128	3274.0	1.1549
LOX-RP1	1	22.266	3087.45	1.1146
MR: 2.6	5	22.699	3299.64	1.1228
	10	22.898	3395.24	1.1265
	25	23.171	3524.59	1.1315
	50	23.385	3623.92	1.1353

Table 3-7: Error introduced in density (Eq. (3-3)), specific heat (Eq. (3-1)) and local sound velocity when assuming ideal gas in combustion chamber and nozzle

		Ideal gas result			CEA result			Percentage error		
	p [bar]	ρ [kg/m^3]	c_p [J/kgK]	a [m/s]	ρ [kg/m^3]	c_p [J/kgK]	a [m/s]	ρ [%]	c_p [%]	a [%]
LOX	1	0.0472	6612.2	1542.7	0.0472	14197	1542.7	0.0	53.43	0.0
-LH2	5	0.2277	6028.7	1579.2	0.2272	10939	1580.3	0.2	44.89	0.1
MR:	10	0.4484	5776.3	1595.4	0.4480	9677.4	1595.9	0.1	40.31	0.0
5.0	25	1.1009	5467.5	1615.3	1.1007	8292.5	1615.4	0.0	34.07	0.0
	50	2.1759	5254.8	1629.1	2.1757	7437.7	1629.2	0.0	29.35	0.0
MMH	1	0.0870	3551.5	1137.4	0.0870	7856.0	1137.8	0.0	54.79	0.0
-N2O4	5	0.4189	3252.5	1164.7	0.4177	6262.4	1166.2	0.3	48.06	0.1
MR:	10	0.8243	3124.3	1177.0	0.8233	5630.3	1178.2	0.1	44.51	0.1
1.9	25	2.0208	2965.6	1192.4	2.0199	4913.3	1193.7	0.1	39.64	0.1
	50	3.9881	4449.5	1203.3	3.9868	2855.0	1204.9	0.0	35.83	0.1
LOX	1	0.0867	3631.8	1133.6	0.0867	11680.1	1133.6	0.0	68.91	0.0
-RP1	5	0.4137	3349.1	1164.9	0.4137	9342.9	1165.0	0.0	64.150	0.0
MR:	10	0.8111	3233.5	1178.5	0.8111	8462.9	1178.5	0.0	61.79	0.0
2.6	25	1.9767	3087.6	1196.3	1.9767	7407.7	1196.3	0.0	58.32	0.0
	50	3.8806	2983.4	1209.5	3.8805	6686.2	1209.5	0.0	55.63	0.0

where A is the cross-sectional area at a certain point in the thrust chamber and A_t the throat cross-sectional area. Eq. (3-5) will yield two solutions for M, a subsonic and a supersonic Mach number; from the requirement that the flow must be subsonic before the throat and supersonic after the throat one can eliminate the none applicable solution.

The velocity that corresponds with a Mach number yields from:

$$v = M \cdot a \tag{3-6}$$

where the local speed of sound is given by:

$$a = \sqrt{\gamma \cdot R \cdot T} \tag{3-7}$$

To validate this assumption again results are compared with CEA in Table 3-7. The molar mass, temperature and ratio of specific heats for random chosen pressure and mixture ratio combinations are obtained from CEA and are tabulated in Table 3-6. These values are substituted into the ideal gas local speed of sound relation (Eq. (3-7)) and the result is compared to the speed of sound calculated with CEA. Table 3-7 clearly shows that the assumption of ideal gases does not lead to differences with the CEA code. Hence either CEA also assumes ideal gas theory which means NASA sees this as a valid assumption, or the assumption does not lead to significant reduction in accuracy; this was not further investigated as it doesn't matter for the purposes of this work.

Main combustion chamber Mach number and total conditions.

Along any point in a steady, isentropic (hence adiabatic and reversible), inviscid flow, the local temperature, local pressure and local density are a function of the specific heat ratio, local Mach number and total temperature (T_0), total pressure (p_0) or total density (ρ_0) respectively. As for these types of flows the total temperature, pressure and density remain constant along a streamline, Eq. (3-8), Eq. (3-9) and Eq. (3-10) can be used to calculate the temperature, pressure and density at any place in the nozzle:

$$\frac{T_0}{T} = 1 + \frac{\gamma - 1}{2} \cdot M^2 \tag{3-8}$$

$$\frac{p_0}{p} = \left(1 + \frac{\gamma - 1}{2} \cdot M^2\right)^{\frac{\gamma}{\gamma - 1}} \tag{3-9}$$

$$\frac{\rho_0}{\rho} = \left(1 + \frac{\gamma - 1}{2} \cdot M^2\right)^{\frac{1}{\gamma - 1}} \tag{3-10}$$

In order to solve Eq. (3-8), Eq. (3-9) and Eq. (3-10), the Mach number in the combustion chamber must be calculated or assumed. A common design choice is to take Mach numbers in the range 0.1 to 0.6 with M=0.1 being conservative as this will lead to the longest dwell time required and thus longest combustion chamber length. However Huble et al. give in [31] an empirical relation, Eq. (4-31), to estimate the contraction ratio of the combustion chamber from the throat diameter; since the nozzle throat diameter is known from the nozzle exit diameter and nozzle area ratio, the Mach number in the combustion chamber does not need to be assumed but but can be calculated by inserting the result of Eq. (4-31) back into the area-Mach number relation given by Eq. (3-5). Solving the latter equation for M then yields the Mach number in the combustion chamber (M_{mcc}).

Next using Eq. (3-6) the velocity in the combustion chamber (v_{mcc}) can be determined which then allows to find the combustion chamber's total mass flow $\dot{m}_{mcc}$ using the continuity equation:

$$\dot{m} = \rho \cdot A \cdot v \tag{3-11}$$

hence

$$\dot{m}_{mcc} = \rho_{mcc} \cdot A_{mcc} \cdot v_{mcc} \tag{3-12}$$

where the combustion chamber cross-sectional area is estimated using relation 4-31.

Having the combustion chamber Mach number, the total conditions in the combustion chamber can be found (using Eq. (3-8), Eq. (3-9) and Eq. (3-10)).

Flow expansion through nozzle.

As the nozzle exit conditions such as exit pressure, temperature or density are not known beforehand, the change in conditions in the nozzle is done step by step starting from the throat towards the nozzle exit. In other words the nozzle calculations are done by dividing the nozzle in segments (see for example Figure 3-7) and as flow properties such as heat flux vary greatly along the nozzle axis this approach is also useful for cooling calculations as will be explained in Section 3-3. According to Humble et al. when performing cooling calculations typically each tube segment is 1% to 10% of the total tube length [31]; hence with this in mind it is convenient to segment the nozzle in fragments with a length of 1% to 10% of the total nozzle divergence length even when the nozzle is not cooled.

For expander cycles where the temperature of the coolant is of major importance for the sizing of the turbine and pumps, it is suggested to use segments which are each 1% of the total length. Increasing the length of the segments can affect the temperature rise significantly as will be explained in Section 3-3, but also significantly speeds up the engine analysis. However as the engine analysis run time with 1% of the total nozzle length was found to be very lengthy during optimisation, a length of 5% was chosen as compromise for standard nozzle segmentation length.

First for each segment the Mach number is calculated using the local cross-sectional area and the specific heat ratio at the exit of the previous segment which is assumed to have not changed that much such that the error introduced by doing so in the following calculations is negligible. Then the assumption is made that the specific heat ratio and Mach number are constant over the whole segment. Having these two properties allows to calculate other properties such as pressure, temperature, density, molar mass, specific heat capacity, velocity, viscosity, conductivity and Prandtl number in the segment. The specific heat ratio for the calculations of the next segment is then found using the found pressure of the current segment. If a conical nozzle is assumed, the local cross-sectional area is calculated using the following relations (see also Figure 3-8):

$$r = \left(\frac{d_t}{2}\right) + x \cdot \tan(\alpha) \tag{3-13}$$

$$A = \pi \cdot r^2 \tag{3-14}$$

where the local cross-sectional area A follows from the local radius r which is determined by the throat diameter d_t, the distance from the throat towards the nozzle exit x and the value of the nozzle half angle α is given by Eq. (4-29).

Thrust coefficient and characteristic velocity.

Now all parameters to calculate the performance parameters thrust coefficient (C_F) and characteristic velocity (c^*) are known:

$$C_F = \Gamma \cdot \sqrt{\left(\frac{2 \cdot \gamma}{\gamma - 1}\right) \cdot \left(1 - \left(\frac{p_e}{p_{mcc}}\right)^{\frac{\gamma-1}{\gamma}}\right)} + \left(\frac{p_e}{p_{mcc}} - \frac{p_a}{p_{mcc}}\right) \cdot \frac{A_e}{A_t} \tag{3-15}$$

$$c^* = \frac{1}{\Gamma} \cdot \sqrt{\frac{R_A}{\hat{M}_{mcc}} \cdot T_{mcc}} \tag{3-16}$$

where p_a is the atmospheric pressure. Knowing the thrust coefficient and characteristic velocity allows to calculate the thrust chamber specific impulse ($(I_{sp})_{ideal}$) through:

$$(I_{sp})_{ideal} = \frac{F}{\dot{m} \cdot g_0} = \frac{C_F \cdot c^*}{g_0} \tag{3-17}$$

where g_0 is the standard gravitational constant.

Table 3-7 shows that for the combustion gases assuming ideal gas does not introduce a significant error in the calculation of the local sound velocity and thus, since the combustion chamber flow Mach number is known at this stage, Eq. (3-6) can be used to calculate the chamber velocity. Knowing the chamber flow velocity allows the calculation of the chamber mass flow using Eq. (3-12). Having the total mass flow through the combustion chamber then allows the calculation of the oxidiser and fuel mass flows at the combustion chamber injector ends which follow from using the specified mixture ratio in the combustion chamber:

$$\dot{m}_{mcc,fuel} = \frac{\dot{m}_{mcc}}{MR_{mcc} + 1} \tag{3-18}$$

$$\dot{m}_{mcc,ox} = MR_{mcc} \cdot \dot{m}_{mcc,fuel} \tag{3-19}$$

However as ideal rocket theory is used, the performance parameters C_F and c^* or $(I_{sp})_{ideal}$ are ideal parameters and must be corrected to obtain more realistic values. Instead of correcting the thrust coefficient and characteristic velocity to obtain a more realistic specific impulse, the approach has been chosen to correct directly the specific impulse instead as data on specific impulse is more readily and abundant available in literature.

The disadvantage of this approach with respect to correcting the thrust coefficient and characteristic velocity separately is that while the end result remains the same in either case, when optimizing the user loses insight in which of the two should be tuned more than the other to get to the desired specific impulse. Hence it is desirable to correct both separately from this point of view.

Validation and correction of specific impulse.

The ideal rocket engine set of equations as presented up till now are solved for different rocket engines. Two specific impulse corrections factors (ζ_s) are calculated; one for vacuum specific impulse ($(\zeta_s)_{vac}$) and the other for sea level specific impulse $(\zeta_s)_{sl}$. In Table 3-8 the obtained vacuum or sea level specific impulse is compared with the vacuum or sea level specific impulse found in literature and the required correction factor is calculated. The correction factor that

Table 3-8: Isp correction table using data from [32], [33], [4], [34], [35], [36], [37], [38] and [39]

Engine	Real $(I_{sp})_{vac}$ [s]	Calc. $(I_{sp})_{vac}$ [s]	$(\zeta_s)_{vac}$ [—]	Real $(I_{sp})_{sl}$ [s]	Calc. $(I_{sp})_{sl}$ [s]	$(\zeta_s)_{sl}$ [—]
Aestus	324	369.3	0.8774			
Aestus 2	340	396.0	0.8586			
F-1	304.8	341.8	0.8917			
H-1	292	320.6	0.9107			
HM7B	446	503.3	0.8861			
J2	424	464.5	0.9128			
J2S	436	477.0	0.9140			
LE-5	450	511.1	0.8804			
LE-7	445.6	480.4	0.9277	349.9	378.6	0.9241
RD-120	350	388.7	0.9005			
RD-170	337	365.9	0.9211	309	337.7	0.9150
RL10A-3-3A	446.4	494.2	0.9032			
RL 10B-2	462	522.9	0.8836			
RS-27	294	320.9	0.9161	257	283.7	0.9058
S-4(MA-3)	308.7	352.7	0.8753			
SSME	452.9	491.4	0.9217	363	401.4	0.9044
Vinci	465	521.1	0.8923			
Vulcain	440	479.6	0.9174	326	370.6	0.8796
Vulcain 2	429	471.7	0.9094	318	355.9	0.8936
AVG:			0.9000			0.9038
STD:			0.0192			0.0157

Calc: calculated ζ_s: specific impulse correction factor

will be used in the program is the average (AVG) of the correction factors that were found this way; hence $(\zeta_s)_{vac} = 0.9000$ and $(\zeta_s)_{sl} = 0.9038$. Both values are within range of what is found in literature; Sutton mentions a correction factor in the range of 0.8 to 0.9 [4] while Huzel has a slightly shifted range of 0.85 to 0.95 [40].

The corrected Isp is then found using

$$I_{sp} = \zeta_s \cdot (I_{sp})_{ideal} \tag{3-20}$$

where ζ_s follows from Table 3-8 and hence is taken equal to 0.9028 when dealing with vacuum and 0.9038 when the calculations are executed under sea level conditions.

Thrust.

Finally the thrust produced in the main combustion chamber then follows from:

$$F = \dot{m}_{mcc} \cdot I_{sp} \cdot g_0 \tag{3-21}$$

The momentum loss in the nozzle is accounted for through the specific impulse correction factor.

3-2-2 Injector

The fluids going into the combustion chamber are vaporized and form a low density gas mixture [11]. In case one or both of the fluids is/are first used as coolant it is likely it/they is/are already

in gaseous state when injected into the main combustion chamber. In either case the assumption is made that a gas mixture exists after the injector plate.

According to Humble et al. [31] the pressure loss over the injector face has a typical value of 20% of the chamber pressure for unthrottled engines, and 30% of the chamber pressure for throttled engines. The injectors are designed to have such high pressure drops for combustion stability reasons; the interested reader is referred to reference [11] (Zandbergen) for further explanation. Hence the propellant pressure before the injector has to be:

$$p_{inj,in} = p_{inj,out} + (\Delta p)_{inj} \tag{3-22}$$

where the pressure loss over the injector is given by

$$(\Delta p)_{inj} = \begin{cases} 0.2 \cdot p_{mcc} & \text{for unthrottled engines} \\ 0.3 \cdot p_{mcc} & \text{for throttled engines} \end{cases} \tag{3-23}$$

Though throttling is not modelled, the user has the choice of modelling the engine as it were throttled or not such that the correct pressure drop over the injector is used.

In the combustion chamber itself also a pressure loss due to flow acceleration is present; in [11] Zandbergen uses the conservation of mass to calculate the pressure drop; it leads to following relation:

$$p_{i_{out}} - p_{mcc} = \rho_{mcc} \cdot v_{mcc}^2 = \gamma_{mcc} \cdot p_{mcc} \cdot M_{mcc}^2 \tag{3-24}$$

Hence from Eq. (3-24) one can see that the pressure required just behind the injector face is directly dependent on the chamber pressure, chamber specific heat ratio and chamber flow velocity.

It is assumed that the propellants are ignited in the combustion chamber and thus just after the injector plate a mixture of two liquids, vapours or gases is present. If it is assumed no energy is lost from the system, then energy is conserved and the heat lost from one liquid or gas equals the heat gained by the other and thus the temperature of the mixture can be found using conservation of energy [41]:

$$\begin{aligned} \dot{m}_{ox} \cdot c_{p_{ox}} \cdot (T_{mix} - T_{ox}) &= \dot{m}_{fuel} \cdot c_{p_{fuel}} \cdot (T_{fuel} - T_{mix}) \\ \Rightarrow T_{mix} &= \frac{\dot{m}_{ox} \cdot c_{p_{ox}} \cdot T_{ox} + \dot{m}_{fuel} \cdot c_{p_{fuel}} \cdot T_{fuel}}{\dot{m}_{ox} \cdot c_{p_{ox}} + \dot{m}_{fuel} \cdot c_{p_{fuel}}} \end{aligned} \tag{3-25}$$

The molar mass of the mixture ($\hat{M}_m$) is found using the following relation [11]:

$$\left.\begin{aligned} \hat{M}_m &= \tfrac{n_{ox} \cdot \hat{M}_{ox} + n_{fuel} \cdot \hat{M}_{fuel}}{n_{ox} + n_{fuel}} \\ MR &= \tfrac{m_{ox}}{m_{fuel}} = \tfrac{n_{ox} \hat{M}_{ox}}{n_{fuel} \hat{M}_{fuel}} \end{aligned}\right\} \Rightarrow \hat{M}_m = \frac{\hat{M}_{fuel} \cdot (MR + 1)}{\left(\frac{\hat{M}_{fuel}}{\hat{M}_{ox}} \cdot MR\right) + 1} \tag{3-26}$$

The heat capacity of a gas mixture is given by following relation [4]:

$$c_p = \frac{\sum_i n_i \cdot c_{p_i}}{\sum_i n_i} \tag{3-27}$$

As only bi-liquid engines are considered the ratio of amount of moles (n) of oxidiser and fuel is found as follows:

$$\left.\begin{aligned} n &= \tfrac{m}{\hat{M}} \\ MR &= \tfrac{m_{ox}}{m_{fuel}} \end{aligned}\right\} \Rightarrow n_{ox} = n_{fuel} \cdot \frac{\hat{M}_{fuel}}{\hat{M}_{ox}} \cdot MR \tag{3-28}$$

where m denotes the mass of of the substance considered.

However as the propellants can also be injected as liquid or vapours, Eq. (3-27), which is only valid for gases, is not suitable and another relation should be used. Jamieson and Cartwright have proposed the following equation to obtain the heat capacity of nonaqueous mixtures [42] [2]:

$$C_{p,mix} = (w_1 \cdot C_{p,1} + w_2 \cdot C_{p,2}) \cdot (1 + \alpha + \beta) \tag{3-29}$$

where

$$\alpha = \left(0.0014 \cdot |\Delta H_1 - \Delta H_2|^{0.88} - 0.08\right) \cdot w_1 \cdot w_2 \tag{3-30}$$

$$\beta = \left(5 \times 10^{-5}\right) \cdot |\Delta H_1 - \Delta H_2| \cdot \sin\left(360 \cdot w_2\right) \tag{3-31}$$

with ΔH the heat of evaporation of each substance (see Table 3-9) and w_1 and w_2 the weight fractions of the substances. Hence:

$$w_1 = \frac{m_{ox}}{m_{ox} + m_{fuel}} = \frac{\dot{m}_{ox}}{\dot{m}_{ox} + \dot{m}_{fuel}} \tag{3-32}$$

$$w_2 = \frac{m_{fuel}}{m_{ox} + m_{fuel}} = \frac{\dot{m}_{fuel}}{\dot{m}_{ox} + \dot{m}_{fuel}} \tag{3-33}$$

To obtain the specific heat capacity Eq. (3-29) simply needs to be divided by the molar mass of the mixture obtained in Eq. (3-26):

$$c_{p,mix} = \frac{C_{p,mix}}{\hat{M}_{mix}} \tag{3-34}$$

Teja, Jamieson and Cartwright further state in [43] that from testing Eq. (3-29) for 215 nonaqueous mixtures, which resulted in a total of 1083 data points, a maximum error of 9.1%, with 95% of values lying within +-5% error range, was obtained.

According to Zandbergen [11] the velocity distribution along the combustion chamber is relatively uniform and thus the velocity right after the injector plate can be assumed to be about the same as the velocity of the flow at the end of the combustion chamber; hence:

$$v_{inj} = v_{mcc} \tag{3-35}$$

The specific heat ratio cannot be easily found; the most correct way would be to find a method to calculate the specific heat at constant volume (c_v) and divide the specific heat at constant pressure (c_p) by it as $\gamma = \frac{c_p}{c_v}$. But the main reason why one would want to know the specific heat ratio is to calculate the Mach number. However in order to calculate the Mach number after the injector plate one would need to calculate the local speed of sound. In case one would assume an ideal gas mixture after the injector plate Eq. (3-7) could be used. In that case the specific heat ratio is also found easily using ideal gas theory:

$$\left.\begin{aligned} \gamma &= \tfrac{c_p}{c_v} \\ R &= \tfrac{R_A}{\hat{M}} = c_p - c_v \end{aligned}\right\} \gamma_m = \frac{c_{p,m}}{c_{p,m} - \frac{R_A}{\hat{M}_m}} \tag{3-36}$$

The use of this equation is also suggested by Sutton [4] for the use in ideal rocket theory, but the assumption of ideal gases after the injector plate leads just as was the case in the main combustion

[2] This is the original document where the equation is derived and discussed. However as this document was not available freely on the internet a more recent paper by A.S. Teja that cites the equation and some of the accompanying discussion of the original was used. This paper is found in reference [43]

chamber, to large errors. For example the local speed of sound using Eq. (3-7) leads to high subsonic or even supersonic Mach numbers while the Mach number should be a low subsonic value. However because the Mach number and consequently also the specific heat ratio are not of interest nor of importance for further calculations, it is decided that these parameters are not calculated.

3-3 Heat Exchanger

In a rocket engine the purpose of a heat exchanger can be twofold; the thrust chamber wall gets extremely hot and needs to be cooled down such that the material limits are not reached. Several methods of cooling exist, when active cooling like regenerative cooling is applied, a liquid coolant is passed through small channels along the thrust chamber wall, the coolant gasifies in the process and hence can be used for tank pressurisation or driving turbines. In this section the heating mechanism of the heat exchanger as modelled in LiRA is explained. Important characteristics of this component can be summarised as follows:

- **component function(s)**: heat coolant to gaseous state to drive turbine(s).
- **component modelling goal(s)**: model heat exchange between thrust chamber and liquid coolant, calculate pressure loss over heat exchanger.
- **important assumption(s)**: fixed coolant velocity through channels.
- **important limitations(s)**: cooling options limited to regenerative cooling with straight cooling channels and fuel as coolant.

The model supports the following two engine cooling architectures for nozzle (including throat) and/or combustion chamber:

1. no cooling
2. regenerative cooling

Except for the option of no cooling at all, only regenerative cooling is considered as this cooling method can cause considerable pressure drops and thus is of importance for the sizing of the turbo-pumps. Further heat exchange by regenerative cooling is essential in expander cycles as the hot gases formed need to drive the turbine(s). When an engine is regeneratively cooled the coolant which is often the fuel because oxidisers at high temperatures lead to corrosion issues, is passed in cooling channels along the nozzle and/or combustion chamber before it is injected into the combustion chamber.

Other cooling methods such as dump cooling, radiative cooling, film cooling and ablative cooling are not considered because these have no or negligible effect on the overall engine sizing in the current model. Therefore thrust chamber parts that are either dump, film, ablative or radiation cooled are modelled as if 'no cooling' is present.

The cooling circuits are often only covering part of the thrust chamber and can have different orientations with respect to the thrust chamber center line. Either the cooling channels are running parallel to the center axis of the hot gas flow (see Figure 3-9) or they are running with

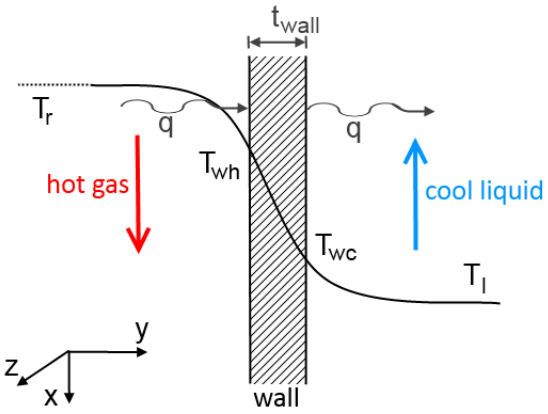

Figure 3-4: Regenerative cooling heat transfer mechanism (xy view)

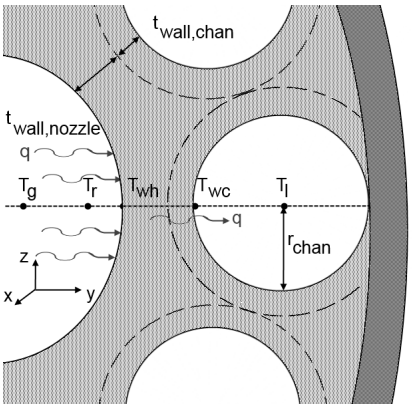

Figure 3-5: Detail view cooling channel geometry (yz view)

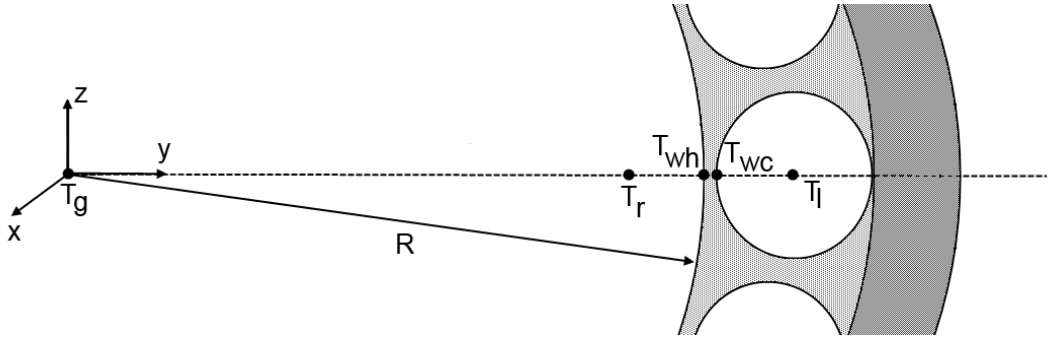

Figure 3-6: Cross section thrust chamber/nozzle with cooling channels (yz view)

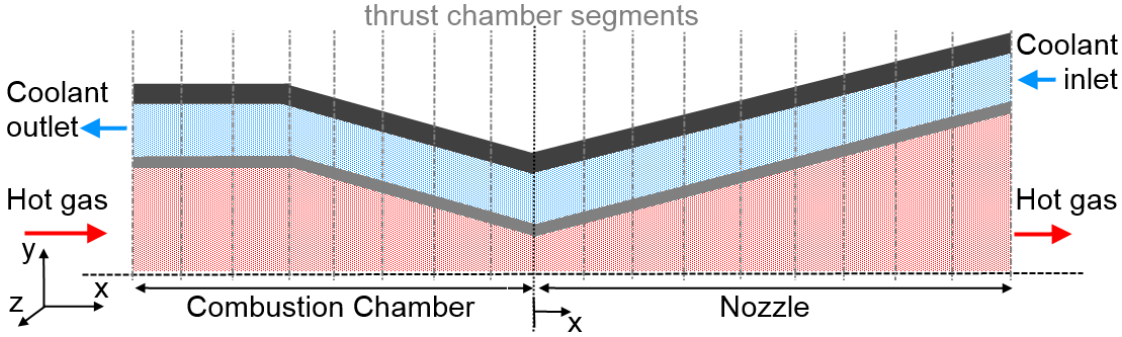

Figure 3-7: Cross section thrust chamber/nozzle with cooling channels (xy view)

an inclination with respect to the center axis of the hot gas flow and thus the coolant is spiralling around the circumference of the thrust chamber (see Figure 3-10). Because detailed modelling of the cooling channels is only making the model more restrictive as more user input and constrains would be required, only the straight circular cooling channels are considered.

3-3-1 Enthalpy and Determination of State

During the heat exchange calculations it is important to know in which state the coolant is. The enthalpy (h [J/kg]) of a substance is defined by its heat capacity (c_p [J/kgK]) and temperature (T [K]):

$$h = c_p \cdot T \tag{3-37}$$

The specific heat of vaporization (Δh_{evap} [J/kg]) is the amount of energy per kilogram of the substance, in other words increase in enthalpy, needed to transform a given quantity of this substance from the liquid to the gaseous phase. At low and moderate pressures the heat of vaporization can be assumed to be constant over the temperature ranges of interest because changes in this value are negligible. [44] While pressures in rocket engine cycles can be quite elevated, this assumption is made nevertheless because the scope of this work is not to model the heat exchange in detail. Hence the enthalpy of the substance when it is fully gaseous, at the end of boiling, is:

$$h_{\text{end boiling}} = h_{\text{start boiling}} + \Delta h_{evap} \tag{3-38}$$

To determine the enthalpy at which the substance starts boiling one must determine the boiling temperature under a certain pressure. The boiling temperature can be determined using the Clausius-Clapeyron equation [45] [46]:

$$\ln\left(\frac{p_2}{p_1}\right) = \frac{\Delta H}{R_A} \cdot \left(\frac{1}{T_1} - \frac{1}{T_2}\right) \tag{3-39}$$

Eq. (3-39) is a general equation; in case the boiling temperature at a certain pressure (usually atmospheric pressure or at 1 bar) together with the heat of vaporization[3] under that same pressure is known, Eq. (3-39) can be rewritten to find the boiling temperature at any pressure:

$$T_b = \left(\frac{1}{T_0} - \frac{R_A}{\Delta H_{evap}} \cdot \ln\left(\frac{p}{p_0}\right)\right)^{-1} \tag{3-40}$$

where T_b is the boiling temperature at a known pressure p_0 and p is the pressure in the system for which the boiling temperature is to be found. ΔH_{evap} is the heat of vaporization at pressure p_0. The boiling temperatures and specific heats of vaporization of several substances at 1 bar that have been taken from [47], [30] and [17] are listed together in [48]. The for this model relevant boiling temperatures at 1 bar and corresponding heat of vaporization are listen in Table 3-9: Note that in Table 3-9 the specific heat of vaporization (Δh_{evap}) is given, to obtain the heat of vaporization ΔH_{evap} use:

$$\Delta H_{evap} = \Delta h_{evap} \cdot \hat{M} \tag{3-41}$$

[3] the heat of vaporization (ΔH_{evap}) [J/mol] is the product of the specific heat of vaporization (Δh_{evap}) [J/kg] with the molar mass ($\hat{M}$) [kg/mol] of the substance

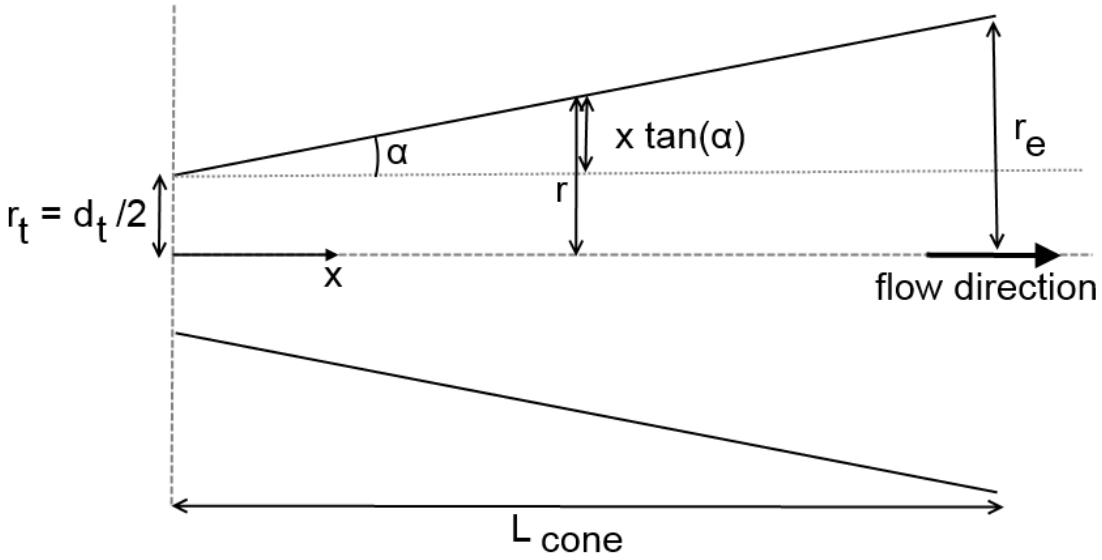

Figure 3-8: Conical nozzle

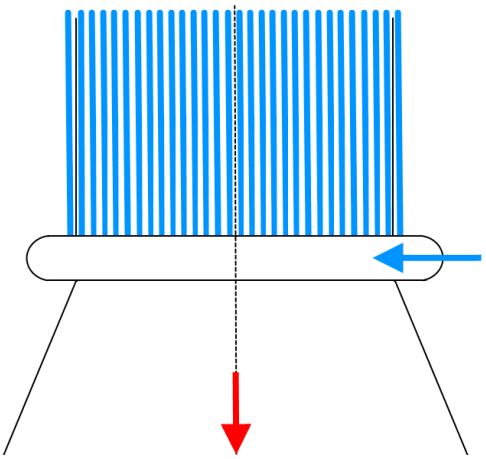

Figure 3-9: Straight cooling channels parallel to thrust chamber center axis

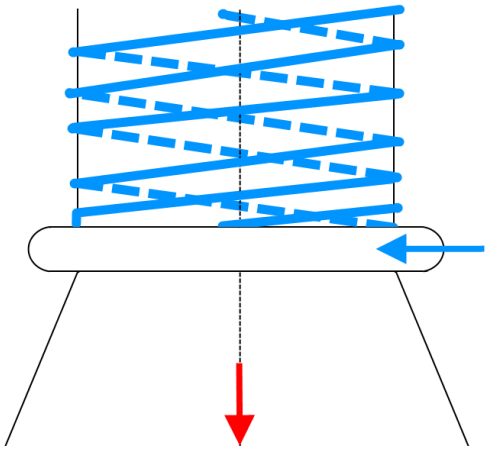

Figure 3-10: Inclined cooling channels spiralling around thrust chamber center axis

Table 3-9: Boiling temperature and specific heat of vaporization of several substances at $1\,\mathrm{bar}$ adapted from [48]

Substance	Pressure (p_0) [bar]	Boiling temperature (T_0) [K]	Specific heat of vaporization (Δh_{evap}) [kJ/kg]
N_2O_4	1	294.3	413
LOX	1	90.15	213
LH_2	1	20.25	446
$RP1$	1	489.45	246
MMH	1	360.65	709

This method was found by the author to work very well, except for hydrogen at pressures above 208 bar where the boiling temperature suddenly becomes deeply negative. This is not correct and thus a limitation of above method. It however only forms a problem for engine cycles such as the staged combustion cycle where high pressure hydrogen (for example in the heat exchanger or in the lines feeding the pre-burner) is present. Therefore as under the high pressures it is logical that for the temperatures encountered in rocket engine cycle lines the state should be liquid, it is assumed in LiRA that the state of hydrogen is liquid for any temperature when the pressure is higher than 208 bar.

Knowing the boiling temperature allows to find the enthalpy at which the substance under a given pressure will start boiling:

$$h_{\text{start boiling}} = c_p \cdot T_b \tag{3-42}$$

Now three states can be defined depending on the enthalpy of the coolant:

$$\text{state} = \begin{cases} \text{liquid} & h < h_{\text{start boiling}} \\ \text{gas-liquid} & h_{\text{start boiling}} \leq h \leq h_{\text{end boiling}} \\ \text{gas} & h > h_{\text{end boiling}} \end{cases} \tag{3-43}$$

3-3-2 Heat Transfer

The heat transfer rate from or into a substance is given by following relation:

$$Q = \dot{m} \cdot c_p \cdot \Delta T \tag{3-44}$$

Eq. (3-44) can be used to find the temperature increase over a segment. However during a phase change, boiling (vapourisation) in this case, the temperature remains constant as can be seen from Figure 3-11. Thus at the coolant side the increase in temperature is then given by:

$$T_{out} = \begin{cases} T_{in} + \frac{Q_{\text{hot gas}\rightarrow\text{coolant}}}{\dot{m}_{coolant} \cdot (c_p)_{coolant}} & h < h_{\text{start boiling}}, h > h_{\text{end boiling}} \\ T_{in} & h_{\text{start boiling}} \leq h \leq h_{\text{end boiling}} \end{cases} \tag{3-45}$$

At the hot gas side the decrease in temperature of the free stream hot gas is assumed negligible and thus not taken into account.

The heat transfer rate is the product of the heat flux with the contact area:

$$Q = q \cdot A \tag{3-46}$$

where the heat flux from the gas into the wall and from the wall into the liquid is constant (see also Figure 3-4), (full derivation see [11]) hence:

$$q = \frac{T_r - T_c}{\frac{1}{h_g} + \frac{1}{h_c} + \frac{\delta}{k}} \tag{3-47}$$

where δ is the wall thickness through which the conduction takes place and T_c the coolant temperature. According to Zandbergen [11] the reference temperature (T_r) in the combustion

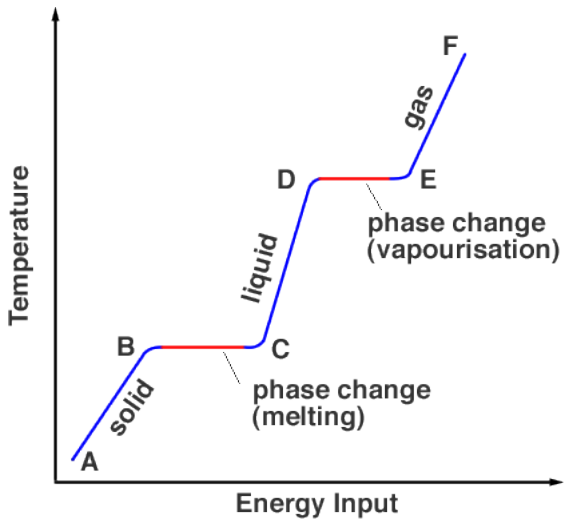

Figure 3-11: Phase change diagram. Phase changes are indicated by flat regions where heat energy is used to overcome attractive forces between molecules. [49]

chamber is typically taken equal to the combustion chamber temperature (T_{mcc}) and in the throat and nozzle to the adiabatic wall emperature (T_{aw}).:

$$T_r = \begin{cases} T_{mcc} & \text{combustion chamber cooling} \\ T_{aw} = T_{hg} \cdot \left(1 + rf \cdot \frac{\gamma-1}{2} \cdot M^2\right) & \text{throat and nozzle cooling} \end{cases} \tag{3-48}$$

with the recovery factor (rf) dependent on the Prandtl number according to [11] as follows:

$$rf = \begin{cases} Pr^{1/2} & \text{for laminar boundary layers} \\ Pr^{1/3} & \text{for turbulent boundary layers} \end{cases} \tag{3-49}$$

While the thermal conductivity is solely dependent on the material or substance, the calculation of the coefficient of convective heat transfer on the hot gas side (h_g) or coolant side (h_c) can be done by several approaches.

Here the approach by Cornelisse et al. [50] is used for the combustion chamber and nozzle cooling. The coefficient of convective heat transfer on hot gas side is then given by:

$$h_g = 1.213 \cdot a \cdot m_g^{0.8} \cdot \mu_g^{0.8} \cdot c_{p,g} \cdot Pr^{-\frac{2}{3}} \cdot d_g^{-1.8} \tag{3-50}$$

with $a = 0.023$ in the combustion chamber and $a = 0.025 - 0.028$ in the nozzle region. [50] Here $a = 0.0265$ will be taken for the calculations in the nozzle region as this value is in the middle of the range given by Cornelisse et al.

For both the throat and nozzle cooling the relation for the liquid heat transfer coefficient by Sieder-Tate states that:

$$h_c = 0.025 \cdot \frac{k}{d} \left(Re^{0.8} \cdot Pr^{0.4}\right) \cdot \left(\frac{T_c}{T_{wc}}\right) \tag{3-51}$$

Table 3-10: Best case fabrication criteria found in literature [51], [52]

Parameter	Unit	Value
Channel width (w_{chan})	[mm]	≥ 0.510
Channel height (h_{chan})	[mm]	≤ 5.100
Land thickness (w_{rib})	[mm]	≥ 0.510
Aspect ratio (h_{chan}/w_{chan})	[–]	≤ 8.000
Wall thickness (t_{wall})	[mm]	≥ 0.635

where T_{wc} is the wall temperature at coolant side and d is the (equivalent) cross-sectional diameter of the cooling channels which is the diameter that a circular cooling channel with the same area would have; as circular cooling channels are assumed in the first place the equivalent diameter and diameter of the circular cooling channels are the same. The Reynolds (Re) and Prandtl (Pr) number are given by:

$$Re = \frac{\rho \cdot v \cdot L}{\mu} \tag{3-52}$$

$$Pr = \frac{\mu \cdot c_p}{k} \tag{3-53}$$

3-3-3 Cooling Channel Geometry, Pressure Loss and Wall Material

The cooling channel geometry can have many designs, Table 3-10 gives some minimum and maximum values that follow from fabrication criteria. The thrust chamber is divided in small segments over which the heat transfer, the resulting temperature rise and pressure loss is calculated. The temperature increase is given by Eq. (3-45). The pressure drop over the channels is assumed to be in each channel equal and according to Huzel and Huang given by [53]:

$$\Delta p = f \cdot \frac{L}{d} \cdot \frac{1}{2} \cdot \rho \cdot v^2 \tag{3-54}$$

where f is a friction loss coefficient, L is the length and d the -equivalent- diameter of the cooling channel respectively. According to Sutton, the pressure drop over the cooling jacket is typically between 5% to 25% of the main combustion chamber pressure.[4]

If the cooling channels are modelled like pipes then some empirical relations stated by Zandbergen in [11] can be used to calculate the friction factor f:

- for smooth pipes with $Re < 1 \times 10^6$ Zandbergen proposes to use among others the following relationships by Poisseuille and Blasius [11]:

$$f = \begin{cases} \frac{64}{Re} & Re < 2320 \\ 0.316 \cdot \left(\frac{1}{Re}\right)^{0.25} & 2320 < Re < 2 \times 10^4 \\ 0.184 \cdot \left(\frac{1}{Re}\right)^{0.2} & 2 \times 10^4 < Re < 2 \times 10^6 \end{cases} \tag{3-55}$$

- for non-smooth pipes with $Re > 1 \times 10^6$, Zandbergen [11] proposes using the following relation by Nikuradse.

$$f = 8 \cdot \left(2.457 \cdot \log\left(3.707 \cdot \frac{1}{e/d}\right)\right)^{-2} \tag{3-56}$$

with d again the equivalent cooling channel diameter and e the height of the wall roughness; typical values of the latter parameter for several tubes according to Zandbergen [11] are:

$$e = \begin{cases} 0.0002 \times 10^{-3}\,\text{mm} & \text{aluminium} \\ 0.015 \times 10^{-3}\,\text{mm} & \text{stainless steel} \\ 0.05 \times 10^{-3}\,\text{mm} & \text{titanium} \end{cases} \tag{3-57}$$

The channel wall thickness and the nozzle inner wall thickness, assuming cylindrical channels and cylindrical nozzle segments, are found using:

$$t = f_s \cdot \frac{p}{2 \cdot (\sigma_{ult})_{\text{wall material}}} \tag{3-58}$$

where f_s is a safety factor (typically taken equal to 2 in the nozzle region [11]), p the pressure in the cylinder (hence here inside the cooling channel or inside the nozzle respectively) and σ_{ult} is the ultimate strength; in this case of the wall material. The outer nozzle wall can be of a different material then the inner wall; the required thickness of the inner wall is dependent on the pressure inside the nozzle, while the thickness of the outer wall is dependent on the pressure inside the cooling channels.

For simplicity, it is assumed that the nozzle wall thickness and the cooling channel thickness are equal to the thickness at its most critical point, the throat, and remain constant over the nozzle length, then knowing the radius of the nozzle at the throat yields the amount of cooling channels.

If no nozzle wall material is defined, Inconel 600 will be assumed. Similarly for the combustion chamber Narloy Z is taken for computations if no choice by the user has been specified. Properties of some common thrust chamber wall materials can be found in Table H-1.

Figure 3-12 gives an overview of the calculated steps performed when modelling regenerative cooling.

3-3-4 Impact of Number of Segments on Cooling Mechanism

When the amount of combustion chamber and/or nozzle segments increases, the amount of heat transfer rate per segment is smaller as the contact surface area of the segment is smaller. Since the heat flux varies rapidly along the thrust chamber wall, the heat transfer does to and thus larger segments overestimate the heat transfer and consequentially temperature rise over a single segment. This can clearly be seen in Figure 3-13 where the Vinci is taken as example; the first plot, Figure 3-13a has a coolant exit temperature of 1167 K while the second plot, Figure 3-13b has only a coolant exit temperature of 813 K. Hence sufficient small nozzle segmentation is essential for accuracy, however this will greatly impact the program execution time; in this example for the Vinci engine the program execution time is 13.9 s for 1 % segmentation while it is only 7.0 s for 5 % segmentation. This time difference might not be significant when running the simple engine analysis routine, but it will severely impact the execution time of the uncertainty and sensitivity analysis and optimisation routine as here the engine analysis routine is ran repeatedly for many times.

3-4 Gas Generator or Pre-burner

A gas generator or a pre-burner operates exactly the same and hence are a single component. The purpose of this component is to generate gas from (partial) combustion of the propellants to drive

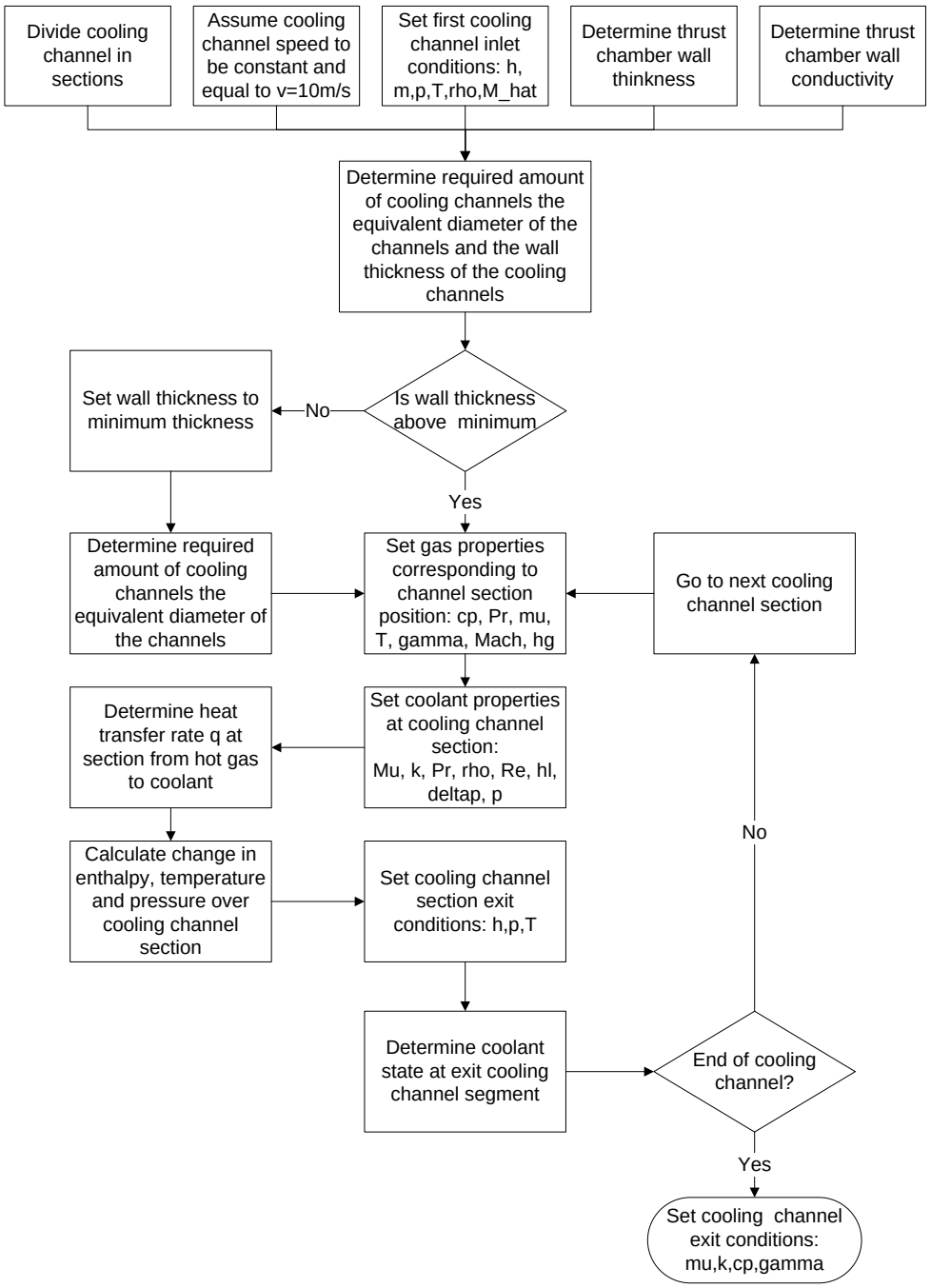

Figure 3-12: Iterative calculation scheme of cooling channels

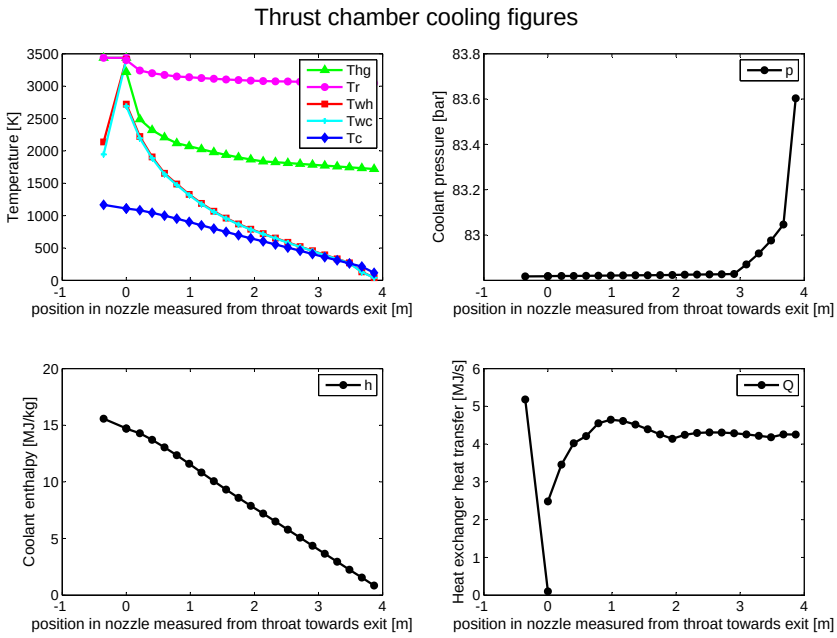

(a) With thrust chamber segments of 5 % of total length

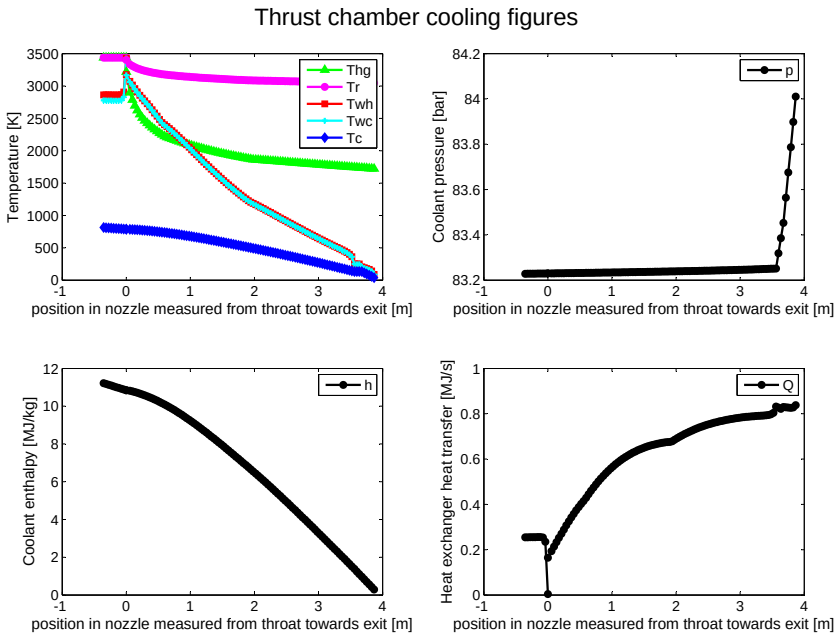

(b) With thrust chamber segments of 1 % of total length

Figure 3-13: Coolant temperature, pressure, enthalpy and heat transfer development in heat exchanger of the Vinci expander cycle engine

the turbine. The most important characteristics of the gas generator or pre-burner component are:

- **component function(s)**: generate gas to drive turbine(s)
- **component modelling goal(s)**: model combustion of propellants
- **important assumption(s)**: fixed chamber velocity of Mach 0.2, fixed percentage pressure drop over gas generator injector.
- **important limitation(s)**: amount of gas generators or pre-burners limited to a single one; this makes the modelling of full flow staged combustion impossible.

In theory a gas generator operates the same as a combustion chamber and thus one could ask oneself why a separate component is needed. The answer lies in the fact that in the main combustion chamber more properties are calculated such as flow velocity, flow viscosity, flow conductivity and Prandtl number which are of no importance for the components after the gas generator or pre-burner the way they are modelled in LiRA. Note that these properties are likely to become of importance when more detailed model of the turbine is applied.

For an open cycle the turbine exhaust is decoupled from the main flow and thus the gas generator chamber pressure is not dependent on the pressure in the main combustion chamber. In the closed cycles the flow is injected into the main combustion chamber and the turbine discharge pressure should be equal to the pressure of the main combustion chamber increased with the pressure losses along the lines to the main combustion chamber. For the gas generator (or pre-burner) it is assumed that over the gas generator injector also a pressure drop of 20% of the gas generator pressure is needed. Therefore in a gas generator cycle the average pump discharge pressure is used to estimate the gas generator pressure:

$$p_{gg} = \frac{(p_{pump,disch})_{avg}}{1.2} \tag{3-59}$$

while in a staged combustion cycle where the required pressure at turbine inlet and hence in the pre-burner is known, the required pump discharge pressure, on fuel side for a fuel rich pre-burner and on oxidiser side for a oxygen rich pre-burner, can be calculated:

$$(p_{pump,disch})_{\text{fuel side}} = 1.2 \cdot p_{gg} \tag{3-60}$$

$$(p_{pump,disch})_{\text{ox side}} = 1.2 \cdot p_{gg} \tag{3-61}$$

In some engines dedicated pumps are used to pressurise the flow that is going to the gas generator but this is not possible in the current version of LiRA. Further also no typical pressure loss over the gas generator injector was found in literature hence this component was not taken into account separately and instead is considered part of the gas generator component.

The mixture ratio in the gas generator or pre-burner is usually fuel rich [4] to minimize the production of oxygen and atomic oxygen and to obtain a lower combustion temperature, both can be devastating to the turbine components, especially combined. One exception exist when hydrocarbons such as RP-1 are used as fuel, in these engines, especially Russian staged combustion engines, a oxygen rich mixture is chosen [4] to minimize the production of carbon which can lead to clogging of the turbine components. Therefore when the user does not specify a mixture ratio, in case RP-1 was chosen as fuel, LiRA will balance the cycle using a oxygen rich mixture ratio in

the gas-generator or pre-burner. A value for the mixture ratio in the gas generator is obtained by using the desired or required turbine inlet temperature and looking up in the thermal data tables which mixture ratio corresponds with the desired temperature and the calculated gas generator pressure. If no temperature is defined a typical value needs to be assumed; this value corresponds to the maximal allowed turbine inlet temperature which is discussed in Section 3-6-5.

Having the mixture ratio, pressure, oxidiser, fuel and total mass flow required by the turbine(s) as input, the combustion temperature, ratio of specific heats, molar mass,specific heat capacity, fuel mass flow, oxidiser mass flow and density are determined and outputted by the component.

The combustion temperature, the specific heat ratio, the molar mass and specific heat capacity in the gas generator follow from the pressure and mixture ratio, and is found by using the with CEA created tables.

The fuel and oxidiser portion of the mass flow through the gas generator follows from the total mass flow and the mixture ratio in the gas generator:

$$\dot{m}_{gg_{fuel}} = \frac{\dot{m}_{gg}}{MR_{gg} + 1} \tag{3-62}$$

$$\dot{m}_{gg_{ox}} = MR_{gg} \cdot \dot{m}_{gg_{fuel}} \tag{3-63}$$

The mass flow through the pumps is then:

$$\dot{m}_{fuel} = \dot{m}_{mcc,fuel} + \dot{m}_{gg_{fuel}} \tag{3-64}$$

$$\dot{m}_{ox} = \dot{m}_{mcc,ox} + \dot{m}_{gg_{ox}} \tag{3-65}$$

While for the performance modelling in LiRA the velocity of the flow in the gas generator is of no importance, it is of importance to size the gas generator which is done in Section 4-1-6. Because a gas generator is like a combustion chamber and in Section 3-2-1 it was stated that typical chamber Mach numbers are between 0.1 and 0.6, the arbitrary design choice, within this range, of Mach 0.2 is made. This value cannot be altered by the user unless the value is directly changed in the source code.

3-5 Pump

In order to have low pressures in the storage tanks but still have high pressures in the main combustion chamber a pump is needed to increase the propellant pressure. This section discusses how the pump component is modelled and how its required power is determined. Important characteristics of the pump component can be summarised as follows:

- **component function(s)**: increase propellant pressure.
- **component modelling goal(s)**: increase propellant pressure and determine power needed to achieve this.
- **important assumption(s)**: black box modelling; among others the type of pump, number of pump stages, pump rotational speed and pump cavitation are not considered.
- **important limitations(s)**: maximum one pump per (oxidiser and fuel) side available; there is no possibility to use a boost pump.

Relations.

The pump component determines the required pump power (P_p); it does this from the mass flow ($\dot{m}$) passing the pump, the required pressure rise over the pump (Δp), the density of the propellant (ρ) and the efficiency of the pump (η_p). The type of pump is of no importance for this level of modelling.

The pump power follows from:

$$P_{p_{ox}} = \frac{1}{\eta_{p_{ox}}} \cdot \dot{m}_{ox} \cdot \frac{\Delta p_{ox}}{\rho_{ox}} \tag{3-66}$$

$$P_{p_{fuel}} = \frac{1}{\eta_{p_{fuel}}} \cdot \dot{m}_{fuel} \cdot \frac{\Delta p_{fuel}}{\rho_{fuel}} \tag{3-67}$$

where Humble et al. [31] give for the pumps following typical design efficiency values:

- oxidiser pump

$$\eta_{p,ox} = 0.80 \tag{3-68}$$

- fuel pump

$$\eta_{p,fuel} = \begin{cases} 0.75 & \text{LH2} \\ 0.80 & \text{otherwise} \end{cases} \tag{3-69}$$

The uncertainty in the pump efficiency is not addressed by Humble et al, but is estimated in Table 9-7.

Validation.

Table 3-11 gives for the A1 stage by Huzel and Huang the pressure rise over the pumps, the pump efficiency and density of the propellant; from this the estimated required pump power obtained using Eq. (3-66) and Eq. (3-67) can be compared to the values stated by Huzel and Huang. The difference is less than 1.5 percent for both pumps and thus the relationships used can be considered to be sufficient accurate for conceptual design modelling.

3-6 Turbine

When having pumps, a turbine is required to drive these pumps and therefore the required pump power determines the required turbine power. The turbine itself is driven by hot gas either created by a gas generator, or by gasified coolant. The amount of gas flow needed is dependent on the turbine power required, desired turbine inlet temperature and the possible turbine pressure ratio. All these aspects are addressed in this section. The most important characteristics about the pump component in LiRA can be summarised as follows:

- **component function(s)**: drive pumps.

Table 3-11: Validation of pump power relations (Eq. (3-66) and Eq. (3-67)) with A1 stage by Huzel and Huang [53]

	Unit	Oxidiser side	Fuel side
Propellant	[−]	LOX	RP1
Propellant density	[kg/m^3]	1143.4	808.1
Mass flow	[kg/s]	892.5	404.7
Pump pressure rise	[bar]	100.0	115.5
Pump efficiency	[−]	0.707	0.658
Real pump power	[kW]	10922	8672
Calculated pump power	[kW]	11040	8791
Percentage error ($E_{\%}$)	[%]	1.1	1.4

- **component modelling goal(s)**: determine required pressure ratio over the turbine or determine required inlet pressure for given outlet pressure and fixed pressure ratio such that enough power to the pumps is delivered.

- **important assumption(s)**: black box modelling; among others the type of turbine, number of turbine stages, turbine pitch rotational speed, turbine blade material are not considered.
- **important limitations(s)**: maximum one turbine per (oxidiser and fuel) side available, turbine arrangements are limited to geared or parallel dual shafts.

3-6-1 Turbine Power and Required Mass Flow

The turbine output power follows from [11]:

$$P_T = \eta_T \cdot m_T \cdot c_p \cdot T_{in} \cdot \left(1 - (p_{out}/p_{in})^{\frac{\gamma-1}{\gamma}}\right) \tag{3-70}$$

where the turbine output power (P_T) must equal the demanded power by the pump(s) and η_T is the turbine efficiency.

In case of a single turbine driving both pumps, the mass flow through the gas generator and turbine is the same. In case each pump is driven by a dedicated turbine, the gas produced by the gas generator is divided over the turbines, in this case the sum of the mass flow through the oxidiser turbine and the fuel turbine must be equal to the mass flow through the gas generator.

Hence for one turbine:

$$m_{gg} = m_T \tag{3-71}$$

where

$$m_T = \frac{P_T}{\eta_T \cdot c_p \cdot T_{in} \cdot \left(1 - (p_{out}/p_{in})^{\frac{\gamma-1}{\gamma}}\right)} \tag{3-72}$$

with

$$P_T = \frac{1}{\eta_m}\left(P_{p,ox} + P_{p,fuel}\right) \tag{3-73}$$

where η_m is the mechanical efficiency of the power transfer of the turbine to the pump.

For two turbines the mass flow through the gas generator is:

$$m_{gg} = m_{T_{ox}} + m_{T_{fuel}} \tag{3-74}$$

where:

$$m_{T_{ox}} = \frac{P_{T,ox}}{\eta_{T_{ox}} \cdot c_p \cdot T_{in} \cdot \left(1 - (p_{out}/p_{in})_{ox}^{\frac{\gamma-1}{\gamma}}\right)} \tag{3-75}$$

$$m_{T_{fuel}} = \frac{P_{T,fuel}}{\eta_{T_{fuel}} \cdot c_p \cdot T_{in} \cdot \left(1 - (p_{out}/p_{in})_{fuel}^{\frac{\gamma-1}{\gamma}}\right)} \tag{3-76}$$

with

$$P_{T,ox} = \frac{1}{\eta_m} \cdot P_{p,ox} \tag{3-77}$$

$$P_{T,fuel} = \frac{1}{\eta_m} \cdot P_{p,fuel} \tag{3-78}$$

3-6-2 Turbine Efficiency

Humble et al. [31] give for turbines a typical design efficiency value of 70%. For a geared Turbo-Pump Assembly (TPA), the gearbox leads to an additional power loss between the turbine output and the pump, to account for this loss the mechanical efficiency η_m is used. In case no gearbox is present there will still be a small loss in the bearings and shaft connecting pump and turbine, however this loss will be assumed to be negligible. Walsh and Fletcher state in [54] that gas turbine gearboxes have at design operating point an efficiency between 97.5% and 99%. At off-design conditions however this efficiency can reduce to 65%. [54] When the user does not define a turbine and/or mechanical efficiency the following values will be used:

- mechanical efficiency

$$\eta_m = \begin{cases} 0.975 & \text{geared turbo-pump assembly} \\ 1 & \text{direct drive, dual shafts turbo-pump assembly} \end{cases} \tag{3-79}$$

- turbine efficiency:

$$\eta_T = 0.7 \tag{3-80}$$

The uncertainty in turbine efficiency values is not addressed by Humble et al, but is estimated using real engine data in Table 9-7.

3-6-3 Turbine Pressure Ratio

If the pressure ratio $(\frac{p_{in}}{p_{out}})$ over the turbine is not defined by the user, typical design values given by Humble et al. will be used [31].

- in case one turbine drives both oxidiser and fuel pump:

$$\frac{p_{in}}{p_{out}} = 20 \tag{3-81}$$

- in the case each pump is driven by a separate turbine then for the oxidiser turbine:

$$\frac{p_{in}}{p_{out}} = \begin{cases} 2.5 & \text{LOX} \\ 20 & \text{otherwise} \end{cases} \tag{3-82}$$

similarly for the fuel turbine:

$$\frac{p_{in}}{p_{out}} = \begin{cases} 8.0 & \text{LH2} \\ 20 & \text{otherwise} \end{cases} \tag{3-83}$$

These values are design values that should be used only for first order estimates; for a good design the turbine ratio should be part of an engine optimisation.

Currently in LiRA either a single turbine is driving both pumps through a gear system or each pump has a dedicated turbine. As LiRA is currently also not capable of modelling turbines in series two turbines are always modelled as dual shaft parallel turbines (see Figure 4-2). As a single gas generator (or pre-burner) or hot gas tap-off of the heat exchanger is feeding both turbines, it is assumed that the flow is delivered under the same conditions (pressure, temperature) at both turbines. In closed systems the additional requirement that also the same conditions at the outlet are needed is assumed; hence the inlet pressure, inlet temperature and pressure ratio of two turbines must be the same and the only difference in power delivered can come from the amount of mass flow going through the turbine.

3-6-4 Turbine Functioning within Cycle

If no number of turbines is specified by the user, two turbines will be assumed. The functioning of the turbine itself is fairly simple; it is modelled more or less as a black box as the type of turbine and its components are of no importance for the level of modelling. The turbine component takes the inlet temperature, inlet pressure, required pump power, turbine efficiency and mechanical efficiency, oxidiser, fuel and mixture ratio as input; in the expander cycles where only fuel is driving the turbine no oxidiser and mixture ratio is needed. From these parameters the turbine component calculates the specific heat ratio and specific heat capacity of the flow at the inlet, turbine power, required turbine mass flow, turbine outlet pressure, outlet temperature, outlet density, outlet molar mass and outlet specific heat capacity.

3-6-5 Turbine Inlet Temperature

Figure 3-14 shows some allowable maximum temperature and flow velocity combinations for different turbine blade materials; depending on which source is cited design temperatures for uncooled turbine blades are typically in the range of $900\,\text{K} - 1350\,\text{K}$ [4] while a maximum of $1100\,\text{K}$ is given by [31]. While in [7] using $1000\,\text{K}$ is suggested as design upper limit of uncooled blades. Huzel and Huang state in [53] that the gas generator usually produces gas at a temperature between $900\,\text{K}$ and $1200\,\text{K}$. It follows from Figure 3-14 that a design inlet temperature of

maximum 800 K should be taken when advanced materials (because of for example cost reasons) cannot be used. This temperature also allows for higher mean pitch-line velocities, resulting in more efficient turbines. [31] These temperature restrictions have an impact on the gas generator in the generator and staged combustion cycles and on the heat exchanger in expander cycles.

LOX-LH2 operating engines are always fuel rich in the gas generator as aforementioned turbine inlet temperature can only be obtained with such mixture ratios as can be seen from Figure 3-15a. However as stated earlier, Russian staged combustion cycles that run LOX and a hydrocarbon are usually oxygen rich in the gas generator and thus have no problem having temperatures as low as 800 K as can be seen from Figure 3-15b, American staged combustion engines running a LOX-hydrocarbon gas generators are usually fuel rich and are observed to have a higher gas generator combustion temperature due to the much lower mixture ratios that are required to reach such low temperatures. With fuel rich mixtures temperatures below 1000 K are practically impossible to obtain for LOX-RP1. Figure 3-15c shows that with fuel rich N2O4-MMH mixtures it is difficult to get to temperatures below 1300 K and hence turbine cooling will be required. Therefore when the user does not specify a maximum allowable turbine inlet temperature and/or a gas generator mixture type, it is suggested that gas generators have a suggested combustion temperature value of 1000 K and that the mixture is suggested to be fuel rich for LOX-LH2 combinations and oxygen rich for hydrocarbon combinations such as 'N2O4-MMH and RP1'.

For expander cycles the temperature upper limit is set to 1350 K, if this temperature is exceeded an warning to the user will be returned.

Hence in summary, the suggested design turbine inlet temperature is:

$$T_{in} = 1000\,\mathrm{K} \tag{3-84}$$

which is suggested to be obtained using a fuel rich mixture in the gas generator when the engine runs on LOX-LH2 and a oxygen rich mixture ratio when using the LOX-RP1 or N2O4-MMH combination. For a good design practice, the turbine inlet temperature should be part of the optimisation process.

3-7 Propellant Tanks

The propellant tanks have the function to store the oxidiser and fuel under the right conditions for use in the engine cycle. The pressure is a very important factor for the tank mass as will be explained later in the mass model. For LiRA the most important characteristics of the propellant tanks are:

- **component function(s)**: store propellants under sufficient pressure.
- **component modelling goal(s)**: determine tank pressure and temperature.
- **important assumption(s)**: pressure and temperature in tanks remain constant.
- **important limitations(s)**: currently only the option of a single fuel and a single oxidiser tank in an engine cycle is possible.

Table 3-12: Typical tank storage temperature

Substance	Storage temperature [K]
LH2	20.27
LOX	90.17
MMH	300
N2O4	300
RP1	300

Tank pressure.

Once the thruster has been sized the injector inlet pressure ($p_{inj,inlet}$) is known and the required pressure in tanks or after the pump can be estimated. Because LiRA currently is only considering steady state systems, it is assumed that the pressure in the tanks is constant.

For pressurised feed systems the propellant tanks typically operate at an average pressure between 1.3 MPa and 9 MPa [4]; the required pressure is estimated using Eq. (3-85):

$$MEOP_{\text{propellant tank}} = p_{inj,inlet} + \Delta p_{losses} \tag{3-85}$$

where the pressure losses (Δp_{losses}) in the current model can only come from losses over the heat exchanger. Once the pressure losses are known the pressure in the tank is iteratively corrected when balancing the feed system.

Similarly for turbo-pump fed systems, once a tank pressure is defined or assumed, the required pressure rise over the pumps can be estimated using Eq. (3-86). This estimate does not take into account any pressure losses between the tanks or pumps and the injector but allow for a first design iteration. For turbo-pump fed systems it is only necessary to pressurize the propellant tanks slightly (in order to suppress pump cavitation [4]); average values are found between 0.07 MPa and 0.34 MPa [4]. Based on these ranges, if no pressure in the tanks is defined by the user a pressure of 3 bar for turbo-pump fed systems will be assumed.

Tank temperature.

In case the user does not define a temperature for the oxidiser or fuel tank, a typical value, given in Table 3-12, is assumed. For cryogenic substances the boiling point value is taken while for storable substances 300 K, which is about room temperature, is assumed.

3-8 Pressurant Tank

The pressurant tank stores a gas under very high pressure which is injected in the propellant tanks in order to force propellant out under a desired pressure. In LiRA a single pressurant tank always pressurises both oxidiser and fuel tank. Currently no other options alike separate tanks, or tank pressurisation by gas tap-off is possible. Important characterisitcs about the pressurant tank component in LiRA are:

- **component function(s)**: store pressurant.

- **component modelling goal(s)**: determine pressurant pressure and temperature

- **important assumption(s)**: constant temperature
- **important limitations(s)**: single pressurant tank for pressurisation of both oxidiser and fuel tanks with no option to not pressure one of them.

If the initial pressure and temperature are not defined by the user, typical values will be used. A typical pressurant which is often used is helium with a typical initial pressurant pressure and temperature of 400 bar and 300 K respectively; these values follow from personal experience during an internship in Astrium.

3-9 Feed Lines

The feed lines are the lines connecting the components and thus transport the propellants through the cycles. Currently in LiRA the lines are not modelled physically in the sense that they are a real component and have a certain length and make changes, such as pressure loss or temperature change, to the flow going through them. They are theoretical schematic lines and are used to store information on how the flow left the component where they originate from and thus at which conditions the flow is delivered to the component were the line ends into. The most important characteristics of the feed lines in LiRA can be summarised as follows:

- **component function(s)**: transport flows between components.

- **component modelling goal(s)**: store flow conditions at component in-and-outlets.

- **important assumption(s)**: no pressure losses, no temperature changes.

- **important limitations(s)**: not a physical component that interacts with the flow.

Pressure in lines.

The pressure in the line directly after the propellant tank is assumed to be equal to the Maximum Expected Operating Pressure in the tank itself. Pressure losses in the lines themselves are not considered. The flow inside the lines is assumed to be isentropic; this means that no heat is added to the flow and no energy transformations occur due to friction or dissipation.

Hence in the case of a pressure fed system the pressure at the injector oxidiser side is equal to the Maximum Expected Operating Pressure of the oxidiser tank, and analogous the pressure at the fuel side injector inlet is equal to the Maximum Expected Operating Pressure of the fuel tank. In case of the presence of pumps this means the pressure at the pump inlet is equal to the maximum pressure of the propellant tank that is feeding them.

The pressure after a pump at its outlet is simply calculated by adding the pressure rise over the pump to the pressure at the pump inlet. The required pressure rise (Δp) follows from using Eq. (3-86).

$$(\Delta p)_{\mathrm{p}} = p_{p,disch} - p_{MEOP_{\text{propellant tank}\rightarrow\text{pump}}} \tag{3-86}$$

where $p_{p,disch}$ is the sum of the combustion chamber pressure and all the pressure losses or differences up till the pump; losses considered are the pressure loss from injector face to main combustion chamber, the pressure ratio needed over the injector, the pressure ratio over the turbine in closed cycles and the pressure loss over the heat exchanger if applicable.

However the required pressure rise over the pump is not know yet at this point and is to be found using the balancing (iteration) schemes represented in Figure 5-3, Figure 5-5, Figure 5-7 and Figure 5-9. As estimate for the first iteration, the pump discharge pressure is assumed to be equal to the injector inlet pressure, hence from Eq. (3-86) then follows:

$$\begin{aligned} p_{\text{ox. pump,disch}} &= p_{inj,inlet} \\ &\Rightarrow (\Delta p)_{\text{ox. pump}} = p_{inj,inlet} - p_{MEOP_{\text{ox. tank}}} \end{aligned} \tag{3-87}$$

$$\begin{aligned} p_{\text{fuel pump,disch}} &= p_{inj,inlet} \\ &\Rightarrow (\Delta p)_{\text{fuel pump}} = p_{inj,inlet} - p_{MEOP_{\text{fuel tank}}} \end{aligned} \tag{3-88}$$

this estimate will be, if necessary, iteratively corrected when balancing the feed system.

Temperature in lines.

Just as the pressure, it is assumed that the temperature in the line directly after the propellant tank is equal to the propellant temperature inside the tank. No heat is added to the flow, and no energy transformations occur due to friction or dissipative effects, hence up till the injector on oxidiser side and up till the cooling channels on fuel side in case of a pressure fed system, the temperature remains constant. For turbo-pump fed systems it is assumed that the change in temperature of the liquid over the pump is negligible and thus the liquid exits the pump at the same temperature as it has entered.

Molar mass.

In the feed lines the molar mass is of importance to determine the state of the flow under certain pressure and temperature; see Eq. (3-41) in the next section. The molar mass of a pure substance remains constant and is the sum of the mass of the atoms that form the molecule. Eq. (3-89) gives an overview of the molar masses of substances that are used in the model.

$$\hat{M} = \begin{cases} 31.998\,\text{g/mol} & LOX \\ 92.01\,\text{g/mol} & N2O4 \\ 2.015\,88\,\text{g/mol} & LH2 \\ 46.0717\,\text{g/mol} & MMH \\ 198.2158\,\text{g/mol} & RP1 \end{cases} \tag{3-89}$$

Specific heat, density, viscosity and conductivity.

The specific heat, density, viscosity and conductivity of the substances will be assumed constant as long as the propellant is liquid (see Table 3-13). This because in liquid state these properties are fairly pressure independent. As soon as the propellant vaporizes and becomes a gas the corresponding values will be read from tables containing these properties for several pressure and temperatures.

Table 3-13: Specific heat, density viscosity and conductivity of several substances at standard conditions (298 K, 1 bar) unless noted otherwise [48]

Substance	Mass density (ρ) [kg/m^3]	Specific heat capacity (c_p) [kJ/kgK]	Dynamic viscosity (μ) [cp]	Thermal conductivity (k) [W/mK]
N_2O_4	1450 @ 293.15 K	1.27 @ 300 K	0.423 @ 293 K	0.131
LOX	1140 @ 90.3 K	1.68 @ 65 K	0.19 @ 90 K	0.149
LH_2	70.9 @ 20.5 K	7.32 @ 14 K	0.013 @ 20 K	0.117
$RP1$	773 @ 298.15 K	1.89 @ 298 K	0.75 @ 289 K	0.137
MMH	874 @ 298.15 K	2.89 @ 293 K	0.855 @ 293 K	0.246

The check to see if a substance is in liquid or gaseous or liquid-gaseous (boiling) state is performed using the method explained for the heat exchanger in Section 3-3.

3-10 Additional Performance Parameters Calculated

When sizing a propulsion system, the design must be such that it can deliver a certain change in velocity to the vehicle of which it is part. Further the ratio of thrust to weight determines the maximum achievable acceleration of the rocket. The requirements of change and velocity and acceleration usually come from a mission design and trajectory model. As these are propulsion system requirements, they are important for the design and hence optimisation of a propulsion system and thus shortly discussed in this section.

Change in velocity (Δv).

When the specific impulse is known and both the total (propulsion system) dry mass and wet mass, the latter two follow from the mass model discussed in Section 4-2, the change in velocity (Δv) value can be calculated using Tsiolkovsky's ideal rocket equation [31]:

$$\Delta v = v_e \ln\left(\frac{m_i}{m_f}\right) - g_0 \cdot t_b \tag{3-90}$$

where m_i is the initial total mass (hence wet mass) and m_f the final total mass (hence dry mass). The effective exhaust velocity (v_e) is the product of the specific impulse with the constant gravitational acceleration [31]:

$$v_e = Isp \cdot g_0 \tag{3-91}$$

Thrust-to-weight ratio.

Another useful parameter to compare engines is the thrust-to-weight ratio (F/W) which is simply thrust delivered by a system divided by its weight [31]:

$$F/W = \frac{F}{m \cdot g_0} \tag{3-92}$$

3-11 Validity of Performance Model

The performance model uses mainly ideal rocket motor theory which is corrected using correction factors that are obtained by calibration. The uncertainty introduced in the results found with the performance model due to uncertainty in the value of these correction factors should be subject of a sensitivity and uncertainty analysis as one is performed in Section 9-5.

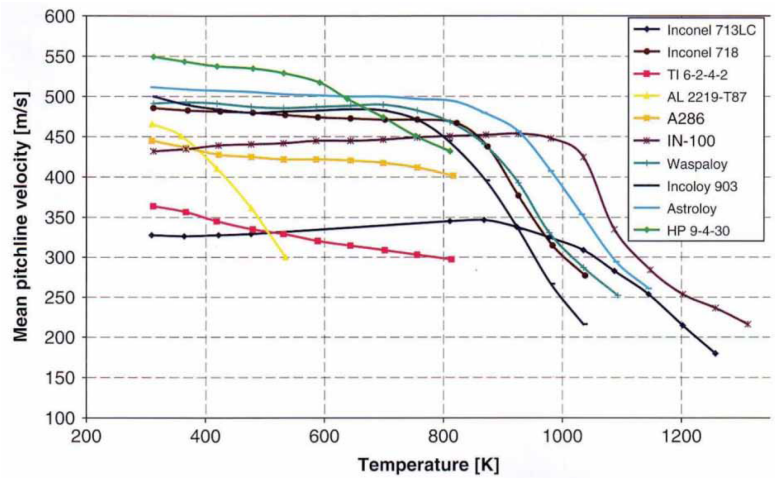

Figure 3-14: Temperature dependence of turbine materials [55]

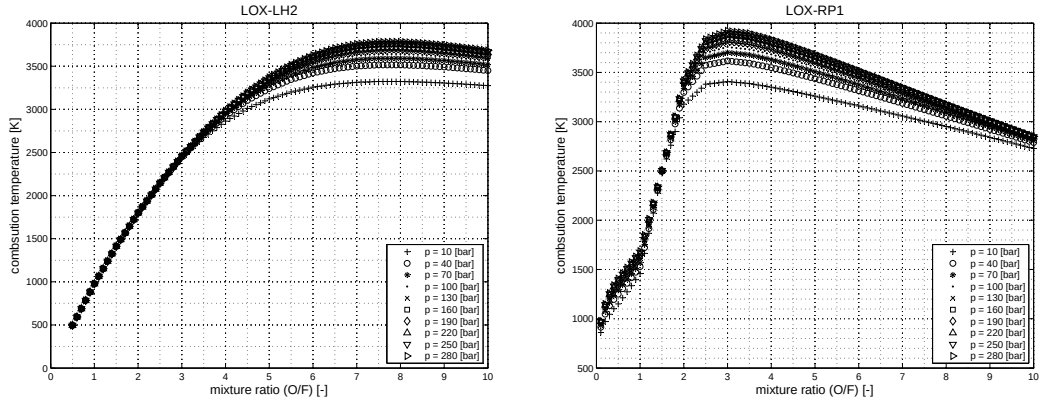

(a) LOX-LH2 **(b)** LOX-RP1

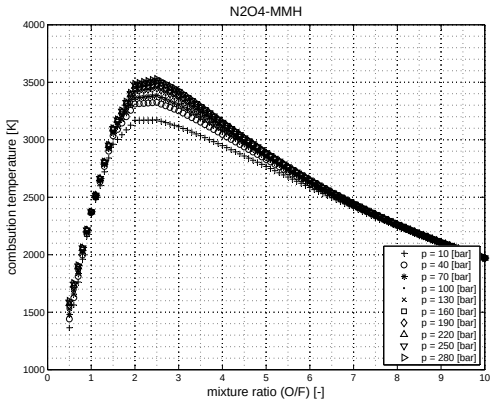

(c) N2O4-MMH

Figure 3-15: Combustion temperature relation with mixture ratio for LOX-LH2, LOX-RP1 and N2O4-MMH following from LiRA's thermodynamic tables

Chapter 4

Mass and Size Model

For propulsion system design the mass and dimensions of the system are important design constraints and therefore need to be included in the program in order to be able to optimise a propulsion system later on. For the mass and sizing simple, often empirical, relations are used. The challenge of this work is not to find relations but how to incorporate them and get meaningful output that can be used for optimisation purposes.

4-1 Size Model

In order to size a space vehicle one needs to know the size or envelope of the propulsion system; this is important for optimisation. The dimensioning model of LiRA estimates engine volume and tank volumes which together yield a total propulsion system volume estimate. Components such as nozzle, combustion chamber, gas generator and turbo-pump are also sized individually, however these estimates are not used for the total propulsion system volume estimate as they are considered part of the engine volume estimation relation used; an engine volume envelope is more than just the addition of the volume of individual components. Using this method, only the overall engine size and the propellant and pressurant tank volumes are of major importance. In this section all dimensioning related equations and methods are given, when an empirical relation is used also a small validation is performed to assess its accuracy.

4-1-1 Overall Engine Size

Relations.

In [56] Zandbergen has created for turbo-pump fed engines several empirical engine sizing relations based on actual engine dimension data. The two relations with the highest coefficient of

Table 4-1: Validation of relations 4-1, 4-2, 4-3 and 4-4

					Real		Calculated		$E_{\%}$	
Engine	Type	F	N	A_e/A_t	L	d	L	d	L	d
		[kN]	[−]	[−]	[m]	[m]	[m]	[m]	[%]	[%]
Aestus	pf	27.5	1	84	2.195	1.263	2.073	1.373	5.6	8.7
AJ10-118K	pf	43.4	1	65	2.69	1.7	2.754	1.754	2.4	3.2
Vulcain	tp	1025	1	45	3.1	2.5	2.442	2.051	21.2	18.0
HM7B	tp	62.2	1	82.9	2.01	0.992	1.345	1.092	33.1	10.1
J2	tp	1023	1	27.5	3.38	2.05	2.376	1.873	29.7	8.7
LE-5	tp	103	1	140	2.7	1.65	1.550	1.375	42.6	16.7
LE-5A	tp	121.5	1	130	2.668	1.625	1.602	1.417	39.9	12.8
LE-7	tp	1080	1	52	3.2	2.57	2.491	2.136	22.2	16.9
RL10-3-3A	tp	73.4	1	240	1.78	1	1.480	1.388	16.9	38.8
RL10-B-2	tp	110	1	285	4.153	2.223	1.636	1.595	60.6	28.3
SSME	tp	2278	1	77.5	4.24	2.39	3.012	2.801	29.0	17.2
vulcain 2	tp	1350	1	60	3.6	2.15	2.640	2.326	26.7	8.2
H-1	tp	945.4	1	45	2.67	1.24	2.398	2.008	10.2	61.9
RD-120	tp	833.6	1	106.7	3.872	1.954	2.445	2.276	36.9	16.5
RS-27	tp	1023	1	12	3.77	1.69	2.270	1.608	39.8	4.9
Aestus II	tp	55.4	1	300	2.286	1.3	1.406	1.342	38.5	3.2
S-4(MA-3)	tp	364	1	25	2.41	1.22	1.873	1.399	22.3	14.7

pf: pressure fed tp: turbo-pump fed

determination, Eq. (4-1) and Eq. (4-2) have been implemented into the model:

$$L = 0.088 \cdot F^{0.255} \cdot N^{-0.40} \cdot (A_e/A_t)^{0.055} \tag{4-1}$$

$$d = 0.026 \cdot F^{0.265} \cdot N^{0.150} \cdot (A_e/A_t)^{0.184} \tag{4-2}$$

where F denotes the thrust, N the number of thrusters and A_e/A_t the expansion ratio respectively.

For pressure fed engines Eq. (4-3) and Eq. (4-4) were established based on pressure-fed rocket engines found in literature. App.F explains how the relations were obtained.

$$L = 1.4921 \cdot \ln(F_{vac}) - 13.179 \tag{4-3}$$

$$d = 0.8364 \cdot \ln(F_{vac}) - 7.1771 \tag{4-4}$$

Again the length and diameter of these engines are the length and diameter of the smallest cylindrical-shaped enclosure that contains the turbo-pump completely.

Validation.

In order to test these relations the length and diameters of several engines using their actual vacuum thrust, number of engines and nozzle area ratio is performed in Table 4-1.

4-1-2 Propellant and Propellant Tank Volume

Humble et al. identify four components of which the tank volume is constructed: [31]

1. Usable propellant volume (V_{pu})
   The theoretical amount of propellant needed to fulfil the burn time
   $$V_{pu} = \frac{m_{prop}}{\rho_{prop}} \tag{4-5}$$
2. Ullage volume (V_{ull})
   This is usually 1% to 3% of the total tank volume. A worst case of 3% will be assumed for the typical case:
   $$V_{ull} = 0.03 \cdot V_{tank,prop} \tag{4-6}$$
3. Boil-off volume (V_{bo})
   This volume is necessary in cryogenic tanks. However this volume will be standard ignored as no general data is available, however the user will still be prompted to give a value.
4. Trapped volume (V_{trap})
   The volume of unusable propellant left in feed lines, valves, tanks and other components after engine shut-down. Sutton defines the expulsion efficiency of a tank and/or propellant piping system as the amount of propellant expelled or available divided by the total amount of propellant initially present; he gives for this efficiency typical values of 97% to 99.7%. [4] Hence on average 1.65% of the total propellant volume is trapped; this value will be assumed for the typical case.

Hence

$$V_{tank,prop} = V_{pu} + V_{ull} = V_{pu} + 0.03 \cdot V_{tank,prop} \Rightarrow V_{tank,prop} = \frac{V_{pu}}{0.97} \tag{4-7}$$

4-1-3 Pressurant and Pressurant Tank Volume

Humble et al. [31] suggest the following method to determine the required pressurant mass, pressurant volume and pressurant tank volume:
The required pressurant mass m_{press} can be determined with the ideal gas law:

$$m_{press} = \frac{V_{press} \cdot p_f}{Z_f \cdot R \cdot T_f} \tag{4-8}$$

with

$$T_f = T_i \cdot \left(\frac{p_f}{p_i}\right)^{\frac{n-1}{n}} \tag{4-9}$$

where Z is a compressibility factor and n is the polytropic index. The latter is:

$$n = \begin{cases} 1 & \text{for an isothermal process (constant temperature)} \\ 1 < n < \gamma & \text{for a quasi-adiabatic process (heat loss is greater than the heat added)} \\ \gamma & \text{for an isentropic process (no heat transfer)} \end{cases}$$

Since for long thrust durations there is insufficient time for heat to transfer from the environment/tanks into the propellant, the propellant will cool down, hence, $n = 1$ is practically not

Table 4-2: Values of A, B, C, D and E in Eq. (4-10) for helium and nitrogen as stated in the NIST chemistry webbook [30]

Pressurant	A	B	C	D	E
He	20.78603	4.850638e-10	-1.582916e-10	1.525102e-11	3.196347e-11
N_2	28.98641	1.853978	-9.647459	16.63537	0.000117

possible. On the other hand a certain amount of heat transfer will take place hence assuming a purely isentropic process, where n is hence equal to γ is also wrong. In reality the process is best modelled as a quasi-adiabatic process where the heat loss during expansion is greater than the heat added to the gas from the environment; thus n having a value between 1 and γ. As no logical method to find a value for n between 1 and *gamma* was found, the choice is made to assume isothermal conditions. The impact of making this assumption and the value of n should be studied, but is not considered important enough for the current scope of LiRA as for comparative purposes the same error is present in each case and does not affect the outcome.

In case the user decides or LiRA is modified to model the tank pressure drop as a quasi-adiabatic or isentropic process, the value of γ can calculated from the molar heat capacity and molar mass of the pressurant combined with Eq. (3-36) and Eq. (3-34). The molar heat capacity can be found using following relation given by NIST [30]:

$$Cp = A + B \cdot t + C \cdot t^2 + D \cdot t^3 + E/(t^2) \tag{4-10}$$

where Table 4-2 gives the values of coefficients A, B, C, D and E for helium and nitrogen as stated in the NIST chemistry webbook [30] and t is the temperature in Kelvin divided by 1000; hence $t = T/1000$. The molar mass of the pressurant is depicted in Table 4-3. Currently only helium and nitrogen are considered as possible pressurants as these are the most widely used. While often also gaseous hydrogen or gaseous oxygen is used to pressurise the fuel or oxygen tank respectively, this option adds complexity to the model which for now is not needed.

For determining the value of the compressibility factor (Z) the Redlich-kwong equation of state represented as an equation for the compressibility factor of a gas, as a function of temperature and pressure is used [57]:

$$Z = \frac{1}{1-h} - \frac{A^2}{B}\frac{h}{1+h} \tag{4-11}$$

where:

$$A^2 = \frac{a}{R^2 \cdot T^{2.5}} \tag{4-12}$$

$$B = \frac{b}{R \cdot T} \tag{4-13}$$

$$h = \frac{B \cdot p}{Z} \tag{4-14}$$

with

$$a = \frac{0.4275 \cdot R^2 \cdot T_{crit}^{2.5}}{p_{crit}} \tag{4-15}$$

$$b = \frac{0.08664 \cdot R \cdot T_{crit}}{p_{crit}} \tag{4-16}$$

Table 4-3: Molar mass, critical pressure and critical temperature for Helium and Nitrogen from NIST tables [30]

Pressurant	$\hat{M}$ $[g/mol]$	p_{crit} $[bar]$	T_{crit} $[K]$
He	4.002602	2.289945	5.19
N_2	28.0134	33.999	126.15

The critical temperature (T_{crit}) and critical pressure (p_{crit}) are taken from NIST chemistry webbook [30], their values are depicted in Table 4-3. The compressibility factor Z can only be found by solving Eq. (4-11) iteratively (taking as initial guess no compressibility, hence $Z = 1$). Note that as the ideal gas law is used twice in the iterative loop, first in Eq. (4-8) then in Eq. (4-19), two compressibility factors need to be calculated; one at initial pressurant tank conditions (Z_i) and one at final pressurant tank conditions (Z_f). Further according to Zandbergen p_f has to minimal 1.5 to 2 times the required tank pressure [11]; here the required tank pressure will be assumed to be equal to the Maximum Expected Operating Pressure (MEOP). In case a single pressurant tank is to be used to pressurize more than one propellant tanks, the maximum MEOP of these tanks is to be used. Hence:

$$p_f = 1.5 \cdot max(MEOP_{ox}, MEOP_{fuel}) \tag{4-17}$$

The pressurant volume is found using:

$$V_{press} = V_{tank,prop} + V_{tank,press} \tag{4-18}$$

where $V_{tank,press}$ is found using the ideal gas law in combination with the initial tank pressure (p_i) and initial tank temperature (T_i):

$$V_{tank,press} = \frac{m_{press} \cdot Z_i \cdot R \cdot T_i}{p_i} \tag{4-19}$$

As one does not know the volume of the pressurant tank, neither its mass in advance, one needs to iterate; the iteration scheme is presented in Figure 4-1.

4-1-4 Nozzle

The throat and exit area follow directly from the input:

$$A_e = \pi \cdot \left(\frac{d_e}{2}\right)^2 \tag{4-20}$$

$$A_t = \frac{A_e}{A_e/A_t} \tag{4-21}$$

The throat diameter then is found using:

$$d_t = 2 \cdot \sqrt{\frac{A_t}{\pi}} \tag{4-22}$$

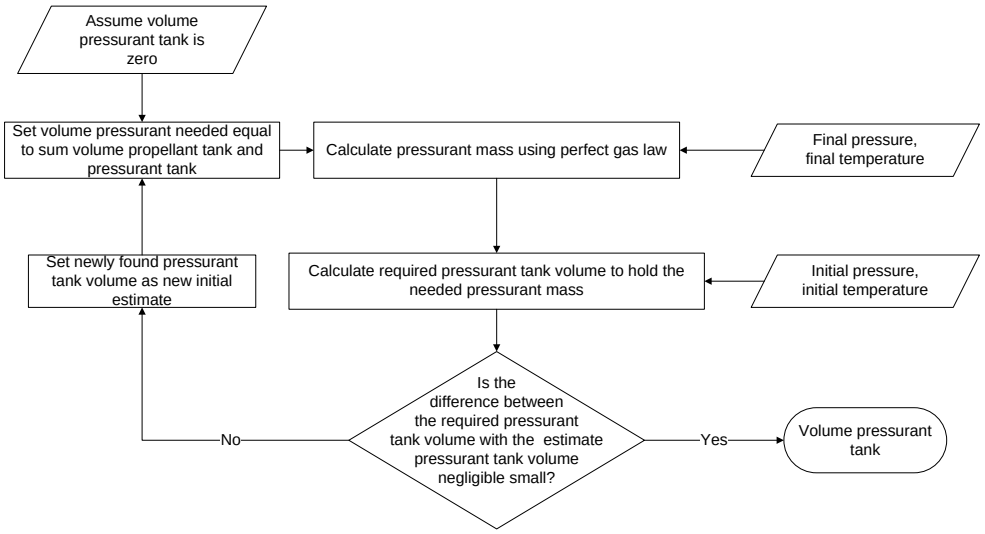

Figure 4-1: Iteration process to find $V_{tank,press}$

Assuming a conical nozzle, the length of the throat region (L_{throat}, the length of the nozzle divergent $L_{divergent}$ and the resulting total nozzle length L_{nozzle} follow from [40] [11]

$$L_{throat} = r_u \cdot \sin\alpha \tag{4-23}$$

$$L_{divergent} = \frac{\left(\sqrt{\frac{A_e}{A_t}} - 1\right) \cdot r_t + r_u \cdot (\sec(\alpha) - 1)}{\tan\alpha} \tag{4-24}$$

$$L_{nozzle} = L_{throat} + L_{divergent} = r_u \cdot \sin\alpha + \frac{\left(\sqrt{\frac{A_e}{A_t}} - 1\right) \cdot r_t + r_u \cdot (\sec(\alpha) - 1)}{\tan\alpha} \tag{4-25}$$

with

$$r_t = \frac{d_t}{2} \tag{4-26}$$

$$0.5 \cdot r_t < r_u < 1.5 \cdot r_t \tag{4-27}$$

The nozzle cone half angle (α) for a conical nozzle is related to the nozzle length and throat and exit radius as follows [31] (see also Figure 3-8):

$$L_{cone} = \frac{r_e - r_t}{\tan(\alpha)} \tag{4-28}$$

where L_{cone} is the length of the conical part of the nozzle measured from the throat. Typically α has values in the range between 12 deg to 18 deg. [31] [4] A small angle means that most of the momentum is axial and thus has the highest specific impulse, however the longer nozzle length that goes with a small divergence angle increases mass. [4] Similarly large divergence angles give short light nozzle designs, but have lower performance. [4] Humble et all state that usually a compromise of $\alpha = 15$ deg is taken [31] for new designs:

$$\alpha = 15\,\text{deg} \tag{4-29}$$

Zandbergen reports in [11] that the throat longitudinal radius (r_u) has an optimal value between 0.5 and 1.5 times the throat radius (r_t); therefore a value of 1 times the throat radius will be taken as this is in the middle of this optimal interval:

$$r_u = 1.0 \cdot r_t \tag{4-30}$$

4-1-5 Combustion Chamber

In [31] an empirical scaling relation between the throat diameter and the combustion-chamber-to-throat-area ratio is given:

$$\frac{A_{mcc}}{A_t} = 8.0 \cdot d_t^{-0.6} + 1.25 \text{ where } d_t \text{ is in cm} \tag{4-31}$$

The chamber diameter (d_{mcc}), chamber volume (V_{mcc}) and actual chamber length (L_{mcc}) then follow from:

$$d_{mcc} = 2 \cdot \sqrt{\frac{A_{mcc}}{\pi}} \tag{4-32}$$

$$V_{mcc} = L^* \cdot A_t \tag{4-33}$$

$$L_{mcc} = \frac{V_{mcc}}{\pi \cdot \left(\frac{d_{mcc}}{2}\right)^2} \tag{4-34}$$

The characteristic length (L^*) has a typical range of values for certain propellant combinations. Upper and lower values for several combinations are found in [11] and [31]. Here the highest values mentioned in Humble et al for L^* will be used as this represents the worst case scenario [31]:

$$L^* = \begin{cases} 1.02\,\text{m} & LOX - LH2 \\ 1.27\,\text{m} & LOX - RP1 \\ 0.89\,\text{m} & N2O4 - MMH \end{cases} \tag{4-35}$$

4-1-6 Gas Generator or Pre-burner

Since a gas generator is basically a combustion chamber, it is assumed it can be sized in exactly the same way as the main combustion chamber. Therefore the length of the gas generator combustion chamber L_{gg} and its volume V_{gg} follow from using Eq. (4-34) and Eq. (4-33) respectively. To solve Eq. (4-34) and Eq. (4-33) the cross-sectional area, diameter and throat cross-sectional area of the gas generator need to be found.

The gas generator cross-sectional area and the diameter is found by using the continuity equation given by Eq. (3-11) and assuming the Mach number at the end of the gas generator or pre-burner has a typical Mach number equal to that in the combustion chamber, hence:

$$M_{gg} = 0.2 \tag{4-36}$$

Then using Eq. (3-6) to find the velocity of the flow in the gas generator leads to the following relation to find the cross-sectional area of the gas generator:

$$A_{gg} = \frac{\dot{m}_{gg}}{\rho \cdot v_{gg}} = \frac{\dot{m}_{gg}}{\rho \cdot (M_{gg} \cdot a_{gg})} = \frac{\dot{m}_{gg}}{\rho \cdot \left(M_{gg} \cdot \sqrt{\gamma_{gg} \cdot \frac{R_A}{\bar{M}_{gg}} \cdot T_{gg}}\right)} \tag{4-37}$$

The gas generator diameter d_{gg} then follows from using Eq. (4-32).

The gas generator throat cross-sectional area is found by assuming that the empirical scaling relation between the throat diameter and the combustion-chamber-to-throat-area ratio given by Eq. (4-31) is also valid for gas generators. Since know one is interested in the throat area for a known combustion chamber cross-sectional area which was found earlier using the continuity equation, one has to solve Eq. (4-31) iteratively for A_t. Note that $d_t = 2 \cdot \sqrt{\frac{A_t}{\pi}}$. As first estimation for A_t the chamber cross-sectional area could be taken.

4-1-7 Turbo-pump

Relations.

In [58] Zandbergen proposes to use the following relations to estimate length and diameter of the smallest cylindrical-shaped enclosure that contains the turbo-pump completely [58]:

$$L = (L/d) \cdot P \cdot P_\rho \tag{4-38}$$

$$d = \frac{1}{(L/d)} \cdot P \cdot P_\rho \tag{4-39}$$

where (L/d) is the length-over-diameter ratio, P the turbo-pump power in MW and P_ρ the power density in $\frac{MW}{m^3}$. Based on actual engine data, Zandbergen [58] gives a L/d range of:

$$L/d = \begin{cases} 1-2 & \text{Direct drive or geared} \\ 0.8-1.3 & \text{Dual shafts} \end{cases} \tag{4-40}$$

The turbo-pump power density is estimated with the following relationship [58]:

$$P_\rho = \begin{cases} 0.5085 \cdot P + 1.3877 & \text{Direct drive or geared} \\ 3.6982 \cdot P + 12.365 & \text{Dual shafts} \end{cases} \tag{4-41}$$

Eq. (4-40) and Eq. (4-41) are dependent on the turbo-pump types which can be either direct drive, geared or dual shaft. Figure 4-2 displays examples of the most common configurations of these types. As can be see from Figure 4-2, turbo-pump of the type direct drive or geared have a single turbine driving both pumps, while turbo-pumps of the type dual shaft always have two turbines; hence the number of turbines defined by the user determines which relation is applicable.

Validation.

Turbo-pump dimension data is hard to find, however the accuracy of the used relations is discussed by Zandbergen, the author of the relations, in [58].

4-2 Mass Model

The mass model has the purpose to estimate the total propulsion system mass such that optimisation of a vehicle or subsystem for mass is possible.

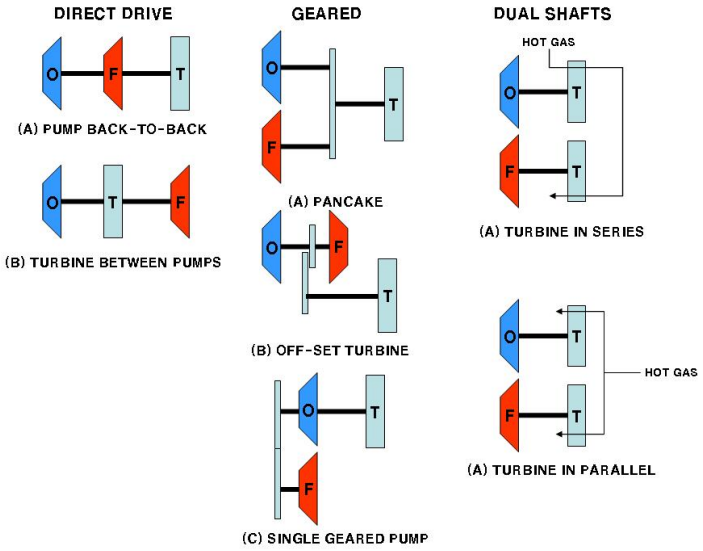

Figure 4-2: Schematic of basic turbo-pump arrangements (taken from Zandbergen [58] based on NASA SP8107 [59])

The major components in a propulsion system are the thrust chamber assembly, the propellant feed control system, the turbo-pump, the gas generator system, the propellant tank pressurization system, the electrical system, the hydraulic control system and the flight instrumentation system. [60] Hence they will also have the largest dry mass contributions to the system. However it is difficult to estimate the mass of the electrical system, the hydraulic control system and the flight instrumentation system; therefore the masses of these components will not be calculated. Also minor components such as injector and starters might have a contribution of several kilograms to the total engine mass but will be left out of the mass calculation because of the difficulty to establish mass estimation relationships for these components.

In a mass breakdown, the propellant mass needed is by far the largest contributor to the total launcher/stage wet mass. According to reference [61], for a launcher the mass contribution consists of 90 percent by the propellants and only 6 percent by the structure (tanks, engines, fins, etc.) and 4 percent by the payload. Hence it is clear that the estimation of propellant mass is far more important than engine dry mass.

The engine component mass relations in LiRA are only used to give the user an idea of the order of magnitude of the mass, the actual total engine dry mass is estimated using a single relation. The tank masses however are however used in combination with the engine dry mas estimate to have a total propulsion system dry mass estimate which on its turn combined together with the propellant and pressurant mass yields the total propulsion system wet mass estimate which is the most important mass output.

In this chapter all mass estimation related equations and methods are given, when an empirical relation is used also a small validation is performed to assess its accuracy. A component wise approach is taken; first the relations to estimate engine dry mass, propellant and pressurant mass and tank dry mass are discussed. As one of the goals is to optimise an engine stage also the correction needed to get from a propulsion system dry mass to a stage dry mass estimate is

discussed. Finally the methods of mass estimation of some major engine sub components are shortly discussed.

4-2-1 Overall Engine Mass

Relations.

Since the engine mass cannot be simply determined from the sum of masses of the subcomponents, another approach is chosen. Zandbergen has created in [56] and [62] several empirical engine mass estimation relations based on actual engine mass data. The relations with the highest coefficient of determination have been implemented into the model:

- pressure fed

$$m_{engine} = \begin{cases} 0.1005 \cdot F^{0.6325} & \text{storable} \\ \text{no relation given} & \text{other} \end{cases} \tag{4-42}$$

  with F, the vacuum thrust in Newton

- turbo-pump fed

$$m_{engine} = \begin{cases} 0.006 \cdot F^{0.858} \cdot p_{mcc}^{0.117} \cdot (A_e/A_t)^{0.034} & \text{cryogenic} \\ (0.001 \cdot F + 49.441) \cdot N^{0.030} \cdot (A_e/A_t)^{0.004} & \text{storable, semi-cryogenic} \end{cases} \tag{4-43}$$

  with F, the vacuum thrust in Newton, p_{mcc} the chamber pressure in bar, (A_e/A_t) the nozzle area expansion ratio and N the amount of thrust chambers.

As can be seen from Eq. (4-42) and Eq. (4-43) Zandbergen makes a distinction between pressure fed and turbo-pump fed engines, further a distinction between cryogenic on one hand and storable or semi-cryogenic liquid propellant engines on the other hand. For pressure fed systems no relation for cryogenic engines is given, this is likely because the combination of pressure-fed and cryogenic or even semi-cryogenic is not usual. In the case the model is ran with this combination, it will be assumed that the mass of cryogenic or semi-cryogenic pressure fed rocket engines can also be estimated using the storable relation.

Validation.

In order to test these relations the dry mass of several engines using their actual vacuum thrust, number of engines, nozzle area ratio and chamber pressure is performed in Table 4-4.

4-2-2 Propellant Tank and Pressurant Tank Mass

One way to calculate the tank mass is to calculate the tank shell mass and multiply the result with a shell tank mass correction factor to account for tank add-ons. [11] However another method presented by Zandbergen in [11] is based on work of Trotsenburg [63] which was conducted under supervision of Zandbergen; here a tank performance factor that relates tank mass to tank volume and MEOP is used. This method has the advantage it does not require the user to make a tank

Table 4-4: Validation of relations 4-42 and 4-43

Engine	Cycle type	Propellant type	F [kN]	N [−]	A_e/A_t [−]	p_c [MPa]	m_{dry} real [kg]	m_{dry} calculated [kg]	$E_{\%}$ [%]
Aestus	pf	storable	27.5	1	84	1.77	111	64.6	41.8
AJ10-118K	pf	semi-cryogenic	43.4	1	65	0.896	124.7	86.2	30.9
Vulcain	tp	cryogenic	1025	1	45	10	1719	1681.0	2.2
HM7B	tp	cryogenic	62.2	1	82.9	3.6	158	137.6	12.9
J2	tp	cryogenic	1023	1	27.5	5.4	1542	1535.5	0.4
LE-5	tp	cryogenic	103	1	140	3.65	255	216.2	15.2
LE-5A	tp	cryogenic	121.5	1	130	3.98	244	251.1	2.9
LE-7	tp	cryogenic	1080	1	52	12.7	1714	1816.8	6.0
RL10-3-3A	tp	cryogenic	73.4	1	240	3.2	138	162.2	17.5
RL10-B-2	tp	cryogenic	110	1	285	4.413	259	239.6	7.5
SSME	tp	cryogenic	2278	1	77.5	206.7	3150	4842.4	53.7
vulcain 2	tp	cryogenic	1350	1	60	11.6	1850	2187.6	18.3
H-1	tp	semi-cryogenic	945.4	1	45	4.12	878.2	1010.1	15.0
RD-120	tp	semi-cryogenic	833.6	1	106.7	16.28	1125	899.7	20.0
RS-27	tp	semi-cryogenic	1023	1	12	4.87	1146.6	1083.2	5.5
Aestus II	tp	storable	55.4	1	300	6	138	107.3	22.3
S-4(MA-3)	tp	semi-cryogenic	364	1	25	4.6	470.4	418.8	11.0

pf: pressure fed tp: turbo-pump fed

wall material choice nor to correct for tank add-ons as this is already included in the performance factor; the tank mass estimate is only dependent on required tank volume, maximum expected operating pressure and aforementioned tank performance factor K:

$$m_{tank} = \frac{V_t \cdot MEOP}{K} \tag{4-44}$$

where the average values for K are [63]:

$$K = \begin{cases} 3.32 \times 10^4, \sigma = 1.04 \times 10^4 & \text{surface tension tanks} \\ 12.2 \times 10^4, \sigma = 3.91 \times 10^4 & \text{composite over-wrapped pressure vessels} \\ 6.43 \times 10^4, \sigma = 0.56 \times 10^4 & \text{titanium tanks} \end{cases} \tag{4-45}$$

Propellant tanks will be modelled as surface tension tanks containing liquid, while pressurant tanks as either composite over-wrapped pressure vessels (COPV) or titanium tanks containing compressed gas; this is because surface tension tanks are not suited for the typical high pressures (up to 400 bar and higher) found in pressurant tanks.

4-2-3 Stage Dry Mass

As the goal of this work is to look at launcher propulsion systems, one is interested in stage wet and dry masses. The sum of the component masses does not simply yield the total propulsion system mass as some major components such as the electrical system, the hydraulic control system and the flight instrumentation system and minor components such as ignitor and starter are not taken into account. Further when considering a whole stage of which the propulsion system is part additional structural weight on top of the weight of the propulsion system needs to be taken into account. A possible approach to account for this problem is to introduce a correction factor.

For the determination of the stage dry mass correction factor several actual stage dry masses are compared to the propulsion system dry mass estimate found with LiRA. For example the Ariane 5 EPS-V stage, which uses the pressure fed Aestus engine is chosen, has a total wet mass of 11.3 metric tonnes of which a propellant mass of 10 metric tonnes. [64] Therefore the stage dry mass is 1.3 metric tonnes. When calculating the propulsion system dry mass with LiRA for the Aestus engine a dry mass value of 641.6 kg is found. This means a correction factor of 2.0 is needed. Similarly the Ariane 5 ESC-A stage, which uses the gas generator cycle HM7B engine, has a total wet mass of 19.4 metric tonnes of which 14.9 metric tonnes are propellant. Therefore the stage dry mass is 4.5 metric tonnes. [64] LiRA gives for a propulsion system using the HM7B engine a dry mass of 831.8 kg. This means a correction factor of 5.5. This is repeated in Appendix G for several stages from which then an average value of 2.53 and standard deviation of 1.44 is obtained.

Hence:

$$m_{total,dry} = (m_{engine} + m_{tank,ox} + m_{tank,fuel} + m_{tank,pressurant}) \cdot K_{\text{dry mass}} \tag{4-46}$$

where

$$K_{\text{dry mass}} = 2.53 \tag{4-47}$$

4-2-4 Propellant Mass

The required propellant mass follows directly from the engine mass flows and burn time:

$$m_{ox} = \dot{m}_{ox} \cdot t_b \tag{4-48}$$

$$m_{fuel} = \dot{m}_{fuel} \cdot t_b \tag{4-49}$$

4-2-5 Pressurant Mass

Once $V_{tank,press}$ has been found m_{press} can be calculated using Eq. (4-8).

4-2-6 Thrust Chamber

The thrust chamber is the assembly of main combustion chamber and nozzle. In [11] it is proposed by Zandbergen to use a mass estimation correction factor (K). This factor is calculated by calculating the thrust chamber shell mass and comparing it to the actual total mass; from this data an average correction factor K can be derived. The thrust chamber shell mass itself is the combination of the combustion chamber shell mass (found with Eq. (4-51)) and the nozzle shell mass (found with Eq. (4-52)); therefore [11]:

$$m_{\text{thrust chamber}} = K \cdot (m_{\text{thrust chamber}})_{shell} = K \cdot [(m_c)_{shell} + (m_{nozzle})_{shell}] \tag{4-50}$$

Combustion chamber shell mass.

The following assumptions are made:

- A cylindrical chamber with two flat ends

- constant thickness for all parts which is equal to the thickness of the cylindrical part
- thin-wall

Under these assumptions the following relation can be derived to compute the shell mass of a combustion chamber (for complete derivation see [11]):

$$(m_c)_{shell} = \left(\frac{1}{\frac{L_{mcc}}{d_{mcc}}} + 2 \right) \cdot \frac{\rho}{\sigma_{ult}} \cdot f_s \cdot p_{mcc} \cdot V_{mcc} \tag{4-51}$$

Nozzle shell mass.

Following from derivations and combinations of relations set out in Zandbergen [11], the following mass estimation equation for the nozzle is found:

$$(m_{nozzle})_{shell} = \frac{\rho}{\sigma_{ult}} \cdot f_s \cdot \left(A_t \cdot \frac{\epsilon - 1}{\sin \alpha} \frac{p_{mcc} \cdot d_{mcc}}{2} \right) \tag{4-52}$$

where ϵ is the nozzle area ratio; $\epsilon \equiv \frac{A_e}{A_t}$.

Calculation of thrust chamber mass correction factor K.

Unfortunately it is difficult to find data for the thrust chamber mass, chamber and nozzle material and length. Therefore a K value was constructed from only three engines. In Appendix H the complete calculation as suggested by Zandbergen is given; the result is a K value of 1.52 with a standard deviation of 0.80.

4-2-7 Gas Generator or Pre-burner

The gas generator or pre-burner is basically a combustion chamber that supplies gases to a turbine instead of to a nozzle; hence it can be treated similarly to a combustion chamber for the calculation of its mass as is also suggested by Manski in [15]. Hence again the following assumptions are made:

- A cylindrical chamber with two flat ends
- constant thickness for all parts which is equal to the thickness of the cylindrical part
- thin-wall

Under these assumptions again the same relation (Eq. (4-51)) by [11] can be used:

$$(m_{gg})_{shell} = \left(\frac{1}{\frac{L_{gg}}{d_{gg}}} + 2 \right) \cdot \frac{\rho}{\sigma} \cdot f_s \cdot p_{gg} \cdot V_{gg} \tag{4-53}$$

If the same rationale as for the thrust chamber is taken, then a mass estimation correction factor K should be used to correct the shell mass calculation to a more accurate mass estimation:

$$m_{\text{gas generator}} = K \cdot (m_{\text{gas generator}})_{shell} \tag{4-54}$$

However as no data on actual gas generator masses could be found and neither an alternative method, this parameter will be set to value 1. The reason for including the correction factor anyway allows the user of the model to adjust the value to his or her own feeling/judgement. The estimate however will not affect the dry mass of the engine, propulsion system or stage as explained earlier.

4-2-8 Turbo-Pump

Relations.

The mass of the turbo-pump system m_{tp} can be estimated using Zandbergen's empirical relation given by Eq. (4-55) [58]:

$$m_{tp} = \begin{cases} \text{Direct drive or geared} \begin{cases} 73.831 \cdot P_T^{0.9176} & \text{Low power} \\ 417.62 \cdot \ln(P_T) - 137.5 & \text{High power} \end{cases} \\ \text{Dual shafts arrangements} \begin{cases} 51.137 \cdot \ln(P_T) + 121.1 & \text{LOX} \\ 81.582 \cdot \ln(P_T) + 25.9 & \text{LH2} \end{cases} \end{cases} \tag{4-55}$$

where P_T is the turbine output power in MW. Zandbergen further states that the low power relation is valid in the range $0.1\,\text{MW} < P_T < 1.75\,\text{MW}$ with a RSE of 20.7 %, the high power relation in the range $2.25\,\text{MW} < P_T < 40\,\text{MW}$ with a RSE of 35.2 %, the LOX relation in the range $2\,\text{MW} < P_T < 18\,\text{MW}$ with a RSE of 12.9 % and finally the LH2 relation in the range $5\,\text{MW} < P_T < 50\,\text{MW}$ with a RSE of 5.2 %.

In case the turbine power of a direct drive or geared turbo-pump system falls in between the low power and high power range, the average of both estimates will be the estimate given by LiRA. In case the power falls outside the ranges a warning will be given that the estimated mass may contain a significant error and hence should be used carefully. For the dual shaft arrangements only relations for LOX and LH2 are given, the reason for this is likely to be because dual shaft turbo-pump arrangements are commonly found for LOX-LH2 bi-propellant rockets. A possible hypothesis for this could be created using Table 3-13; here one can observe a large difference in density of LOX and LH2; this means a significant difference in rotation speed of the pumps and their efficiency. Proof that the density of the propellant directly affects the pump efficiency and rotational speed is given in Appendix E; here it is concluded that a direct drive arrangement is not efficient, as it would need to rotate at the lowest maximum allowable speed of the two pumps, and a geared arrangement would be larger and heavier for the LOX-LH2 combination due to the high reduction ratio needed. For all other propellant combinations the density differences are not that extreme as for LOX-LH2 and thus the pump rotational speeds are not that different and a direct drive or geared arrangement could be lighter than using two separate turbines in a dual shaft arrangement.

Validation.

Turbo-pump mass data is hard to find, however the accuracy of the used relations is discussed by Zandbergen, the author of the relations, in [58].

4-3 Validity of Mass and Size Model

Because the relations used are either empirical relations or first-order of magnitude estimation relations based on the mass or volume of part of the system which is then corrected by a correction factor, a lot of uncertainty in the estimates exist. Because the propulsion system mass and volume estimates are not using the masses or volumes from all components discussed, the source of uncertainty in the volume and mass estimate is limited to those introduced by the methods of estimating the overall engine, propellant tank and pressurant tank estimates. For stage dry mass an additional correction factor is a source of uncertainty. The accuracy of mass and volume estimates is addressed when the Relative Standard Errors of Estimate are determined in Section 7-2. The impact of uncertainty in the correction factors on an estimate always needs to be assessed by means of a sensitivity and uncertainty analysis such as one is performed in section 9-5.

Chapter 5

Program Set-up

LiRA has three main routines all calling the engine analysis module which contains the performance, mass and dimensioning models. The simple engine analysis routine loads an user made engine file defining a single engine cycle and performs the engine performance mass and dimensioning calculations; this is the final output. The uncertainty and sensitivity analysis routine either allows the user to perform the analysis on a certain engine or to fix a delta v and thrust to weight ratio requirement and see how the optimised input and output variables vary with variation in certain parameters. In the first case an engine definition file is loaded before calling the engine analysis routine, in the latter no engine definition, but a constraint file is loaded. All other necessary input needed, must be given by the user through the command window. The final output is written to text files. The optimisation routine requires several input by the user that must be given through the command window and only loads a constraint file. It then generates random input for the input parameters that are to be included in the optimisation before calling the engine analysis routine. The generated input and obtained output is further processed before presented to the user as final output stored in text files. The current version of LiRA has no dedicated Graphical User Interface (GUI) and interacts with the user through MATLAB's command window. A user manual explaining step by step how to use the three different functionalities of LiRA is found in Appendix K.

5-1 Engine Analysis Calculation Order

As can also be seen in Figure 5-2, Figure 5-3, Figure 5-5, Figure 5-7 and Figure 5-9, the model will start at the essence of a rocket engine, the thrust chamber (which is the assembly of combustion chamber and nozzle (extension)) and calculates iteratively outwards from this component until a balance is reached. In the thrust chamber the main tunable parameters, next to the oxidiser and fuel choice, are the mixture ratio and combustion pressure. Once a propellant choice, mixture ratio and combustion pressure are defined the nozzle and injector calculations can be performed. Now the conditions at the injector of the main combustion chamber are known, the required pressure at the exit of the propellant tanks in case of a pressure-fed system or the required

pressure rise over the pumps follows from the pressure losses from the storage tanks to the injector. If applicable, knowing the conditions in the nozzle and main combustion chamber allows for the cooling calculations to be performed and for the calculation of the pressure loss over the heat exchanger. Next step is then, if applicable, to balance the turbo-pump (and if applicable, the gas generator or pre-burner) such that the turbine is capable of providing enough power to the pumps and the pumps pump enough mass flow at high enough pressure to feed the main combustion chamber and turbine. Once this is done the total oxidiser mass flow and fuel mass flow is known and thus the propellant tanks can be sized. After having the size of the propellant tanks, the pressurant tank can be sized and then the engine and its feed system have been modelled from pressurant tank to the atmosphere at the nozzle exit.

So to recap an overview of the computation order is given:

1. load user pre-made input file or create input file by prompting user for input.
2. dimension combustion chamber and nozzle from given input
3. start thruster (main combustion chamber, nozzle and injector) calculations
4. balance feed system
5. (if gas generator or pre-burner present) size gas generator or pre-burner
6. size propellant tanks
7. size pressurant tank
8. perform mass calculations
9. perform dimension calculations

5-2 Model Parameters

As the thrust chamber plays a central role and all other components are dependent on choices made for this component, most of the user required input to the model are related to the thrust chamber. In literature several rules of thumb or typical design values for certain variables can be found. Hence the user does not necessarily has to define a value for all these parameters. In case a parameter is left undefined, the user will be prompted with a message that a parameter is needed but has not been assigned a value and a typical value is suggested. The user then has the choice to either use this value or set a value him or herself. The user is however always encouraged to input custom values for the optional input parameters wherever possible, as this can make the model more refined and lead to better results. Some examples of engine input files that would need to be created for the program to run, are given in Appendix B.

Further thermochemical data needs to be provided to the program; this is combustion temperature, density, molar mass, specific heat ratio, specific heat capacity, viscosity and conductivity data of pure liquid substances and of gas mixtures. The choice of propellant combinations and pressurant substances is therefore also limited as each new option requires more data tables to be made. Currently LiRA supports Liquid Oxygen (LOX) and Dinitrogen Tetroxide (N2O4) as oxidisers and Liquid Hydrogen (LH2), Monomethylhydrazine (MMH) and Rocket Propellant 1 (RP1) as fuels in the following combinations: LOX/LH2, N2O4/MMH and LOX/RP1; these are common combinations in liquid bi-propellant engines and therefore allow the model to analyse a wide variation of engines. Helium is the most often encountered pressurant in pressurant tanks; alternatively nitrogen is sometimes used if Helium is too expensive. Therefore Helium and Nitrogen are the two pressurant options currently available in the model.

For the optimisation additional inputs which give the optimisation requirements and constraints are needed. The optimisation input requirements are given in Table 5-3 and constraints in Table 5-4. Why these requirements and constraints are chosen is discussed in Chapter 8.

Table 5-1: Overview of all independent variable parameters in LiRA

Id.	Parameter	Type	Source	Remark
V-1	Engine cycle choice	Required input	User	
V-2	Oxidiser choice	Required input	User	
V-3	Fuel choice	Required input	User	
V-4	Nozzle exit diameter	Required input	User	
V-5	Nozzle area ratio	Required input	User	
V-6	Atmospheric pressure	Required input	User	
V-7	Burn time	Required input	User	
V-8	Main combustion chamber pressure	Required input	User	
V-9	Main combustion chamber mixture ratio	Optional input/typical value	User/literature	Sec.3-2
V-10	Nozzle cooling method	Optional input/typical value	User/assumption	Sec.3-3
V-11	Main combustion chamber cooling method	Optional input/typical value	User/assumption	Sec.3-3
V-12	Pressurant choice	Optional input/typical value	User/assumption	Sec.4-1-3
V-13	Pressurant initial temperature	Optional input/typical value	User/assumption	Sec.4-1-3
V-14	Pressurant initial pressure	Optional input/typical value	User/assumption	Sec.4-1-3
V-15	Oxidiser initial temperature	Optional input/typical value	User/literature	Sec.3-9
V-16	Fuel initial temperature	Optional input/typical value	User/literature	Sec.3-9
V-17	Nozzle wall material	Optional input/typical choice	User/literature	Sec.3-3
V-18	Combustion chamber wall material	Optional input/typical choice	User/literature	Sec.3-3
V-19	Engine throttled	Optional input/typical choice	User/literature	Sec.3-2-2
V-20	MEOP oxidiser tank	Optional input/typical value	User/literature	Sec.3-9
V-21	MEOP fuel tank	Optional input/typical value	User/literature	Sec.3-9
V-22	Oxidiser pump efficiency	Optional input/typical value	User/literature	Sec.3-5
V-23	Fuel pump efficiency	Optional input/typical value	User/literature	Sec.3-5
V-24	Number of turbines	Optional input/typical value	User/assumption	Sec.3-6
V-25	Turbine efficiency*	Optional input/typical value	User/literature	Sec.3-6
V-26	Turbine pressure ratio*	Optional input/typical value	User/literature	Sec.3-6
V-27	Turbine mechanical efficiency*	Optional input/typical value	User/literature	Sec.3-6
V-28	(max allowed) Turbine inlet temperature*	Optional input/typical value	User/literature	Sec.3-6-5
V-29	Mixture type in gas generator	Optional input/typical value	User/literature	Sec.5-6-4

* in case of two turbo-pumps, this parameter is defined for oxidiser- and fuel side separately

Table 5-2: Overview of all independent non-variable parameters in LiRA

Id.	Parameter	Type	Source	Remark
NV-1	Propellant tank ullage volume fraction	Typical value	Literature	Sec.4-1-2
NV-2	Propellant tank boil off volume fraction	Typical value	Literature	Sec.4-1-2
NV-3	Propellant tank trapped volume fraction	Typical value	Literature	Sec.4-1-2
NV-4	Specific impulse correction factor	Correction factor	Calculated	Sec.3-2
NV-5	Thrust chamber mass correction factor	Correction factor	Calculated	Sec.4-2-6
NV-6	Gas generator mass correction factor	Correction factor	Calculated	Sec.4-2-7
NV-7	Propellant tank performance factor	Correction factor	Literature	Sec.4-2-2
NV-8	Pressurant tank performance factor	Correction factor	Literature	Sec.4-2-2
NV-9	Total propulsion system dry mass correction factor	Correction factor	Calculated	Sec.4-2-3

Table 5-3: Overview of all optimisation requirement inputs in LiRA

Id.	Parameter	Type	Source	Remark
R-1	Change in velocity (ΔV)	Required input	User	
R-2	Thrust-to-weight ratio (F/W)	Required input	User	
R-3	Payload mass	Required input	User	

Table 5-4: Overview of all possible optimisation constraint inputs in LiRA

Id.	Parameter	Type	Source	Remark
C-1	Total wet mass of propulsion system	Optional input	User	
C-2	Total diameter of propulsion system	Optional input	User	
C-3	Total length of propulsion system	Optional input	User	
C-4	Total volume of propulsion system	Optional input	User	
C-5	L/d tanks	Optional input	User	

5-3 Overview of Typical, Calculated and Assumed Parameter Values Used in LiRA

As discussed in the performance, mass and sizing model, several typical, calculated and assumed values are used throughout the engine analysis. Some parameter values can be set by the user (Table 5-1) while others (Table 5-2) can't. Table 5-5 gives an overview of all non-user defined values used by the program. (Remember that a non-user defined value can also be a user variable input that is optional and left undefined.)

5-4 Overview Components

An example engine scheme, in this case of an oxygen rich staged combustion cycle, with a lot of components and feed lines can be seen in Figure 5-1. Every component has a unique C-number (C being short for component), while the lines connecting the components get a S-number (S standing for data-Set). The S number name consists of the two component numbers it connects. C-numbered components are attributed characteristics such as cross sectional area, efficiency, power, etc. Flow properties like pressure, temperature, density, mass flow, etc are calculated and stored in the S-numbered lines. However some components such as the main combustion chamber and gas generator also contain information such as pressure, temperature and mass flow through the component as this might be more intuitive for some users. This approach has the advantage of easy understanding the program flow and reading the flow characteristics in the line; however the assumption is made that the characteristics are constant in the entire line and thus no line losses are taken into account. Further also no pressure losses over valves or splits and joints are considered. These could be incorporated by creating a 'pipe' and 'valve' component that has to be placed in between two components or two lines respectively that have a flow in between them and which then acts as a component changing flow properties due to pipe effects and/or line losses. In the most simple case the pipe and valve component would just contain a user-defined pressure loss coefficient to calculate the pressure loss (and the consequently change in other flow properties like temperature and density).

Piping and valves are not included in the model. These components are important for accurately modelling pressure losses, however for cycle relative comparison from a mass, dimension and performance perspective point of view, the ignoring of these losses is assumed to have an equal effect on all cycles and thus is assumed to be not required for the scope of this work.

Table 5-5: Overview of typical, calculated and assumed parameter values used in LiRA

Id.	Parameter	When used	Value	Unit	Condition
V-9	MCC mixture ratio	If undefined	2.77	[−]	LOX-RP1
			4.83	[−]	LOX-LH2
			2.37	[−]	N2O4-MMH
V-10	Nozzle cooling method	If undefined	reg. cooling	[−]	ce, be
			no cooling	[−]	otherwise
V-11	MCC cooling method	If undefined	reg. cooling	[−]	ce, be
			no cooling	[−]	otherwise
V-12	Pressurant choice	If undefined	helium	[−]	-
V-13	Pressurant initial temperature	If undefined	300	[K]	-
V-14	Pressurant initial pressure	If undefined	400	[bar]	-
V-15	Oxidiser initial temperature	If undefined	90.17	[K]	LOX
			300	[K]	otherwise
V-16	Fuel initial temperature	If undefined	20.27	[K]	LH2
			300	[K]	otherwise
V-17	Nozzle wall material	If undefined	Inconel 600	[−]	-
V-18	Combustion chamber wall material	If undefined	Narloy Z	[−]	-
V-19	Engine throttled	If undefined	unthrottled	[−]	pressure fed
			throttled	[−]	otherwise
V-20	MEOP oxidiser tank	If undefined	3	[bar]	-
V-21	MEOP fuel tank	If undefined	3	[bar]	-
V-22	Oxidiser pump efficiency	If undefined	80	[%]	-
V-23	Fuel pump efficiency	If undefined	75	[%]	LH2
			80	[%]	otherwise
V-24	Number of turbines	If undefined	2	[−]	-
V-25	Turbine efficiency	If undefined	70	[−]	-
V-26	Turbine pressure ratio	If undefined	2.5	[−]	LOX
			8.0	[−]	LH2
			20.0	[−]	otherwise
V-27	Turbine mechanical efficiency	If undefined	100	[%]	1 turbine
			97.5	[%]	2 turbines
V-28	(max allowed) Turb. inlet temp.	If undefined	1000	[K]	used for gg and sc design
			1350	[K]	used as expander cycle limit
V-29	Mixture type in gas generator	If undefined	oxygen rich	[−]	LOX-RP1, N2O4-MMH
			fuel rich	[−]	otherwise
NV-1	Prop. tank ullage volume fraction	Always	3	[%]	-
NV-2	Prop. tank boil off volume fraction	Always	0	[%]	LOX,LH2
NV-3	Prop. tank trap. volume fraction	Always	1.65	[%]	-
NV-4	Specific impulse correction factor	Always	0.9000	[−]	vacuum
			0.9038	[−]	sea level
			0.9	[−]	altitude
NV-5	TC mass correction factor	Always	1.52	[−]	-
NV-6	GG mass correction factor	Always	1.0	[−]	gg, sc
NV-7	Propellant tank performance factor	Always	3.32×10^4	$[m^2/s^2]$	-
NV-8	Press. tank performance factor	Always	12.2×10^4	$[m^2/s^2]$	COPV
			64.3×10^4	$[m^2/s^2]$	titanium
NV-9	Total propulsion system dry mass correction factor	Always	2.53	[−]	-

pf: pressure fed cycle | gg: gas generator cycle | MCC: main combustion chamber
sc: staged combustion cycle | ce: closed expander cycle | TC: thrust chamber
be: bleed expander cycle | reg.: regenerative | GG: gas generator
turb: turbine | press.: pressurant | prop: propellant

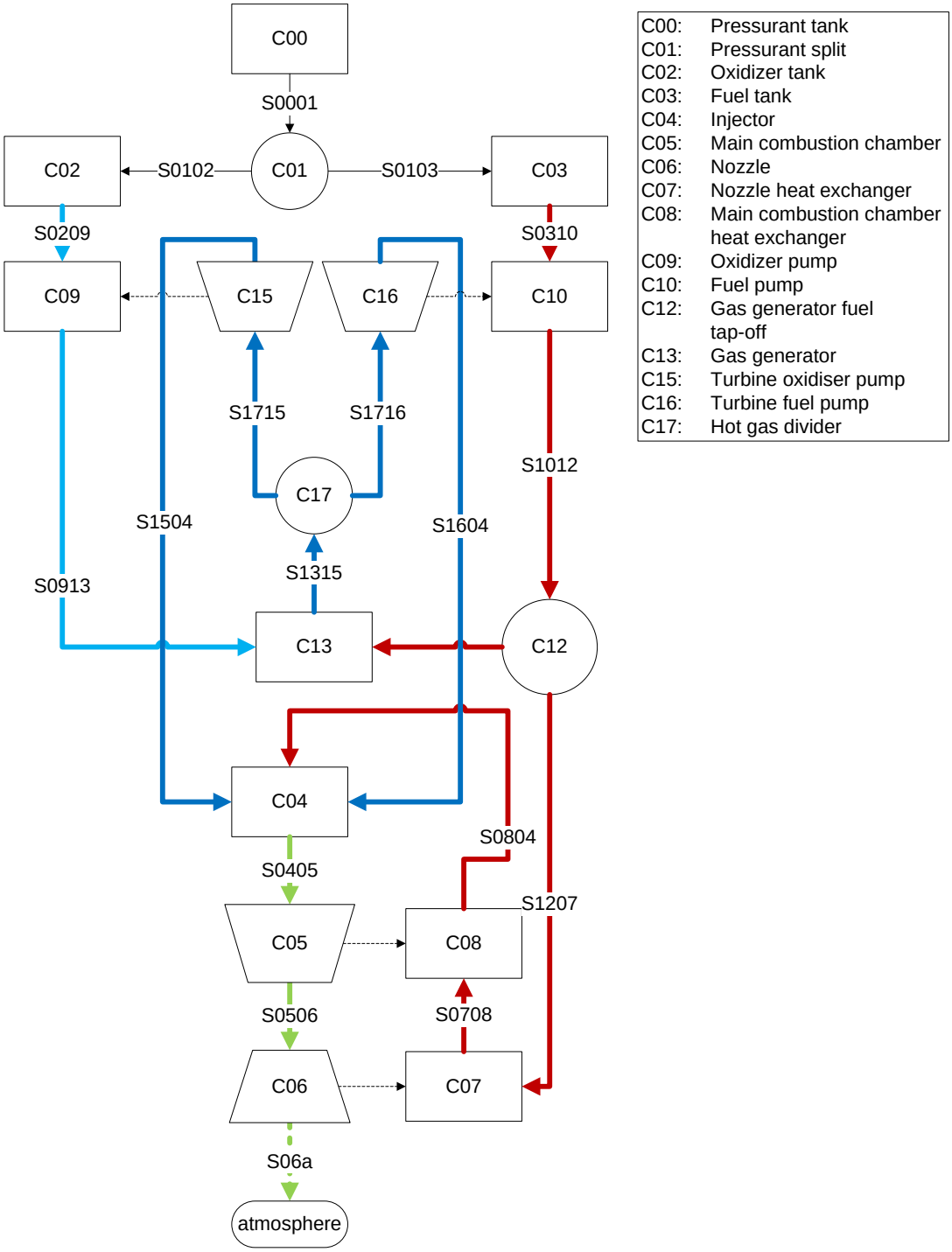

Figure 5-1: Oxygen rich staged combustion cycle with double turbines with regenerative chamber and nozzle cooling

A more elaborate overview of some possible engine cycles and cycle variation options is given in Appendix A. The components naming, required input and given output is described in Appendix C. Though in the ideal case the user would be able to construct his or her own engine using a component library in a way similar to EcoSimPro, this approach is hard to achieve in MATLAB. Simulink was considered but found unsuitable for the reason it cannot easily handle loops and the components need to be connected in order of calculation rather than the architecture which would mean the whole point of using a visual component library would be lost. Therefore the choice was made to let the user only choose from pre-defined cycle options. Initially this will only be pressure-fed, gas generator, staged combustion, closed expander cycle and bleed expander cycle, with either chamber and nozzle regenerative cooling, regenerative chamber cooling only or no cooling at all. Further also the choice of one or two turbines and if applicable an oxygen or fuel rich mixture in the gas generator or pre-burner is given. While the amount of possibilities is hence not unlimited, the model is made such that new cycles or new architectural options of existing can easily be added.

5-5 Model Output

Some examples of how model output can be visualised are given in Figure 7-1 and Figure 7-2.

Flow properties.

The model calculates or estimates the flow properties in terms of velocity (v), Mach number (M), molar mass ($\hat{M}$), density (ρ), pressure (p), temperature (T), specific heat capacity (c_p), specific heat capacity ratio (γ), Prandtl number (Pr), Reynolds number (Re), viscosity (μ) and conductivity (k) at all relevant points in the engine cycle.

Cycle properties.

Next to aforementioned properties, characteristics of the engine such as pressure difference over the pump (Δp_p), pump power (P_p), turbine power (P_t), gas generator mixture ratio (MR_{gg}), gas generator pressure (p_{gg}), gas generator combustion temperature (T_{gg}), main combustion chamber temperature (T_{cc}), mass flow ($\dot{m}$) in the lines, over the pumps ($\dot{m}_p$) and in the main combustion chamber ($\dot{m}_{mcc}$) and nozzle ($\dot{m}_{nozzle}$) are calculated.

Propulsion system performance, dimensions and mass.

In every engine analysis run, the performance of the engine and the mass and dimensions of the individual components are estimated. Performance output, given both for vacuum and at sea level conditions, are specific impulse (Isp), thrust (F), characteristic velocity (c^*) and thrust coefficient (C_F). The mass (m) of the components are the pressurant tank mass ($m_{\text{press tank}}$), oxidiser tank mass ($m_{\text{ox tank}}$), fuel tank mass ($m_{\text{fuel tank}}$), turbo-pump mass (m_{tp}), gas generator mass (m_{gg}), thrust chamber mass (m_{tc}), pressurant mass (m_{press}), oxidiser (m_{ox}) and fuel (m_{fuel}) mass. And finally dimensions are engine length $(L)_{engine}$ and diameter $(d)_{engine}$, turbo pump length (L_{tp}) and diameter (d_{tp}), gas generator or pre-burner length (L_{gg}) and diameter (d_{gg}), oxidiser tank volume ($V_{\text{ox tank}}$), fuel tank volume ($V_{\text{fuel tank}}$) and pressurant tank volume ($V_{\text{press tank}}$).

Sensitivity and uncertainty analysis.

During one-at-the-time sensitivity and uncertainty analysis a text file containing the sensitivity coefficients and estimated standard deviations of the considered parameters is created.

For sampling based sensitivity and uncertainty analysis using simple Monte Carlo analysis the values generated for the varied uncertainty parameters and the responses to the selected performance, mass and dimension parameters is stored to a text file.

More elaborate information is found in Chapter 9 and Appendix B, the latter also shows an example of the generated output files.

Optimisation.

The optimisation routine creates a text file containing all essential information on the optimisation ran and the results. More information is found in Chapter 8 and Appendix B, the latter also shows an example of a generated output file.

5-6 Balancing of Propulsion System

The method of iterative matching of pressure and power of the feed system of an engine cycle such that the system delivers the right amount of propellants under the correct pressure to the thrust chamber and at the same time sustains itself, hereafter referred to as balancing, differs from cycle to cycle. Therefore in this section the balancing of the feed system is discussed per engine cycle. The thrust chamber assembly calculations are however independent of the feed system, hence engine cycle. As they determine the requirements of the feed system they are discussed first.

The balancing schemes are large figures and therefore only the balancing scheme of the pressure fed cycle is given in this chapter; the schemes of the other cycles are found in Section 5-8.

5-6-1 Thrust Chamber Assembly Calculation Routine

Of the thrust chamber, first the main combustion chamber calculations are performed which yield the total conditions and the velocity in the chamber and the required oxidiser and fuel mass flow that needs to be supplied to the chamber. Next the injector and the nozzle calculations are performed; the injector calculations yield the required pressure at which the propellants need to be supplied to the thruster while the nozzle calculations yield the engine thrust, specific impulse, ΔV, thrust coefficient, characteristic velocity, etc. The component specific calculations are discussed in Section 3-2.

5-6-2 Balancing of the Feed System in the Presure-fed Cycle

First a typical pressure in the propellant tanks is assumed and the heat exchanger (cooling channel) calculations are performed; now the pressure loss over the heat exchanger is known the pressure required in the propellant storage tanks is corrected and the system is balanced. The procedure of achieving this is given schematically in Figure 5-2.

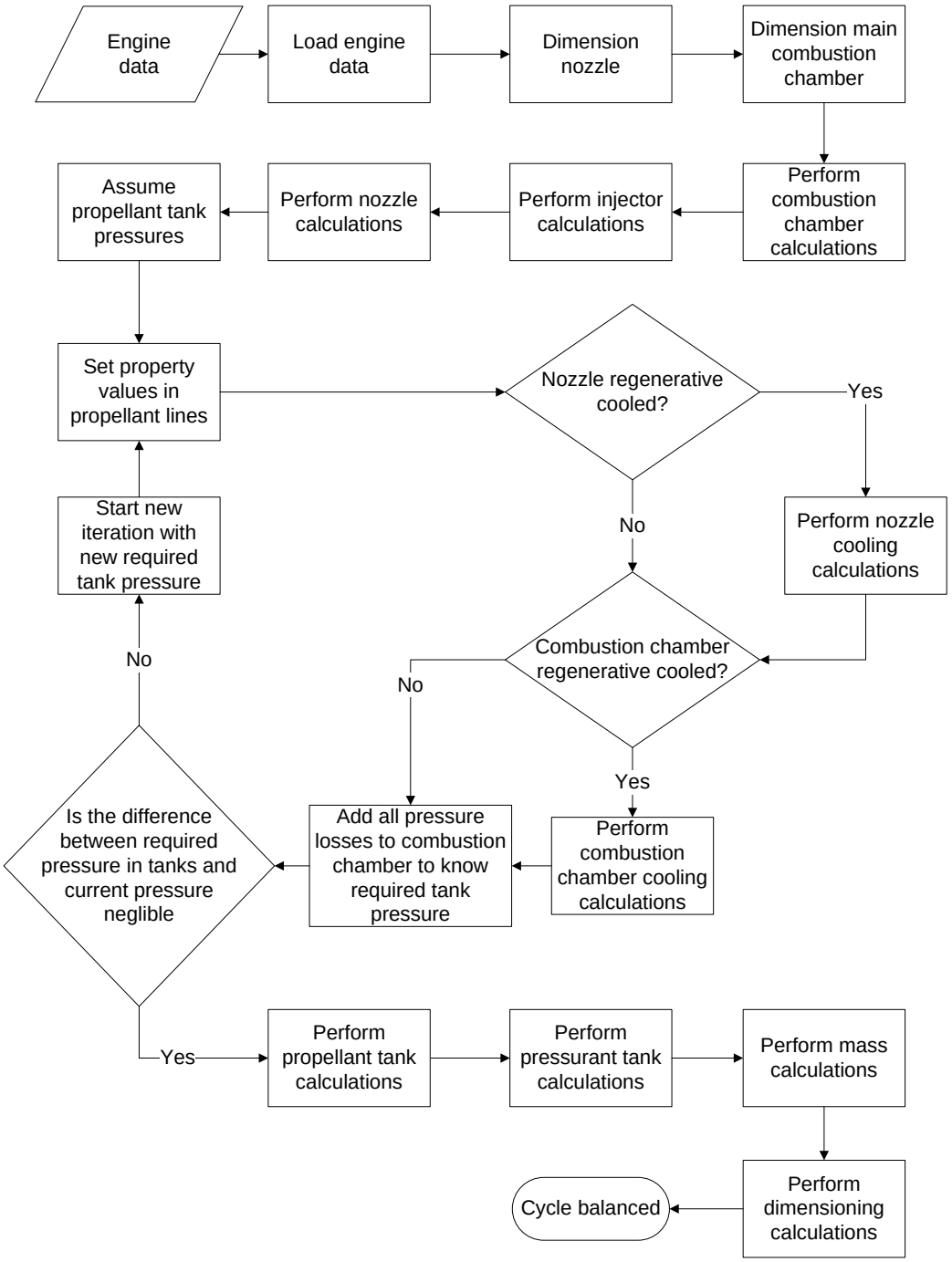

Figure 5-2: Pressure fed cycle balancing scheme

5-6-3 Balancing of the Feed System in the Gas Generator Cycle

In LiRA neither the gas generator pressure nor mixture ratio are user defined. Further each pump is either driven by an individual turbine or a single turbine drives both pumps (through a gearbox). The possibility to have each individual turbine be driven by a separate gas generator, this is for example the case in full flow staged combustion engines, is not yet considered as this configuration adds complexity which does not add any additional value in answering the research questions set in this work and is thus ignored at this point. In case a gearbox is needed, it does not need to be modelled as the rotation speeds are not playing a role in the current model; however the mass of a gearbox should be included in the turbo-pump mass estimation.

It is assumed that the flow properties remain the same from the gas generator to the turbine, even if the flow is split from the gas generator to two separate turbines. As the mass flow through the generator (m_{gg}) nor through the turbine(s) (m_T or $m_{T_{ox}}$ and $m_{T_{fuel}}$) is not known one needs to iterate for the mass flow(s) until estimated mass flow corresponds with the (sum of the) calculated mass flows through the turbine(s). The iteration scheme for balancing the gas generator cycle is illustrated by Figure 5-3.

The initial guess for the mass flow through turbine follows from the knowledge that the mass flow through the gas generator is usually about 2 % to 5 % of the total mass flow [31]; so then when 2 % is assumed:

$$\left.\begin{aligned} \dot{m}_{tot} &= \dot{m}_{mcc} + \dot{m}_{gg} \\ \dot{m}_{gg} &= 0.02 \cdot \dot{m}_{tot} \Rightarrow \dot{m}_{tot} = \tfrac{\dot{m}_{gg}}{0.02} \end{aligned}\right\} \dot{m}_{gg} = \frac{0.02 \cdot \dot{m}_{mcc}}{0.98 \cdot \dot{m}_{mcc}} = \frac{\dot{m}_{mcc}}{49} \tag{5-1}$$

and then the initial guess becomes:

$$\begin{cases} \dot{m}_T = \dot{m}_{gg} & \text{one turbine} \\ \dot{m}_{T,ox} = \dot{m}_{T,fuel} = 0.5 \cdot \dot{m}_{gg} & \text{two turbines} \end{cases} \tag{5-2}$$

where in case of two turbines it is assumed as first guess that each turbines receives half of the mass flow produced by the gas generator.

The pressure drop over the turbine is an input hence the pressure and temperature after the turbine follow from:

$$p_{out} = \frac{p_{out}}{p_{in}} \cdot p_{in} \tag{5-3}$$

$$T_{out} = T_{in} \cdot \left(\frac{p_{out}}{p_{in}}\right)^{\left(\frac{\gamma-1}{\gamma}\right)} \quad \text{where } T_{in} \approx T_{gg} \tag{5-4}$$

where for Eq. (5-4) the isentropic relation has been used. The iterative process of finding the mass flow through the turbine(s) is shown in Figure 5-4.

5-6-4 Balancing of the Feed System in the Staged Combustion Cycle

For the staged combustion cycle the important assumption is made that when a fuel rich mixture in the pre-burner is chosen, all the fuel needed in the main combustion chamber is coming from the pre-burner and in the main combustion chamber only additional oxidiser is added to balance the mixture ratio. Similarly when a oxygen rich mixture is set by the user in the pre-burner,

it is assumed that all oxygen needed in the main combustion chamber is passing through the pre-burner while additional fuel is added in the main combustion chamber to balance the mixture ratio. In other words though that in the pre-burner already fuel and oxidiser is mixed, ignited and combusted partially, it is assumed that the flow which is created and injected into the main combustion chamber has been mixed but has not undergone any combustion. This assumption will hence lead to too optimistic combustion in the main combustion chamber and underestimation of the required propellant mass flow and hence mass. The procedure of balancing the cycle is depicted in Figure 5-5.

For the balancing of the turbine initially a pressure ratio of 1.01 over the turbine is assumed, knowing the required outlet pressure this will yield a required inlet pressure and thus a required pump pressure rise. This will yield a required pump power and thus a new required mass flow through the turbine(s), however as the total mass flow through the turbine(s) is fixed in a staged combustion cycle the pressure ratio over the turbine will need to be increased or decreased in order to tune the required pump power to the power delivered by the turbine, this iterative process is shown in Figure 5-6.

5-6-5 Balancing of the Closed Expander Cycle

The closed expander cycle works the same as the staged combustion cycle with that difference that no pre-burner is present. The turbo-pump is driven by hot gaseous fuel created by heat exchange of the thrust chamber and fuel feed lines (regenerative cooling). In these designs the heat exchange is important as the turbine inlet temperature should be such that it is as high as the turbine inlet allows, in order to have minimal required mass flow and minimal required pressure ratio and thus a minimal turbo-pump mass. However as argued in Section 3-3, the modelling detail and thus accuracy of the cooling channels is limited to straight channels and hence the results obtained when balancing the closed expander cycle might not be the optimal ones. The schemes for solving the closed expander cycles are given by Figure 5-7 and Figure 5-8.

5-6-6 Balancing of the Feed System in the Bleed Expander Cycle

Just as the closed expander cycle works the same as the staged combustion cycle with that difference that no pre-burner is present, in theory the bleed expander cycle, (also called open expander cycle) works the same as the gas generator cycle with the difference no gas generator is present. Instead of tapping off cool fuel of the feed lines, hot gaseous fuel is tapped off of the fuel flow just before it is injected into the main combustion chamber. This hot gaseous fuel is created by passing cool fuel through a heat exchanger connected to the thrust chamber (regenerative cooling). The tapped off gaseous fuel is passed through a turbine and then dumped into the atmosphere; often through a small nozzle to generate some additional thrust, or the flow is injected at the end of the nozzle of the main combustion chamber to increase the mass flow (and thus Isp and thrust). However it was observed that many bleed expander cycles have a fuel bypass which leads fuel after the pump directly to the main combustion chamber without passing the heat exchanger. This thought to be due to the fact that when all fuel passes the heat exchanger, the mass is too large to be heated sufficiently to have the turbine work. On the other hand when only the fuel required by the turbine is passing the heat exchanger often the fuel temperature is too hot for the turbine blades and hence an adaptation to the cycle has been made such that the fuel is partially bypassing the heat exchanger as can be seen in Figure A-6. To determine the pressure ratio over the turbine(s) the same rationale as was the case for the gas

generator cycle is used. The balancing schemes of the bleed expander cycle are given in Figure 5-9 and Figure 5-10.

5-7 Overview Developed Code

The only functions not developed by the author of this work are the standard Matlab build-in functions and the function called `progressbar.m`[1] which creates, as the name suggests, the progress bars when running the code. All code of LiRA developed is summarised in Section 5-8, Table 5-6, Table 5-7 and Table 5-8. In total 6518 lines source code and 656 lines of comment have been written distributed over 90 files of which three are main execution files and the other functions (hence subroutines) of these three.

5-8 Large Figures and Tables

Figure 5-3 shows the the iteration scheme for balancing the gas generator cycle where Figure 5-4 shows the balancing of the turbo-pump.

Figure 5-5 shows the the iteration scheme for balancing the gas generator cycle where Figure 5-6 shows the balancing of the turbo-pump.

Figure 5-7 shows the the iteration scheme for balancing the gas generator cycle where Figure 5-8 shows the balancing of the turbo-pump.

Figure 5-9 shows the the iteration scheme for balancing the gas generator cycle where Figure 5-10 shows the balancing of the turbo-pump.

[1] developed by Steve Hoelzer and freely available here: [65]

Table 5-6: Overview of developed code for LiRA (1/3)

Function	# sl	# cl	Short description of function
Main routines			
main	59	4	Run normal engine analysis routine for a engine definition file
main_sensitivity_analysis.m	151	3	Run sensitivity and uncertainty analysis routine
main_optimisation.m	159	15	Run optimisation routine
Main subroutines			
run_engine_analysis.m	71	1	Run engine analysis routine
FOSA	107	15	Run first order one-at-the-time sensitivity analysis
SMCA	271	8	Run simple Monte Carlo uncertainty analysis
optimisation_routine	311	22	Run optimisation routine
Component related			
combustionchamber.m	132	19	Perform combustion chamber performance related calculations
chambercooling.m	340	54	Perform chamber heat exchanger performance related calculations
dimensioning.m	130	12	Calculate size of a component
calculatemass.m	177	10	Calculate mass of a component
gasgenerator.m	35	0	Perform gas generator performance related calculations
injector.m	152	13	Perform injector performance related calculations
pressuranttank.m	62	15	Perform pressurant tank performance related calculations
nozzle.m	106	11	Perform nozzle performance related calculations
propellanttank.m	48	8	Perform propellant tank performance related calculations
pump.m	2	0	Perform pump performance related calculations
setdimensions.m	16	1	Set dimensions of all components that have not been sized yet
setmasses.m	28	10	Set masses of all components
setpropellantdata.m	378	18	Set propellant properties in feed lines
turbine.m	31	5	Perform turbine performance related calculations
throatandnozzlecooling.m	227	31	Perform nozzle heat exchanger performance related calculations
Balancing routines			
balance_bleedexpandercycle.m	209	14	Balance bleed expander cycle feed system
balance_closedexpandercycle.m	256	22	Balance closed expander cycle feed system
balance_gas_generator_cycle.m	84	9	Balance gas generator cycle feed system
balance_pressure_fed_cycle.m	74	5	Balance pressure fed cycle feed system
balance_stagedcombustion.m	169	5	Balance staged combustion cycle feed system
turbopumpbalance_gasgenerator.m	173	12	Balance turbo pump in the gas generator cycle feed system
turbopumpbalance_preburner.m	301	11	Balance turbo pump in the staged combustion cycle feed system

sl: number of source code lines # cl: number of comment lines

Table 5-7: Overview of developed code for LiRA (2/3)

Function	# sl	# cl	Short description of function
Data load, read and save routines			
characteristiclength.m	21	2	Return characteristic length for a given propellant combination
conductivity_pure_substance.m	37	1	Return conductivity of a pure substance in (gas-)liquid state
density_pure_substance.m	37	1	Return density of a pure substance in (gas-)liquid state
loadconstraints.m	17	0	Load constraints from text file
loadenginedata.m	168	0	Load input parameter values from engine definition file
materialdata.m	53	0	Return material ultimate strength, density and conductivity
molarmass_pure_substance.m	13	0	Return molar mass of a pure substance in (gas-)liquid state
parameterrange.m	161	2	Return minimum, maximum, average and standard deviation of an input parameter
physical_properties.m	23	6	Return of a pure substance in liquid state its specific heat of vapourisation the reference pressure and temperature for which this value holds
pressurantdata.m	27	2	Return molar mass, specific heat ratio, critical temperature and critical temperature of a pressurant
reset_all_parameters.m	87	0	Clear all parameters who's values interfere with further calculations
save_mc_sensitivity_study_to_file.m	100	2	Save the results of the uncertainty study with Monte Carlo to a text file
save_optimisation_to_file.m	55	0	Save results of optimised propulsion systems to file
searchlibrary.m	75	5	Return a property of a gas or gas mixture
specificheat_pure_substance.m	37	1	Return specific heat ratio of a pure substance in (gas-)liquid state
useTypicalDesignValue.m	190	20	Return a typical or calculated value for an undefined parameter or return a correction parameter value
viscosity_pure_substance.m	37	1	Return viscosity of a pure substance in (gas-)liquid state
Other functions			
addannotation.m	2	0	Add an annotation to a plot
drawellipse.m	9	0	Draw ellipse in plot
filterdata.m	118	1	Filter out data that does not meet constraints of optimisation
find_min_req_mflow_heatexchanger.m	158	11	Find minimal required mass flow that needs to go through the heat exchanger of an expander cycle to have an acceptable turbine inlet temperature.
generatesamples.m	13	0	Generate a specified number of samples with a chosen distribution
generatesamples_within_range.m	14	0	Generate a specified number of samples with a chosen distribution within a specified range
makeplot.m	99	5	Make specified plot
promptuser.m	31	4	Prompt the user with a request for input
setparameter.m	96	0	Set (or change) a parameter value
sortdata.m	9	2	Sort data arrays along a column
std_2D.m	28	4	Calculate standard deviation along semi-major axis, standard deviation along semi-minor axis and angle of rotation of the standard deviational ellipse for a given two dimensional data array
wallthickness.m	13	1	Determine if wall thickness meets minimum thickness and if not set to minimal thickness

sl: number of source code lines # cl: number of comment lines

Table 5-8: Overview of developed code for LiRA (3/3)

Function	# sl	# cl	Short description of function
Basic calculation functions			
calculateMach.m	22	1	Calculate Mach number from area-Mach relation
calculatemachfromvelocity.m	5	0	Calculate Mach number from a given velocity
calculatespecificheatratio.m	3	0	Calculate specific heat ratio from specific heat and molar mass
calculatevelocityfrommach.m	5	0	Calculate velocity form given Mach number
characteristicvelocity.m	5	0	Calculate characteristic velocity
combustionchamberarea.m	3	4	Determine combustion chamber cross-sectional area
combustionchamberlength.m	2	0	Determine combustion chamber length
compressibilityfactor.m	19	1	Calculate gas compressibility factor
convectiveheatcoefficient_gasside.m	12	1	Calculate convective heat transfer coefficient at hot gas side
convectiveheatcoefficient_liquidside.m	2	0	Calculate convective heat transfer coefficient at coolant side
densitynozzle.m	2	1	Calculate flow density at given location in thrust chamber
determinecoolingcase.m	53	20	Determine cooling case
determinepropellantcase.m	16	0	Determine propellant case
determinestate.m	23	6	Determine state of substance
determine_boiling_point.m	7	3	Determine boiling point of substance
gasgeneratorthroatarea.m	12	1	Determine gas generator cross-sectional area
heattransferrate.m	10	0	Calculate heat transfer rate
massflow.m	4	5	Calculate oxidiser, fuel and total mass flow from mixture ratio and continuity equation
mixtureratio_mixture.m	64	5	Determine the mixture ratio of a mixture for a given combustion pressure and temperature
nozzlepressure.m	2	1	Calculate flow pressure at given location in thrust chamber
nozzletemperature.m	2	5	Calculate flow temperature at given location in thrust chamber
pipepressureloss.m	22	2	Calculate pressure loss over pipe or cooling channel (segment)
Prandtl.m	2	0	Calculate Prandtl number
pressureinjector.m	9	3	Calculate pressure loss over injector and combustion chamber
Reynolds.m	2	0	Calculate Reynolds number
specificheat_liquidmixture.m	15	9	Calculate specific heat of a mixture of liquids
specificimpulse.m	19	4	Calculate specific impulse
thrust.m	6	3	Calculate thrust
thrustcoefficient.m	7	3	Calculate thrust coefficient
totalconditions.m	4	0	Calculate total pressure, temperature and density
Vandenkerckhovefunction.m	2	0	Calculate Vandenkerckhove value

sl: number of source code lines # cl: number of comment lines

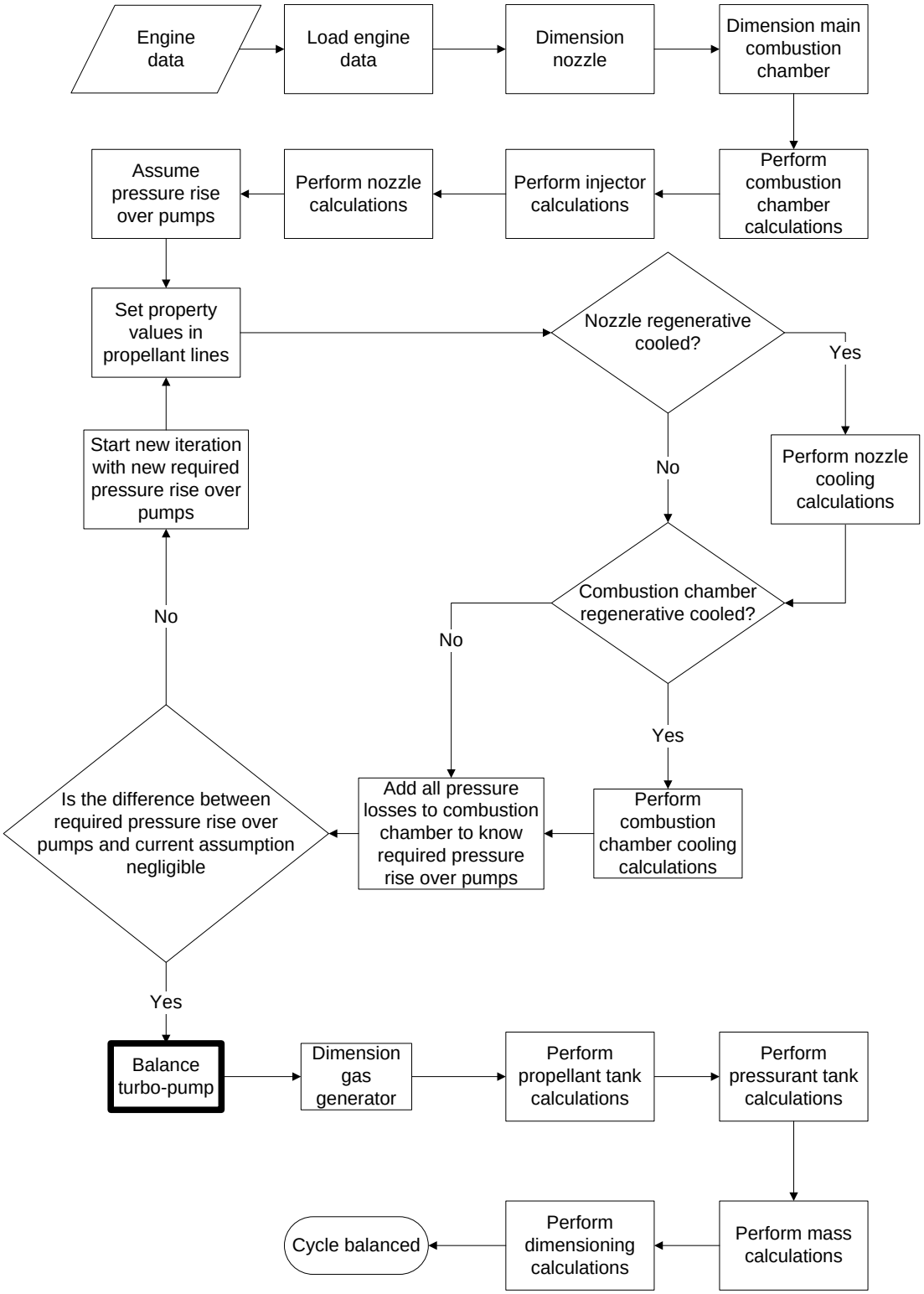

Figure 5-3: Gas generator cycle balancing scheme

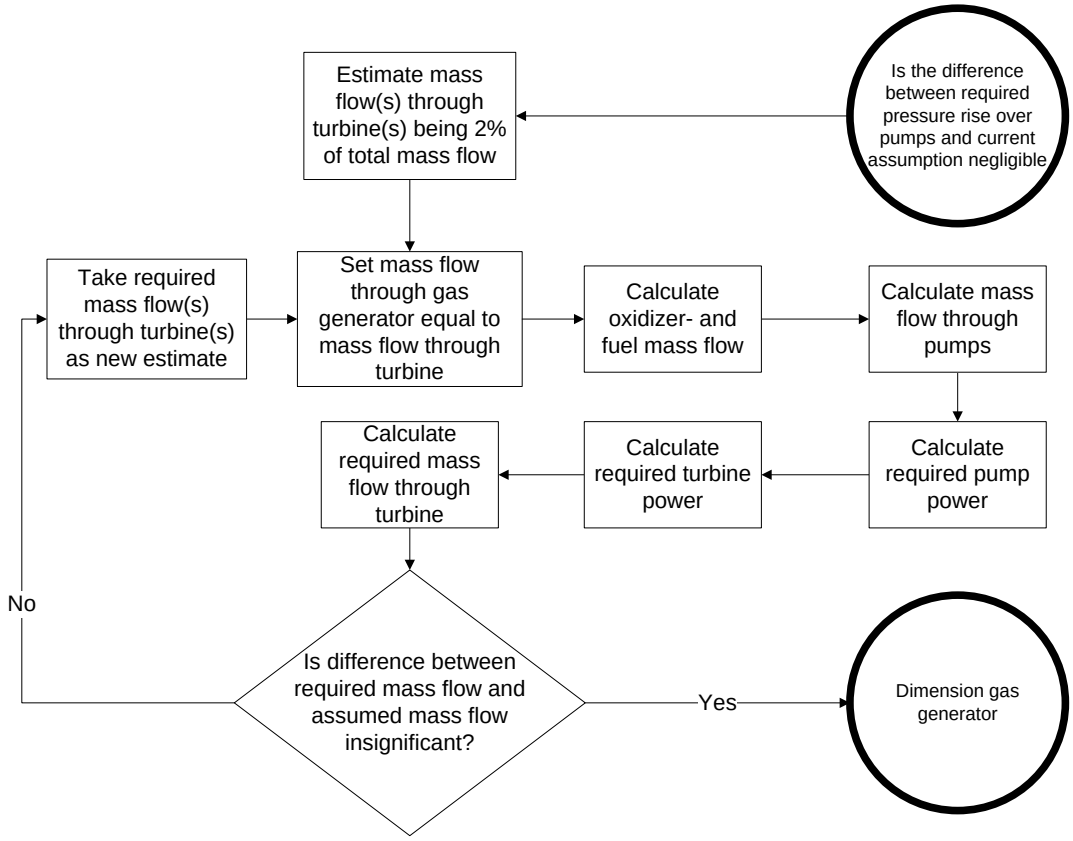

Figure 5-4: Gas generator cycle turbo-pump balancing scheme

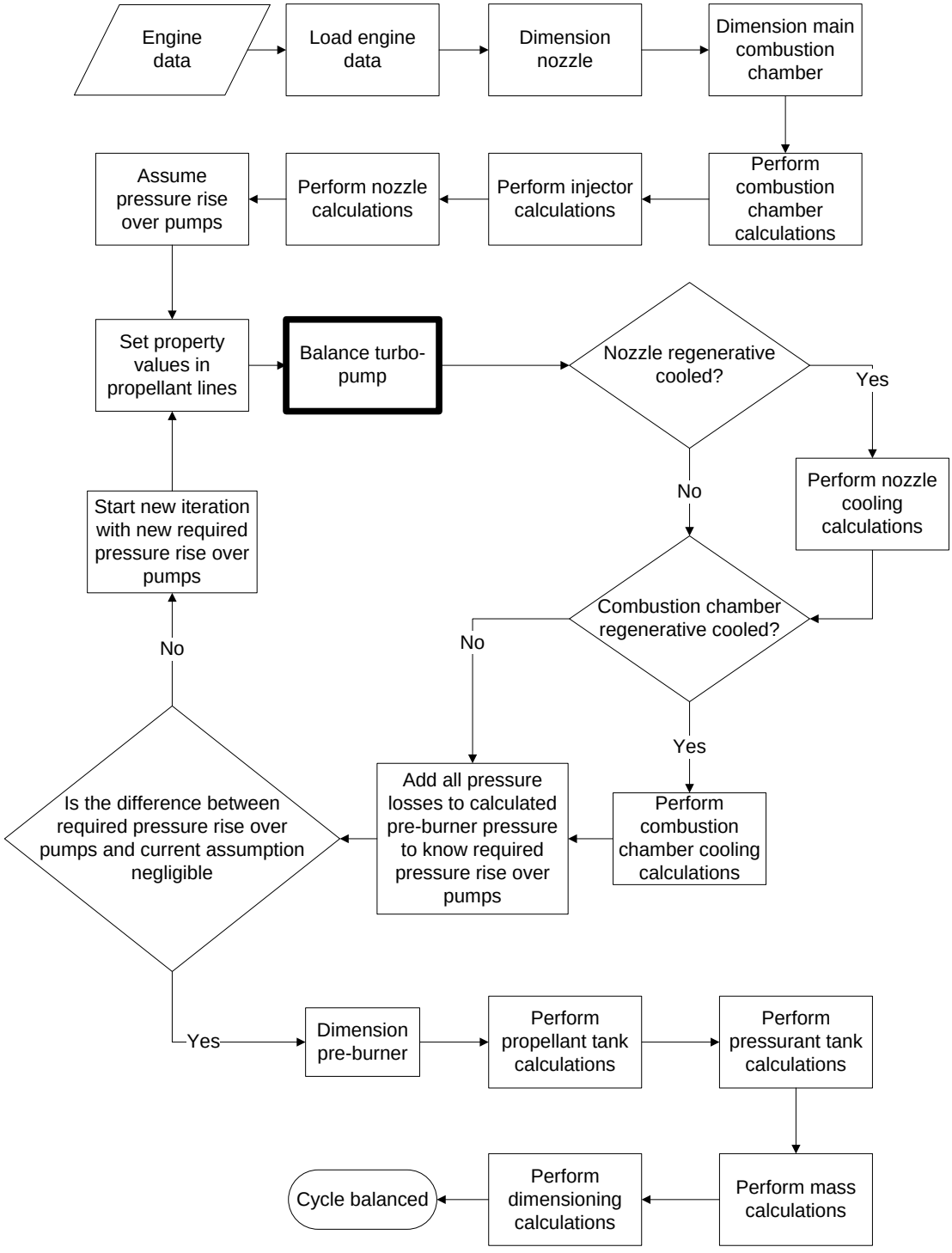

Figure 5-5: Staged combustion cycle balancing scheme

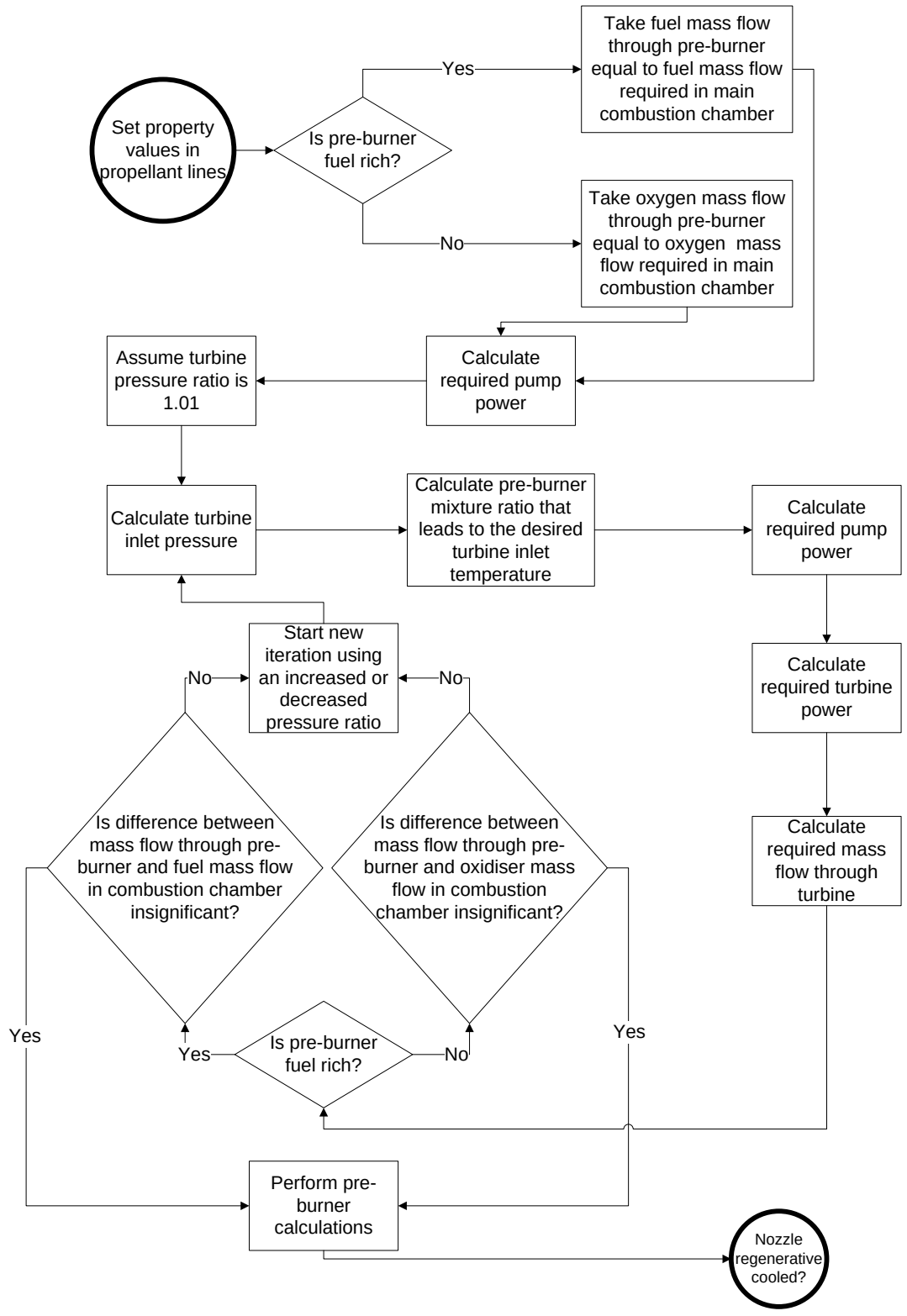

Figure 5-6: Staged combustion cycle turbo-pump balancing scheme

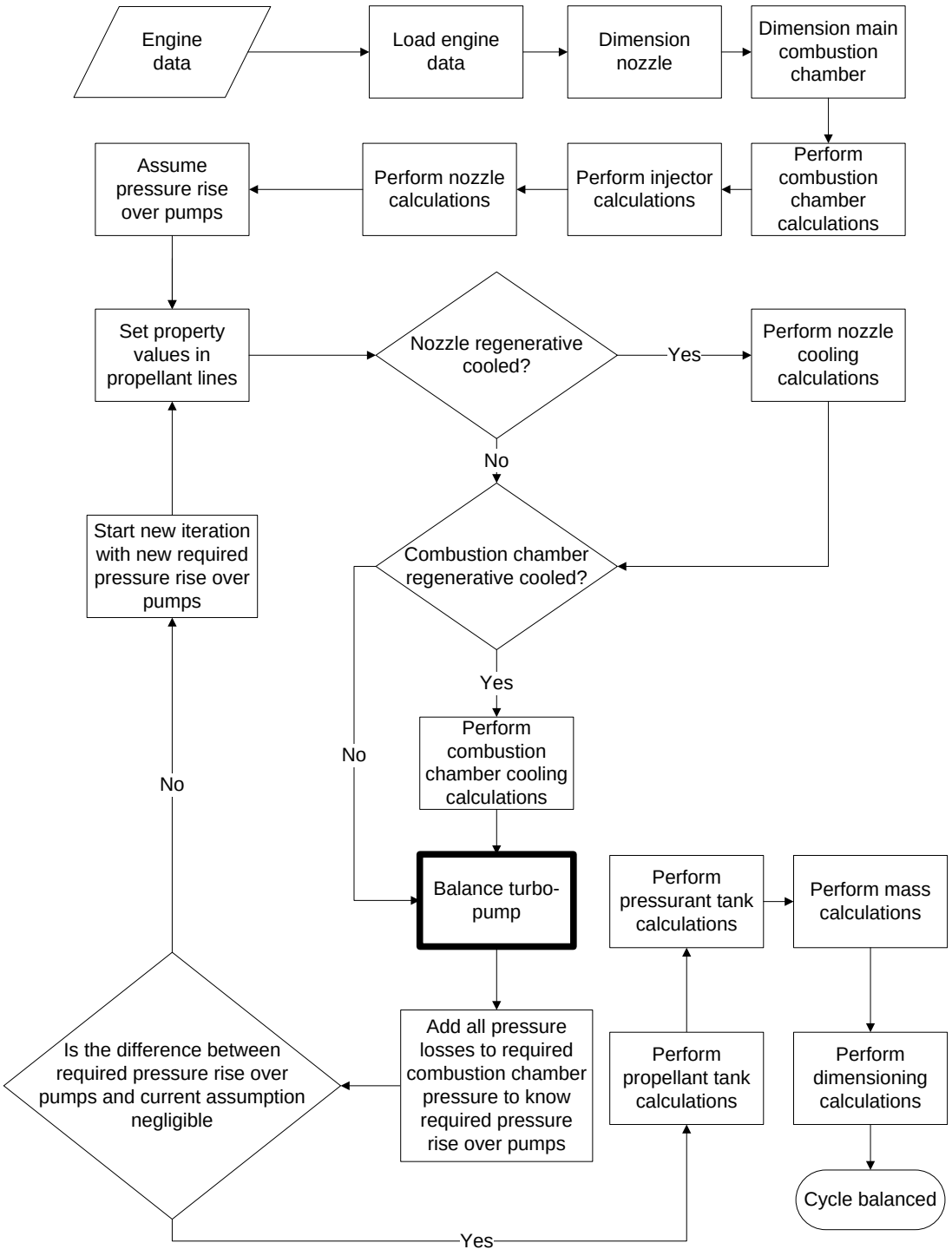

Figure 5-7: Closed expander cycle balancing scheme

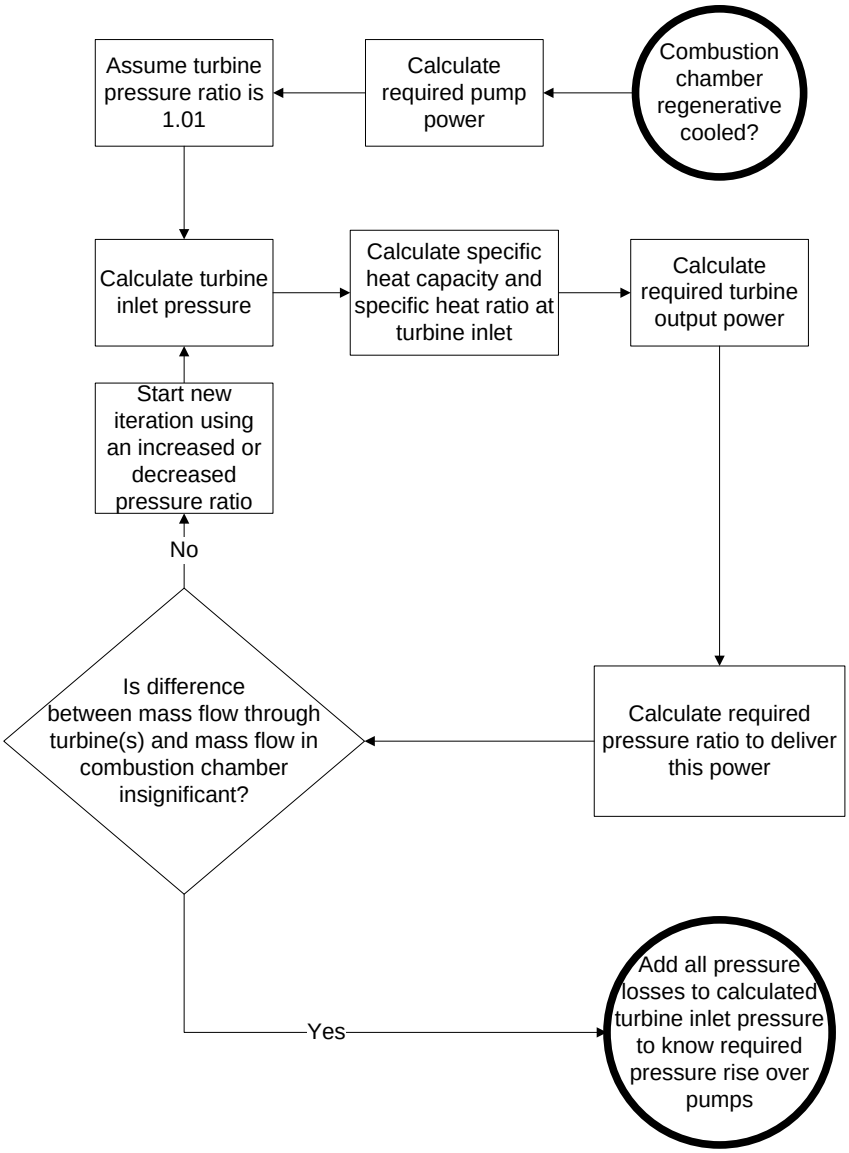

Figure 5-8: Closed expander cycle turbo-pump balancing scheme

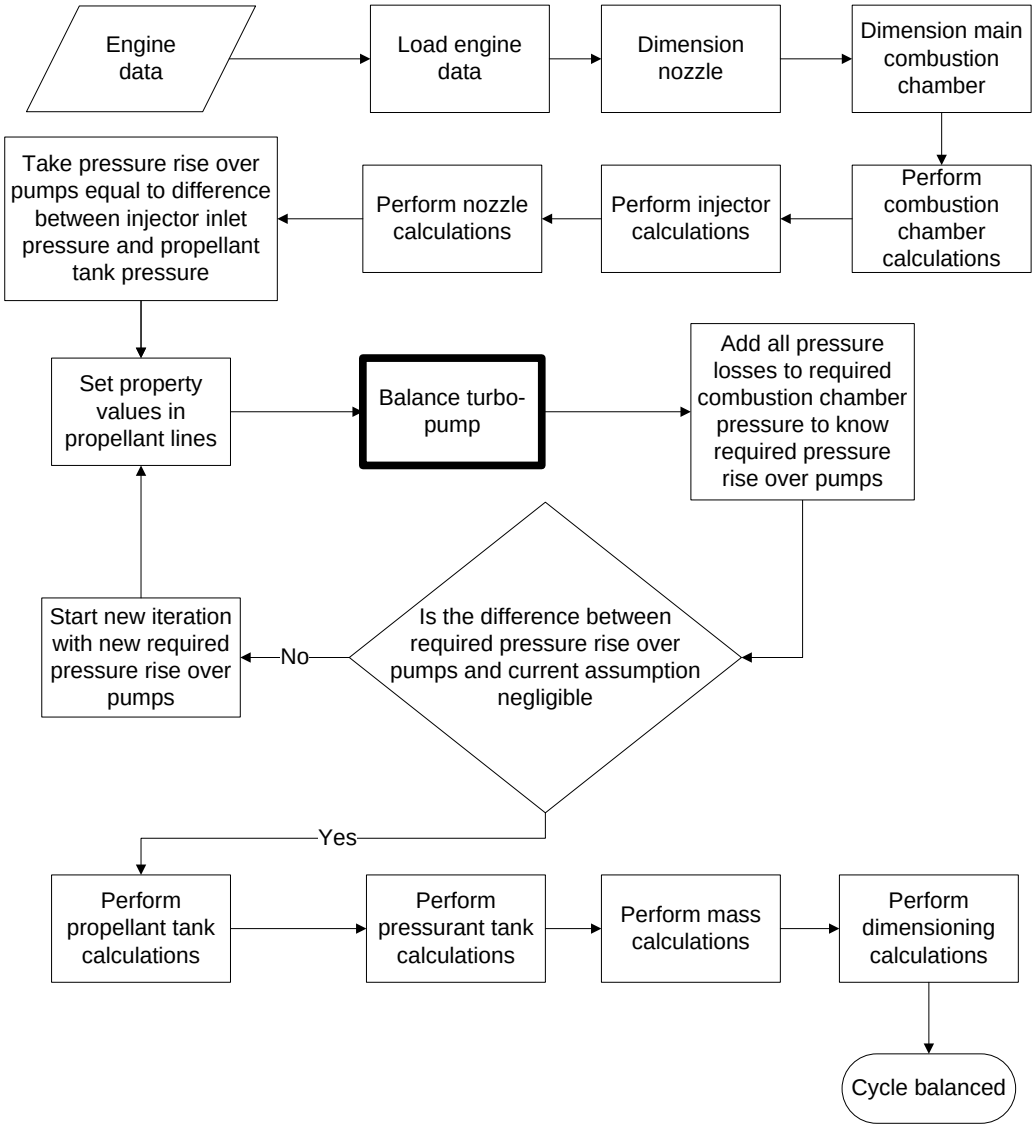

Figure 5-9: Bleed expander cycle balancing scheme

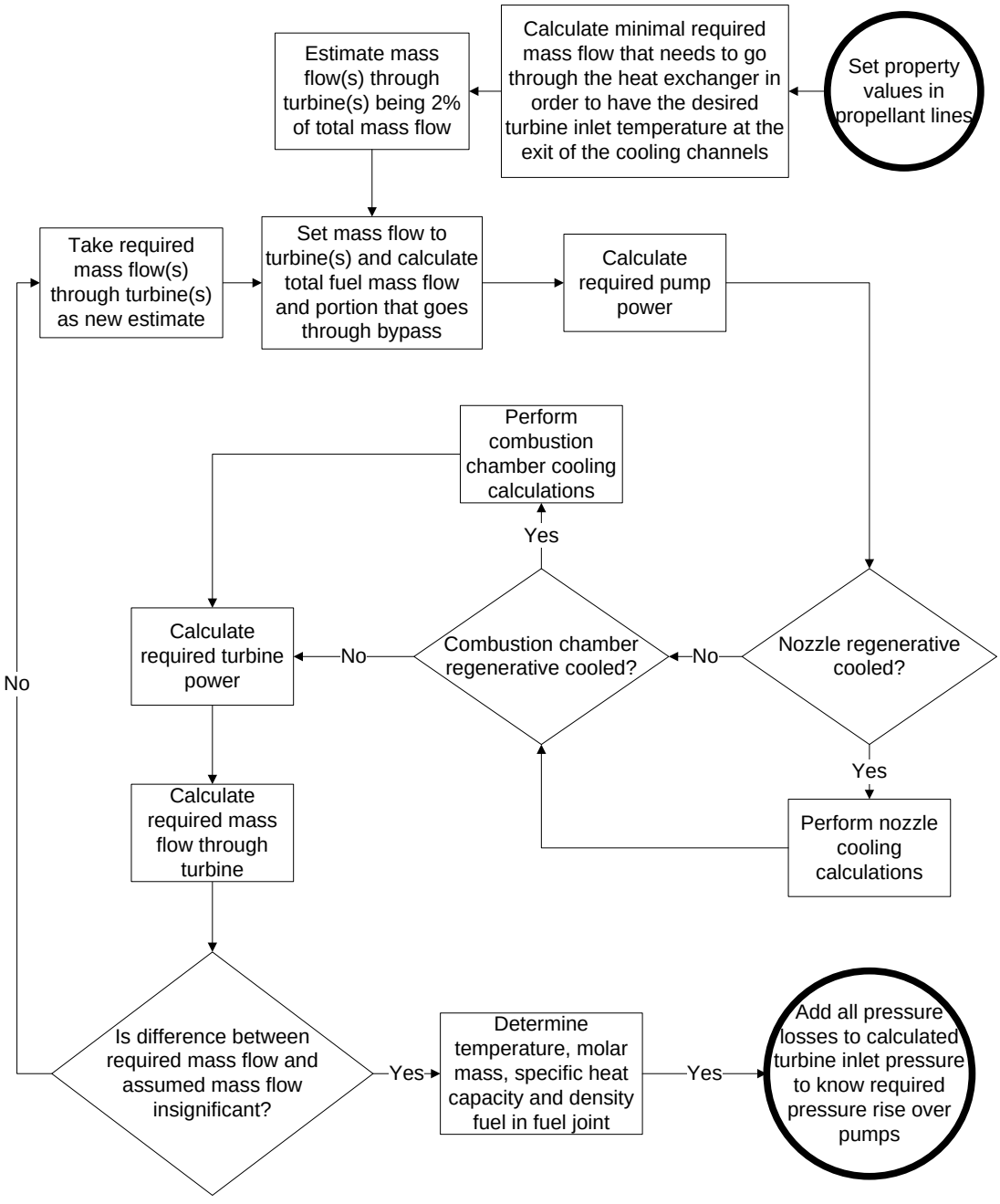

Figure 5-10: Bleed expander cycle turbo-pump balancing scheme

Chapter 6

Important General Statistical Analysis Theory Used for Verification, Validation and Sensitivity Analysis

The model applicability and usefulness are to a significant extend dependent on the accuracy and precision of the output. In the ideal case the model is both accurate (close to true value) and precise (low scatter, hence small standard deviation, variance and coefficient of variance); however precision has the priority as accuracy is due to systematic errors which can be corrected by calibration and precision is not. A systematic error is present in each outcome and means that results can still be compared relative to each other to draw conclusions. Accurate results with a low precision on the other had may have overlap in estimation range due to uncertainty in the outcome that makes comparison and conclusion drawing hard to impossible.

For example when several propulsion system with different engine cycles are optimised to meet a given set of requirements at minimal mass an accurate and precise system would be close to the true optimum and give every time the optimisation is run (almost) the same solutions for the optimised inputs. An accurate but in precise optimisation would give results close to the true optimum, but every time the optimisation is ran a different solution for the optimised inputs is found. A precise but inaccurate optimisation would yield every time it is performed almost identical set of optimised inputs but in reality be far from the true optimum. Finally a imprecise and inaccurate optimisation yields every time it is ran a totally different set optimised of optimised inputs which are often also far from the true optimum.

When having a precise but inaccurate system, still meaningful relative analysis of the results of the different optimised propulsion systems can can be performed knowing that when accuracy is improved, the relative trends observed, values found and conclusions made should not change which is not the case for an imprecise system even though it might be accurate.

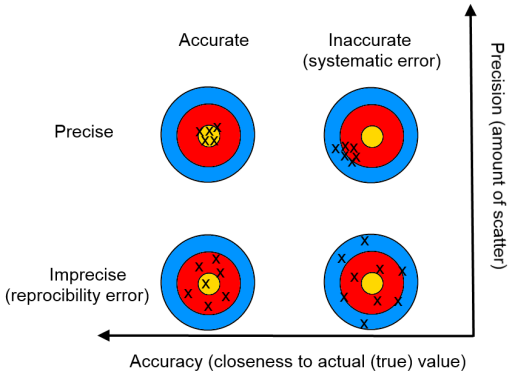

Figure 6-1: Archer analogy for explaining precision versus accuracy

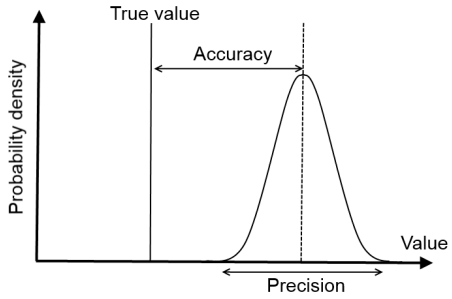

Figure 6-2: Precision versus accuracy

So in summary precision is expressed in terms of deviation of a mean value and has no relation with the actual value while accuracy determines how large the error is in the estimation method; Figure 6-1 and Figure 6-2 graphically explain the difference and relation between accuracy and precision.

Two types of errors are related to accuracy and precision and thus of importance for further study:

1. systematic (or determinate) errors which affect the accuracy of the results; these are being investigated by means of verification and validation.
2. random (or indeterminate) errors which affect the precision and are part of the uncertainty analysis.

6-1 Verification and Validation

The actual difference between an estimate and an expected (real) value is called the approximation error and can be expressed as an absolute error (E_{abs}), relative error (E_{rel}) or percentage error ($E_{\%}$):

$$E_{abs} = |y_i - f(x_i)| \tag{6-1}$$

$$E_{rel} = \left| \frac{y_i - f(x_i)}{y_i} \right| \tag{6-2}$$

$$E_{\%} = 100 \cdot \left| \frac{y_i - f(x_i)}{y_i} \right| \tag{6-3}$$

When having a collection of errors for a certain parameter, one can determine the standard deviation of these errors; the standard deviation of the errors in prediction is called the standard

error of estimation SEE [66]:

$$SEE = \sqrt{\frac{1}{N-1} \cdot \sum_{i=1}^{N} (y_i - f(x_i))^2} \tag{6-4}$$

The standard error of estimation (SEE) of Eq. (6-4) is to be interpreted just the same as a regular standard deviation (SD) of Eq. (6-5); the latter is an indication of how spread out a distribution of estimates is with respect to the mean of the distribution of estimates while the former (SEE) indicates the spread of predictions/estimates with respect to their expected/real values as given by the estimation function. [67].

6-2 Sensitivity Analysis

The standard deviation (from the mean) (SD) and standard error (of the mean) SE of the results obtained are found using following relations:

$$SD = \sqrt{\frac{1}{N-1} \cdot \sum_{i=1}^{N} (y_i - \bar{y})^2} \tag{6-5}$$

$$SE = \frac{SD}{\sqrt{N}} \tag{6-6}$$

with N the number of estimates, y_i the estimated value and $\bar{y}$ the mean value of the estimates. The standard deviation is an indication on how much variation there is around the estimation while standard error is a measure of the uncertainty of the standard deviation as one does not truly know the true value of the mean around which the standard deviation is constructed.

Let Z denote a standard normal random variable, $\phi(z_0)$ the area under the bell shape of a normal standard distribution function (depicted in Figure 6-3) from $z = 0$ till z_0; then the probability P that Z lies within z_0 standard deviations from the mean is given by [68]:

$$P(-z_0 \leq Z \leq z_0) = 2 \cdot \phi(z_0) \tag{6-7}$$

where the value of $\phi(z_0)$ can be obtained from normal curve area table such as given in Figure 6-3.

When the average value is an estimate, there is an uncertainty in the estimate of the average itself. However the central limit theorem of mathematical statistics states that the average (AVG) of a large number of independent values should have nearly a normal distribution [69], this means that $100 \cdot (2 \cdot \phi(z_o))$ percent of the time the actual true mean value for the output parameter considered must lie within the interval [68]:

$$AVG \pm z_0 \cdot SE \tag{6-8}$$

6-3 Data Interpretation and Acceptance

Statistics are always tricky regarding interpretation. When having a collection of estimates (or results) and actual values, the average of the estimates is simply found by summation of the

results and division by the number of estimates:

$$AVG = \frac{\sum_{i=1}^{N} y_i}{N} \tag{6-9}$$

The magnitude of the standard deviation (and thus also standard error) depends on the magnitude of the estimations and is inconvenient for comparison with estimates of another magnitude; the Relative Standard Deviation (RSD) and Relative Standard Error (RSE) allow to compare the obtained results for the different collection of estimates, for example for different cycles in this work. The RSD is the standard deviation divided by the mean, similarly RSE is calculated by dividing the SD by the estimate itself. The RSD and RSE are thus found by using following relations:

$$RSD[\%] = 100 \cdot \frac{SD}{AVG} \tag{6-10}$$

$$RSE[\%] = 100 \cdot \frac{SE}{f(x_i)} \tag{6-11}$$

When assuming the samples are normally distributed then the estimate($f(x_i)$) in Eq. (6-11) equals the average of the estimates found using Eq. (6-9). Estimates with high RSE values are considered less reliable than estimates with low RSE values; but where to put the boundary is subjective.

For example the US National Center for Health Statistics states in [70] that their estimates are "*considered statistically unreliable and are suppressed if 1) the denominator is based on fewer than 70 sample cases, or 2) the relative standard error (RSE) of the estimate (expressed as a percent) is greater than 30 percent.*". In [58] and [56] Zandbergen also states a relative standard error of estimate limit of maximum 30 percent should be taken in order to consider the estimate reliable. The Australian Bureau of Statistics however states on their website, see [71], that *"Estimates with a RSE of 25% or greater are subject to high sampling error and should be used with caution."*.

These examples show that no consensus exist though 30% seems to be the practical upper limit for the relative standard error of estimate to still consider the estimate reliable, and hence this limit will be taken when discussing results. Concerning the minimum amount of sample cases needed, no limit is set as it is not easy to find engine data, hence the determination of the accuracy and reliability of the estimates must be carefully interpreted.

6-4 Repeatability or reproducibility

Repeatability or reproducibility expresses the closeness of analysis results for the same input conditions over time. For some cases like optimisation a small variation in outcome is generally permitted as long as the conclusions are not affected. LiRA's main engine analysis routine and its results are all deterministic hence have perfect reproducibility. For the optimisation routine however use is made of (pseudo-)random generated values during Monte Carlo analysis and thus a different outcome than the one reported might be obtained. This is further discussed in Section 8-4.

6-5 Large Figures and Tables

Figure 6-3 contains a scan of a normal curve area table.

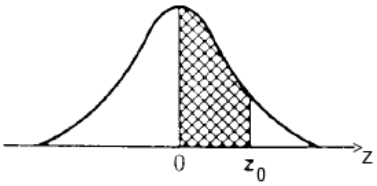

z_0	.00	.01	.02	.03	.04	.05	.06	.07	.08	.09
0.0	.0000	.0040	.0080	.0120	.0160	.0199	.0239	.0279	.0319	.0359
0.1	.0398	.0438	.0478	.0517	.0557	.0596	.0636	.0675	.0714	.0753
0.2	.0793	.0832	.0871	.0910	.0948	.0987	.1026	.1064	.1103	.1141
0.3	.1179	.1217	.1255	.1293	.1331	.1368	.1406	.1443	.1480	.1517
0.4	.1554	.1591	.1628	.1664	.1700	.1736	.1772	.1808	.1844	.1879
0.5	.1915	.1950	.1985	.2019	.2054	.2088	.2123	.2157	.2190	.2224
0.6	.2257	.2291	.2324	.2357	.2389	.2422	.2454	.2486	.2517	.2549
0.7	.2580	.2611	.2642	.2673	.2704	.2734	.2764	.2794	.2823	.2852
0.8	.2881	.2910	.2939	.2967	.2995	.3023	.3051	.3078	.3106	.3133
0.9	.3159	.3186	.3212	.3238	.3264	.3289	.3315	.3340	.3365	.3389
1.0	.3413	.3438	.3461	.3485	.3508	.3531	.3554	.3577	.3599	.3621
1.1	.3643	.3665	.3686	.3708	.3729	.3749	.3770	.3790	.3810	.3830
1.2	.3849	.3869	.3888	.3907	.3925	.3944	.3962	.3980	.3997	.4015
1.3	.4032	.4049	.4066	.4082	.4099	.4115	.4131	.4147	.4162	.4177
1.4	.4192	.4207	.4222	.4236	.4251	.4265	.4279	.4292	.4306	.4319
1.5	.4332	.4345	.4357	.4370	.4382	.4394	.4406	.4418	.4429	.4441
1.6	.4452	.4463	.4474	.4484	.4495	.4505	.4515	.4525	.4535	.4545
1.7	.4554	.4564	.4573	.4582	.4591	.4599	.4608	.4616	.4625	.4633
1.8	.4641	.4649	.4656	.4664	.4671	.4678	.4686	.4693	.4699	.4706
1.9	.4713	.4719	.4726	.4732	.4738	.4744	.4750	.4756	.4761	.4767
2.0	.4772	.4778	.4783	.4788	.4793	.4798	.4803	.4808	.4812	.4817
2.1	.4821	.4826	.4830	.4834	.4838	.4842	.4846	.4850	.4854	.4857
2.2	.4861	.4864	.4868	.4871	.4875	.4878	.4881	.4884	.4887	.4890
2.3	.4893	.4896	.4898	.4901	.4904	.4906	.4909	.4911	.4913	.4916
2.4	.4918	.4920	.4922	.4925	.4927	.4929	.4931	.4932	.4934	.4936
2.5	.4938	.4940	.4941	.4943	.4945	.4946	.4948	.4949	.4951	.4952
2.6	.4953	.4955	.4956	.4957	.4959	.4960	.4961	.4962	.4963	.4964
2.7	.4965	.4966	.4967	.4968	.4969	.4970	.4971	.4972	.4973	.4974
2.8	.4974	.4975	.4976	.4977	.4977	.4978	.4979	.4979	.4980	.4981
2.9	.4981	.4982	.4982	.4983	.4984	.4984	.4985	.4985	.4986	.4986
3.0	.4987	.4987	.4987	.4988	.4988	.4989	.4989	.4989	.4990	.4990

Source: Abridged from Table 1 of *Statistical Tables and Formulas*, by A. Hald, John Wiley & Sons, 1952. Reproduced by permission of John Wiley & Sons.

Figure 6-3: Normal curve areas, source [86]

Chapter 7

Verification and Validation of LiRA

When attempting to model a process, one will only succeed of approaching but never matching reality due to the need of simplifications, limited knowledge and uncertainty and mistakes. On top of this one can make a (almost) flawless product, but it might not suit the requirements and user needs. This is where verification and validation comes in place.

Using the explanation of Professor Easterbrook [72], verification and validation refer to two different types of analysis; validation serves to answer the question *"Is one building the right system?"*, while verification answers the question *"Is one building the system right?"*.

Put in other words validation is needed to check if the model meets the user needs while verification concerns whether the model is well constructed, free of mistakes, etc. [72]

Chapter 6 said that accuracy is determined by study of systematic errors. There are three sources of systematic errors [73]:

1. instrumental errors
   Usually this error refers to errors introduced due to off-sets in measurement equipment hardware; but as LiRA is pure software based, here the 'instruments' refer to the relations used which were acquired by data analysis (actual engine data). These errors can be fixed by calibration. For example when using empirical relations constructed by regression analysis or correction factors, a lower error can be simply obtained by increasing the sampling base used to determine the empirical relation or value of the correction factor respectively. Calibration was performed when introducing correction factors into the ideal rocket motor theory used in the performance model discussed in Chapter 3 and when using mass or sizing correction factors in Chapter 4.

2. methodological errors
   Solving scheme (order of solving, iteration schemes), simplifications, assumptions, etc. could all introduce a small error which sums up to significant differences in results and actual data. Methodological errors are hard to trace on systems level and often require validation on component or process level. The latter is not performed as it is not part of the scope of this work, but strongly recommended for future work when one desires to improve and/or expand LiRA. Validation of the models on system level is performed in Section 7-2.

3. personal errors
   The author of this work is human, and thus prone to human mistakes such as typos when writing code, logical errors when thinking a process through, incorrect reading of data, etc. A method of detecting these errors is by means of verification which is found in Section 7-1.

During verification two actions are needed: first the model itself needs to be checked on coding and logical errors and then in a second step the program operation has to be checked; is the program doing what it should do? For this LiRA's structure, operation, assumptions, required input and generated output are compared to similar programs. Next in order to find out how well the tool performs relative to others and were LiRA's strengths and weaknesses are, a comparison of the results of several test cases ran with LiRA and other similar software is performed. A test case is for example an engine analysis found in a publication of a study using similar modelling software. Ideally the output should be more or less the same (assuming the other software has been validated as well and found to meet user needs); however differences are to be expected and need to be assessed whether they are acceptable.

Some validation such as specific impulse, engine dry mass estimation and others was already performed on relation level when discussing the models. However to validate LiRA as a complete tool the accuracy of LiRA is studied. Here the performance, dimension and mass model are validated separately for several engines using available actual data; the real parameter values for the engines chosen are found in Appendix D. The Relative Standard Error of Estimate (RSE) is a measure of the accuracy of predictions and is determined for each relation separately using LiRA estimates; for some relations taken from work of others, a RSE value is given by the author of the relation, however because the relation input parameters can contain an error themselves, the estimate for a certain engine using the relation is not necessarily the same as the one given by the author of the relation. For example a relation requiring the vacuum thrust as input to yield a mass estimate will give for the same engine a different value when the true vacuum thrust is inserted and when the estimated vacuum thrust by LiRA is inserted; therefore the RSE values will be different too. Finally at the end of this chapter conclusions on the accuracy of LiRA are given.

7-1 Verification

Any program needs to be tested for programming and/or logical errors. The programming errors are detected by comparing hand calculations with the computer calculations while logical errors are detected by comparison of program results and trends with similar work conducted by others.

7-1-1 Checking of Model Code on Errors by Comparison of Results with Hand Calculations

For the gas generator cycle a complete hand calculation for the HM7B engine has been manually performed and compared with the model. During this verification several coding mistakes and some logical errors were found and fixed. Further throughout this work when odd or unexpected values were obtained, hand calculations were performed to check the obtained result. Often a mistake in the code was discovered this way. After this verification one can be fairly certain that no more coding errors exist in the model.

7-1-2 Tool Build-up Structure, Operation, Input and Output Comparison with Other Similar Software

Other similar tools were already introduced during the literature study and state-of-the-art review in Chapter 2. Half of the tools discussed (CEA, RPA and SCORES) are just modelling the combustion and thruster performance, while the other half (SEQ and LRP2, REDTOP PRO and EcoSimPRO) allow the user to model an entire cycle. The latter half uses combustion models based on or similar to the Gordon and McBride code used in CEA and all model the cycles in a modular way by creating components which are balanced in a specific order. Therefore to answer the verification question *"Is one building the system right?"* on can conclude that the tool build-up philosophy of LiRA is almost exactly the same as other similar tools.

7-1-3 Comparison of test cases with other models

RL10A-3-3A closed expander cycle.

The RL10A-3-3A is the upperstage engine of the Atlas and Titan launch vehicles. The engine is a closed expander cycle which operates on LOX and LH2 and produces 73.5 kN of vacuum thrust. Both nozzle and chamber are regeneratively cooled and the hot gas is passed through a single turbine, see Figure 7-4, which drives both oxidiser and fuel pumps through a gear box before entering the main combustion chamber.

This engine is modelled in [29] with REDTOP as test case for comparison and is modelled here again for validation. The output reported in [29] is however very limited and therefore only superficial comparison could be made. The values reported in [29] for the RL10A-3-3A engine and those obtained with LiRA are given in Table 7-1. The difference in mass flow rate could be explained by a different pump and turbine efficiency used.

RS-68 gas generator cycle.

The RS-68 is LOX-LH2 gas generator cycle engine with parallel flow turbines used on the Delta IV. Its main combustion chamber is regenerative cooled, while the nozzle has ablative cooling. Table 7-2 shows a comparison on modelling results between Redtop and LiRA. The difference in specific impulse is negligible, but all other parameters show significant deviations in estimated values. The mass flow rate difference is likely due to difference in gas generator pressure and mixture ratio as this affects the gas generator flow properties and the pump power requirements. As no data in [29] on this is mentioned, nor actual RS-68 engine data stating these values could be found, this hypothesis could not be verified.

The difference in T/W ratio is directly linked to the difference in estimated engine thrust and engine dry mass. The reason for overestimation of thrust by LiRA could not be determined due to the lack of engine data. Concerning engine dry mass, LiRA makes use of an empirical relation which does not make an estimate on basis of the individual component masses, while for REDTOP it is not stated how the mass estimate is done, this could be the difference. The engine length estimate of REDTOP is actually too short, according to [74], the RS-68 has an engine length of 5.2 m hence the LiRA's estimated value is closer to reality than REDTOP's, however it should be noted that the authors in [29] acknowledge a too low value for the length estimate and attribute it to the long powerhead arrangement of the RS-68.

Table 7-1: RL10A-3-3A

	Unit	LiRA	REDTOP-2 [29]	Real [4],[75]
Input				
Engine cycle	[–]	=	Closed expander cycle	
Oxidiser	[–]	=	LOX	
Fuel	[–]	=	LH2	
Nozzle exit diameter	[m]	1.02	N/F	
Nozzle area ratio	[–]	=	61	
Burn time	[s]	600	N/F	
Pressure main combustion chamber	[bar]	=	32.750	
Mixture ratio main combustion chamber	[–]	=	5.5	
Nozzle cooling	[–]	Regenerative cooling	N/F	
Chamber cooling	[–]	Regenerative cooling	N/F	
Oxidiser pump efficiency	[–]	0.64	N/F	
Fuel pump efficiency	[–]	0.555	N/F	
Number of turbines	[–]	1	N/F	
Turbine efficiency	[–]	0.72	N/F	
Turbine pressure ratio	[–]	1.41	N/F	
Output				
Vacuum thrust	[N]	80189	73396	73396
Tank supplied flow rate	[kg/s]	18.62	16.78	16.8
Vacuum Isp	[s]	439.13	443.85	446.4
Vacuum T/W	[–]	48.8:1	52.2:1	N/F
Engine dry mass	[kg]	167.4	143.3	138

=: idem N/F: not found

Table 7-2: RS-68 modelled with Redtop

	Unit	LiRA	REDTOP-2 [29]	Real [74],[39], [4]
Input				
Engine cycle	[–]	=	Gas generator	
Oxidiser	[–]	=	LOX	
Fuel	[–]	=	LH2	
Nozzle exit diameter	[m]	2.5	N/F	
Nozzle area ratio	[–]	=	21.5	
Burn time	[s]	242	N/F	
Pressure main combustion chamber	[bar]	=	97.9	
Mixture ratio main combustion chamber	[–]	=	6.0	
Nozzle cooling	[–]	No cooling	N/F	
Chamber cooling	[–]	Regenerative cooling	N/F	
Number of turbines	[–]	2	N/F	
Mixture type gas generator	[–]	Fuel rich	N/F	
Output				
Vacuum thrust	[kN]	3820.9	3340.6	3341
Tank supplied flow rate	[kg/s]	1019.9	803.8	N/F
Vacuum Isp	[s]	406.0	410.4	409
Sea level Isp	[s]	360.0	359.1	357
Vacuum T/W	[–]	77.1:1	55.1:1	N/F
Sea level T/W	[–]	68.4:1	48.2:1	N/F
Engine dry mass	[kg]	5052.6	6177.9	6800
Engine length	[m]	5.0	3.1	N/F

=: idem N/F: not found

SE-21D bleed expander cycle.

The SE-21D is a LOX-LH2 theoretical bleed expander cycle engine being studied in [28] using the LRP2 tool. Figure 7-6 shows the engine cycle and the conditions at certain locations in the cycle as published in [28] while Figure 7-1 shows the LiRA equivalent engine cycle with the conditions at the same locations in the engine cycle (note: values in bold are input). There is however one important difference in the engine cycle; the original engine cycle has two fuel pumps while in LiRA only one pump can be modelled. When studying Figure 7-6 one can see the the secondary fuel pump is used for the fuel that is tapped off to go as coolant to the heat exchanger after which it is mainly used as hot gas to drive the turbine but also partially is injected into the main combustion chamber. As significant pressure loss finds place over the heat exchanger and the pressure at injector inlet must be higher than the combustion chamber (due to the minimum required pressure ratio over the injector), the portion of fuel used as coolant must be delivered to the heat exchanger at a higher pressure than the fuel that is going directly after passing the first pump into the main combustion chamber. LiRA is currently not capable of adding a second pump and therefore in theory will require a higher pressure rise over the fuel pump.

The thruster performance and flow conditions are very close, however two significant differences are observed; the first is the nozzle exit temperature and exit velocity though the exit Mach number is almost identical. The reason LiRA estimates the exit temperature too high is because the heat loss due to regenerative cooling is not taken into account in the temperature development in the nozzle. Consequentially due to the same reason the local speed of sound at the exit is also higher and hence yields a higher exit velocity value in LiRA even though the Mach numbers are in both models almost the same. The second significant difference is the heat exchanger inlet pressure (and thus also the fuel pump discharge pressure) which in LiRA is about 3 MPa lower than the engine cycle modelled with LRP2. This difference can only be explained by the underestimation of pressure losses over the heat exchanger in LiRA.

Conclusions are hence that LiRA must allow multiple pumps in order to model cycles more accurately and further should have a more elaborate heat exchanger model such that pressure losses are estimated more accurately.

SLME fuel rich staged combustion cycle.

In [18] and [25] different LOX-LH2 staged combustion engine cycles are studied for the use in a SpaceLiner. For the booster, among others, a fuel rich staged combustion engine is studied. The engine cycle and the conditions at certain locations in the cycle, which is modelled in LRP2, as published in [25] is given in Figure 7-8. The equivalent engine cycle and the conditions at the same positions in the cycle when modelled by LiRA are given in Figure 7-2 (note: values in bold are input). There is again one significant difference, namely the original engine cycle makes use of two oxidiser pumps while LiRA only allows the modelling of a single oxidiser pump.

The thruster performance and geometry results are very similar, in the feed system a large difference in pump discharge pressure at fuel side is observed. It seems LiRA heavily underestimates pressure losses over the heat exchanger. The pre burner pressure and mixture ratio estimates in LiRA correspond close to those in LRP2.

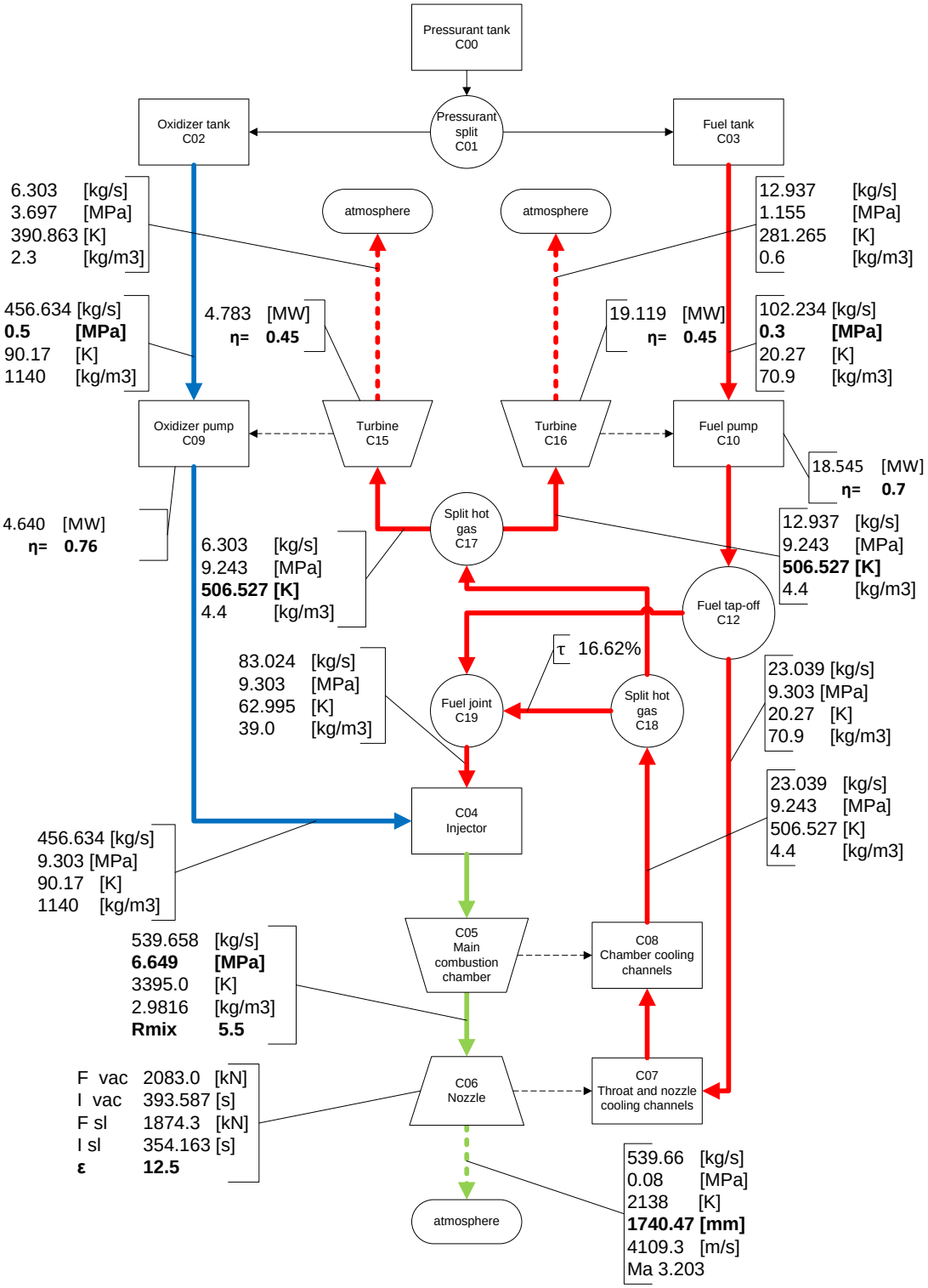

Figure 7-1: Thermodynamic conditions inside expander bleed cycle engine SE-21D calculated with LiRA

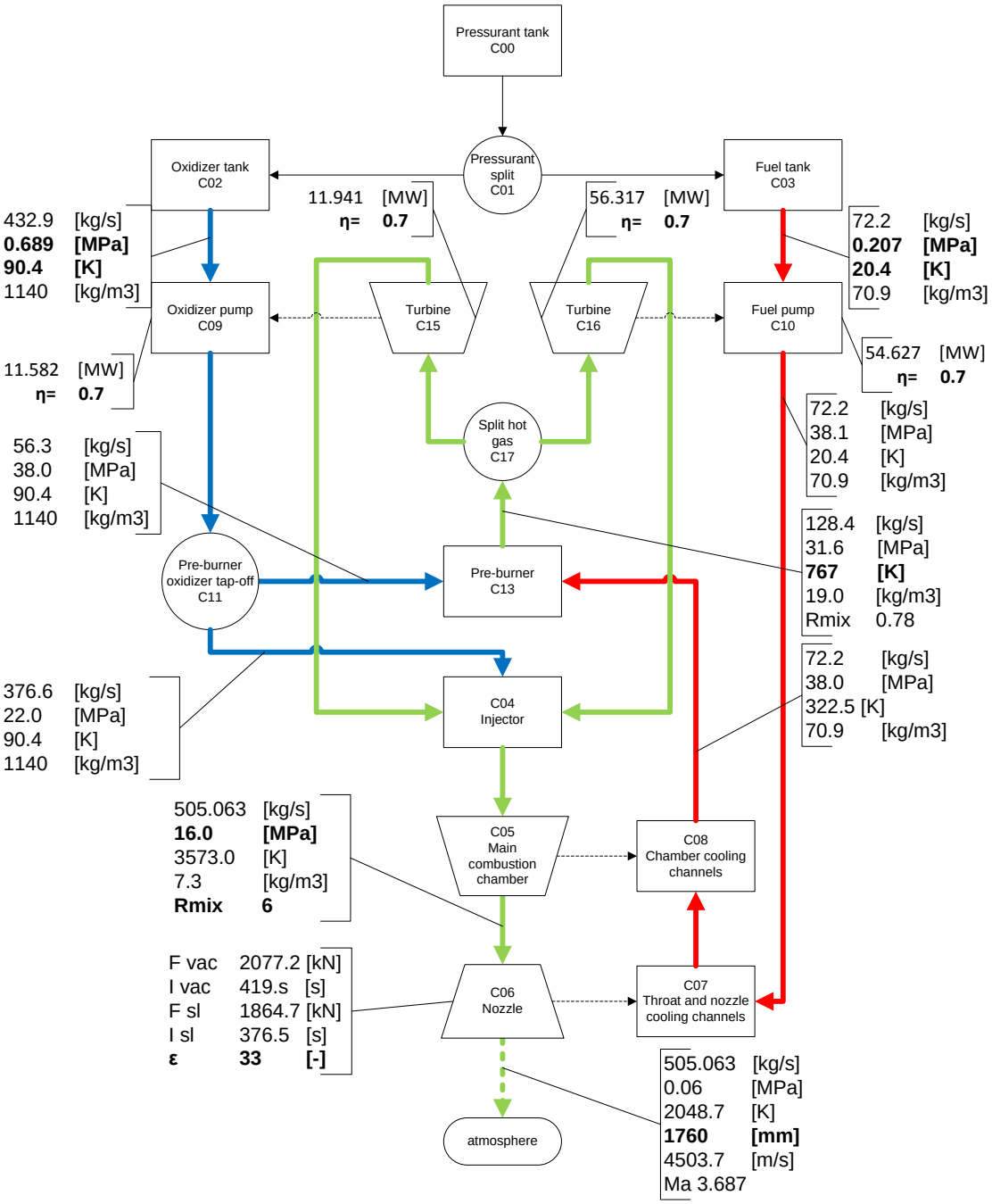

Figure 7-2: SLME Booster Fuel Rich Staged Combustion engine cycle diagram in LiRA

Table 7-3: SLME Booster modelled with LRP2 and LiRA.

	Unit	LRP2 [25]	LiRA	Difference [%]
Input				
Mixture ratio	[−]	6.0	=	
Main combustion pressure	[MPa]	16.0	=	
Turbine entry temperature	[K]	767	=	
Nozzle expansion ratio	[−]	33	=	
Nozzle exit diameter	[m]	1.76	=	
Output				
Fuel rich pre-burner pressure	[MPa]	32.5	29.3	2.5
Fuel rich pre-burner mixture ratio	[−]	0.7	0.78	11.4
Main oxidiser pump discharge pressure	[MPa]	19.5	22.0	11.4
Main fuel pump discharge pressure	[MPa]	50.6	37.8	25.3
Chamber contraction ratio	[−]	2.5	2.3	8.0
Characteristic chamber length	[m]	1.1	1.0	9.1
Throat radius	[m]	0.153	0.153	0.0
Total thrust chamber length	[m]	2.7	2.8	3.7
Specific impulse in vacuum	[s]	437.2	419.4	4.1
Specific impulse at sea level	[s]	388.8	376.5	3.2
Thrust in vacuum	[kN]	2206	2077.2	5.8
Thrust at sea level	[kN]	1961	1864.7	4.9

=: idem

LRB gas generator cycle.

The LRB is a LOX-RP1 gas generator cycle under study for liquid booster stage in [27]; the engine cycle as it looks in SEQ and the one as it looks in LiRA are shown in Figure 7-7 and Figure 7-3 respectively. Table 7-4 compares the results obtained in LiRA with those reported in [27] to be obtained with SEQ.

The high gas generator pressure is due to the method of estimating the gas generator where the pressure over the gas generator injector is assumed to be 20% of the gas generator pressure. This error has further no consequences as the turbine output power is determined by the pressure ratio, which is a fixed value in LiRA for gas generator cycles. The difference in mass flow and pump power can be explained by the observations of Kauffmann et al. in [27] that for fuel rich hydrocarbon mixtures the estimates of CEA (such as combustion temperature) show significant discrepancies with tabulated data in other publications and with experimental data. Kauffman further elaborates on the problem and identifies the cause being that CEA allows the cracking of long hydrocarbon chains into any theoretical possible smaller hydrocarbon, pure carbon and hydrogen molecules. [27] However in the combustion of highly fuel rich mixtures there are substantial amounts of unburned chain molecules to be expected. [27] As CEA splits them, a higher temperature is obtained than observed experimentally. [27] For a more elaborate explanation the interested reader is referred to his work. The important conclusion of the problem is that CEA combustion temperature estimates for a certain pressure and fuel rich mixture ratio are significantly higher than experiments or other publications show (differences can be up to about 300 K, see Table 7-11).

Kauffmann et al. solve the problem of wrong combustion temperature estimate by running two separate calculations of CEA in the extreme fuel regime; one normal call as before, but the second is a heavily reduced version of thermodynamic database where a lot of species are omitted. The values used are an interpolation between the results of these two sets.

Table 7-4: LRB SEQ and LiRA modelling results comparison

	Unit	SEQ [27]	LiRA	Difference [%]
Input				
Thrust chamber pressure	[bar]	65.00	=	
Thrust chamber MR	[–]	2.40	=	
Exit diameter	[m]	2.02	=	
Expansion Ratio	[–]	15.0	=	
Performance				
Sea-level thrust	[kN]	2118.14	2038.5	3.8
Vacuum thrust	[kN]	2444.41	2321.7	5.0
Sea-level specific impulse	[s]	260.83	269.33	3.3
Vacuum specific impulse	[s]	301.00	306.75	1.9
Thrust chamber temperature	[K]	3453.97	3578.5	3.6
Total mass flow	[kg/s]	832.08	782.87	5.9
Engine MR	[–]	2.17	2.43	12.0
C^*	[m/s]	1687.38	1796.5	6.5
Fuel pump power	[MW]	4.06	3.45	15.0
Oxidiser pump power	[MW]	6.21	5.70	8.21
GG chamber pressure	[bar]	56.88	70.5	23.9
GG chamber temperature	[K]	886.62	1000	12.8
GG mass flow	[kg/s]	38.095	14.0	63.2
GG MR	[–]	0.30	0.14	53.3
Dimensions				
Char. chamber length	[m]	1.30	1.27	2.3
Chamber length	[m]	0.81	0.64	21.0
Nozzle length	[m]	2.64	2.90	9.8
Total length†	[m]	3.45	3.54	2.6
Throat radius	[m]	0.26	0.26	0.0
Contraction ratio	[–]	1.80	2.00	11.1
Mass				
Chamber/nozzle assembly	[kg]	1147	1416	23.5
Turbo-machinery	[kg]	1671	763	54.3
Misc.	[kg]	254	-	-
Total‡	[kg]	3071	2397	21.9

†: total thrust chamber length, not total engine length ‡: engine dry mass
=: idem

Table 7-5: Comparison of performance results of A-1 stage Alpha Vehicle by Huzel and Huang with results obtained in LiRA (sea level conditions)

Parameter	Unit	Huzel and Huang	LiRA	Difference [%]
Thrust chamber				
Thrust	[kN]	3336.2	3560.7	6.7
Specific impulse	[s]	270	275.0	1.9
Nozzle stagnation pressure	[bar]	68.9	79.8	15.8
Oxidiser mass flow rate	[kg/s]	880.4	926.3	5.2
Fuel mass flow rate	[kg/s]	375.1	394.2	5.1
Characteristic velocity (ideal)	[m/s]	1725	1798.2	4.2
Thrust coefficient (ideal)	[−]	1.532	1.6593	8.3
Contraction ratio	[−]	1.6	1.9	18.8
Oxidiser side				
Pump inlet pressure	[bar]	3.8	3.8	0.0
Pump discharge pressure	[bar]	103.8	106.6	2.7
Pump shaft power	[kW]	11073	11859	7.1
Fuel side				
Pump inlet pressure	[bar]	3.1	3.1	0.0
Pump discharge pressure	[bar]	118.6	164.8	39.0
Pump shaft power	[kW]	8791	13420	52.7
Turbine				
Inlet pressure	[bar]	44.1	113.1	156.5
Inlet temperature	[K]	1033.2	1000	3.2
Shaft power	[kW]	20238	26061	28.8
Mass flow rate	[kg/s]	41.7	27.9	33.1
Gas generator				
Oxidiser mass flow rate	[kg/s]	12.1	3.6	70.2
Fuel mass flow rate	[kg/s]	29.6	27.9	5.7

LiRA hence is not able to reach the low gas generator combustion temperature modelled by SEQ using a fuel rich RP1-LOX mixture. The gas generator in the LiRA analysis hence has a higher combustion temperature leading to a higher turbine output power for a lower mass flow (because the pressure ratio is fixed); the lower mass flow leads to less mass flow passing the pumps hence a lower pump power requirement and thus consequentially a lower turbine output power requirement.

A possible solution to LiRA's problem is to use the same method as Kauffmann et al. proposes, however it therefore either needs another table with properties or LiRA must b e modified such that it is also able to call CEA directly.

Comparison with first stage of hypothetical "alpha vehicle" of Huzel and Huang.

In Design of Liquid Rocket Engines by Huzel and Huang, a hypothetical four-stage launcher, called the "Alpha vehicle", is used as case for explanatory example calculations. The first stage of this hypothetical vehicle is a LOX-RP1 gas generator cycle operating at sea level which will be used for comparison. The quantitative comparison is found in Table 7-5.

A performance comparison in results between those obtained by Huzel and Huang and those obtained by LiRA is given in Table 7-5.

There are some significant differences in the results obtained by Huzel and Huang and LiRA, a first reason is the fact Huzel an Huang calculate combustion with frozen composition conditions, while LiRA uses chemical equilibrium, this can make a significant difference in specific heat capacity

and conductivity of the combustion products and thus in the Prandtl number. The fuel pump discharge pressure is much overestimated in LiRA due to the large pressure loss over the heat exchanger, Huzel and Huang calculate a pressure drop of 290 psi or 20 bar over the cooling jacket and manifold while in LiRA the pressure drop over the heat exchanger is 58.254 bar. Further due to the problem Kauffmann et al. have observed in [27] with estimating the combustion temperature of LOX-RP1 using CEA tabulated values leads to problems with the gas generator mixture ratio and thus fuel and oxidiser mass flow.

7-2 Validation

In order to assess the credibility of the values returned by LiRA it is validated against real data. Table 7-6 expresses accuracy in terms of relative standard error of estimation.

Most parameters tested show acceptable errors ($RSE < 30\,\%$) in combination with a sufficient large sampling base ($N \geq 5$); additionally a lot of parameters tested do have an acceptable Relative Standard Error of Estimate (RSE) value but are disputable due to the limited amount of samples.

The pressure-fed engine dry mass estimate and the propellant tank mass estimate are unacceptable but this could be deceptive due to the limited amount of samples; all RSE values that are based on a small sampling base should be treated with care.

The turbine output power for gas generator cycles at fuel side shows errors which are just unacceptable. The reason is due to the error in fuel pump discharge pressure. This is due to the over or underestimation in pressure drop over the heat exchanger. Improving the heat exchanger model means adding design details such as detailed cooling channel geometry and lay-out which will lead to more variables which are hard for the user to define without performing a dedicated nozzle cooling optimisation study. Therefore this error is accepted.

The gas generator mass flow estimates, the combustion chamber length estimate and the COPV pressurant tank estimate show high RSE values while sufficient samples are available, and hence are undoubtedly unacceptable. However because in gas generator cycles the mass flow of the gas generator is typically only around 2 % of the total mass flow [31], the error on the total mass flow and propellant required is minimal and thus it is decided to not further attempt to reduce this error to acceptable estimation errors. Similarly the combustion chamber length estimate will not be used for total engine wet mass estimations during sensitivity study and optimisation nor in the application of LiRA, and thus this error requires no immediate attention and is not attempted to be improved. Regarding the COPV pressurant tank estimate it is reasoned that though unacceptable the impact on the total wet mass is small (see Section 4-2) and will be present in all cycles and can thus be neglected for the scope of this work.

As the scope of this work is in the first place to build a precise model to allow for comparative studies it has been decided to accept this error and warn the user to not use mass values for these components as accurate estimates.

7-3 Conclusions on Verification and Validation

However unlike LiRA, none of these tools explicitly mention the existence of integrated optimisation routine nor an uncertainty and sensitivity analysis capability. Hence LiRA, though

Table 7-6: Overview of RSE of performance, mass and dimension estimation relationships on systems level

Component	Relation	N†	RSE [%]	Acceptable
Vacuum specific impulse	Eq. (3-17)	19	2.1	Yes
Vacuum thrust	Eq. (3-21)	19	17.5	Yes
Oxidiser mass flow rate - pressure fed	Eq. (3-65)	1	TBD	No
Oxidiser mass flow rate - gas generator	Eq. (3-65)	9	18.1	Yes
Oxidiser mass flow rate - staged combustion	Eq. (3-65)	4	9.9	Yes
Oxidiser mass flow rate - expander cycle	Eq. (3-65)	4	9.3	Yes
Fuel mass flow rate - pressure fed	Eq. (3-64)	1	TBD	No
Fuel mass flow rate - gas generator	Eq. (3-64)	9	28.6	Yes
Fuel mass flow rate - staged combustion	Eq. (3-64)	4	7.0	Yes
Fuel mass flow rate - expander cycle	Eq. (3-64)	4	15.4	Yes
Gas generator mass flow rate - gas generator		9	156.6	No
Gas generator mass flow rate - staged combustion		2	27.0	Yes
Turbine output power ox side - gas generator	Eq. (3-70)	2	7.4	Yes
Turbine output power ox side - staged combustion	Eq. (3-70)	0	TBD	No
Turbine output power ox side - expander cycle	Eq. (3-70)	0	TBD	No
Turbine output power fuel side - gas generator	Eq. (3-70)	7	34.5	No
Turbine output power fuel side - staged combustion	Eq. (3-70)	0	TBD	No
Turbine output power fuel side - expander cycle	Eq. (3-70)	0	TBD	No
Pump discharge pressure ox side	Eq. (3-87)	7	5.4	Yes
Pump discharge pressure fuel side	Eq. (3-88)	7	19.6	Yes
Pressure gas generator (gas generator cycle)		9	35.1	No
Mixture ratio gas generator (gas generator cycle)		9	26.4	Yes
Combustion chamber length	Eq. (4-34)	14	259.3	No
Combustion chamber diameter	Eq. (4-32)	14	18.5	Yes
Combustion chamber contraction ratio	Eq. (4-31)	14	21.0	Yes
Thrust chamber mass	Eq. (4-50)	3	21.6	Yes
Turbo-pump assembly mass - direct drive or geared‡	Eq. (4-55)	6	$\leq$ 26.3	Yes
Turbo-pump assembly mass - dual shafts‡	Eq. (4-55)	9	$\leq$ 11.7	Yes
Turbo-pump length - direct drive or geared	Eq. (4-38)	?	TBD	No
Turbo-pump length - dual shafts	Eq. (4-38)	?	TBD	No
Turbo-pump diameter - direct drive or geared	Eq. (4-39)	?	TBD	No
Turbo-pump diameter - dual shafts	Eq. (4-39)	?	TBD	No
Propellant tank mass - surface tension tanks	Eq. (4-44)	4	30.5	No
Pressurant tank mass - COPV	Eq. (4-44)	13	38.3	No
Pressurant tank mass - titanium	Eq. (4-44)	15	27.9	Yes
Propellant tank volume ox side	Eq. (4-7)	3	28.8	Yes
Propellant tank volume fuel side	Eq. (4-7)	3	18.8	Yes
Pressurant volume		1	TBD	No
Engine overall length - pressure fed	Eq. (4-3)	2	18.4	Yes
Engine overall length - cryogenic tp fed	Eq. (4-1)	10	23.8	Yes
Engine overall length - non-cryogenic tp fed	Eq. (4-1)	5	14.9	Yes
Engine overall diameter - pressure fed	Eq. (4-4)	2	22.3	Yes
Engine overall diameter - cryogenic tp fed	Eq. (4-2)	10	18.6	Yes
Engine overall diameter - non-cryogenic tp fed	Eq. (4-2)	5	13.3	Yes
Engine dry mass - pressure fed	Eq. (4-42)	2	50.3	No
Engine dry mass - cryogenic tp fed	Eq. (4-43)	10	10.3	Yes
Engine dry mass - non-cryogenic tp fed	Eq. (4-43)	5	21.1	Yes

†: number of samples TBD: To Be Determined

‡ N and RSE are values stated by Zandbergen in [58]

at this stage not as extensive in engine cycle choice and detail as the other tools, offers wider applicability. The performance model shows good correspondence with other simulation software estimates and reality for the thrust chamber, the turbo-pump assembly and gas generator or pre-burner have some larger differences; this is mainly related to the estimated pressure difference between gas generator and pump discharge pressure and the estimation of pressure drop over the heat exchanger. While the numbers are not all satisfactory corresponding, the trends are good and no unrealistic values which would indicate a significant error in modelling were encountered.

7-4 Large Figures and Tables

Figure 7-4 shows the RL10A-3-3A operating schematic.

Figure 7-5 shows the RS-68 operating schematic.

Figure 7-6 shows the thermodynamic conditions inside expander bleed cycle engine calculated by DLR's cycle analysis tool LRP2.

Figure 7-7 shows the LRB engine cycle diagram.

Figure 7-8 shows the SLME Booster FRSC engine cycle diagram.

Figure 7-9 shows the A-1 stage engine operation parameters.

Figure 7-9 shows the A-1 stage engine performance diagram.

Figure 7-11 shows the hydrocarbon properties in extreme fuel rich environment.

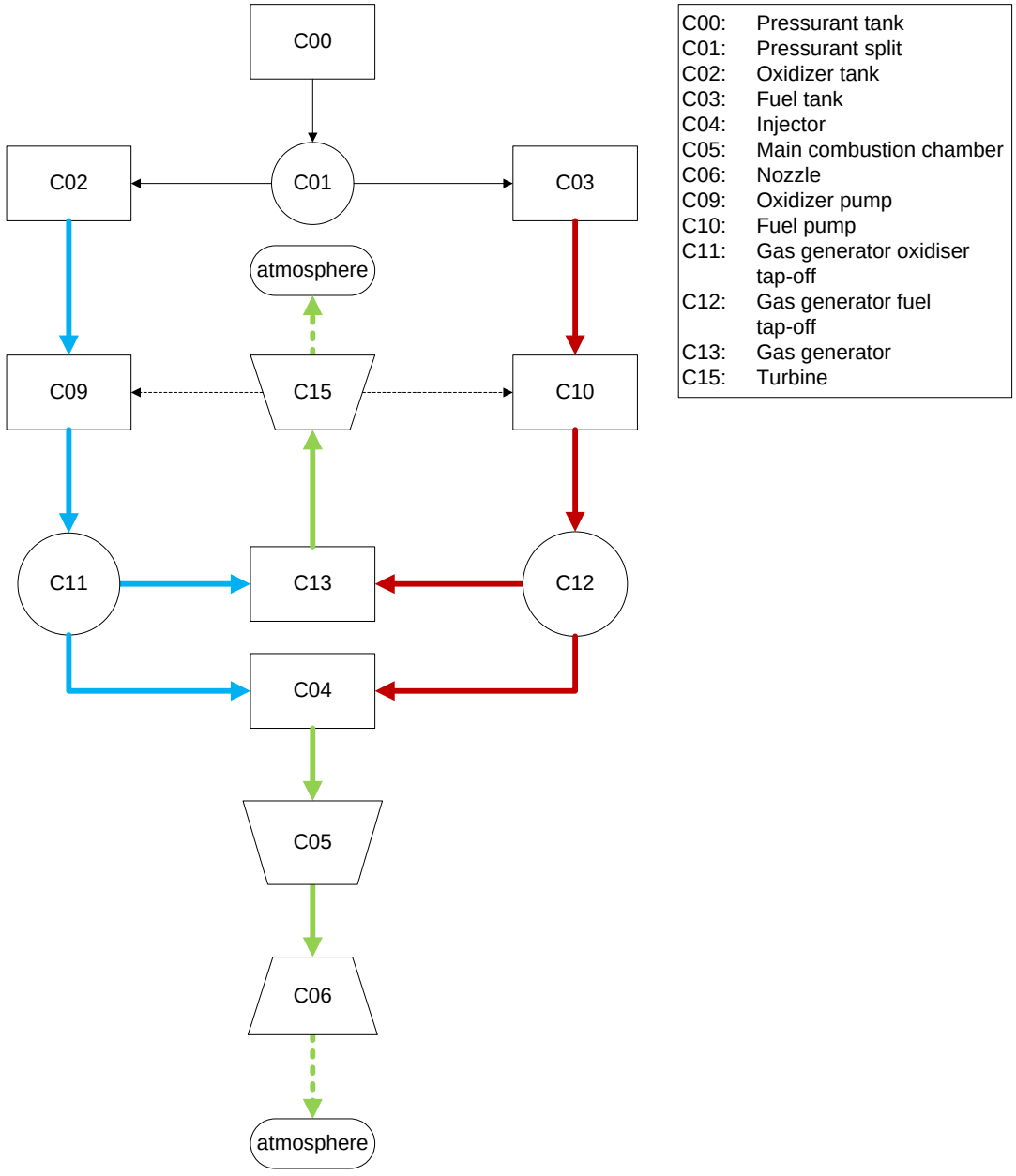

Figure 7-3: LRB engine cycle diagram as modelled in LiRA

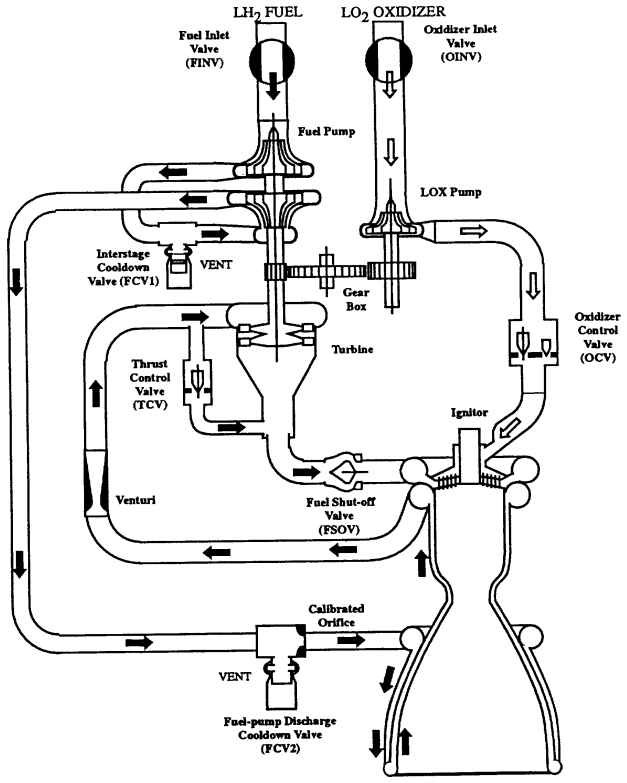

Figure 7-4: RL10A-3-3A Operating schematic [87]

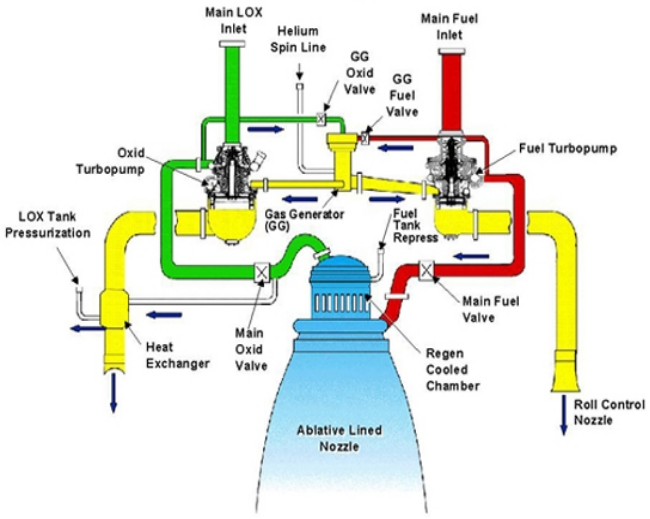

Figure 7-5: RS-68 Operating schematic [74]

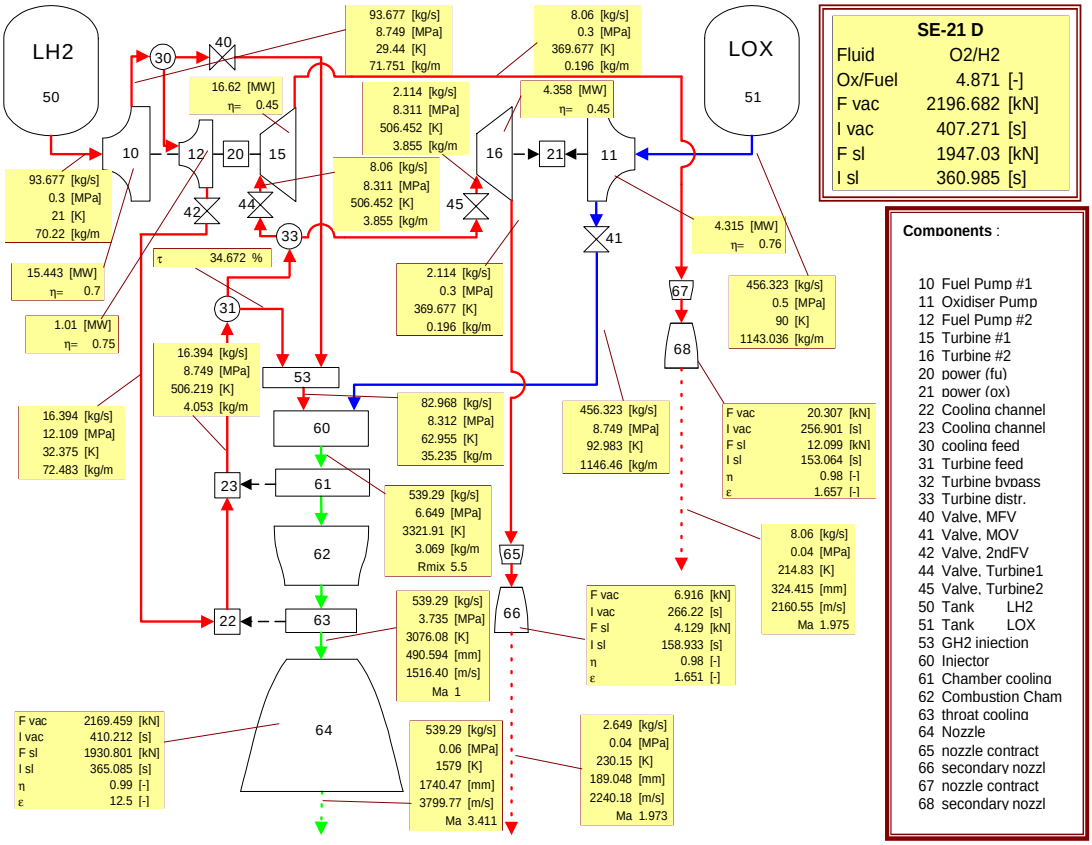

Figure 7-6: Thermodynamic conditions inside expander bleed cycle engine calculated by DLR's cycle analysis tool LRP2 [26] [28]

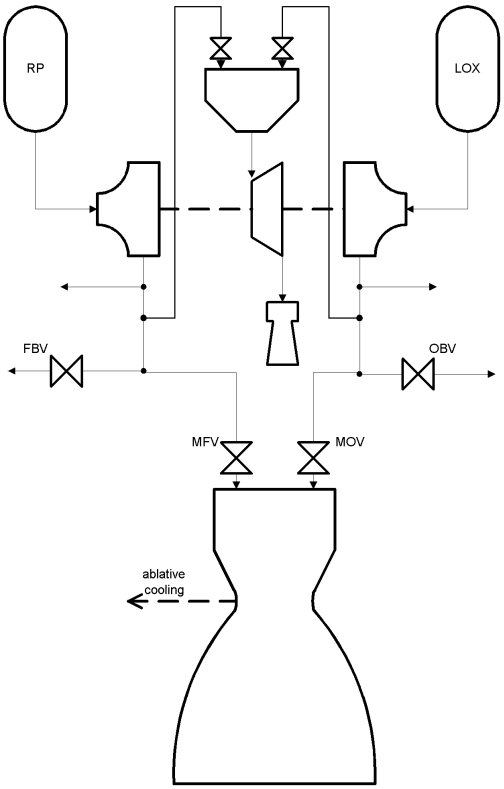

Figure 7-7: LRB engine cycle diagram [27]

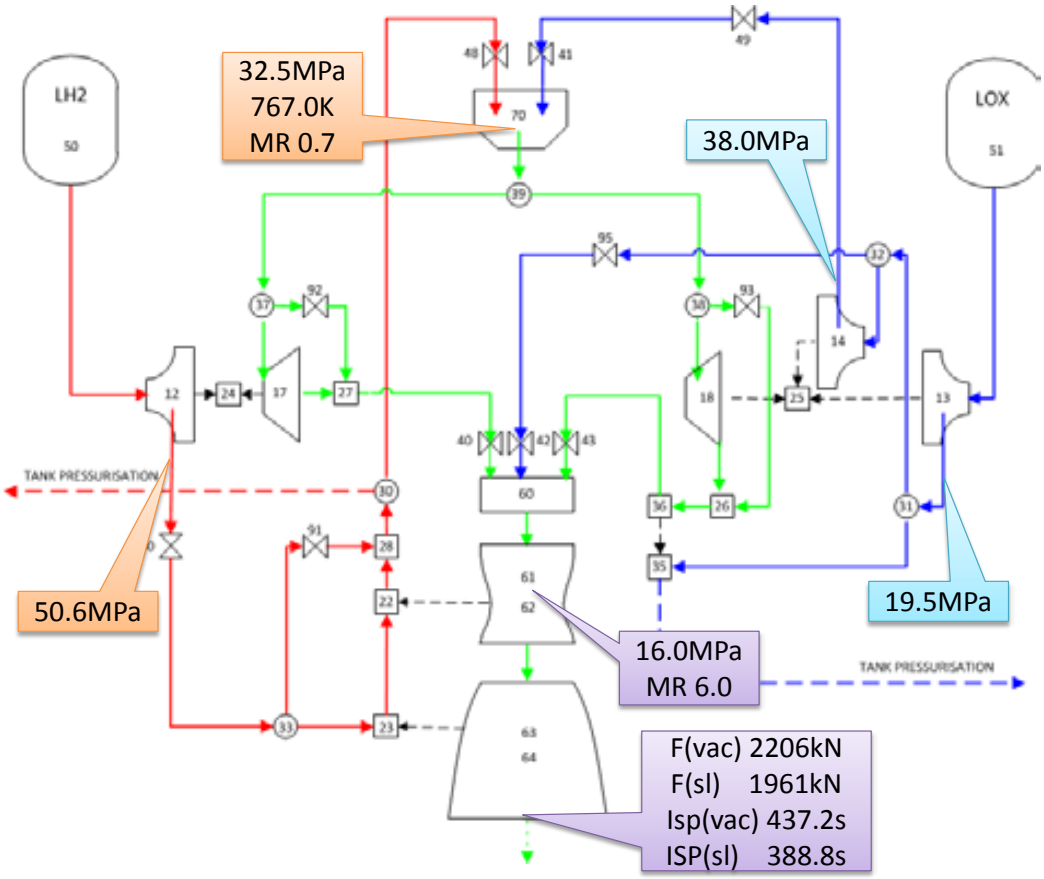

Figure 7-8: SLME Booster FRSC engine cycle diagram [25]

TABLE 3-2.–*750K A-1 Stage Engine Operating Parameters*
[Sea-level conditions]

Engine (turbopump feed):		
Thrust	lb	750 000
Nominal single-firing duration	sec	165
Specific impulse	sec	262.4
Oxidizer LO_2:		
Flow rate	lb/sec	1967.7
Density	lb/ft^3	71.38
Fuel RP-1:		
Flow rate	lb/sec	892.3
Density	lb/ft^3	50.45
Mixture ratio	O/F	2.20
Thrust chamber (tubular wall construction regeneratively cooled by fuel):		
Thrust	lb	747 000
Specific impulse	sec	270
Injector end pressure	psia	1095
Nozzle stagnation pressure	psia	1000
Oxidizer flow rate	lb/sec	1941
Fuel flow rate	lb/sec	827
Mixture ratio	O/F	2.35
c^* efficiency	Percent	97.5
c^*	ft/sec	5660
C_f efficiency	Percent	98
C_f		1.532
Contraction ratio	A_c/A_t	1.6
Expansion ratio	A_e/A_t	14
Throat area A_t	in^2	487
L^*	in	45
Nozzle contour		80 percent bell
Oxidizer side:		
Injector pressure drop	psi	200
Torus dome pressure drop	psi	150
Line pressure drop	psi	25
Main valve pressure drop	psi	35
Pump inlet pressure	psia	55
Pump discharge pressure	psia	1505
Developed pump head	ft	2930
Pump:		
Flow rate	lb/sec	1971
Shaft power	bhp	14 850
Efficiency	Percent	70.7
Shaft speed	rpm	7000
Heat exchanger	lb/sec	3
Fuel side:		
Injector pressure drop	psi	200
Jacket and manifold pressure drop	psi	290
Line pressure drop	psi	10
Main valve pressure	psi	15
Calibration orifice pressure drop	psi	110
Pump:		
Inlet pressure	psia	45
Discharge pressure	psia	1720
Developed pump head	ft	4790
Pump:		
Flow rate	lb/sec	892
Shaft power	bhp	11 790
Efficiency	Percent	65.8
Shaft speed	rpm	7000
Turbine:		
Inlet pressure	psia	640
Inlet temperature	°F	1400
Pressure ratio		23.7
Gas flow rate	lb/sec	92
Shaft power	bhp	27 140
Efficiency	Percent	58.2
Shaft speed	rpm	7000
Shaft torque	in-lb	20 380
Auxiliary drive:		
Shaft power	bhp	500
Gas generator system:		
Oxidizer side:		
Flow rate	lb/sec	26.7
Entrance loss	psi	25
Line pressure drop	psi	25
Control-orifice pressure drop	psi	615
Valve pressure drop	psi	10
Injector pressure drop	psi	120
Fuel side:		
Flow rate	lb/sec	65.3
Entrance loss	psi	25
Line pressure drop	psi	25
Control-orifice pressure drop	psi	800
Valve pressure drop	psi	20
Injector pressure drop	psi	140
Gas generator:		
Mixture ratio	O/F	0.408
Injector end pressure	psia	710
Combustor pressure drop	psi	70
Thrust vector control:		
Minimum acceleration	rad/sec^2	1
Maximum velocity	deg/sec	10
Displacement	deg	±14

Figure 7-9: A-1 Stage engine operation parameters [53]

66 DESIGN OF LIQUID PROPELLANT ROCKET ENGINES

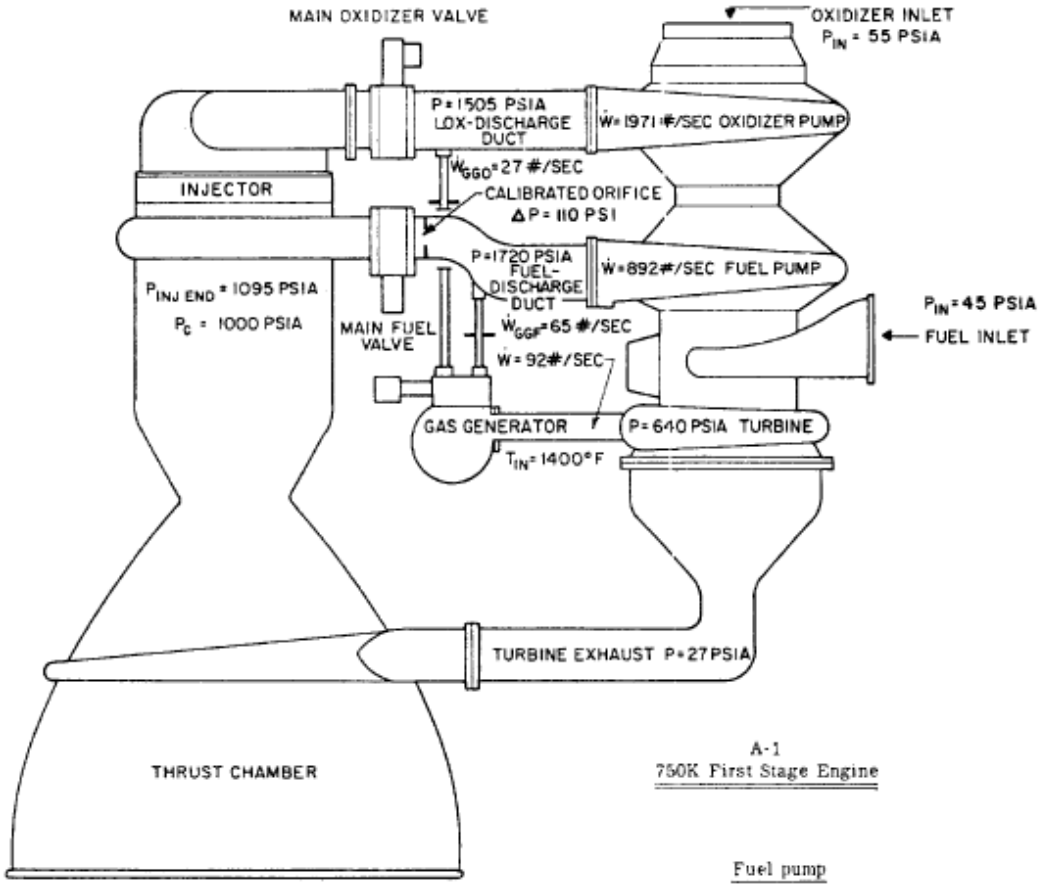

A-1
750K First Stage Engine

Nominal engine parameters

Propellants:	
Liquid oxygen density	71.38 lb/ft^3
RP-1 density	50.45 lb/ft^3
Thrust (sea level)	750 000 lb
Specific impulse	262.4 sec
Mixture ratio	2.20

Thrust chamber

Expansion area ratio	14
Throat area	487 in^2
Thrust	747 000 lb
Specific impulse	270 sec
Mixture ratio	2.35
Flow rates:	
oxidizer	1941 lb/sec
fuel	827 lb/sec

Fuel pump

Developed head	4790 ft
Flow rate	892 lb/sec
Efficiency	65.8%
Horsepower	11 790 bhp
Speed	7000 rpm

Oxidizer pump

Developed head	2930 ft
Flow rate	1971 lb/sec
Efficiency	70.7%
Horsepower	14 850 bhp
Speed	7000 rpm

Turbine

P_{in}	640 psia
Pressure ratio	23.7
$Temp_{in}$	1400° F
Efficiency	58.2%
Horsepower	27 140 bhp
Exhaust thrust	3000 lb

Figure 3-1.–A-1 engine performance diagram.

Figure 7-10: A-1 Stage engine performance diagram [53]

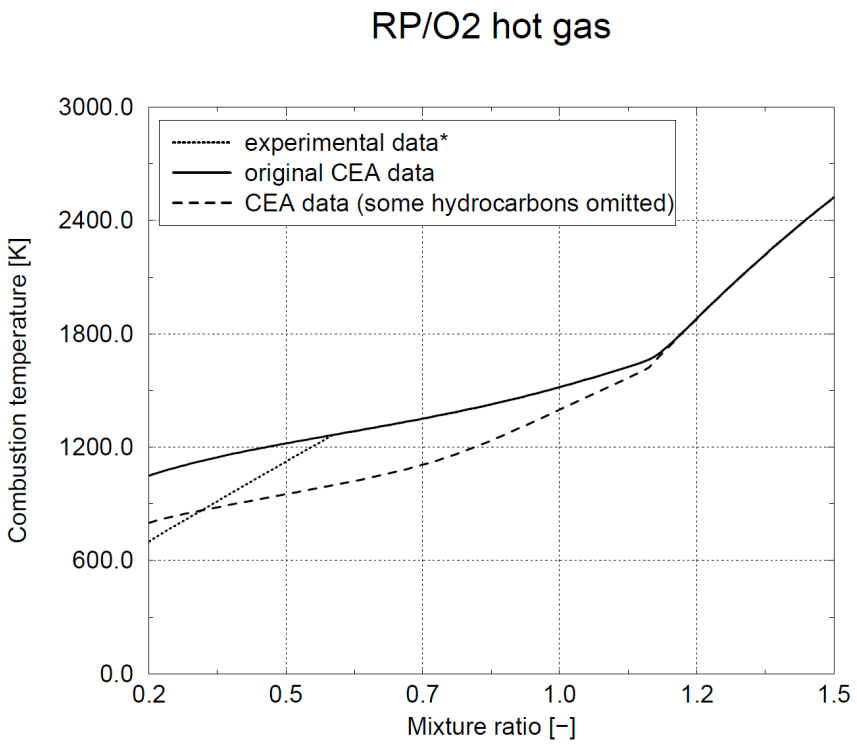

Figure 7-11: Hydrocarbon properties in extreme fuel rich environment [27]

Chapter 8

Optimisation with LiRA

When designing a propulsion system a designer needs to play with a lot of often related parameters. Thrust is dependent on specific impulse and mass flow. In order to achieve a certain thrust level whilst needing as little propellant possible, one should attempt to maximise specific impulse and minimise mass flow as can be seen from Eq. (3-17). The achievable mass flow through the thrust chamber depends on area ratio and nozzle exit diameter as is explained in Section 3-2. Therefore for a required mass flow an optimal area ratio and exit diameter needs to be found. The specific impulse is dependent on chamber pressure, nozzle area ratio and mixture ratio through the thrust coefficient and characteristic velocity where the mixture ratio affects the combustion temperature, the ratio of specific heats and the molar mass of the flow.

The designer will notice that increasing specific impulse by simply increasing area ratio and chamber pressure alone will have negative consequence for the total mass. Area ratio affects, depending on the engine cycle (see Eq. (4-42) and Eq. (4-43)), the engine dry mass. Main combustion chamber pressure determines tank pressure in pressure fed systems and thus tank mass. Therefore he will try to increase specific impulse by optimising mixture ratio and propellant choice. Varying the mixture ratio and propellant choice however is also not without consequence as the density of an oxidiser and fuel can differ considerably and thus on one hand can strongly affect the tank volumes and hence tank dry mass and on the other lead to high pump power requirements, hence a heavy turbo-pump.

Other parameters like pump and turbine efficiency, turbine pressure ratio, turbine inlet temperature and tank pressures will also affect the performance and thus efficiency of the cycle and component mass and volumes. A more elaborate qualitative analysis is found in Section 9-1. So in order to find the optimal combination of parameter values that meet the set requirements and have minimal mass, volume, cost or maximal reliability, or a combination of those, an optimisation needs to be performed.

As LiRA only has a performance, mass and sizing model, the optimisation is restricted to output related to these models. First a rationale of how the optimisation should look like is presented, then a general overview of optimisation methods is given. Next the most important optimisation parameters are identified followed by the description of the optimisation routine created. Finally

an example optimisation of a stage is performed where the results are subjected to sensitivity and uncertainty analysis and are validated before discussion of observations and drawing conclusions.

8-1 Optimisation Rationale

The main reasoning behind the optimisation set-up of the engine cycle is that the user has a certain set of requirements and constraints that have to be met and wants to know which cycle design provides the most optimal solution. A trade between all solutions that meet the constraints will be need to be performed, having trade-parameters such as performance, mass, dimensions, cost, reliability, etcetera. However as the model currently only includes performance, mass and dimensions models, it can only include these aspects in the optimisation.

An engine stage is usually designed such that the stage itself with all the stages above it and the payload undergoes a certain velocity change (ΔV). The amount of change in velocity needed follows from a trajectory model. When no opposing forces are present, this change in velocity can be achieved with any amount of thrust as long as the burn time is unlimited. However in reality the drag, gravitational pull and limited burn time constraint will set a minimal required thrust. As LiRA has no trajectory nor an atmospheric model a required thrust-to-weight ratio is required as additional input. The change in velocity required should be taking into account the mass of the stage itself as well as the stages above it and the payload (the stages above the to be optimised staged can in a certain sense also be considered as payload to that specific stage). The thrust to weight ratio at this moment could be obtained by looking to a similar stage and calculating its thrust-to-weight ratio and setting it as requirement for this optimisation. Further in LiRA all mass above the stage for which the propulsion system is designed should be considered payload mass ($m_{payload}$). An overview of the optimisitation input requirements is also given in Table 5-3.

8-2 Optimisation Methods

Liberti and Kucherenko give in [78] a compact overview of global optimisation methods. According to them global optimisation methods can be more or less classified to be either deterministic or stochastic.

Zhang et al. give in [79] some examples of deterministic and stochastic methods along with a description. Examples stated of deterministic models are Branch and Bound Global Optimisation, Homotopy Continuation Methods and Interval Analysis while some examples of stochastic methods are Random Search, Simulated Annealing, Genetic Algorithm, Tabu Search, Differential Evolution, Particle Swarm Optimisation, Random Tunneling Algorithm, Ant Colony Optimisation, Harmony Search and some Hybrid Methods combining several techniques. [79]

Deterministic models have a theoretical guarantee of locating the global minimum or at least a local minimum whose value differs at worst by a certain amount from the global one. [78] Stochastic methods offer only a guarantee in probability of locating the global minimum. [78] The big advantage of stochastic methods however is that they are usually faster in locating a global optimum compared to deterministic methods. [78] Liberti and Kucherenko further state that for black-box formulations and extremely ill-behaved functions stochastic methods are better adapted. [78] Also they found that deterministic methods are incapable of solving practical problems with more than 10 variables. [78]

Monte Carlo is a stochastic estimation procedure that relies on the law of large numbers which says that when enough independent samples are taken, the average of these samples must be close to the true value. [80] Additionally the central limit theorem dictates that this average has a Gaussian distribution around the true value. [80] Monte Carlo is often used when the distribution of a variable is unknown or when one does not want to solve integrals numerically.

While in theory the Monte Carlo samples need to be generated independently in practice they can have dependencies as long as every point is visited as many times as it would with independent samples; the reason for using dependent samples is that it could significantly increasing the speed of converging the estimates to the true average. [80] Shalizi explains in [80] several of these improved Monte Carlo methods.

All above methods are very complex with the exception of Monte Carlo which is basically a brute trial and error guessing method. Nevertheless this method, the simple Monte Carlo, not one of the improved, is chosen as it is easily implemented. However the optimisation routine used in LiRA makes one small modification to the method and adds one extra step before accepting the simple Monte Carlo result which will be explained in the next sections.

8-3 Optimisation Routine

As explained earlier Simple Monte Carlo analysis has been chosen for the optimisation. In contrary to sensitivity analysis where the values for the knowledge variables were generated randomly, here they will be fixed to typical values and most of the values for the decision variables will be generated randomly.

In order to speed up optimisation for now only the engine and not the feed system is optimised, this means that the main combustion chamber pressure, main combustion chamber mixture ratio, nozzle exit diameter and nozzle area ratio are optimised to lead to the lowest total wet stage mass for a given change in velocity, thrust-to-weight ratio and payload mass requirement. The burn time follows during the optimisation from these requirements as will be explained later on. The user further is also asked to choose an atmospheric pressure value, nozzle cooling method and chamber cooling method for each engine cycle as these parameters cannot be optimised. All other variables, such as efficiencies, tank pressures, tank temperature, turbine pressure ratios and turbine inlet temperatures, which should be optimised for in a full optimisation, but aren't, are assigned a typical value (for values see Table 5-5). Hence LiRA's optimisation routine currently does not allow the user to optimise for tank pressures, tank storage temperatures, turbine inlet temperatures, turbo-pump component efficiencies and turbine pressure ratios. This approach is justified by the findings of input parameter analysis which is described in Section 9-4

The routine followed is shown schematically in Figure 8-1.

The optimisation goes as follows; first a required stage thrust is guessed, let's denote this guess as F_{guess}, now the main combustion chamber mixture ratio, nozzle exit diameter and nozzle area ratio of the thrust chamber need to be found such that this thrust is delivered. To do this a certain amount of samples containing random values limited to certain search ranges are generated and evaluated; those samples that differ less than a certain percentage of the desired thrust F_{guess} are filtered out. As there are many combinations possible that meet this requirement, it is likely there are multiple samples to chose from; as one desires to minimise mass, the one which leads to the lowest wet mass is chosen. However in order to have wet mass estimates a burn time is needed. For each sample the required burn time that is needed to meet the required change in

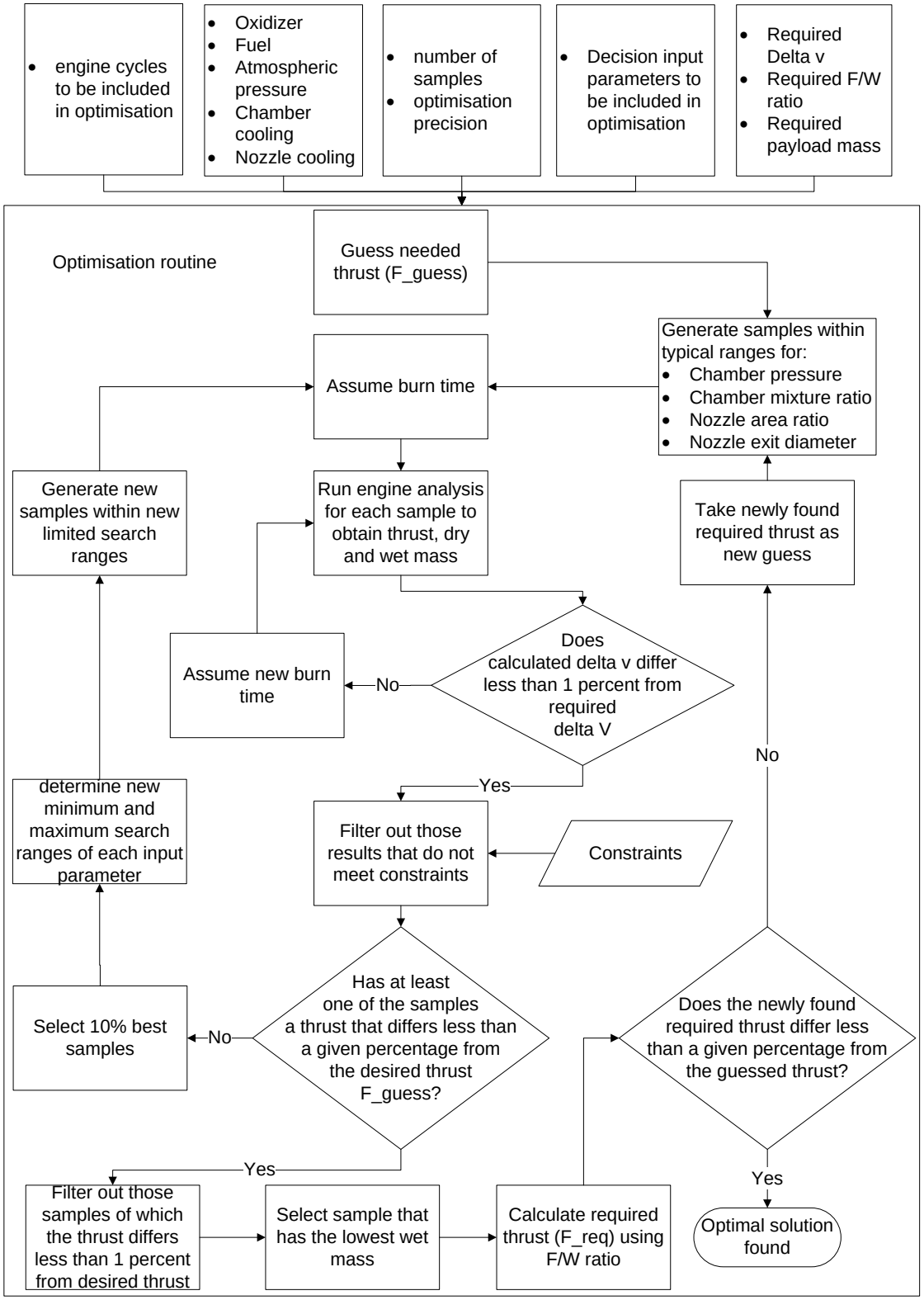

Figure 8-1: Stage propulsion system optimisation routine

velocity is calculated iteratively. Some of these samples might not meet the other constraints set by the user and are also filtered out. In the case none of the samples meet the constraints or lead to a thrust that differs less than a certain specified amount of percent from the desired thrust, a new set of samples is generated. This is repeated until a set is found that gives a thrust that equals or does not differ more than a specified amount of percent from F_{guess}. Once a sample that delivers this thrust, and in case of multiple candidates has the lowest wet mass, is selected the required thrust to weight ratio is used to calculated the required thrust. If this required thrust does not match the earlier guessed thrust, a new iteration where the new guessed thrust is set equal to the newly found require thrust is needed. This is repeated until the guessed thrust and the required thrust doe not differ more than a user specified percentage.

The constraints the user can choose from are all mass and dimension related as these often form the practical limitations to a propulsion system. An overview of the available constraint options is given in Table 5-4; all constraints are optional and in case no value is defined zero or infinity will be assumed and thus the constraint will have no effect.

Hence to summarise, the optimisation requires user defined values for change in velocity, thrust-to-weight ratio and payload mass (see also Table 5-3) and optimises main combustion chamber pressure, main combustion chamber mixture ratio, nozzle exit diameter and nozzle area ratio and calculates the burn time such that the required change in velocity and thrust to weight ratio with a given payload mass and a given set of constraints (see Table 5-4) are met.

When one would like to optimise the complete propulsion system, a loop calling current optimisation routine with random generated values for the remaining decision parameters (such as maximum tank operating pressure, tank temperature, turbine pressure ratio, pump and turbine efficiencies) should be created. As this will increase the optimisation computation time significantly without any additional value for the goals that are set in this work, this loop is not created but left for future work.

8-4 Precision and Reproducibility of Results and Impact of Allowed Tolerance in Requirements and Number of Samples Used on the Outcome

Because the optimisation relies on the use of random generated samples, every time the routine is ran different samples are generated. The chance of finding the global minimum point and not a local minimum increases with the amount of samples used. Also the chances that exactly the same solution is returned when repeating the optimisation increases with number of samples as the search range is better covered. Trial and error has shown that using 200 samples is sufficient to find in most cases a solution in the first try; when using less samples the possibility exists that no optimum is found and the routine needs to be ran again which hence is time intensive.

The user sets requirements for the optimisation, how fast a final solution is found depends on the tolerance the user gives that these requirements must be met. For the change in velocity requirement a tolerance of 1 percent is suggested as the iteration to meet this value is located in an inner loop of the routine and converges fast. However this is not the case for the thrust-to-weight ratio as this ratio is determined in the most outer loop of the optimisation routine and therefore each iteration requires to run an analysis for the many newly generated samples again. Therefore a 5 percent tolerance is suggested.

The impact of number of samples and requirement tolerance is not quantified due to time constraints and is hence left to be determined in future work.

The precision of the results is studied by repeating the optimisation and comparing the optimised input and the corresponding output of each run.

8-5 Example Optimisation of an Upper Stage

In this section the study of the effect of choosing different engine cycles for an upper stage similar to the Ariane 5 is chosen as a practical example case to demonstrate the capabilities of LiRA. The normal Ariane 5 has three possible upper stage engines depending on the configuration; the Aestus pressure fed engine for the storable propellant upper stage Etage à Propergols Stockables (EPS), the HM7B gas generator cycle engine for the cryogenic upper stage Etage Supérieur Cryogénique type A (ESC-A) and the Vinci closed expander cycle for the cryogenic upper stage ESC-B. For the Ariane 5 Midlife Extension (Ariane 5 ME), it was chosen to abandon the Aestus (used in the EPS-B stage) and HM7B (ESC-A stage) engine and use only the Etage Supérieur Cryogénique type B (ESC-B) upper stage with Vinci.

The choice of using Vinci in the new upper stage design results from completed and ongoing studies for new generation upper stage cryogenic engines in Europe which have the objective of increasing reliability, increasing performance, have engines with restart capability and low recurring cost. These studies indicate the Vinci closed expander cycle as most promising option. [1]

Now given the dimensions of Ariane V's upper stage and the thrust requirements of the engine and neglecting the requirement of restart capability, what would according to LiRA be the influences on the Ariane upperstage when using different engine cycles which have been optimised for a minimum wet mass for a given change in velocity and thrust to weight ratio equal to that of the Ariane V cryogenic upperstage (ESC-A)?

It is expected that the closed expander cycle should be a better choice than the current gas generator cycle. Also because closed cycles are said to be more efficient, the staged combustion cycle is expected to perform better. If this is not the case validation must point out why.

To speed up the optimisation in the example optimisation no thrust chamber cooling except for the expander cycles, where heat exchange is required, is chosen. The outcome with cooling is likely to have some differences as the pressure drop over the heat exchanger will lead to higher pump discharge pressures and hence higher pump powers or higher tank pressures; therefore also mass and volume will increase. The impact should be studied but is hence left to be determined in future work.

8-5-1 Requirements and Constraints

Ariane 5 ESC-A has a dry mass of 4.4 metric tons and a total mass of 19 tons. The vacuum Thrust and Isp are 63 kN and 446s respectively. Ariane 5 ECA can bring maximal 10 tons of payload to GTO but when looking to actual payload masses it can be seen the total payload mass is around 8 metric tons. Hence assuming the fairing is already ejected when the ESC-A stage is activated, the total initial (wet) mass is about $19 \times 10^3\,\mathrm{kg} + 8.0 \times 10^3\,\mathrm{kg} = 27.0 \times 10^3\,\mathrm{kg}$

and its total final (dry) mass about $4.4 \times 10^3\,\text{kg} + 8.0 \times 10^3\,\text{kg} = 12.4 \times 10^3\,\text{kg}$. This means a change in velocity and thrust to weight ratio of:

$$\begin{aligned}\Delta v &= 446\,\text{s} \cdot 9.806\,65\,\text{m/s}^2 \cdot \ln\left(\frac{27.0 \times 10^3\,\text{kg}}{12.4 \times 10^3\,\text{kg}}\right) \\ &= 3403.4\,\text{m/s} \end{aligned} \tag{8-1}$$

$$\begin{aligned}F/W &= \frac{65 \times 10^3\,\text{N}}{27.0 \times 10^3\,\text{kg} \cdot 9.806\,65\,\text{m/s}^2} \\ &= 0.245 \end{aligned} \tag{8-2}$$

If the data of Ariane 5 ESC-A is used as they are the constraints would be:

- engine diameter $< 5.4\,\text{m}$
- oxidiser tank diameter $< 5.4\,\text{m}$
- fuel tank diameter $< 5.4\,\text{m}$
- pressurant tank diameter $< 5.4\,\text{m}$

Further the ESC-A stage has an approximate length of 7.150 m from nozzle exit to top of stage dome, but this is not taken as a constraint, instead the stage length is left open in order to see the different solutions for the different cycles.

However the shape and location of the propellant and pressurant tanks are not as modelled in LiRA. In LiRA one cylindrical oxidiser and one cylindrical fuel tank, each with flat heads, and a single spherical pressurant tanks that are all placed on top of each other are assumed.

The maximal diameter of the parts cannot exceed 5.4 m. Further the length to diameter ratio of the storage tanks cannot exceed a certain ratio to guarantee structural integrity; high stresses in the bottom of the tanks occur due to the gravitational forces which are even stronger during launch and could lead to tank rupture. A typical tank length to diameter ratio value of 3 for vertical tanks found is found in literature such as [81] and [82]; hence this value will be taken as maximum.

The storable liquid Ariane stages use N2O4 and MMH as propellants and a pressure fed engine while the cryogenic stages use LOX and LH2 as propellants with a turbo-pump fed engine. Cryogenic pressure fed engines do exist, also for use as main engine on small upper stages, see for example [83], but the delivered thrust of production engines has however been kept limited; nevertheless both a storable as a liquid pressure fed engine are included in the study to observe the impact.

An overview of the used requirements and fixed input for the optimisation of the upperstage with different engine cycles is given in Table 8-1

8-5-2 Results for a Stage with a Gas Generator Cycle

In order to determine the precision and validity of the results obtained with the optimisation method first a single engine cycle is considered. The gas generator cycle is chosen as the Ariane 5 ESC-A on which the requirements used here are based also has a gas generator cycle propulsion system and thus allows for easier and directer comparison.

To assess the precision of the optimisation, the optimisation is performed five times with exactly the same requirements and fixed input after which the optimised input and corresponding output

Table 8-1: Ariane 5 LiRA upperstage engine optimisation requirements and fixed inputs

Parameter	Unit	Engine cycle					
		pf (stor.)	pf (cryo.)	gg	sc	ce	be
Requirements							
Change in velocity	[m/s]			3403.4			
Thrust-to-weight ratio	[−]			0.245			
Payload mass	[kg]			8000.0			
Fixed input							
Oxidiser choice	[−]	N2O4	LOX	LOX	LOX	LOX	LOX
Fuel choice	[−]	MMH	LH2	LH2	LH2	LH2	LH2
Atmospheric pressure	[bar]	0.0	0.0	0.0	0.0	0.0	0.0
Regenerative nozzle cooling	[−]	No	No	No	No	Yes	Yes
Regenerative chamber cooling	[−]	No	No	No	No	Yes	Yes
Number of turbines	[−]	N/A	N/A	2	2	2	2
Mixture type gas generator	[−]	N/A	N/A	fuel rich	fuel rich	N/A	N/A
Engine throttle	[−]	No	No	Yes	Yes	Yes	Yes
Other: see Table 5-5							

are compared. The discussion on the precision takes place first as it is important for the validity of further discussion. Though not verified, the findings for the other cycles should be very similar. This is a reasonable assumption as exactly the same optimisation routine is followed.

Next the results are validated and findings of good and/or badness of the method and results are presented and discussed.

In Section 8-7, Table 8-6 the results of the five optimisation runs can be found, reported in Table 8-2 are the found average value, standard deviation and relative standard deviation.

8-5-2-1 Precision

When studying the relative standard deviations of the results in Table 8-2 one immediately notices that the optimised input is quite different for every run. However when looking at the output (see also Table 8-6) one can see from Table 8-2 that the optimisation gives near identical results with exception for the throat diameter as this one is a direct result of the nozzle exit diameter and nozzle area ratio which are optimised input parameters.

The optimisation attempts to minimise the total wet mass including payload; this value has a relative standard deviation of less than a percent while the optimised inputs have quite large relative standard deviations.

The observation of returning very different optimised input parameters can be due to three causes:

- too little samples are used and the global minimum is not found
- there are many local minima that have a value close to the global minimum and therefore even with a large amount of samples chances are higher to find a local minimum than the global minimum.
- or the tolerances on the requirements set are too high such that a requirement is met too easily and a new iteration, which refines the search for a minimum, is not performed. In this case the solution with the lowest mass of the last iteration is accepted as solution while

Table 8-2: Ariane 5 LiRA upperstage with gas generator cycle optimisation average results of five consecutive runs with same requirements and same fixed input

Parameter	Unit	Average	St. dev	Relative st. dev [%]
Optimised input				
Chamber pressure	[bar]	35.1	15.4	43.8
Chamber mixture ratio	[−]	4.8	0.350	7.3
Nozzle exit diameter	[m]	1.5	0.390	25.7
Nozzle area ratio	[−]	221.2	35.3	16.0
Output				
Thrust	[kN]	48.4	488.4	1.0
Isp	[s]	476.6	4.9	1.0
Delta V	[m/s]	3425.5	6.1	0.2
Thrust to weight ratio	[−]	0.2	0.004	1.4
Burn time	[s]	970.0	11.0	1.1
Engine oxidiser mass flow	[kg/s]	8.7	0.243	2.8
Engine fuel mass flow	[kg/s]	1.9	0.112	5.9
Engine total mass flow	[kg/s]	10.6	0.184	1.7
Engine dry mass	[kg]	113.2	5.1	4.5
Pressurant tank mass	[kg]	164.3	8.0	4.9
Oxidiser tank mass	[kg]	69.9	1.5	2.1
Fuel tank mass	[kg]	246.3	16.3	6.6
Total dry mass	[kg]	1502.0	66.4	4.4
Pressurant mass	[kg]	25.6	1.2	4.9
Oxidiser mass	[kg]	8407.9	180.7	2.1
Fuel mass	[kg]	1842.4	121.9	6.6
Propellant mass	[kg]	10275.8	139.4	1.4
Total wet mass	[kg]	11777.8	165.6	1.4
Payload mass	[kg]	8000.0	0.000	0.0
Total dry mass incl. payload	[kg]	9502.0	66.4	0.7
Total wet mass incl. payload	[kg]	19777.8	165.6	0.8
Engine overall length	[m]	1.9	0.016	0.8
Engine overall diameter	[m]	1.2	0.034	2.8
Volume oxidiser tank	[m^3]	7.7	0.166	2.1
Volume fuel tank	[m^3]	27.3	1.8	6.6
Volume pressurant tank	[m^3]	0.5	0.024	4.9
Engine volume	[m^3]	2.2	0.141	6.5
Total volume	[m^3]	37.7	1.7	4.5
Nozzle throat diameter	[m]	0.1	0.020	20.1
Oxidiser tank length (for 5.4m diameter)	[m]	0.338	0.007	2.1
Fuel tank length (for 5.4m diameter)	[m]	1.190	0.079	6.6
Pressurant tank length (for 5.4m diameter)	[m]	0.022	0.001	4.9
Stage total length	[m]	3.402	0.069	2.0

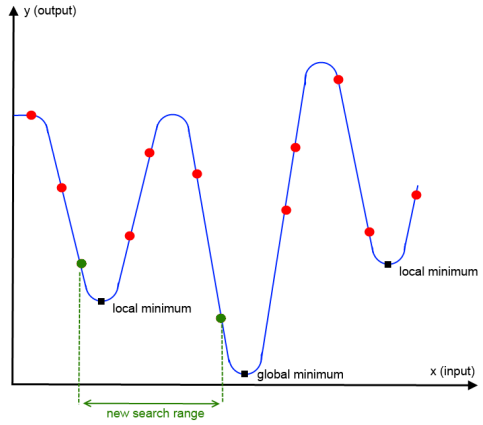

Figure 8-2: New search range optimisation for first iteration in attempt to find global minimum when too little samples are used; a local minimum will be found

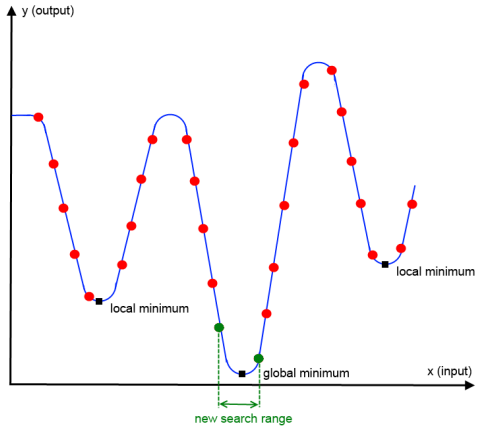

Figure 8-3: New search range optimisation for first iteration in attempt to find global minimum when sufficient samples are used; the global minimum will be found

this solution might not be the global minimum and even not be a local minimum; just the minimum of all samples.

Either way the global minimum (hence global optimum) is not found; the first cause is solved by increasing the amount of samples used, as is visualised by using only two dimensions in Figure 8-2, and Figure 8-3. The second cause can in theory also be solved by increasing the amount of samples, however one could not treat it as problem in the first place. When many local minima (hence local optima) exist with values close to the global, this is beneficial for the designer as one has much space to vary design parameters without significant penalty on the mass. The third cause can only be solved by decreasing the tolerances set on the requirements.

As the minimised mass in the output has near identical values, the second explanation is the most likely one and thus the optimisation space has many local minima that have values close to the global minimum. Two approaches to verify this cold be on one hand to run the optimisation with a huge amount of samples, this is however very time consuming, or alternatively use a deterministic optimisation methods which guarantees to find the global minimum as explained in section 8-2, and compare it to the minima found with Monte Carlo. If the same observations are made, the hypothesis of many local minima with values close to global minimum is correct.

One must thus conclude that while the precision of the output is good, additional optimisation goals need to be set to let the optimisation find a single solution. Nevertheless the output can be used for discussion as it does not change significantly with each optimisation run.

8-5-2-2 Validation of Optimisation Results

In order to assess whether or not the obtained results are realistic the optimised upper stages are compared with the current real upper stages

When comparing the turbo-pump fed stage dry masses (hence without payload) of the optimisation with the current Ariane 5 ESC-A it can be seen that during the optimisation the dry mass is likely

Table 8-3: Overview several upper stages for validation, sources: [64], [84], [85]

	Unit	EPS-V	H10-3	ESC-A	2nd stage	Centaur T	ECA-B
Launcher	[–]	Ariane 5	Ariane 4	Ariane 5	Delta IV 4m	Titan 4	Ariane 5
Engine	[–]	Aestus	HM7B	HM7B	RL10B-2	RL10A-3-3A	Vinci
Cycle	[–]	pf	gg	gg	ce	ce	ce
Oxidiser	[–]	N2O4	LOX	LOX	LOX	LOX	LOX
Fuel	[–]	MMH	LH2	LH2	LH2	LH2	LH2
Burn time	[s]	1000	780	945	840	600	720
Vac. Isp	[s]	321	445.1	446	460.4	444	467
Vac. F	[kN]	29	62.8	63.0	109.9	147.1	175
Stage wet mass	[t]	11.3	13.5	19.4	23.2	23.9	-
Stage propellant mass	[t]	10.0	11.8	14.9	20.4	21.0	28
Stage dry mass	[t]	1.3	1.7	4.5	2.8	2.9	-
Maximal payload capacity to GTO	[t]	7.55	2.17	10.05	6.16	5.76	12
Calc. Δv with max. payload	[m/s]	2380.1	6104.3	3084.0	5358.7	5360.3	-
Calc. F/W with max. payload	[–]	0.157	0.409	0.218	0.382	0.506	-

pf: pressure fed cycle gg: gas generator cycle be: bleed expander cycle
sc: staged combustion cycle ce: closed expander cycle

underestimated. However is not surprising as when the average value of the dry mass correction factor was determined in Appendix G, the Ariane 5 ESC-A had needed a correction factor of 5.58 which is 120.6% higher than the average factor determined.

However when comparing the original dry mass obtained by the optimisation with the dry mass of the H10-3 stage of the Ariane 4 suddenly the estimates are in the same order of magnitude. The dry mass of the H10-3 is also significantly lighter than the ESC-A.

When calculating the propellant to stage wet mass ratios one find a ratio of 0.87 for the H10-3 and 0.77 for the ESC-A suggesting that the dry mass contribution to the total wet mass is larger in the ESC-A than it is the case for the H10-3. The Ariane 4 H10-3 uses the same HM7B engine as the Ariane 5 ESC-A stage, hence the engine and engine support mass should be about the same. The difference in burn time and a slightly different mixture ratio also have an effect but can't be the cause that the ESC-A dry mass is more than two times higher than that of the H10-3. Therefore the difference must be sought in structural mass. The following hypothesis is put forward: the stage structural mass is strongly dependent on the total mass it has to support and the accelerations that it undergoes. Therefore stage dry mass increases not only with propulsion system mass as currently is assumed, but also with payload mass (under which not only the scientific payload but also all masses of any other stages and structures above the considered stage is understood) and with acceleration (as the acceleration can significantly increase forces and thus stresses in the structure, which hence needs to have sufficient thickness to withstand them). Therefore for accurate dry mass estimation one must know the acceleration profile of the whole launcher as the structure of a stage needs to be designed for the highest accelerations to which it is subjected even if these accelerations do not take place when the stage is active; this is often the case for upper stages. This implies that the optimisation routine must be integrated into a larger launcher design tool that has a trajectory model, where the stage dry mass and propulsion system mass is iteratively updated during launcher and trajectory design.

Further when propellant masses are compared, one can see that the estimated amount of propellant needed for the optimised stages is much lower than the current Ariane 5 ESC-A stage. This is

because the achieved specific impulse in the optimised engines is considerably larger than the specific impulse of the HM7B engine in the real ESC-A stage. As during the optimisation one optimises for lowest wet mass, automatically samples with high specific impulse will be selected. The reason that these high specific impulses can be reached is found in the fact that currently no limit is set on nozzle length and as a consequence large area ratios are possible; the HM7B only has an area ratio of 83.1 [33]. Further as can be seen in Figure 8-5, the nozzle tends to stick out of the stage and thus needs to be protected by an interstage skirt. The longer the nozzle, the larger and heavier this interstage skirt will become, this is not accounted for in current model.

Hence in order to improve accuracy one should:

- replace current method of estimating stage dry mass with an iterative method where first a stage mass is assumed, then a structural dry mass estimate is obtained from complete launcher design for a given payload mass in combination with accelerations obtained with a trajectory design module. Next the mass of the propulsion system of the stage for a required change in velocity and thrust-to-weight-ratio should be determined by optimisation as is currently performed by LiRA and added to the stage structural mass to find a new total stage dry mass and a new iteration can start.

- make specific impulse estimate closer to values seen in real engines by setting nozzle length constraints (which automatically implies a constraint on the nozzle area ratio as there is also a minimal throat diameter) and thus lead to a more accurate propellant mass estimate.

Nevertheless still a meaningful discussion is possible by comparing the different optimised engine cycles as they all have the same flaw.

8-5-3 Results for Other Cycles

The optimisation routine is ran using the suggested change in velocity tolerance of 1 percent and thrust-to-weight tolerance of 5 percent; the results of the optimisation are tabulated in Table 8-4.

8-5-4 Discussion of Results for All Cycles

Verification

The optimisation routine gives for the example a result for every engine cycle. To verify the results, it is manually checked if the requirements are met. The change in velocity is obtained using the rocket equation given in Eq. (3-90). The thrust to weight ratio relation is given by Eq. (3-92). Using the specific impulse, total dry mass including payload, total wet mass including payload one can see that the change in velocity returned is indeed the correct one. Similarly by using the thrust and total wet mass including payload also one can see that for every cycle the thrust-to-weight ratio returned is the correct one. In Table 8-5 it is verified if the returned values for Δv and F/W ratio match the ones obtained using hand calculates and if they are within the set tolerance and thus meet the requirements.

Table 8-4: Ariane 5 LiRA upperstage engine optimisation results

Parameter	Unit	Engine cycle					
		pf (stor.)	pf (cryo.)	gg	sc	ce	be
Optimised input							
Chamber pressure	[bar]	15.5	6.3	40.7	82.1	60.2	23.9
Chamber mixture ratio	[–]	2.39	6.57	4.19	3.94	3.80	5.28
Nozzle exit diameter	[m]	2.713	3.318	1.244	1.059	1.118	1.807
Nozzle area ratio	[–]	195.1	175.8	199.9	296.9	237.4	252.3
Output							
Thrust	[kN]	89.8	60.5	47.5	47.3	47.8	47.8
Isp	[s]	340.6	443.5	478.3	486.0	480.8	474.6
Delta V	[m/s]	3436.0	3394.1	3420.6	3391.0	3391.0	3427.5
Thrust to weight ratio	[–]	0.253	0.239	0.243	0.247	0.246	0.249
Burn time	[s]	860.0	1000.0	990.0	1000.0	1000.0	990.0
Engine oxidiser mass flow	[kg/s]	19.0	12.1	8.3	7.9	8.0	8.6
Engine fuel mass flow	[kg/s]	7.9	1.8	2.1	2.0	2.1	1.7
Engine total mass flow	[kg/s]	26.9	13.9	10.4	9.9	10.1	10.3
Engine dry mass	[kg]	136.5	106.3	114.2	125.2	120.7	108.8
Pressurant tank mass	[kg]	645.2	487.3	178.5	173.8	181.3	151.1
Oxidiser tank mass	[kg]	681.4	266.8	68.4	65.8	66.6	71.1
Fuel tank mass	[kg]	482.2	653.2	275.1	268.6	282.2	219.6
Total dry mass	[kg]	**4921.7**	**3829.4**	**1609.7**	**1602.6**	**1646.5**	**1392.9**
Pressurant mass	[kg]	100.3	75.8	27.8	27.0	28.2	23.5
Oxidiser mass	[kg]	16298.5	12070.2	8230.8	7921.0	8015.7	8557.2
Fuel mass	[kg]	6824.8	1838.1	2058.3	2009.7	2111.3	1642.8
Propellant mass	[kg]	**23223.7**	**13984.1**	**10316.9**	**9957.8**	**10155.2**	**10223.5**
Total wet mass	[kg]	**28145.4**	**17813.5**	**11926.6**	**11560.4**	**11801.7**	**11616.4**
Payload mass	[kg]	8000.0	8000.0	8000.0	8000.0	8000.0	8000.0
Total dry mass incl. payload	[kg]	12921.7	11829.4	9609.7	9602.6	9646.5	9392.9
Total wet mass incl. payload	[kg]	36145.4	25813.5	19926.6	19560.4	19801.7	19616.4
Engine overall length	[m]	3.8	3.2	1.8	1.9	1.9	1.9
Engine overall diameter	[m]	2.4	2.0	1.2	1.3	1.2	1.3
Volume oxidiser tank	[m^3]	11.6	11.1	7.6	7.3	7.4	7.9
Volume fuel tank	[m^3]	8.2	27.2	30.4	29.7	31.2	24.3
Volume pressurant tank	[m^3]	2.0	1.5	0.5	0.5	0.6	0.5
Engine volume	[m^3]	16.8	10.5	2.1	2.4	2.2	2.3
Total volume	[m^3]	**38.6**	**50.3**	**40.6**	**40.0**	**41.4**	**34.9**
Nozzle throat diameter	[m]	0.2	0.3	0.1	0.1	0.1	0.1
Oxidiser tank length (ϕ5.4 m)	[m]	0.505	0.485	0.331	0.318	0.322	0.344
Fuel tank length (ϕ5.4 m)	[m]	0.358	1.187	1.329	1.298	1.364	1.061
Pressurant tank length (ϕ5.4 m)	[m]	0.086	0.065	0.024	0.023	0.024	0.020
Stage total length	[m]	4.8	5.0	3.5	3.5	3.6	3.3

pf: pressure fed cycle | gg: gas generator cycle | be: bleed expander cycle
sc: staged combustion cycle | ce: closed expander cycle | N/A: Not Applicable
stor.: storable | cryo.: cryogenic | ϕ: diameter

Table 8-5: Verification of optimisation results

	Cycle				
		Returned by LiRA		Is result the same as manual calculation?	
		ΔV [m/s]	F/W [–]	ΔV	F/W ratio
Required value	all	3403.4	0.245	-	-
Optimisation result	stor. pf	3436.0	0.253	yes	yes
	cryo. pf	3394.1	0.239	yes	yes
	gg	3420.6	0.243	yes	yes
	sc	3391.0	0.247	yes	yes
	ce	3391.0	0.246	yes	yes
	be	3427.5	0.249	yes	yes
		difference		requirements met?	
		ΔV [%]	F/W [%]	ΔV	F/W ratio
Allowed tolerance	all	1.0	5.0	-	-
Difference between required and returned value	stor. pf	1.0	3.4	yes	yes
	cryo. pf	0.3	2.5	yes	yes
	gg	0.5	0.7	yes	yes
	sc	0.4	0.7	yes	yes
	ce	0.4	0.4	yes	yes
	be	0.7	1.5	yes	yes

pf: pressure fed cycle gg: gas generator cycle stor.: storable
sc: staged combustion cycle ce: closed expander cycle cryo.: cryogenic
be: bleed expander cycle -: Not Applicable

Validation

Due to the flaw in current stage dry mass calculation method, discussion on stage level is meaningless, however when focusing on propulsion system level still insightful discussions can be performed and conclusions can be drawn.

By studying the results in Table 8-4 one finds that cryogenic propulsion systems using a turbo-pump fed cycle have both a dry mass and propellant mass advantage, which automatically results also in a wet mass advantage, over systems with a storable or cryogenic pressure fed cycle. And that of those cryogenic turbo-pump fed propulsion systems, the ones with a closed cycle have a propellant advantage.

The lower energetic content of storable propellants decreases the achievable specific impulse (see also Table 3-3) and therefore increases the required total mass flow to attain a certain thrust (see Eq. (3-17)) compared to cryogenic fuels; this leads to a larger propellant mass. This effect is strengthened by the fact that the required thrust of a propulsion system also increases with its own mass for a fixed thrust-to-weight ratio, thus increasing the required mass flow again if the specific impulse is already at an optimum. On top of this a pressure fed system has heavier tanks due to the higher operating pressure; hence switching from a low energetic storable propellant combinations like N2O4-MMH to high energetic cryogenic propellants like LOX-LH2 leads to an improvement in mass as can be seen in Table 8-4.

When considering total propulsion system volume however, storable propellants tend to lead to a smaller tank volume because a storable oxidiser and fuel like N2O4 and MMH have a considerable higher density than cryogenic oxidiser and fuel like LOX and LH2. However when looking at the cryogenic propellant combinations in Table 8-4 only, turbo-pump fed systems appear to have a lower total volume than pressure fed systems; this is due to smaller engine size value for turbo-pump fed systems with similar tank volumes as the advantage of high density propellants does no longer apply.

While it does not have an significant impact on the results, it is noted that when comparing for the optimised engine cycles the nozzle exit diameter with the estimated engine diameter, one can see that estimated engine diameter can be smaller than the optimised nozzle exit diameter which hence is contradicting. Therefore one should use value of whichever of these two is the largest. Eq. (4-1), Eq. (4-2), Eq. (4-3) and Eq. (4-4) show a dependency of engine size on thrust; from the observation that turbo-pump fed systems have a lower required thrust with respect to pressure fed engines according to the optimisation, one can conclude that also the engine diameter and length should be smaller. Therefore it is possible that even though storable pressure fed systems have compacter tanks, the volume of the total propulsion system of a cryogenic turbo-pump system is smaller due to the smaller engine size.

While from a mass point of view only it is clear turbo-pump systems lead to considerable mass savings with respect to pressure-fed systems and possible also volume savings depending on the propellant choice, it is however harder to say which turbo-pump engine cycle is the best choice; the uncertainty in the dry mass and volume estimates of the turbo-pump cycles leads to overlapping estimations and thus makes a final engine choice indecisive. However when looking at the propulsion mass alone it can be clearly seen that the closed cycles (staged combustion cycle and closed expander cycle) have a mass in the order of a few hundred kilograms lower than the open cycles; therefore confirming that closed cycles are more propellant efficient.

8-6 Validity of Optimisation

Though the accuracy of the optimisation should be improved as discussed before, the routine has confirmed known trends such as:

- dry mass savings for pump fed systems with respect to pressure fed systems due to lighter tanks because of lower tank pressures.
- propellant mass savings for pump fed systems with respect to pressure fed systems due to higher chamber pressures which lead to increased specific impulse
- less propellant needed when switching from storable to cryogenic propellants.
- efficiency increases when switching from open to closed cycle

This indicates that the optimisation works and can be used for comparative means. However for actual stage design, the aforementioned flaws in specific impulse estimation and dry mass estimation must be solved.

8-7 Large Figures and Tables

Figure 8-4 shows an extract from the Ariane 5 user manual containing data on the Ariane 5 stages. Figure 8-5 is an information poster containing detailed data on the Ariane 5 ESC-A stage.

Table 8-6 tabulates the results of the 5 consecutive Ariane 5 LiRA upperstage gas generator cycle propulsion system optimisation runs performed in order to determine the precision and reproducibility.

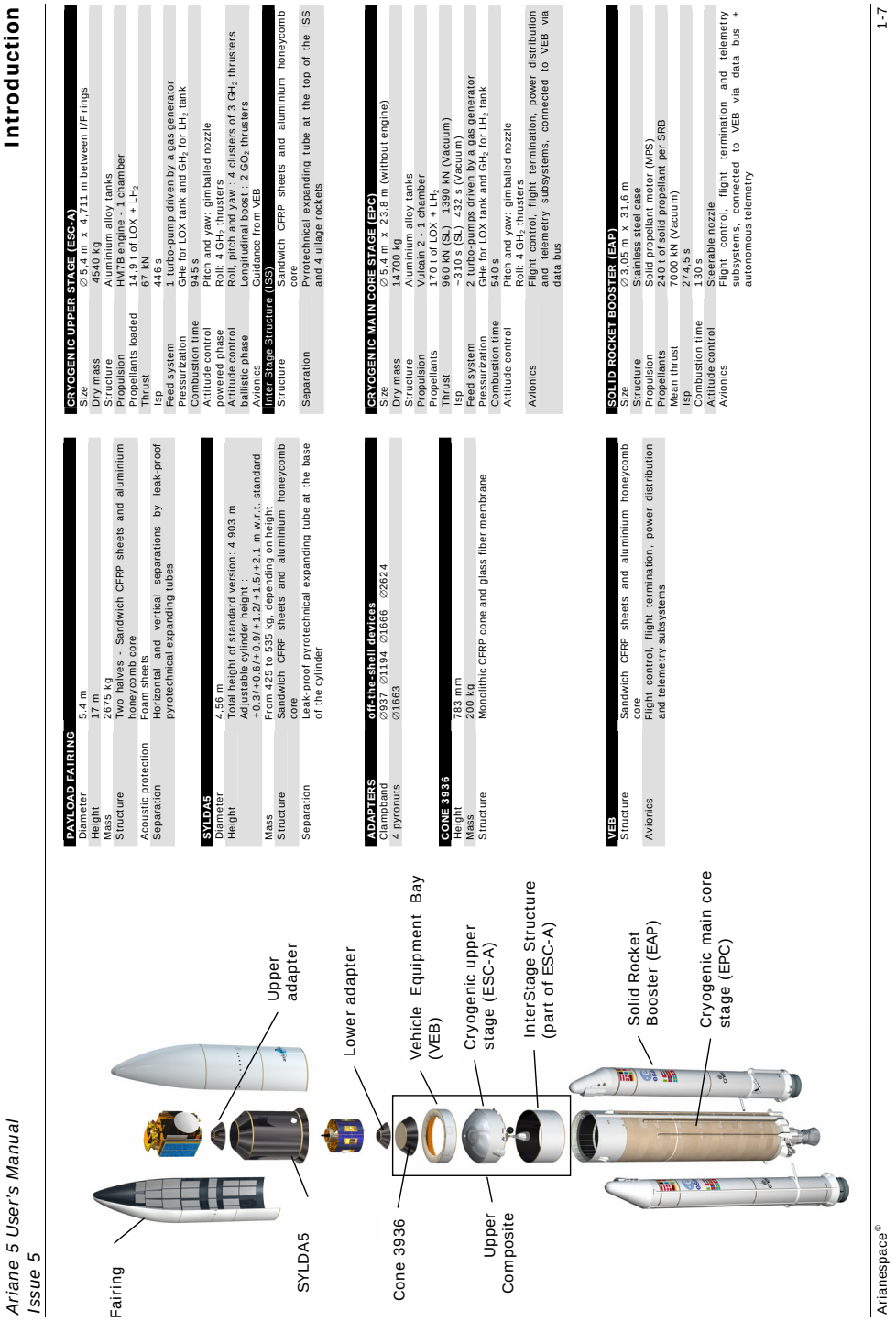

Figure 8-4: Ariane 5 data sheet [88]

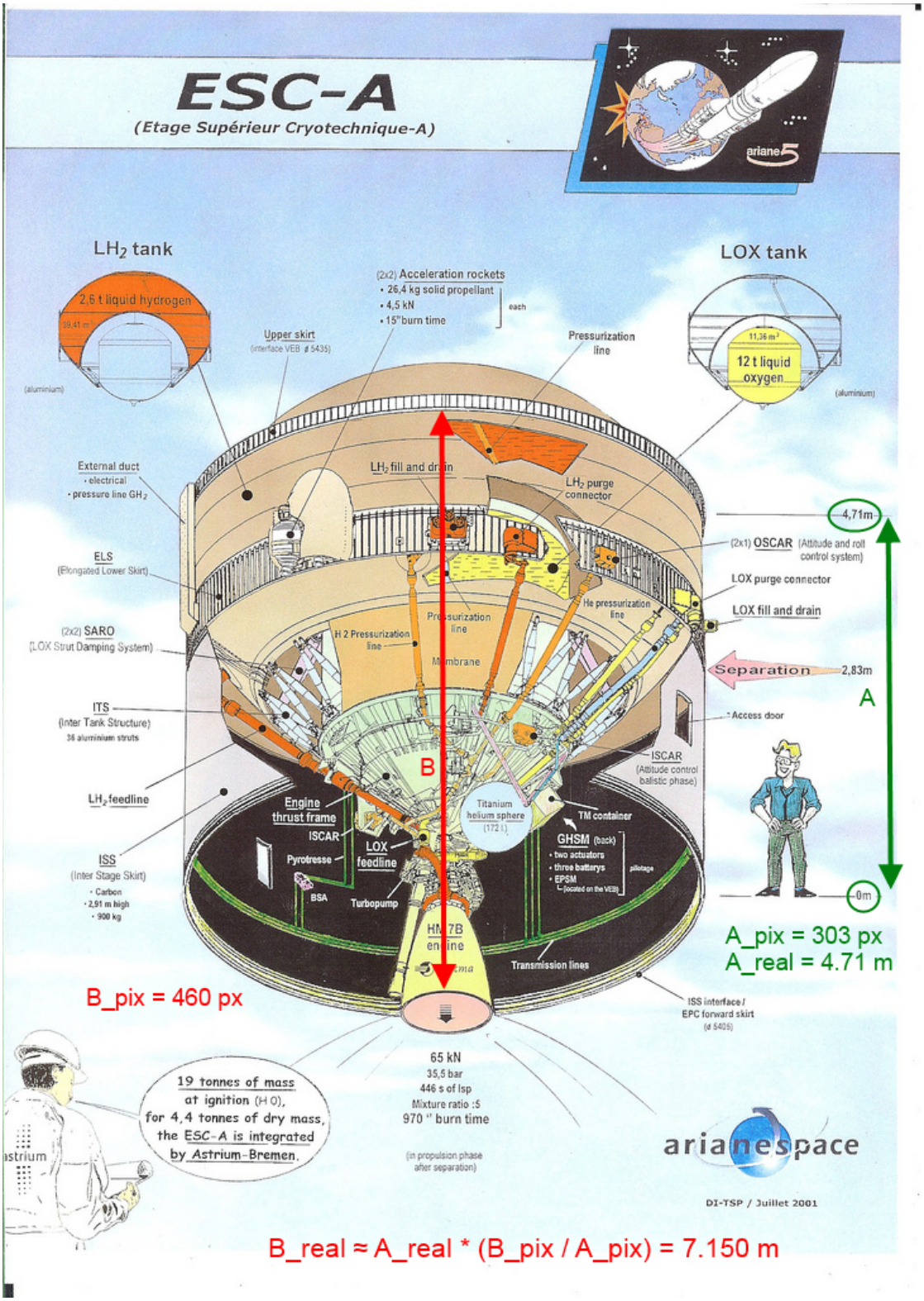

Figure 8-5: Ariane 5 ESC-A [89]

Table 8-6: Results of 5 consecutive Ariane 5 LiRA upperstage gas generator cycle propulsion system optimisation

Parameter	Unit	First run	Second run	Third run	Fourth run	Fifth run
Requirements						
Change in velocity	[m/s]			3403.4		
Thrust-to-weight ratio	[−]			0.245		
Payload mass	[kg]			8000.0		
Fixed input						
Oxidiser choice	[−]			LOX		
Fuel choice	[−]			LH2		
Atmospheric pressure	[bar]			0.0		
Regenerative nozzle cooling	[−]			No		
Regenerative chamber cooling	[−]			No		
Number of turbines	[−]			2		
Mixture type gas generator	[−]			fuel rich		
Other: see Table 5-5						
Optimised input						
Chamber pressure	[bar]	40.7	62.4	18.1	27.8	26.8
Chamber mixture ratio	[−]	4.19	4.81	4.75	5.28	4.92
Nozzle exit diameter	[m]	1.244	1.083	2.222	1.510	1.514
Nozzle area ratio	[−]	199.9	231.1	286.1	198.5	190.4
Output						
Thrust	[N]	47535.9	48315.9	48392.2	48704.9	48988.8
Isp	[s]	478.3	478.6	483.7	469.6	472.6
Delta V	[m/s]	3420.6	3431.6	3430.1	3429.2	3416.0
Thrust to weight ratio	[−]	0.243	0.248	0.254	0.250	0.252
Burn time	[s]	990.0	960.0	970.0	970.0	960.0
Engine oxidiser mass flow	[kg/s]	8.3	8.7	8.5	9.0	8.9
Engine fuel mass flow	[kg/s]	2.1	2.0	1.8	1.8	1.9
Engine total mass flow	[kg/s]	10.4	10.7	10.3	10.7	10.7
Engine dry mass	[kg]	114.2	122.3	106.7	111.5	111.4
Pressurant tank mass	[kg]	178.5	167.2	158.3	156.4	161.0
Oxidiser tank mass	[kg]	68.4	69.6	68.4	72.3	70.7
Fuel tank mass	[kg]	275.1	252.1	236.3	228.7	239.1
Total dry mass	[kg]	1609.7	1546.4	1441.4	1439.3	1473.0
Pressurant mass	[kg]	27.8	26.0	24.6	24.3	25.0
Oxidiser mass	[kg]	8230.8	8372.3	8224.6	8702.6	8509.0
Fuel mass	[kg]	2058.3	1886.3	1767.8	1710.7	1788.8
Propellant mass	[kg]	10316.9	10284.6	10017.0	10437.7	10322.8
Total wet mass	[kg]	11926.6	11831.1	11458.4	11877.0	11795.9
Payload mass	[kg]	8000.0	8000.0	8000.0	8000.0	8000.0
Total dry mass incl. payload	[kg]	9609.7	9546.4	9441.4	9439.3	9473.0
Total wet mass incl. payload	[kg]	19926.6	19831.1	19458.4	19877.0	19795.9
Engine overall length	[m]	1.8	1.9	1.9	1.8	1.8
Engine overall diameter	[m]	1.2	1.2	1.3	1.2	1.2
Volume oxidiser tank	[m^3]	7.6	7.7	7.6	8.0	7.8
Volume fuel tank	[m^3]	30.4	27.9	26.1	25.3	26.5
Volume pressurant tank	[m^3]	0.5	0.5	0.5	0.5	0.5
Engine volume	[m^3]	2.1	2.2	2.4	2.1	2.1
Total volume	[m^3]	40.6	38.3	36.6	35.9	36.8
Nozzle throat diameter	[m]	0.088	0.071	0.131	0.107	0.110

Chapter 9

Sensitivity and Uncertainty Analysis with LiRA

As the goal of LiRA is to help in the design of propulsion systems, an optimisation routine is build around the engine analysis routine. However for efficient optimisation it is desirable to know which input parameters have the largest impact on the design; for this a sensitivity analysis of relevant parameters is needed. Once an optimised design is obtained there still remains uncertainty in the output which should be quantified for meaningful discussion and conclusion drawing; for this an uncertainty analysis is needed.

This chapter has three goals; first to distinguish the different types of variabilities in a model, next to perform a qualitative sensitivity analysis to get a better understanding of the importance of certain variables and to identify those who will be of importance in quantitative analysis.

Finally the method of quantitative sensitivity analysis and quantitative uncertainty analysis are explained and applied to the in Chapter 8 optimised upper stage. First the quantitative sensitivity analysis theory is applied on the user variable input parameters in order to identify the most important ones that hence will be of the most importance during optimisation. Followed by the subjection of the optimisation results to quantitative uncertainty analysis to determine to uncertainty in optimisation results.

Saltelli et al give the following possible definition for sensitivity analysis: *"The study of how uncertainty in the output of a model (numerical or otherwise) can be apportioned to different sources of uncertainty in the model input."*[76] Loucks and van Beek rephrase this in [69] as *"A sensitivity analysis attempts to determine the change in model output values that result from modest changes in model input values."* Sensitivity analysis is not to be confused with uncertainty analysis which, according to Loucks and van Beek, *"attempts to describe the entire set of possible outcomes, together with their associated probabilities of occurence."*.[69]

In other words; an uncertainty analysis studies the effect of uncertainty in the model input parameters on the uncertainty of the output results (and thus affects the precision) while a sensitivity analysis attempts to identify those input parameters that affect the output results the

strongest and hence should be carefully chosen. The methods of performing this analyses are the same; they only differ in the type of parameters that are varied.

There are three types of model variabilities:

1. Natural variability:
   This uncertainty applies when input is time-related. For example during start or engine shut-off some input parameters such as pressure may be time varying, however as LiRA considers steady state solutions only and thus does not include a time dimension, this type of uncertainty is not present.
2. Knowledge uncertainty:
   Uncertainty related to approximations; e.g. use of typical values, correction factors and coefficients
3. Decision sensitivity:
   Many inputs are required to be user defined, e.g. nozzle exit diameter, expansion ratio, etc. but the user can take any value for these parameters which can have a great impact on the output.

Since there are many input parameters and even more output, the analysis will be limited to the study of only the most essential output parameters. Further a distinction is made between knowledge uncertainty parameters and decision sensitivity parameters; when studying the effect of variability of the decision variables on the output one speaks of sensitivity analysis, while when the effect of variability of the knowledge uncertainty parameters on the output is studied one speaks of uncertainty analysis.

The knowledge uncertainty parameters will be used to map the uncertainty in output results; they will be subjected to both one-at-the time and Monte Carlo analysis. The first will give insight into the uncertainty of the output while the latter identifies the most important contributor to the output uncertainty and hence shows which knowledge parameters should be studied first in order to improve the model's precision.

The decision sensitivity parameters are only subjected to one-at-the-time sensitivity analysis during which the knowledge uncertainty parameters are kept constant. This way the most important decision parameters for optimisation are identified.

Knowing hence the sources of largest uncertainty allows recommendation for further refinement of the model while knowing the input values which affect the output the most provides advise to the use which parameters must be carefully chosen and which are of minor importance and hence could easily be set to a typical value without having an significant impact on the output.

9-1 Parameter Identification

Candidate parameters to be subjected to uncertainty and sensitivity analysis are those who are independent of other parameters, the input parameters; all independent variable and non-variable parameters are shown in Table 5-1 and Table 5-2 respectively. All other parameters are hence a direct consequence of the choices made.

The most important output parameters are those that serve to compare engine cycles in terms of performance, mass and dimensions. Concerning performance change in velocity (ΔV) and thrust-to-weight ratio (F/W) are the most important as it defines the capabilities of a propulsions

system. Therefore thrust and specific impulse are important output parameters as well. Regarding mass and dimensions of the system, as discussed earlier, there are three main contributors; the engine, tanks and the propellant. Component masses and volumes have in the current way of modelling no impact on the total dry mass or total volume and can be safely left out for comparison purposes.

The reason for discussing dimensions in terms of volume and not in shape measurement parameters such as length, width, height and/or diameter is because for propellant tanks smart shapes are often used to minimise the waste of space further when expressing propellant tanks in length (or height) and diameter neglects the fact that due to momentum and inertia certain ratio's of length over diameter are undesired. The engine volume is the volume occupied by the smallest cylindrical-shaped enclosure that contains the engine completely. Based on the volume it can hence be decided if an engine and/or its propellants fit in a launcher stage.

In the next two subsections the independent variable and non-variable parameters (see Table 5-1 and Table 5-2) are grouped along their function in an optimisation while giving a rationale, linking to relevant relations discussed earlier, how they affect above identified important parameters that serve to compare engine cycles in terms of performance, mass and dimensions.

9-1-1 Decision Parameters

Non numeric decision parameters describe a characteristic of a propulsion system for which cannot be optimised, it is simply a characteristic choice of a propulsion system. Thee parameters hence need to be set by the user prior optimisation. An overview of parameters meeting this criterion is given in Table 9-1.

Some numeric parameters can be in theory varied over a range but in practice are often found almost always the same or with little variation and thus can be assumed to have a fixed typical value during optimisation. Parameters meeting this criterion are tabulated in Table 9-2

Hence the decision parameters left that can have values over a large range and considerably affect the functioning of a propulsion system are those found in Table 9-3 and Table 9-3.

9-1-2 Knowledge Parameters

All correction parameters have a calculated or typical value which is are not design variables, but have a significant impact the outcome of the design. Uncertainty in the value of these parameters directly affects the uncertainty of the outcome of an propulsion system analysis or optimisation. All concerning parameters are found in Table 9-5.

9-2 Parameter Ranges

Either the average and standard deviation is known or they are unknown but the minimum and maximum value are either known or can be deducted from a logical thought process. In either case it is assumed that the parameter is standard normal distributed and the minimum and maximum mark the 5 to 95 percentile range[1]. Hence in the first case where the nominal value(the average)

[1] the distance between the 50th and 95th percentile is 1.645 standard deviations (see normal curve area table in Figure 6-3) and thus the distance between the 5th and 95th percentile is $2 \cdot 1.645 = 3.3$

Table 9-1: Model non numeric decision parameters that need to be fixed during an optimisation

Parameter	Important parameters (in)directly affected	Rationale
Propellant combination	• specific impulse • thrust • turbo-pump mass • thrust chamber dimensions • thrust chamber mass	Oxidiser choice determines in combination with the fuel choice the the energetic values of the combustion process and thus directly affect specific impulse and thrust performance. The thrust chamber dimensions are also dependent on this combination through the propellant combination determined characteristic length, see Eq. (4-35). The same is true for the thrust chamber mass, see Section 4-2-6. The density of the propellants chosen contributes to the pump power required to pressurise that propellant(see Eq. (3-66)). Pump power determines required turbine power (see Eq. (3-70)) and thus affects the turbo-pump mass through Eq. (4-55).
Nozzle cooling method	• turbo-pump mass	If regeneratively cooling using oxidiser and or fuel is applied, a pressure drop takes places over the cooling channels and thus increases pump pressure rise, hence turbo-pump power (see Eq. (3-66) and Eq. (3-67)) which determine turbo-pump mass and dimensions (see Eq. (4-55) and Section 4-1-7 respectively).
Main combustion chamber cooling method	• turbo-pump mass	See rationale nozzle cooling method choice

and the standard deviation are known, the minimum and maximum are taken $avg \pm 1.645\sigma$. In the second case where the extrema are known, the average is simply the mean value of the two maximum and minimum value, while the standard deviation can be approximated by:

$$\sigma[X] = \frac{X_{high} - X_{low}}{3.3} \tag{9-1}$$

where X denotes the value of the parameter considered.

9-3 Methods of Quantitative Sensitivity and Uncertainty Analysis

Two types of quantitative sensitivity and uncertainty analyses are applied; first a one-at-the-time approach is taken to study the influence of a single parameter on the selected set of important output parameters related to performance, dimensions and mass. However as the one-at-the-time approach does not allow to study the impact of several parameters varying at the same time, a sampling based sensitivity analysis using Monte Carlo sampling is performed as well.

9-3-1 One-at-the-time First Order Analysis

For the most important output parameters, total wet mass and total propulsion system volume, a probabilistic error analysis is performed by defining probability distributions of the values for the various input parameters.

Table 9-2: Model numeric decision parameters that don't vary much in practice and thus for which optimisation is ineffective

Parameter	Important parameters (in)directly affected	Rationale
Pressurant initial temperature	• Pressurant mass • Pressurant volume • Pressurant tank mass • Pressurant tank volume	In combination with the pressure, the temperature affects the density and consequentially also the volume of the pressurant.
Pressurant initial pressure	• Pressurant mass • Pressurant volume • Pressurant tank mass • Pressurant tank volume	The pressure in the pressurant tank determines its wall thickness, thus mass of the tank and in combination with the temperature, the pressure affects the density and consequentially also volume of the pressurant itself and the tank.
Nozzle wall material	• Thrust chamber mass • Turbo-pump mass • Turbo-pump volume	In first place the material choice determines the mass of the thrust chamber. But in a regenerative cooled system, its thermal conductivity also determines the amount of heat transferred to the coolant and thus influences he pressure drop over the cooling channels which on its turn affects the required pressure rise over the pump(s) and thus influences the turbo-pump volume and mass.
Combustion chamber wall material	• Thrust chamber mass • Turbo-pump mass • Turbo-pump volume	See rationale nozzle wall material choice
Propellant tank ullage volume fraction	• Oxidiser tank mass • Oxidiser tank volume • Fuel tank mass • Fuel tank volume • Pressurant mass • Pressurant tank mass • Pressurant tank volume	Increases the propellant tank volume and therefore its mass as well. Larger propellant tanks mean, more pressurant needed, hence increase in pressurant mass, pressurant tank volume and pressurant tank mass as well.
Propellant tank boil off volume fraction	• Oxidiser tank mass • Oxidiser tank volume • Fuel tank mass • Fuel tank volume • Oxidiser mass • Fuel mass • Pressurant mass • Pressurant tank mass • Pressurant tank volume	See rationale propellant tank ullage volume fraction
Propellant tank trapped volume fraction	• Oxidiser tank mass • Oxidiser tank volume • Fuel tank mass • Fuel tank volume • Oxidiser mass • Fuel mass • Pressurant mass • Pressurant tank mass • Pressurant tank volume	Increases the amount of oxidiser and fuel needed and therefore also the volume and consequentially the mass of the tanks. Larger propellant tanks mean, more pressurant needed, hence increase in pressurant mass, pressurant tank volume and pressurant tank mass as well.

Table 9-3: Model numeric decision parameters for which optimisation is possible (1/2)

Parameter	Important parameters (in)directly affected	Rationale
Main combustion chamber pressure	• Gas generator mass • Turbo-pump mass • Specific impulse • Thrust • Oxidiser tank mass (pressure fed only) • Fuel tank mass (pressure fed only)	Both the pressure in the nozzle and in the gas generator or pre-burner when applicable, follow from the pressure in the main combustion chamber. The wall thickness of these components are determined through the pressure and consequentially the thrust chamber and gas generator masses are affected. Further the required pressure rise over the pumps is dependent on the pressure rise required over the pumps or in case of a pressure fed system, the pressure in the propellant tanks. Finally the main combustion chamber pressure choice determines in combination with the mixture ratio and the propellant choice the the energetic values of the combustion process and thus directly affect specific impulse and thrust performance.
Main combustion chamber mixture ratio	• Specific impulse • Thrust	The mixture ratio choice determines in combination with the main combustion chamber pressure and the propellant choice the the energetic values of the combustion process and thus directly affect specific impulse and thrust performance.
Nozzle exit diameter	• Thrust chamber dimensions • Thrust chamber mass	See Section 4-1-4, Section 4-1-5 and Section 4-2-6
Nozzle area ratio	• Specific impulse • Thrust • Thrust chamber dimensions • Thrust chamber mass	The area ratio has a direct influence in the thrust coefficient (see Eq. (3-15)) and further determines the Mach number of the flow throughout the thrust chamber and thus specifies the specific impulse and thrust relations through the resulting flow properties (see Section 3-2).
Atmospheric pressure	• Specific impulse • Thrust	The thrust coefficient is dependent on the atmospheric pressure through Eq. (3-15). Hence the latter also influences the specific impulse and thrust through Eq. (3-17) and 3-21
Burn time	• Oxidiser volume • Fuel volume • Pressurant volume • Oxidiser mass • Fuel mass • Pressurant mass • Oxidiser tank volume • Fuel tank volume • Pressurant tank volume • Oxidiser tank mass • Fuel tank mass • Pressurant tank mass	The longer the burn time the more propellant needed, the larger the propellant tanks, the more pressurant needed, the larger the pressurant tank. Larger tanks mean larger tank masses and larger tank volumes.
Number of turbines (turbo-pump configuration)	• Turbo-pump mass	The amount of turbo-pumps evidently directly affects the total turbo-pump mass.
Pump efficiency	• Turbo-pump mass • Turbo-pump volume	The pump efficiency affects turbo-pump power through Eq. (3-66) and Eq. (3-67) and therefore turbo-pump mass and volume.

Table 9-4: Model numeric decision parameters for which optimisation is possible (2/2)

Parameter	Important parameters (in)directly affected	Rationale
Turbine efficiency	• Turbo-pump mass • Turbo-pump volume	The turbine efficiency affects turbo-pump power and therefore turbo-pump mass and volume.
Turbine mechanical efficiency	• Turbo-pump mass • Turbo-pump volume	The turbine mechanical efficiency affects turbo-pump power through Eq. (3-70) and therefore turbo-pump Mass and volume
Turbine pressure ratio	• Turbo-pump mass • Turbo-pump volume	The turbine pressure ratio affects turbo-pump power through Eq. (3-72) and therefore turbo-pump mass and volume.
Turbine inlet temperature	• Turbo-pump mass • Turbo-pump volume	The turbine inlet temperature relates to the turbine-power through Eq. (3-75) and/or Eq. (3-76)
Propellant initial temperature	• Oxidiser tank mass • Oxidiser tank volume • Pressurant mass • Pressurant tank mass • Pressurant mass	The propellant temperature determines its density and consequentially also volume of the propellant and the tank. The amount of pressurant needed is dependent on the propellant tank size, and thus both pressurant mass and pressurant tank mass are influenced by this parameter.
MEOP oxidiser tank	• Oxidiser tank mass • Oxidiser tank volume • Pressurant tank mass • Pressurant tank volume • Turbo-pump mass • Turbo-pump volume	Propellant tank pressure determines propellant density and volume and hence tank volume. It also defines the wall thickness, thus mass of the tank. The required amount of pressurant increases with the propellant tank volume, hence also the pressurant tank mass and volume are affected. Further the higher the pressure in the propellant tank, the lower the required pressure rise from the pumps, hence the smaller and lighter the turbo-pump.
MEOP fuel tank	• Fuel tank mass • Fuel tank volume • Pressurant tank mass • Pressurant tank volume • Turbo-pump mass • Turbo-pump volume	see rationale MEOP fuel tank

Table 9-5: Model knowledge parameters

Parameter	Important parameters (in)directly affected	Rationale
Specific impulse correction factor	• Specific impulse • Thrust	Directly affects specific impulse and thrust through Eq. (3-20). For a given thrust requirement, the specific impulse value affects the mass flow rate through Eq. (3-21) and thus propellant and propellant tank mass.
Thrust chamber mass correction factor	• Thrust chamber mass	Affects thrust chamber mass
Gas generator mass correction factor	• Gas generator mass	Affects gas generator mass
Propellant tank performance factor	• Oxidiser tank mass • Fuel tank mass	Affects oxidiser tank mass and fuel tank mass
Pressurant tank performance factor	• Pressurant tank mass	Affects Pressurant tank mass

Table 9-6: Knowledge uncertainty parameter ranges

Parameter	Unit	Mean	St. dev	Min	Max	Rationale
Specific impulse correction factor	[−]	0.9000	0.0192	0.8684	0.9316	see Table 3-8
Thrust chamber mass correction factor	[−]	1.52	0.80	0.204	2.836	*
Gas generator mass correction factor	[−]	1.52	0.80	0.204	2.836	†
Propellant tank performance factor	[−]	33200	10400	16092	50308	see Section 4-2-2
Pressurant tank performance factor	[−]	122000	39100	57680.5	186319.5	see Section 4-2-2
Dry mass correction factor	[−]	2.53	1.44	0.1612	4.8988	‡

* mean and standard deviation are calculated in Appendix H.
† No value was found for this factor (see Section 4-2-7), however as a thrust chamber and a gas generator are very similar the same bounds will be taken as uncertainty.
‡ mean and standard deviation are calculated in Appendix G

Table 9-7: Decision sensitivity parameter ranges

Parameter	Unit	Min	Max	Rationale
Main comb. chamber pressure	[bar]	5	25	pressure fed⋆
		5	105	gas generator*
		10	70	expander*
		70	210	staged combustion*
Main comb. chamber mix. ratio	[–]	2.0	4.0	LOX-RP1 †
		3.0	7.0	LOX-LH2 †
		2.37	3.0	N2O4-MMH †
Nozzle exit diameter	[m]	1	5	‡
Nozzle area ratio	[–]	8	300	△
Atmospheric pressure	[bar]	0	1.01325	◦
Burn time	[s]	100	1500	◇
Pressurant initial pressure	[bar]	150	331	#
MEOP oxidiser tank	[bar]	13.0	90.0	pressure fed ⊙
		1.1	3.4	turbo-pump fed ⊙
MEOP fuel tank	[bar]	13.0	90.0	pressure fed ⊙
		1.1	3.4	turbo-pump fed ⊙
Pump efficiency	[–]	0.585	0.795	⋆⋆
Turbine efficiency	[–]	0.345	0.723	⋆⋆
Turbine mechanical efficiency	[–]	0.65	0.975	**
Turbine pressure ratio	[–]	1.85	22.0	††
Turbine inlet temperature	[K]	800	1350	‡‡

⋆ lower limit taken at 5 bar to avoid pressure becoming below zero during expansion in nozzle, upper limit based on maximum chamber pressure found of pressure fed engines of which data is available in literature (see Table D-1)
* limits based on ranges given in Figure 9-1, except for the gas generator cycle the lower limit is taken at 5 bar to avoid pressure becoming below zero during expansion in nozzle
† typical mixture ratio ranges were discussed in Section 3-2 and are given in the fifth and sixth column of Table 3-5
‡ these limits are assumptions.
△ range bounds are the minimum and maximum of Table D-5
◦ minimum is vacuum and maximum is standard sea level pressure
◇ These limits are assumptions. The shortest burn times can be as low as 5s according to Sutton [4], but in reality for launchers 100s is a more practical lower limit. An upper limit is also hard to define, but is set to 1500, 300 seconds more than the burn time of the Aestus on Ariane V EPS.
minimum and maximum of Table I-12
⊙ typical ranges are discussed in Section 3-9. However for turbo-pump fed systems the lower bound has been set to 1.1 bar because lower pressures could lead to excessive turbo-pump requirements for high main combustion chamber pressure. This lower bound was found by running the model for the maximum supported main combustion chamber pressure (100 bar and finding the lowest propellant tank pressure which could still be solved without errors being thrown by the model.
⋆⋆ range boundaries are the average plus and minus 1.645 standard deviation determined in Table E-1
** see subSection 3-6-2
†† This ratio is only used in the open cycles (gas generator and bleed expander). The min and max are the minimum and maximum value of the available engine data of Table D-10
‡‡ Minimum and maximum values are those found in literature (see sec. 3-6-5)

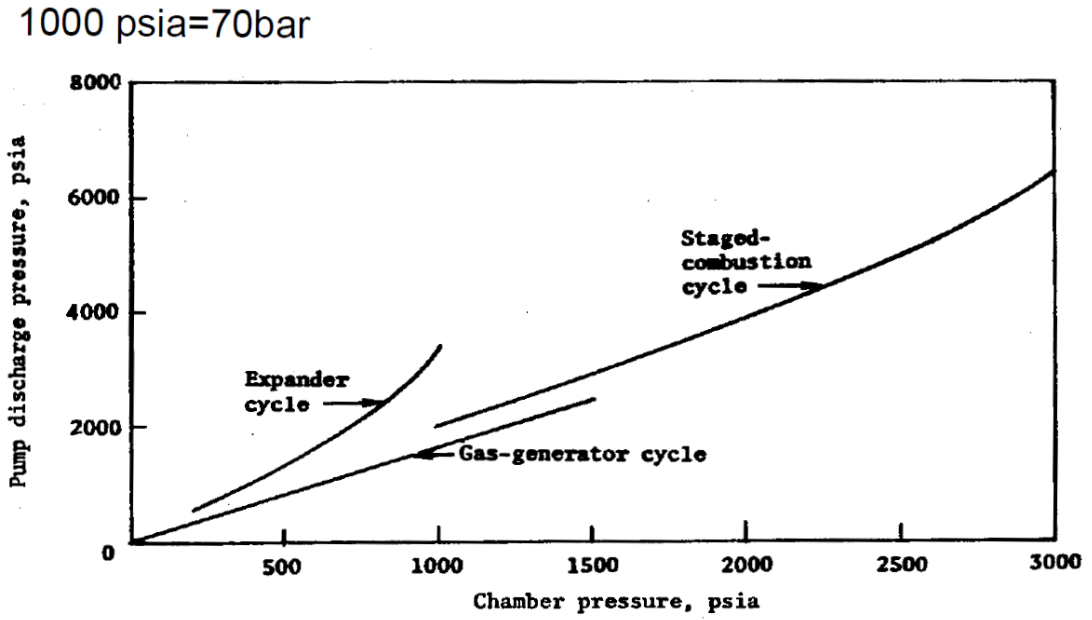

Figure 9-1: Ranges of applicability of different cycles [7])

Each investigated input variable is assigned a high and low value based on either the difference in known maximum and minimum for this value or from a known parameter's distribution. The model is executed varying each parameter one at the time to evaluate the impact of those variations on the model output. To limit the amount of executions only worst and best cases are considered, meaning the model is run for each input parameter one time with its lowest and one time with its highest value. The assumptions made here that all input parameters are independent from each other.

The first order one-at-the-time sensitivity analysis follows the method suggested by Loucks and van Beek in [69]. Let I represent the 'system performance indicator' which is the model output being observed while X is the model input parameter which is varied. The impact that an input parameter X has on the output I is given by the contribution its error variance ($Var[X_i]$) makes to the total error variance ($Var[I]$). (Error variance means the spread of the errors generated by the variability of parameter X. A small variance indicates that the estimates are close to the mean and thus have small standard deviation, which is simply the square root of the variance, and thus the estimates have high precision.) In other words:

$$\% = 100 \cdot \frac{Var[X_i]}{Var[I]} \tag{9-2}$$

where

$$Var[I] = \sum \left[\left(\frac{\delta I}{\delta X_i} \right)^2 \cdot Var[X_i] \right] \tag{9-3}$$

with $\frac{\delta I}{\delta X_i}$ is the sensitivity coefficient which can be approximated by:

$$\frac{\delta I}{\delta X_i} = \frac{I_{i,high} - I_{i,low}}{X_{i,high} - X_{i,low}} \tag{9-4}$$

and the variance of parameter X is the square of the parameter's standard deviation:

$$Var[X] = (\sigma[X])^2 \tag{9-5}$$

once the total error variance is known, the total parameter standard deviation follows from the square root:

$$\sigma[I] = \sqrt{Var[I]} \tag{9-6}$$

The lower and higher value for parameter X (X_{low} and X_{high}) and its standard deviation ($\sigma[x]$) are found in the tables in Section 9-2

9-3-2 Sampling Based Simple Monte-Carlo Analysis

According to Hickman et al. Monte Carlo simulation is the most direct approach of quantitative uncertainty propagation when input uncertainties are given as distributions over a certain parameter. [77]. The spread of results of subjecting the knowledge uncertainty parameters to Monte Carlo analysis gives an indication of the uncertainty range of the solutions while subjecting the decision parameters to Monte Carlo analysis would yield the solution space; however the latter is not performed as its results are not useful for the scope of the sensitivity study. In sampling based sensitivity and uncertainty analysis using simple Monte-Carlo analysis random model input parameter combinations are generated with a certain distribution of which the boundaries are assumed known for each parameter studied. The spread of the output parameters yields an average and standard deviation which hence give a quantitative measure of uncertainty of the output.

9-4 Identification of Optimisation Input Parameters

In order to find which decision parameters need to be variable in the optimisation and which can be taken constant to reduce computation time, a sensitivity study of the output to the decision parameters is performed. Output parameters of importance are change in velocity (Δv) and thrust-to-weight ratio (F/W) as these are the parameters to optimise for. Both affect hence the required thrust and the mass with respect to this required thrust.

Because all thruster related parameters (main combustion chamber pressure, main combustion chamber mixture ratio, nozzle exit diameter and nozzle area ratio) determine the specific impulse and mass flow they are expected to have the largest impact on the specific impulse hence thrust and consequentially change in velocity and thrust-to-weight ratio. Though the burn time should also have a major impact on the mass, its value is dependent on the change in velocity requirement, as will be explained in more detail later on, and hence will be left out of the sensitivity analysis.

For the optimisation of an upper stage it is reasonable that the atmospheric pressure is low enough to assume vacuum; hence the atmospheric pressure is also left out of the analysis.

Table 9-8: Input used for study of sensitivity of change in velocity, thrust-to-weight-ratio and total wet mass to selected decision parameters

Parameter	Unit	pf	gg	sc	ce	be
Oxidiser	[–]	N2O4	LOX	LOX	LOX	LOX
Fuel	[–]	MMH	LH2	LH2	LH2	LH2
Nozzle exit diameter	[m]	1.315	0.992	1.737	1.02	1.625
Nozzle area ratio	[–]	84	82.9	52	61.1	130
Atmospheric pressure	[Pa]	0	0	0	0	0
Burn time	[s]	531	970	346	600	400
Pressure main combustion chamber	[bar]	11	36	131.7	32.6	39.8
Mixture ratio main combustion chamber	[–]	1.9	4.565	6.0	5.0	5.0
Nozzle cooling	[–]	No cooling	No cooling	No cooling	Regenerative cooling	Regenerative cooling
Chamber cooling	[–]	No cooling	Regenerative cooling	No cooling	Regenerative cooling	Regenerative cooling
Number of turbines	[–]	N/A	1	1	1	2
Engine throttle	[–]	No	Yes	Yes	Yes	Yes
Other parameters see Table 5-5						

pf: pressure fed cycle
gg: gas generator cycle
sc: staged combustion cycle
ce: closed expander cycle
be: bleed expander cycle
N/A: Not Applicable

In order to run the computations test cases are needed, so assuming existing engines are optimised systems, let's vary their 'decision parameters' in order to see how it affects their change in velocity, thrust-to-weight-ratio and total wet mass. Note that by varying the decision input parameters the engines evidentially change as well, the goal is not to see how other parameters must change in order to keep the system the same but to see which decision parameters affect the aforementioned output parameters the strongest.

For the computations test cased based on the Aestus engine for the pressure fed cycle, HM7B engine for the gas generator cycle, LE-7 engine for the staged combustion cycle , RL10A-3-3A for the closed expander cycle and LE-5A engine for bleed expander cycle, are used. Input data used is given in Table 9-8. Some of this input data is hence not fixed but varied during the computations. All not shown input data such as pressurant choice, pressurant initial temperature, pressurant initial pressure, etcetera are assumed to have the typical values discussed earlier in Chapter 3 and Chapter 4 and who are summarised in Table 5-5. These typical values are assumed automatically when LiRA is ran and no value is specified in the input file for the concerning parameters. The value of the parameter is also shown in the command window output.

Table 9-9 shows the sensitivity of the change in velocity, thrust-to-weight ratio and total wet mass to variation in the decision parameters. The values are the percentages that the decision parameter contributes to the variation of the observed change in velocity, thrust-to weight ratio and total wet mass; they hence do not tell how large the variation is. The latter is of no importance as it is the task of optimisation to find optimal decision parameter values.

As expected Table 9-9 confirms that the thruster related parameters, main combustion chamber pressure, main combustion chamber mixture ratio, nozzle area ratio and nozzle exit diameter affect the change in velocity, thrust-to-weight ratio and achievable thrust significantly.

The tank maximum operating pressure also has a considerable impact as it affects the tank mass

Table 9-9: OAT comparison of approximate decision sensitivity parameter sensitivity for all studied engine cycles

Output parameter	Input parameter	Parameter sensitivity [%]				
		pf	gg	sc	ce	be
Vacuum change in velocity (Δv)						
	Main combustion chamber pressure	89.3	0.1	0.1	0.1	0.1
	Main combustion chamber mixture ratio	0.2	16.5	25.3	17.7	18.7
	Nozzle exit diameter	1.4	1.1	8.8	3.2	8.9
	Nozzle area ratio	9.1	42.9	30.9	39.8	34.0
	Pressurant initial pressure	0.0	0.1	0.1	0.1	0.1
	MEOP oxidiser tank	N/A	3.6	5.1	4.3	4.1
	MEOP fuel tank	N/A	35.7	29.7	34.8	34.0
	Pump efficiency	N/A	0.0	0.0	0.0	0.0
	Turbine efficiency	N/A	0.0	0.0	0.0	0.0
	Turbine mechanical efficiency	N/A	0.0	0.0	0.0	0.0
	Turbine pressure ratio	N/A	0.0	0.0	0.0	0.0
	Turbine inlet temperature	N/A	0.0	0.0	0.0	0.0
Vacuum thrust to weight ratio (F/W)						
	Main combustion chamber pressure	41.2	2.9	0.1	0.1	0.0
	Main combustion chamber mixture ratio	2.4	0.1	0.7	0.0	0.1
	Nozzle exit diameter	0.5	0.1	0.9	0.3	1.2
	Nozzle area ratio	55.9	91.5	95.0	95.5	94.0
	Pressurant initial pressure	0.0	0.0	0.0	0.0	0.0
	MEOP oxidiser tank	N/A	0.5	0.5	0.5	0.6
	MEOP fuel tank	N/A	3.9	2.8	3.6	4.0
	Pump efficiency	N/A	0.1	0.0	0.0	0.0
	Turbine efficiency	N/A	0.5	0.0	0.0	0.1
	Turbine mechanical efficiency	N/A	0.1	0.0	0.0	0.0
	Turbine pressure ratio	N/A	0.2	0.0	0.0	0.0
	Turbine inlet temperature	N/A	0.0	0.0	0.0	0.0
Total wet mass ($m_{total,wet}$)						
	Main combustion chamber pressure	1.2	1.0	0.8	0.5	0.4
	Main combustion chamber mixture ratio	0.0	0.0	0.0	0.0	0.0
	Nozzle exit diameter	50.4	76.2	47.1	84.2	15.8
	Nozzle area ratio	48.4	22.8	52.1	15.3	83.7
	Pressurant initial pressure	0.0	0.0	0.0	0.0	0.0
	MEOP oxidiser tank	N/A	0.0	0.0	0.0	0.0
	MEOP fuel tank	N/A	0.0	0.0	0.0	0.0
	Pump efficiency	N/A	0.0	0.0	0.0	0.0
	Turbine efficiency	N/A	0.0	0.0	0.0	0.0
	Turbine mechanical efficiency	N/A	0.0	0.0	0.0	0.0
	Turbine pressure ratio	N/A	0.0	0.0	0.0	0.0
	Turbine inlet temperature	N/A	0.0	0.0	0.0	0.0

pf: pressure fed cycle
gg: gas generator cycle
sc: staged combustion cycle
ce: closed expander cycle
be: bleed expander cycle
N/A: Not Applicable

and thus dry and wet mass of the propulsion system. While it can be seen in Table 9-9 that the effect of tank pressure for the total wet mass is small compared to other parameters studied, the change in velocity is affected more severe as it is a function of the natural logarithm of the ratio of wet to dry mass. The thrust-to-weight ratio is also affected more severe as the mass is multiplied with the gravitational acceleration, hence about a factor 10, in order to obtain weight.

Thus in conclusion based on above analysis, when optimising the propulsion system for given change in velocity and given thrust-to-weight ratio, the input parameters that are important to consider are main combustion chamber pressure, main combustion mixture ratio, nozzle exit diameter, nozzle area ratio, maximum operating pressure of the oxidiser tank and maximum operating pressure of the fuel tank. All other decision parameters can be assumed typical constant values without having a significant impact on the change in velocity, thrust to weight ratio or total wet mass.

As will be explained in the next section, the maximum operating pressure of the oxidiser and fuel tank will not be varied during optimisation of the stage because this requires an additional loop which demands too much computation time.

9-5 Sensitivity and Uncertainty Analysis of Ariane 5 LiRA Upperstage Optimisation Results

In the models several correction factors were used which have an uncertainty, this leads to uncertainty in the output. Since the thrust chamber mass and gas generator mass are not used for the total dry mass estimation, their correction factors have no impact on the outcome of the optimisation. This means that the specific impulse correction factor, propellant tank performance factor, pressurant tank performance factor and dry mass correction factor should be subjected to uncertainty analysis.

By varying the values of these knowledge uncertainty parameters, running the optimisation again and observing the output, conclusions can be drawn from the variation in output.

First the knowledge parameter that causes the most uncertainty in the results is determined using one-at-the-time uncertainty analysis. Next the average and standard deviation of the engine total wet mass, total volume and thrust are determined with sampling based uncertainty analysis using simple Monte-Carlo analysis.

Because this uncertainty analysis takes very long, it is only performed for a single engine as demonstration. The choice has been set to the gas generator engine as the HM7B gas generator engine is currently used in Ariane 5's cryogenic upper stage and thus results can be more easily compared to real results.

Application of on-at-the-time sensitivity and uncertainty analysis to example

Table 9-10 shows the sensitivity of the optimised input and output parameters to the uncertainty in the knowledge uncertainty parameters. The values are the percentages that the knowledge uncertainty parameter contributes to the uncertainty of the observed optimised input or output parameter; they hence do not tell how large the variation (hence uncertainty) is. The uncertainty itself is given by the standard deviation which is found in the last column of Table 9-10. The higher the standard deviation, the larger the spread of estimates is and hence the more uncertainty

Table 9-10: Sensitivity of optimised input and output to the uncertainty in the knowledge uncertainty parameters for the gas generator cycle

Parameter	Dry mass corr. fac.	Spec. imp. corr. fac.	Prop. tank perf. fac.	Press. tank perf. fac.	St.dev.
Optimised input					
Chamber pressure	0.65	92.51	6.80	0.04	13.2 bar
Chamber mixture ratio	4.78	8.05	79.67	7.50	0.67
Nozzle exit diameter	37.37	60.82	0.15	1.67	0.260 m
Nozzle area ratio	13.76	35.91	49.89	0.44	10.9
Output					
Thrust	39.44	0.97	42.65	16.94	6.9 kN
Burn time	16.67	16.67	0.00	66.67	7.4 s
Total dry mass incl. payload	44.46	0.10	41.82	13.62	1416 kg
Total wet mass incl. payload	41.87	1.00	46.06	11.07	2978 kg
Total volume	55.68	1.32	8.23	34.77	3.9 m^3

there is in an estimate. So now let's say one thinks the uncertainty in total dry and total wet mass is too high then the sensitivity coefficients tell us that the uncertainty in the dry mass correction factor and in the propellant tank performance factor contribute the most to the uncertainty in these output parameters.

Hence one can conclude that:

1. in order to reduce the uncertainty in the total dry and wet mass estimate (which means reducing the standard deviation) significantly one must focus on decreasing the uncertainty in:

   - dry mass correction factor.
   - propellant tank performance factor.

   And in a second place in the pressurant tank performance factor. The uncertainty in the specific impulse factor has only a small contribution to the uncertainty in the mass estimates.
2. in order to reduce the uncertainty in total propulsion system volume estimate significantly, the results show one must in first place focus on decreasing the uncertainty in:

   - dry mass correction factor.
   - pressurant tank performance factor.

   And in a second instance on the propellant tank performance factor. The uncertainty of the specific impulse correction factor has a minimal contribution to the uncertainty in the total propulsion system estimate.

Application of sampling based sensitivity and uncertainty analysis using simple Monte Carlo analysis to example.

The standard deviations found in Section 9-5 are based on one-at-the-time variations and thus do not account for simultaneous variations of the knowledge parameters. Hence in order to assess the uncertainty in the output for combined uncertainty in the knowledge parameters one must

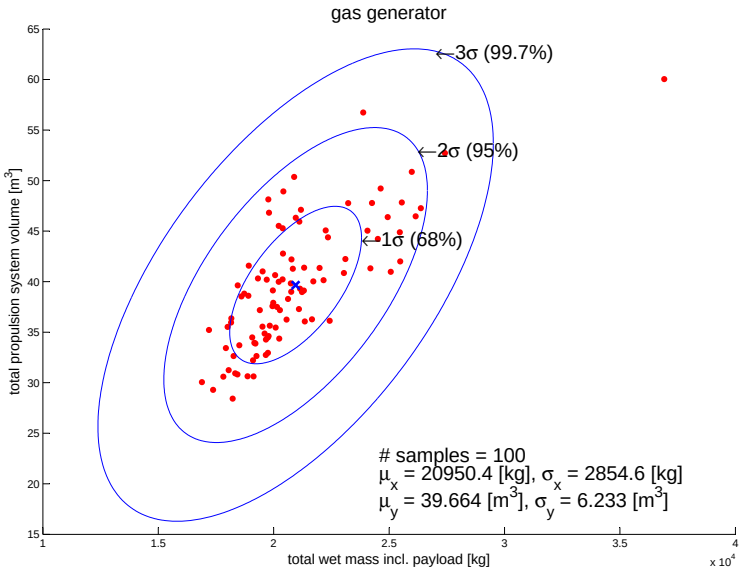

Figure 9-2: Total propulsion system volume versus total wet mass including payload dispersion of solutions for the Ariane 5 upper stage gas generator cycle case

try out several random combinations and determine a standard deviation based on the obtained output. For this the simple Monte Carlo analysis is used.

Figure 9-2 gives the results of the Monte Carlo analysis where the total estimated propulsion system volume is plotted against the total estimated stage wet mass. The other plots are found in Section 9-6, Figure 9-3 and Figure 9-4.

Comparison of one-at-the-time with Monte Carlo results.

Table 9-11 compares the standard deviations found with one at the time parameter variation with the one obtained with simultaneous variation, further the standard error, average, relative standard deviation and relative standard error of the Monte Carlo analysis are tabulated. The difference between the standard deviation obtained using the one-at-the-time approach (SD_{OAT}) and the one using simple Monte Carlo analysis indicates the dependency of the variables. It can be clearly seen that for the cycles for which the analysis was performed, the mass and thrust standard deviations are about the same meaning that the simultaneous variation of the knowledge input parameters does not strongly influence the outcome differently than the one-at-the time approach and therefore the knowledge parameters are not strongly correlated regarding mass and thrust. For volume however the standard deviation resulting of the Monte Carlo analysis is almost double of the one-at-the-time analysis; therefore there is a strong volume correlation between the studied knowledge parameters.

The standard error (SE_{MC}) gives the range of uncertainty of the estimate (hence the precision in absolute terms), the latter being the average of of all the output generated by the Monte Carlo

Table 9-11: mean, standard deviation and standard error of the knowledge parameters for all studied engine cycles

Cycle	# samples	AVG_{OAT}	AVG_{MC}	SD_{OAT}	SD_{MC}	SE_{MC}	RSD_{MC} [%]	RSE_{MC} [%]
Total wet mass [kg]								
gg	100	19926.6	20950.4	2978	2854.6	285.5	13.6	1.4
Total propulsion system volume [m^3]								
gg	100	40.6	39.664	3.9	6.233	0.623	15.7	1.6
Vacuum thrust [kN]								
gg	100	47.5	50.604	6.9	6.731	0.673	13.3	1.3

OAT: One-At-the-Time
SD: Standard Deviation
RSD: Relative Standard Deviation
AVG: Average
gg: gas generator cycle
MC: Monte Carlo
SE: Standard Error
RSE: Relative Standard Error
TBD: To Be Determined

analysis. Hence following from Eq. (6-8), 95 %[2] of the time the true average lies within the range

$$\begin{aligned} I &= AVG_{\text{MC}} \pm z_0 \cdot SE_{\text{MC}} \\ &= AVG_{\text{MC}} \pm 1.96 \cdot SE_{\text{MC}} \end{aligned}$$

The relative standard deviation (RSD_{MC}) in the one to last column indicates how acceptable the estimate is; a relative standard error of estimate of 30% was found acceptable in Chapter 6, hence so if this threshold is taken here as well one can conclude that the uncertainty in the estimates does not lead to unacceptable results for the cycles for which the analysis was performed.

The relative standard error (RSE_{MC}) in the last column shows that the relative variability of the estimate and thus allows the compare the precision in relative terms. As the RSE of the total wet mass, total propulsion system volume and vacuum thrust are for all investigated engine cycles is less than two percent, it shows the model is very precise and robust.

9-6 Large Figures and Tables

Figure 9-3 gives the results of the Monte Carlo uncertainty analysis where the vacuum thrust is plotted against the total estimated stage wet mass. Figure 9-4 gives the results of the Monte Carlo uncertainty analysis where the vacuum thrust is plotted against the total estimated propulsion system volume.

[2] $P = 2 \cdot \phi(z_0) = 0.95 \Rightarrow \phi(z_0) = 0.475 \Rightarrow z_o = 1.96$ (see normal curve area table in Figure 6-3)

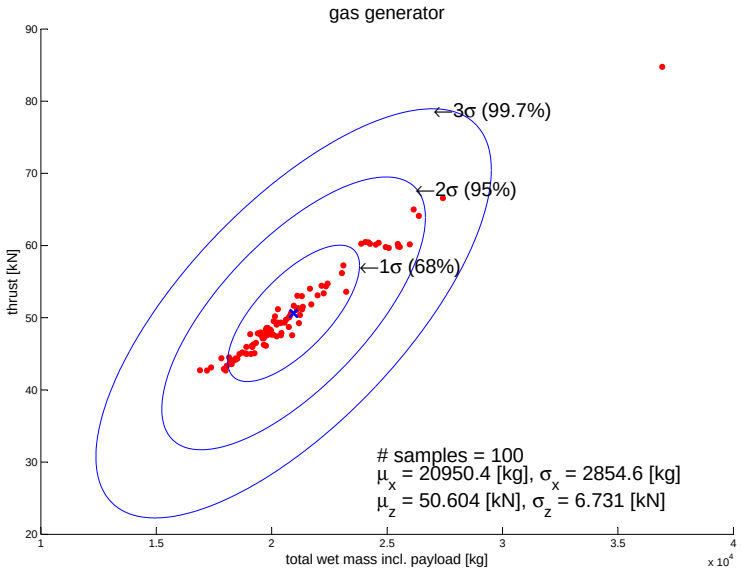

Figure 9-3: Thrust versus total wet mass including payload dispersion of solutions for the Ariane 5 upper stage gas generator cycle case

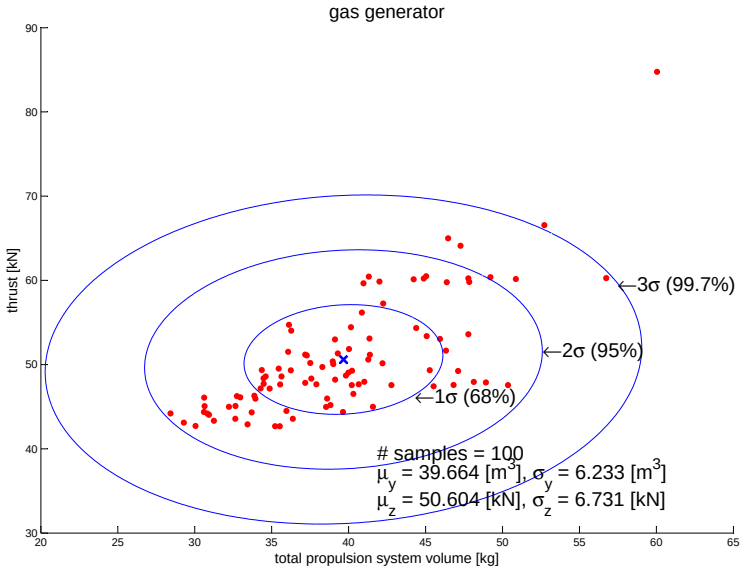

Figure 9-4: Vacuum thrust versus total propulsion system volume dispersion of solutions for the Ariane 5 upper stage gas generator cycle case

Chapter 10

Conclusions and Recommendations

LiRA, a tool comprising a propulsion system performance, dimension and mass model, was created, verified and validated. An optimisation routine to optimise the propulsion system of a launcher stage was build around the propulsion system analysis routine and its inputs and outputs were subjected to uncertainty and sensitivity analysis and were validated against real systems.

For the propulsion system analysis routine, validation showed for most parameters satisfactory accuracy in terms of relative standard error of estimate. Those parameters which showed significant deviations from reality have little impact on the total system in terms of mass, dimension or performance and were hence accepted.

Though the neglecting of line losses and losses over valves proved not to lead to significant reduction in accuracy, it is recommended to create a pipe and valve element when further refining the program.

Propellant flow properties of pure substances and mixtures were obtained using NASA CEA and NIST chemistry web-book. Though the modelling of the combustion is satisfactory in the current performance model, it is restricted to only the pressure, mixture ratio and temperature ranges supported by the tables. It is therefore recommended to either integrate an external tool such as CEA or to write a custom thermodynamic modelling routine, for example using equilibrium flow analysis via minimization of Gibbs Free Energy supporting a certain amount of species as is the case for Redtop.

During the analysis of several engine cycles it was observed that expander cycles might need a bypass which leads part of the fuel directly to the main combustion chamber, instead of directing all fuel through the heat exchanger, in order to work more efficient or in some cases to operate at all. The reason for this is that for too high mass flows the heat exchange does not warm up the fuel to sufficient high temperatures for the turbine to operate efficiently; in some cases where cryogenic hydrogen was used, it was observed that the fuel arrives at the turbine inlet at a temperature barely higher than the temperature it had when leaving the tank. Hence it is recommended to allow an expander cycle to have a fuel tap off, after the fuel pump, which leads fuel to the main combustion chamber without passing the heat exchanger. For an example of a bleed expander cycle using this method see the SE-21 D engine cycle design in [26].

Regarding optimisation, when the reproducibility of the optimisation results was studied, it was observed that for the same requirements and constraints, quite different optimised input results are obtained whilst the output like mass, performance and dimensions does not differ significantly. The hypothesis is put forward that there are many local minima that have a value close to the global minimum. However this was not confirmed and hence is recommended to be included into further work.

Uncertainty analysis of non-variable parameters, such as correction factors, showed that during optimisation the uncertainty in knowledge of the dry mass correction factor, pressurant tank performance factor and propellant tank performance leads to major uncertainty in the total system mass volume estimates; it is therefore recommended to alter the pressurant tank and propellant tank mass estimation method. An alternative method could be calculating the required thickness of a spherical tank or cylindrical tank with hemispherical ends and applying a mass correction factor to it to account for other structural mass. This approach hence requires more detailed modelling of the geometry of the tanks and demands a material choice from the user.

Validation of the optimisation results uncovered two points of improvement. The first one is that the method of using a dry mass correction factor based on propulsion system dry mass only to estimate stage dry mass, can significantly over- or underestimate the latter. The hypothesis is put forward that this is due to the structural mass dependency on launch loads imposed on the system of which the size is a function of acceleration, inclination and the mass of the payload and all structures above the considered stage. The only approach to improve the stage dry mass estimate is hence by adding to LiRA (or combining LiRA with) a trajectory model and a full launcher design module in which iteratively loads and masses are updated such that the propulsion system is also updated along the way. The second point of improvement is to make the estimate of specific impulse more realistic. This can be done by adding additional constraints like limited nozzle length.

Despite the assumptions and simplifications made and the remaining issues, cycle analysis clearly confirms known trends and cycle characteristics. It was shown that closed systems are more propellant efficient and therefore can have significant lower mass and volume relative to open systems. The staged combustion cycle (also known as topping cycle) is especially at high thrust levels superior over all other cycles studied in terms of both propulsion system mass and volume. However due to the uncertainty in the mass estimates no absolute numbers can be given. Nevertheless no matter which turbo-pump cycle is chosen, a clear mass advantage is found for cycles using a pump over a pressure fed cycle; the reason being the lower tank masses due to lower pressure in the propellant storage tanks.

The tool has proven to help the user to gain deep insight in the operation of an engine cycle. While the general characteristic differences between a pressure fed, gas generator, staged combustion, closed expander and bleed expander cycle have been studied, still more aspects remain to be investigated.

The current tool only allows for the fuel rich or oxygen rich partial staged combustion architectures with a single pre-burner and a single or double turbine. However there also exists another variant of the staged combustion cycle, called the full flow staged combustion cycle, where all the oxygen and fuel is passed through two pre-burners which feed the turbines on oxidiser side and fuel side separately. This cycle is said to have advantages such as increased efficiency over partial staged combustion cycles; in [25] and [18] a comparison of a partial staged combustion and full flow staged combustion cycle for the use in a space plane (called SpaceLiner) is made and advantages such as higher Isp, higher efficiency, lower pump discharge pressure and consequently a lower mass flow required through the turbines are identified.

During optimisation semi-cryogenic propellants such as LOX-RP1 were not considered nor was the impact of using oxygen rich pre-burners investigated. Further non-thrust chamber related parameters such as tank pressure, turbine pressure ratio, turbine inlet temperature and turbine and pump efficiency, amount of turbines were not included in the optimisation. The inclusion of these parameters however requires an expansion of the current written routine by adding another loop.

Further work that wants to continue with launcher stage propulsion system optimisation, should hence focus first on resolving the problems with accuracy and uncertainty of which the use of a trajectory model and launcher design model are part of the solution. Next the propulsion system optimisation routine should be expanded such that tank pressure, turbine pressure ratio, turbine inlet temperature and turbine and pump efficiency and amount of turbines are included in the optimisation loop. And finally the tool should be expanded by adding cost and reliability modules to be able to improve the trade that needs to be made by a designer.

LiRA is in summary hence a very capable tool that has been proven to be precise, to behave robust and to predict trends correctly, though the accuracy should be improved through further calibration and elaboration before one can start considering using it for non comparative purposes.

Bibliography

[1] A. Lekeux, J. Pander, and J. Mansouri, "From qualification to 4th year of exploitation : Hm7b on esc a," in *45th AIAA/ASME/SAE/ASEE Joint Propulsion Conference & Exhibit, 2 - 5 August 2009, Denver, Colorado*, 2009. AIAA 2009-5036.

[2] J. Vandamme, "Assisted-launch performance analysis: Using trajectory and vehicle optimization," Master's thesis, Delft University of Technology, 2012.

[3] C. Goertz, "A modular method for the analysis of liquid rocket engine cycles," in *31st AIAA/ASME/SAE/ASEE Joint Propulsion Conference and Exhibit, San Diego, CA*, 1995.

[4] G. P. Sutton and O. Biblarz, *Rocket Propulsion Elements*. John Wiley & Sons, Inc., 2001. ISBN 0471326429.

[5] M. Kaufmann, "Design criteria for high-pressure rocket engines," *ELDO Technical Review*, vol. 3, no. 1, pp. 3–28, 1968.

[6] O. J. Haidn, "Advanced rocket engines," *Advances on Propulsion Technology for High-Speed Aircraft*, vol. 1, pp. 6–1 – 6–40, 2008. Educational Notes RTO-EN-AVT-150, Paper 6.

[7] H. Martensson, A. Sonny, S. Trollheden, and B. Staffan, "Rocket engines: Turbomachinery." http://ftp.rta.nato.int/public/PubFullText/RTO/EN/RTO-EN-AVT-150/EN-AVT-150-05.pdf, 2007.

[8] S. Dr. Chakroborty and T. P. Dr. Bauer, "Using pressure-fed propulsion technology to lower space transportation costs," in *40th AIAA/ASME/SAE/ASEE Joint Propulsion Conference and Exhibit, Fort Lauderdale, Florida*, 2004.

[9] J. M. Seitzman, "Rocket propulsion reacting flow issues." http://soliton.ae.gatech.edu/people/jseitzma/classes/ae6450/thermochemistry.pdf, 2006. AE6450 Rocket Propulsion.

[10] W. Welland, B. Brauers, and E. Vermeulen, "Future igniter technologies," tech. rep., Aerospace Propulsion Products, 2010.

[11] B. Zandbergen, *Thermal Rocket Propulsion*. Delft University of Technology, 2.04 ed., 2012. Reader AE4S01.

[12] J. Sisco, "Liquid rocket engine cycles." https://engineering.purdue.edu/AAE/Academics/Courses/aae539/2007/spring/handouts/EngineCycles.ppt, 2007. slides AAE 539: Advanced Rocket Propulsion.

[13] G. P. Sutton and O. Biblarz, *Rocket Propulsion Elements*. John Wiley & Sons, Inc., 8 ed., 2011.

[14] M. Kaufmann, "The topping cycle -its potential and its limits-," in *XVIIth Congress of the International Astronautical Federation, Madrid*, 1966.

[15] J. A. Manski, Deflet; Martin, "Optimization of the propulsion cycles for advanced shuttles part 1: Propulsion mass model methodology," in *AIAA/ASME/SAE/ASEE 25th Joint Propulsion Conference, Monterey, CA*, 1989.

[16] J. A. Manski, Delfet; Martin, "Optimization of the propulsion cycles for advanced shuttles part 2: Performance model methodology," in *AIAA/SAE/ASME/ASEE 26th Joint Propulsion Conference, Orlando, FL*, 1990.

[17] D. J. Zehe, "Chemical equilibrium with applications." http://www.grc.nasa.gov/WWW/CEAWeb/, March 2010.

[18] M. Sippel, R. Yamashiro, and F. Cremaschi, "Staged combustion cycle rocket engine design trade-offs for future advanced passenger transport," in *SPACE PROPULSION 2012, BORDEAUX, 7TH Ű 10TH MAY 2012*, 2012.

[19] A. Ponomarenko, "Rpa: Tool for liquid propellant rocket engine analysis c++ implementation." http://propulsion-analysis.com/downloads/1.0/docs/RPA_LiquidRocketEngineAnalysis_II.pdf, May 2010. Main website see http://propulsion-analysis.com/.

[20] D. W. Way and D. J. R. Olds, "Scores: Web-based rocket propulsion analysis for space transportation system design," in *35th AIAA/ASME/SAE/ASEE Joint Propulsion Conference and Exhibit, 20-24 June 1999, Los Angeles, California*, 1999. AIAA 99-2353.

[21] Spaceworks Software, "Redtop pro product comparison." http://www.spaceworkssoftware.com/products/desktop/redtop-pro.shtml, 2014.

[22] Técnicas Reunidas S.A., "Ecosimpro modelling & simulation tool." http://www.ecosimpro.com/description.php, 2014.

[23] S. Gordon and B. McBride, "Computer program for calculation of complex chemical equilibrium compositions and applications vol. i: Analysis," tech. rep., NASA, 1994. NASA RP-1311.

[24] J. E. Bradford, A. Charania, J. R. Olds, and M. Graham, "Xcalibur a vertical takeoff tsto rlv concept with a hedm upperstage and a scram-rocket booster," in *53rd International Astronautical Congress The World Space Congress - 2002, 10-19 Oct 2002/Houston, Texas*, 2002. IAC-02-S.5.02.

[25] R. Yamashiro and M. Sippel, "Preliminary design study of staged combustion cycle rocket engine for spaceliner high-speed passenger transportation concept," in *International Astronautical Federation. 63rd International Astronautical Congress 2012, 1.-5. Okt. 2012, Naples, Italy*, 2012.

[26] M. Sippel, "Concurrent launcher engineering at dlr," in *Concurrent Engineering Workshop, ESTEC, 2004*, 2004.

[27] J. Kauffmann, A. Herbertz, and M. Sippel, "Systems analysis of a high thrust, low-cost rocket engine," in *Fourth International Conference on Green Propellants for Space Propulsion. 4th International Conference on Green Propellants for Space Propulsion, Noordwijk, The Netherlands, 20-22 June 2001*, 2001.

[28] M. Sippel, A. Herbertz, C. Manfletti, H. Burkhardt, T. Imoto, D. Haeseler, and A. Goetz, "Studies on expander bleed cycle engines for launchers," in *39th AIAA/ASME/SAE/ASEE Joint Propulsion Conference and Exhibit, Huntsville, Alabama 20-23 jul 2003*, 2003. AIAA 2003-4597.

[29] J. E. Bradford, A. Charania, and B. S. Germain, "Redtop-2: Rocket engine design tool featuring engine performance, weight, cost, and reliability," in *40th AIAA/ASME/SAE/ASEE Joint Propulsion Conference and Exhibit, Fort Lauderdale, Florida, July 11-14, 2004*, 2004. AIAA-2004-3514.

[30] National Institute for Standards and Technology, "Nist chemistry webbook - nist standard reference database number 69," 2013. http://webbook.nist.gov/chemistry/.

[31] R. Humble, G. Henry, and W. Larson, *Space Propulsion Analysis and Design*. McGraw-Hill Companies, Incorporated, 1995. ISBN: 9780070313200.

[32] B. Mc Hugh, "Numerical analysis of existing liquid rocket engines as a design process starter," in *31 st AIAA/ASME/SAU/ASEE Joint Propulsion Conference and Exhibit July 10-12,1995/San Diego, CA*, pp. 4–7, 1995. AIAA 95-2970 http://arc.aiaa.org/doi/pdf/10.2514/6.1995-2970.

[33] Astrium, "Launch vehicle propulsion," 2013. http://cs.astrium.eads.net/sp/launcher-propulsion/rocket-engines/index.html.

[34] NPO Energomash, "Rd-120 engines for second stage of the "zenit" launch-vehicle," 2013. http://www.npoenergomash.ru/eng/engines/rd120/.

[35] LPRE.DE, "Rd-170 (11d521) and rd-171 (11d520)," 2013. http://www.lpre.de/energomash/RD-170/.

[36] Braeunig, "Space shuttle," 2013. http://www.braeunig.us/space/specs/shuttle.htm.

[37] NASA, "J-2 engine fact sheet," 1968. http://www.nasa.gov/centers/marshall/pdf/499245main_J2_Engine_fs.pdf.

[38] J. O. Vilja, G. L. Briley, and T. H. Murphy, "J-2s rocket engine," in *AIAA, SAE, ASME, and ASEE, Joint Propulsion Conference and Exhibit, 29th, Monterey*, June 1993. http://adsabs.harvard.edu/abs/1993jpmc.confT....V.

[39] M. Wade, "Encyclopedia astronautica." http://www.astronautix.com/index.html.

[40] D. Huzel and D. Huang, "Design of liquid rocket engines," tech. rep., NASA, Washington DC, 1971.

[41] Cengel-Boles, *Thermodynamics: An engineering approach*. McGraw-Hill, 2009. ISBN 13: 9780390165206.

[42] D. T. Jamieson and G. Cartwright, "Properties of binary liquid mixtures: Heat capacity," Tech. Rep. 648, National Engineering Laboratory: East Kiibride, U.K, January 1978.

[43] A. S. Tela, "Simple method for the calculation of heat capacities of liquid mixtures," *Journal of Chemical and Engineering Data*, vol. 28, no. 1, pp. 83–85, 1983. http://pubs.acs.org/doi/pdf/10.1021/je00031a025.

[44] F. Senese, "What is the clausius-clapeyron equation?." http://antoine.frostburg.edu/chem/senese/101/liquids/faq/clausius-clapeyron-vapor-pressure.shtml, 2010.

[45] the ChemTeam, "The clausius-clapeyron equation," 2013. http://www.chemteam.info/GasLaw/Clasius-Clapeyron-Equation.html.

[46] P. Z. S. Spakovszky, "The clausius-clapeyron equation (application of 1st and 2nd laws of thermodynamics)," 2013. http://web.mit.edu/16.unified/www/FALL/thermodynamics/notes/node64.html.

[47] B. V. Kit and D. S. Evered, *Rocket Propulsion Handbook*. The Macmillan Company, 1960.

[48] B. Zandbergen, "Propellant characteristics 27 october 2010," 2010. http://www.lr.tudelft.nl/fileadmin/Faculteit/LR/Organisatie/Afdelingen_en_Leerstoelen/Afdeling_SpE/Space_Systems_Eng./Expertise_areas/Space_propulsion/Design_details/Rocket_Propellants/Chemical_propellants/Liquid_propellants/Physical_properties/doc/4-Propellant_charact_27_October_2010.pdf.

[49] Splung.com, "Latent heat." http://www.splung.com/content/sid/6/page/latentheat, 2014.

[50] J. Cornelisse, H. Schoyer, and K. Wakker, *Rocket Propulsion and Spaceflight Dynamics*. Pitman Publ. Ltd, London, 1979.

[51] M. F. Wadel, "Comparison of high aspect ratio cooling channel designs for a rocket combustion chamber with development of an optimized design," tech. rep., NASA Lewis research center, 1998. NASA/TM-1998-206313.

[52] R. Schuff, M. Maier, O. Sindiy, C. Ulrich, and S. Fugger, "Integrated modeling and analysis for a lox/methande expander cycle: Focusing on regenerative cooling jacket design," in *42nd AIAA/ASME/SAE/ASEE Joint Propulsion Conference & Exhibit 9-12 July 2006, Sacramento, California*, 2006. AIAA 2006-4534.

[53] D. K. Huzel and D. H. Huang, *Design of Liquid Propellant Rocket Engines*. NASA, second ed., 1967. NASA SP-125 http://ntrs.nasa.gov/archive/nasa/casi.ntrs.nasa.gov/19710019929_1971019929.pdf.

[54] P. Walsh and P. Fletcher, *Gas Turbine Performance*. John Wiley & Sons, second ed., 2008.

[55] W. Ley, K. Wittmann, and W. Hallmann, *Handbook of Space Technology*. John Wiley & Sons, 2009. ISBN: 978-0-470-69739-9.

[56] B. Zandbergen, "Simple mass and size estimation relationships of pump fed rocket engines," November 2013.

[57] J. W. Murdock, *Fundamental fluid mechanics for the practicing engineer*. CRC Press, 1993. ISBN 0-8247-8808-7.

[58] B. Zandbergen, "Turbo-pump assembly mass estimation," December 2013.

[59] A. Sobin and W. Bissell, "Turbopump systems for liquid rocket engines," tech. rep., Nasa, 1974. NASA SP-8107.

[60] NASA, "Saturn v news reference - f-1 engine fact sheet." http://history.msfc.nasa.gov/saturn_apollo/documents/F-1_Engine.pdf.

[61] D. Newman, "The rocket." http://web.mit.edu/16.00/www/aec/rocket.html, May 1996. Aerospace Education Curriculum, a multi-media introduction to the principles of aerospace engineering. MIT Department of Aeronautics and Astronautics.

[62] B. Zandbergen, "Ae1222-ii: Aerospace design & systems engineering elements i," September 2013.

[63] D. R. Trotsenburg, "A design tool for low thrust rocket propulsion systems," Master's thesis, Delft University of Technology, 2004.

[64] E. Kyle, "Space launch report: Launch vehicle data sheets." http://www.spacelaunchreport.com/library.html#lvdata, March 2014.

[65] S. Hoelzer, "progressbar." http://www.mathworks.nl/matlabcentral/fileexchange/6922-progressbar, February 2005.

[66] D. M. Lane, "Online statistics education: An interactive multimedia course of study." http://onlinestatbook.com/, 2014.

[67] J. Stocks, "Standard error of estimate." https://www.msu.edu/user/sw/statrev/strv209.htm, 1999.

[68] P. C. Hurvich, "Handout: The normal distribution." http://pages.stern.nyu.edu/~churvich/MBA/Handouts/8-Normal.pdf. part of the course STATISTICS AND DATA ANALYSIS COR1-GB.1305.03 New York University.

[69] D. P. Loucks and E. van Beek, *Water Resources Systems Planning and Management - An Introduction to Method, Model and Applications*. United Nations Educational, Scientific and Cultural Organization, 2005. ISBN 92-3-103998-9.

[70] R. J. Klein, S. E. Proctor, M. A. Boudreault, and K. M. Turczyn, "Healthy people 2010 criteria for data suppression." http://www.cdc.gov/nchs/data/statnt/statnt24.pdf, 2002.

[71] Australian Bureau of Statistics, "What is a standard error and relative standard error, reliability of estimates for labour force data." http://www.abs.gov.au/websitedbs/d3310114.nsf/Home/What+is+a+Standard+Error+and+Relative+Standard+Error,+Reliability+of+estimates+for+Labour+Force+data.

[72] S. Easterbrook, "The difference between verification and validation." http://www.easterbrook.ca/steve/2010/11/the-difference-between-verification-and-validation/, 2010.

[73] R. D. McCulla, "Statistical treatment of data." http://www.slu.edu/~rmccull2/resources/statistics_for_data.pdf.

[74] B. K. Wood, "Propulsion for the 21st century - rs-68," in *38th Joint Liquid Propulsion Conference, 8Ű10 July 2002, Indianapolis, Indiana*, 2002.

[75] T. M. Tomsik, "A hydrogen-oxygen rocket engine coolant passage design program (recop) for fluid-cooled hrust chambers and nozzles," tech. rep., NASA Lewis Research Center, 1994.

[76] A. Saltelli, M. Ratto, T. Andres, F. Campolongo, J. Cariboni, D. Gatelli, M. Saisana, and S. Tarantola, *Global Sensitivity Analysis: The Primer*. John Wiley & Sons, 2008.

[77] J.W. Hickman, et al., "Pra procedures guide: A guide to the performance of probabilistic risk assessments for nuclear power plants: Chapters 9-13 and appendices a-g (nureg/cr-2300, volume 2)," tech. rep., The American Nuclear Society and The Institute of Electrical and Electronics Engineers, 1983.

[78] L. Liberti and S. Kuchherenko, "Comparison of deterministic and stochastic approaches to global optimization," *International Transactions in Operational Research*, vol. 12, p. 263Ű285, May 2005.

[79] H. Zhang, A. Bonilla-Petriciolet, and G. Rangaiah, "A review on global optimization methods for phase equilibrium modeling and calculations," *The Open Thermodynamics Journal*, vol. 5, pp. 76–82, 2011.

[80] C. R. Shalizi, "Monte carlo, and other kinds of stochastic simulation." http://vserver1.cscs.lsa.umich.edu/~crshalizi/notabene/monte-carlo.html, March 2013.

[81] D. Kirk, "Mae 4262: Rockets and mission analysis - lecture 29: Propellant tank design." http://my.fit.edu/~dkirk/4262/Lectures/, 2008.

[82] ICARUS Corporation, "Icarus reference chapter 10 vessels." http://instruct.uwo.ca/engin-sc/cbe497/Doc/Icarus/ir10.pdf, 1998.

[83] EADS Astrium, "300 n cryogenic rocket engine." http://cs.astrium.eads.net/sp/launcher-propulsion/rocket-engines/300n-cryogenic-rocket-engine.html, 2014.

[84] P. Leroux, "Ariane 5 donnees relatives au vol 157." http://www.capcomespace.net/dossiers/espace_europeen/ariane/annexes/v157-l517-f3.pdf, November 2002. better quality picture can also be found here: http://astronomienfolie.free.fr/images_conquete_espace/ariane5.jpg.

[85] M. J. L. Turner, *Rocket and Spacecraft Propulsion: Principles, Practice and New Developments*. Springer, 3rd ed., 2008. ISBN 978-3-540-69202-7.

[86] E. T. Lee and J. W. Wang, *Statistical Methods for Survival Data Analysis*. John Wiley & Sons, Inc., third edition ed., 2003. ISBN: 9780471369974.

[87] M. Binder, "Rl10a-3-3a rocket engine modeling project," Technical Memorandum 107318, NASA, January 1997.

[88] Arianespace, *Ariane 5 User's Manual Issue 5 Revision 0*. Arianespace, July 2008.

[89] Arianespace, "Esc-a (etage superieure cryogenique-a)." http://farm3.static.flickr.com/2547/3889885274_cdc9b971a5_b.jpg, July 2001.